

IDENTIFICATION OF NOVEL REGULATORS OF PIN POLARITY
AND
DEVELOPMENT OF A NOVEL AUXIN SENSOR

by

Tomáš Prát

12th January 2017

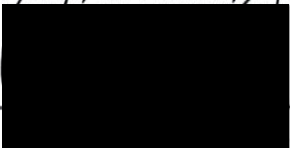
*A thesis presented to the
Graduate School
of the
Institute of Science and Technology Austria, Klosterneuburg, Austria
in partial fulfillment of the requirements
for the degree of
Doctor of Philosophy*



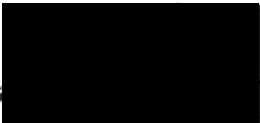
Institute of Science and Technology

The dissertation of Tomáš Prát, titled *Putative regulators of PIN protein polarity and development of novel auxin sensor*, is approved by:

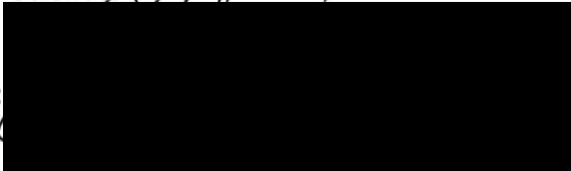
Supervisor: Jiří Friml, IST Austria, Klosterneuburg, Austria

Signature:  _____

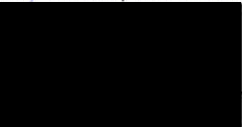
Committee Member: Harald Lukas Janovjak, IST Austria, Klosterneuburg, Austria

Signature:  _____

Committee Member: Christian Luschnig, University of Natural Resources and Life Sciences (BOKU), Vienna, Austria

Signature:  _____

Exam Chair: Laszlo Erdös, IST Austria, Klosterneuburg, Austria

Signature:  _____

© by Tomáš Prát, 12th January 2017

All Rights Reserved

I hereby declare that this dissertation is my own work and that it does not contain other people's work without this being so stated; this thesis does not contain my previous work without this being stated, and the bibliography contains all the literature that I used in writing the dissertation.

I declare that this is a true copy of my thesis, including any final revisions, as approved by my thesis committee, and that this thesis has not been submitted for a higher degree to any other university or institution.

The original title of the draft thesis was 'Putative regulators of PIN protein polarity and development of a novel auxin sensor'. Based on the committee member's suggestion during thesis defense on 12th December 2016 at IST Austria, the title was changed to 'Identification of novel regulators of PIN polarity and development of novel auxin sensor'.

I certify that any republication of materials presented in this thesis has been approved by the relevant publishers and co-authors.

Signature:

A black rectangular box redacting the signature of Tomáš Prát.

Tomáš Prát

12th January, 2017

Abstract

Plant hormone auxin and its transport between cells belong to the most important mechanisms controlling plant development. Auxin itself could change localization of PINs and thereby control direction of its own flow. We performed an expression profiling experiment in *Arabidopsis* roots to identify potential regulators of PIN polarity which are transcriptionally regulated by auxin signalling. We identified several novel regulators and performed a detailed characterization of the transcription factor *WRKY23* (At2g47260) and its role in auxin feedback on PIN polarity. Gain-of-function and dominant-negative mutants revealed that *WRKY23* plays a crucial role in mediating the auxin effect on PIN polarity. In concordance, typical polar auxin transport processes such as gravitropism and leaf vascular pattern formation were disturbed by interfering with *WRKY23* function.

In order to identify direct targets of *WRKY23*, we performed consequential expression profiling experiments using a *WRKY23* inducible gain-of-function line and dominant-negative *WRKY23* line that is defunct in PIN re-arrangement. Among several genes mostly related to the groups of cell wall and defense process regulators, we identified *LYSINE-HISTIDINE TRANSPORTER 1* (*LHT1*; At5g40780), a small amino acid permease gene from the amino acid/auxin permease family (AAP), we present its detailed characterisation in auxin feedback on PIN repolarization, identified its transcriptional regulation, we propose a potential mechanism of its action. Moreover, we identified also a member of receptor-like protein kinase LRR-RLK (*LEUCINE-RICH REPEAT TRANSMEMBRANE PROTEIN KINASE PROTEIN 1*; *LRRK1*; At1g05700), which also affects auxin-dependent PIN re-arrangement. We described its transcriptional behaviour, subcellular localization. Based on global expression data, we tried to identify ligand responsible for mechanism of signalling and suggest signalling partner and interactors. Additionally, we described role of novel phytohormone group, strigolactone, in auxin-dependent PIN re-arrangement, that could be a fundament for future studies in this field.

Our results provide first insights into an auxin transcriptional network targeting PIN localization and thus regulating plant development. We highlighted *WRKY23* transcriptional network and characterised its mediatory role in plant development. We identified direct effectors of this network, *LHT1* and *LRRK1*, and describe their roles in PIN re-arrangement and PIN-dependent auxin transport processes.

Acknowledgments

I would like to first acknowledge my supervisor Jiří Friml for support, kind advice and patience. It was a pleasure to be a part of your lab, Jiří. I will remember the atmosphere present in auxin lab at VIB in Ghent and at IST in Klosterneuburg forever. I would like to thank all past and present lab members for the friendship and friendly and scientific environment in the groups. It was so nice to cooperate with you, guys. There was always someone who helped me with experiments, troubleshoot issues coming from our work *etc.* At this place, I would like to thank especially to Gergo Molnár. I'm happy (and lucky) that I have met him; he naturally became my tutor and guide through my PhD. From no one else during my entire professional career, I've learned that much. I admire also his personality, sense of humour and musical attitude. Köszönöm, Gergo.

I would like to thank to my family for their never-ending support and love. Finally, my very special thanks go to my most beloved person, to my wife. Hanka, you gave me a power to overcome obstacles; you gave me a perspective and stand beside me through my ups and downs. I would like to dedicate this work to you. Thank you so much.

About the Author

Tomáš Prát finished his Bachelor's and Master's degree program in the fields of Cellular and Molecular Diagnostics and Molecular Biology and Genetics at Masaryk University in Brno, respectively. He has started his PhD studies at the VIB Department of Plant Systems Biology in Ghent and continued at IST Austria since April 2013. During his entire career, Tomas has been concentrated on plant hormones, auxin and cytokinin, their interplay and role in essential developmental processes of *Arabidopsis thaliana*. Moreover, he co-worked with Shaul Yalovsky's team from Tel Aviv University on interaction between auxin and ICR1 protein and research results were published in high-impact journal *Proceedings of the National Academy of Sciences of the United States of America*. More recently, his results concerning cytokinin influence on root gravitropism in *Arabidopsis thaliana* were published in *New Phytologist*. Tomas presented his results on several conferences including ACPD conference in Prague in 2014 and EMBO Conference: Signalling in Plant Development in Brno in 2015.

List of Publications Appearing in Thesis

1. Prát T., Grunewald W., Molnár G., Tejos R., Schmid M., Sauer M., and Friml J. 2016. WRKY23 is a component of the transcriptional network mediating auxin feedback on the PIN polarity. Submitted to PLOS Genetics.
2. Prát T., Grunewald W., Molnár G., and Friml J. 2016. WRKY23 downstream target LHT1 transporter mediates auxin-dependent PIN polarization. Manuscript
3. Prát T., Grunewald W., Molnár G., Smakowska E., Belkhadir Y., De Rybel B., and Friml J. 2016. LRRK1, a leucine rich repeat receptor-like kinase and its role in auxin-dependent PIN re-arrangement. Manuscript
4. Zhang J., Medvedova Z., Mazur E., Prát T., Balla J., Reinöhl V., Dun E.A., Yoshida S., Brewer P.B., and Friml J. 2016. Strigolactones interfere with PIN-dependent auxin transport canalization. Manuscript

Table of Contents

Abstract	v
Acknowledgments	vi
List of Figures	xii
List of Supporting Figures	xiii
List of Symbols/Abbreviations	xiv
1 Introduction.....	1
1.1 REFERENCES	5
2 WRKY23 is a component of the transcriptional network mediating auxin feedback on the PIN polarity	9
2.1 SUMMARY	9
2.2 INTRODUCTION	9
2.3 MATERIALS AND METHODS.....	11
2.3.1 <i>Plant material and growth conditions</i>	11
2.3.2 <i>Pharmacological treatments</i>	11
2.3.3 <i>Microarray Analysis</i>	12
2.3.4 <i>RNA Extraction, cDNA Synthesis and Quantitative RT-PCR and Analysis</i>	12
2.3.5 <i>Whole-mount in situ immunolocalization, microscopy and quantitative analysis of PIN relocalization</i>	12
2.3.6 <i>Phenotypic analysis</i>	13
2.3.7 <i>Histological analyses and microscopy</i>	13
2.4 RESULTS.....	13
2.4.1 <i>Identification of components mediating auxin effect on PIN polarity with microarray analysis</i> ..	13
2.4.2 <i>WRKY23 expression is auxin-dependent and is regulated by auxin signalling</i>	16
2.4.3 <i>WRKY23 gain-of-function causes PIN2 lateralization</i>	19
2.4.4 <i>Repression of WRKY23 activity abolishes the auxin effect on PIN2 polarization</i>	19
2.4.5 <i>Misregulation of WRKY23 expression affects growth, responses to environmental stimuli and development in Arabidopsis</i>	21
2.5 DISCUSSION.....	23
2.6 ACKNOWLEDGEMENTS	25
2.7 AUTHOR CONTRIBUTION.....	25
2.8 REFERENCES	26
2.9 SUPPORTING INFORMATION.....	30
3 WRKY23 downstream target LHT1 transporter mediates auxin-dependent PIN polarization.....	35
3.1 SUMMARY	35
3.2 INTRODUCTION	35
3.3 MATERIALS AND METHODS.....	37
3.3.1 <i>Plant material and growth conditions</i>	37
3.3.2 <i>Construction of transgenic lines</i>	38
3.3.3 <i>Phenotypic analysis</i>	38
3.3.4 <i>Pharmacological treatments</i>	39
3.3.5 <i>Microarray analysis</i>	39
3.3.6 <i>RNA extraction, cDNA synthesis, and quantitative RT-PCR and analysis</i>	39
3.3.7 <i>Whole-mount in situ Immunolocalization, microscopy and quantitative analysis of PIN relocalization</i>	40
3.3.8 <i>Histological analyses and microscopy</i>	40

3.3.9	<i>Basipetal auxin transport assay</i>	40
3.4	RESULTS AND DISCUSSION	41
3.4.1	<i>Identification of WRKY23 downstream targets by microarray analysis</i>	41
3.4.2	<i>Defense and stress related genes</i>	42
3.4.3	<i>Cell wall related genes</i>	43
3.4.4	<i>Residual candidates</i>	45
3.4.5	<i>LHT1 transporter</i>	45
3.4.6	<i>Polarity related phenotype analysis narrows down the list of putative regulators</i>	46
3.4.7	<i>Effect of LHT1 gene expression on PIN2 lateralization</i>	49
3.4.8	<i>Expression of LHT1 is regulated by WRKY23 and depends on auxin signalling pathway</i>	50
3.4.9	<i>LHT1 expression regulates auxin abundance/signalling in the root tip</i>	52
3.5	ACKNOWLEDGEMENTS	55
3.6	AUTHOR CONTRIBUTION.....	55
3.7	REFERENCES	56
3.8	SUPPORTING INFORMATION.....	61
4	LRRK1, a leucine-rich repeat receptor-like kinase and its role in auxin-dependent PIN re-arrangement	65
4.1	INTRODUCTION	65
4.2	MATERIALS AND METHODS.....	67
4.2.1	<i>Plant material and growth conditions</i>	67
4.2.2	<i>Construction of transgenic lines</i>	68
4.2.3	<i>Pharmacological treatments</i>	68
4.2.4	<i>IP and MS</i>	69
4.2.5	<i>RNA extraction, cDNA synthesis, and quantitative RT-PCR and analysis</i>	69
4.2.6	<i>Whole-mount in situ Immunolocalization, microscopy and quantitative analysis of PIN relocalization</i>	69
4.2.7	<i>Transient expression in Arabidopsis mesophyll protoplasts</i>	70
4.2.8	<i>Histological analyses and microscopy</i>	70
4.3	RESULTS AND DISCUSSION	70
4.3.1	<i>LRRK1 gain-of-function causes PIN2 lateralization</i>	70
4.3.2	<i>WRKY23 influences auxin signalling-dependent transcription regulation of LRRK1</i>	72
4.3.3	<i>Subcellular localization of LRRK1 and its function in constitutive PIN cycling</i>	74
4.3.4	<i>Application of auxin and flg22 does not lead to LRRK1 internalization</i>	76
4.3.5	<i>Signalling interactors of LRRK1</i>	77
4.3.6	<i>Target interactors of LRRK1</i>	81
4.4	ACKNOWLEDGEMENTS	84
4.5	AUTHOR CONTRIBUTION.....	84
4.6	REFERENCES	85
4.7	SUPPORTING INFORMATION.....	90
5	Strigolactone interfere auxin-dependent PIN re-arrangement in Arabidopsis	97
5.1	INTRODUCTION	97
5.2	MATERIALS	98
5.3	RESULTS.....	98
5.4	REFERENCES	100
6	Development of novel auxin sensor	103
6.1	INTRODUCTION	103
6.1.1	<i>Fluorescent sensors – probes as alternative in monitoring receptor-dependent signalling</i>	105
6.2	RESULTS.....	106
6.2.1	<i>Identification of binding cores for auxin</i>	106
6.2.2	<i>Cloning of selected binding cores, creation of the sensor</i>	107
6.2.3	<i>Testing of the sensor</i>	108
6.2.4	<i>EOS-like sensor</i>	109
6.2.5	<i>FRET based sensor</i>	110

6.2.6	<i>cpGFP sensor</i>	111
6.3	DISCUSSION.....	112
6.4	REFERENCES.....	114
7	Conclusions	118
A.	Appendix – WRKY23 is a component of the transcriptional network mediating auxin feedback on the PIN polarity	120
B.	Appendix - LRRK1, a leucine rich repeat receptor-like kinase and its role in auxin-dependent PIN re-arrangement	131

List of Figures

Figure 2-1 Auxin-dependent PIN re-arrangement and scheme of microarray experiment.....	15
Figure 2-2 <i>WRKY23</i> expression is auxin-dependent and is regulated by auxin signalling.	18
Figure 2-3 <i>WRKY23</i> influences auxin-dependent PIN2 re-arrangement.	20
Figure 2-4 Misregulation of <i>WRKY23</i> expression affects growth, responses to environmental stimuli and development in <i>Arabidopsis</i>	22
Figure 3-1 Expression profiling experiments to identify <i>WRKY23</i> -downstream regulators of PIN repolarization.	42
Figure 3-2 Polarity-related phenotype analysis of mutants in putative regulators.	48
Figure 3-3 Immunolocalization of PIN2 protein in root of <i>LHT1</i> loss- and gain-of-function lines.	49
Figure 3-4 Transcript levels and expression of <i>LHT1</i> during auxin treatments.	52
Figure 3-5 Auxin abundance/signalling in the root tip of <i>LHT1</i> loss- and gain-of-function lines.	53
Figure 4-1 Immunolocalization of PIN2 protein in root of <i>LRRK1</i> gain- and loss-of-function lines.	71
Figure 4-2 Transcript levels of <i>LRRK1</i> during auxin treatments.	73
Figure 4-3 Subcellular localization of <i>LRRK1</i>	75
Figure 4-4 Effect of suggested ligands on <i>LRRK1</i> subcellular localization.	77
Figure 4-5 Expression patterns of <i>LRRK1</i> , <i>PXC2</i> , and <i>RHS16</i> and <i>LRRK1</i> and <i>PXC2</i> mutant venation defects... ..	80
Figure 5-1 Role of strigolactone in the regulation of PIN polarity.	99
Figure 6-1 Pilot experiments to verify usability of streptavidin-biotin assay.	109
Figure 6-2 Results of maleimide reaction on EOS-like sensor with ACP1 binding core.	110
Figure 6-3 Results of FRET sensor with ACP1 binding core.	111
Figure 6-4 Results of two independent experiments with cpGFP sensor containing ACP1 binding core.	112

List of Supporting Figures

Figure S 2-1 Expression pattern of <i>WRKY23</i>	30
Figure S 2-2 <i>WRKY23</i> influences auxin-dependent PIN2 re-arrangement.	31
Figure S 2-3 Morphological phenotypes of <i>WRKY23</i> missregulation.	32
Figure S 3-1 Transcript level confirmation of microarray experiment.	61
Figure S 3-2 Vertical root growth in accordance to gravity vector observed in mutants of candidate gene line.	62
Figure S 3-3 PIN2 re-arrangement in cortex cells in Wt Col-0 and <i>aux1-21 lax1 lax2 lax3</i>	62
Figure S 4-1 Sequence alignment of extracellular domain of LRRK1 show very low identity to other LRR-RLK.	90
Figure S 4-2 Transcript level confirmation of mutant and transgenic plant lines.	92
Figure S 4-3 Output from GENEVESTIGATOR® (Nebion AG) global library of expression data.	94

List of Symbols/Abbreviations

AAAP	amino acid/auxin permease
ACP1	Acid phosphatase locus 1
BA	benzoic acid
BFA	Brefeldin A
CM	Cell membrane
DEX	Dexamethasone
DEX/GR	Dexamethasone-glucocorticoid
DMSO	Dimethyl sulfoxide
ELISA	Enzyme-Linked ImmunoSorbent Assay
GFP	Green Fluorescent protein
GPCRs	G-protein-coupled receptors
HS	Heat-shock
IAA	Indole-3-acetic acid
LHT1	Lysine-histidine transporter 1
LRRK1	Leucine-rich repeat transmembrane protein kinase protein 1
LRR-RLPs	leucine-rich repeat-receptor-like proteins
NAA	Naphtyl-acetic acid
PID	PINOID
PIN	PIN-FORMED
PIP5K	Phosphatidylinositol 4-phosphate 5-kinase
PPAR γ	Peroxisome proliferator activated receptor γ
qRT-PCR	Quantitative real-time PCR
LRR-RLK	Leucine-rich repeat receptor-like protein kinase
TF	Transcription factor
Trp	tryptophan
VGI	Vertical growth index

1 Introduction

Plant hormone auxin and its transport between cells, which depends on PIN auxin transporters, belong to the most important mechanisms controlling plant development. Properties of auxin transport through cellular membranes were predicted by chemiosmotic hypothesis in late 70's. This hypothesis consists of facts known about chemical attribute of Indole-3-acetic acid (IAA) – the basic auxin. IAA is a weak organic acid with indole ring and side carboxyl group moiety at C3 carbon of indole acquiring two molecular states in relation to pH level of their surrounding – dissociated (anionic) IAA^- and undissociated (protonated) IAAH. These two states have different ability of diffusion through cell membrane (CM). Only undissociated state of auxin could be freely transported through CM. The pH of plant cell apoplast is by mechanism of ATP-dependent proton pumps set to 5.5 while in cytoplasm the pH is neutral, around pH 7.0, resulting in accumulation of dissociated form of auxin inside the cell. Therefore, chemiosmotic hypothesis predicted presence of active auxin transporters – auxin efflux proteins. Based on this assumption, there was thought that if transporters are localized on one side of the membrane, if they are polarized, their action could direct auxin flow to one direction allowing the establishment of specific auxin gradients (Rubery & Sheldrake, 1974; Raven & Smith, 1976; Goldsmith & Cleland, 1978). Auxin transport is facilitated by carriers - auxin influx proteins from family AUX/LAX (Bennett *et al.*, 1996), auxin efflux carriers from PIN family (Galweiler *et al.*, 1998) and ABCB proteins (Noh *et al.*, 2001). The most developmentally important and thoroughly studied are PIN (PIN-FORMED) proteins (Adamowski & Friml, 2015). These efflux carriers belong to a plant-specific family of probable proton gradient-driven secondary transporters lacking ATP-binding domain (Zazimalova *et al.*, 2010). According to the length of central hydrophilic domain, eight members of PIN proteins are divided into two groups: (A) shorter, intracellular PINs with partially or entirely reduced central domain and (B) long canonical PINs with long, hydrophilic domain localizing to the CM (Krecek *et al.*, 2009). PIN proteins could be localized symmetrically along the membrane or proteins could be localized polarly – asymmetrically localized: on basal side of the cells in direction to root (rootward side), or localized apically (shootward side). PIN proteins could be localized also on lateral sides of the cells. An asymmetrical localization on membrane has been shown to determine direction of auxin flow within tissues (Wisniewska *et al.*, 2006). Polarity of PIN protein is not generally same in all tissues, depends on cell type, development state of

tissues (Benkova *et al.*, 2003; Friml *et al.*, 2003) but also on environmental stimuli (Friml *et al.*, 2002; Kleine-Vehn *et al.*, 2010; Ding *et al.*, 2011; Rakusova *et al.*, 2011; Rakusova *et al.*, 2015).

Polarly localized PIN auxin exporters and subsequent auxin gradients act also as a polarity cue, establishing new polarity and growth axis of the tissue. Local auxin application induces vascular differentiation in plant tissue but in narrow strands running away from the source rather than in wide field of the cells (Jacobs, 1955). These observations led Tsvi Sachs to propose so called canalization hypothesis in order to explain patterns of vascular strand differentiation *e.g.* in leaf venation and in the reconnection of the stem vasculature strands that were interrupted by wounding (Sachs, 1975). Canalization is a self-organizing pattern of auxin transport in which initially broad domain of auxin-transporting cells is reduced to narrow 'canal' – initial flow of auxin from a source to sink is gradually canalized into files of cells upregulating and polarizing its auxin transport activity by positive feedback control (Bennett *et al.*, 2014). The result of canalization is formation of cell files with high levels of auxin transport polarized towards the auxin sink, these cell files acts as auxin transport canals, connecting the source to the sink. This process has been proposed to mediate multiple key plant developmental processes *i.e.* in establishment of new vasculature (Berleth & Sachs, 2001) and its regeneration after wounding (Sauer *et al.*, 2006; Mazur *et al.*, 2016), competitive control of apical dominance (Booker *et al.*, 2003; Balla *et al.*, 2011) but possibly also establishment of embryonic apical-basal axis (Robert *et al.*, 2013; Wabnik *et al.*, 2013) or organogenesis (Benkova *et al.*, 2003). The mechanism underlying the auxin-mediated polarization is largely unknown but its key component is a feedback regulation of PIN polarity by auxin signalling (Sachs, 1975; Sauer *et al.*, 2006; Bennett *et al.*, 2014).

As a proxy for canalization we used the auxin effect on PIN polarity in *Arabidopsis* root meristems (Sauer *et al.*, 2006). In the root of model plant *Arabidopsis thaliana* are proteins PIN1 localized on basal sides of endodermal and pericycle cells and cells of the vascular tissue. Auxin carriers PIN2 have basal polarity in cells of cortex but apical polarity in epidermis. However, upon 4 hours of treatment by 10 μ M auxin naphthyl-acetic acid (NAA), the localization of PIN1 proteins are changed from basal to inner-lateral side in endodermis and pericycle, while PIN2 auxin carriers undergo change of localization from basal to outer-lateral side of cells in cortex (Sauer *et al.*, 2006). Auxin-dependent PIN lateralization in the root meristem requires a rather prolonged auxin treatment which suggests involvement of a whole

cascade of transcriptional processes. It was shown that this process is transcriptionally dependent on SCF^{TIR1}-Aux/IAA-ARF signalling pathway. This pathway begins with auxin TIR1 coreceptor, as a part of Skp1-Cullin-F-box complex (SCF^{TIR1/AFB1-5}) of SCF E3 type ubiquitin ligase. Auxin acts as molecular glue providing interaction between TIR1 and Aux/IAA (AUXIN/INDOLE-3-ACETIC ACID) proteins (Tan *et al.*, 2007), which are upon auxin binding ubiquitinated and then degraded in proteasome (Salehin *et al.*, 2015). In the absence of auxin, AUX/IAA proteins inactivate ARF (AUXIN RESPONSE FACTOR) transcription factors by heterodimerization and consequently block expression of auxin-dependent genes (Guilfoyle & Hagen, 2007; Salehin *et al.*, 2015). In conditionally expressed mutant line, *HS::axr3-1*, non-degradable version of protein IAA17, as well as in other auxin signalling double mutant *arf7 arf19*, PIN proteins do not undergo the lateralization under the auxin treatment (Sauer *et al.*, 2006). These results suggest that PIN lateralization is dependent on functional SCF^{TIR1}-Aux/IAA-ARF auxin signalling pathway.

Several mechanisms changing characteristics of auxin flow dependent on PIN proteins are known. On transcriptional level, auxin promotes expression of auxin carriers by tissue specific level (Schrader *et al.*, 2003; Vieten *et al.*, 2005). On other hand, the posttranscriptional regulation of auxin carriers by modulation of vacuolar trafficking mechanism indirectly involving also ubiquitination and proteasome activity was suspected in the affection of PIN2 protein stability at CM (Sieberer *et al.*, 2000; Abas *et al.*, 2006; Baster *et al.*, 2013). Third, also posttranscriptional mechanism of clathrin-mediated endocytosis has a key role in decrease of internalization of PIN proteins from cell membrane and thus maintains PIN levels at membrane. Nevertheless, recent publication of Jasik and collaborators disprove this auxin effect on endocytosis (Paciorek *et al.*, 2005; Robert *et al.*, 2010; Xu *et al.*, 2010; Jasik *et al.*, 2016). However, none of these mechanisms influences the direction of intercellular auxin flow.

Mechanism of PIN polarity establishment was thoroughly studied in past 15 years. PIN proteins are undergoing constant recycling between CM and endosomal compartments of the cell. PIN proteins are internalized from CM by clathrin-mediated endocytosis. After internalization, vesicles containing PIN proteins are targeted to a certain side of the membrane driven by ARF-GEF GNOM. ARFs (ADP-ribosylation factor) are a small guanine binding proteins, commonly driving protein transport in *Eukaryotes* (Geldner *et al.*, 2001). At CM, ARF interacts with activators ARF-GEF (ARF-Guanine nucleotide exchange factor), or

inhibitors ARF-GAP (ARF-GTPase activating proteins) respectively (Donaldson & Jackson, 2000). ARF-GEF GNOM dependent endosomal exocytosis is largely important for establishment of basal PIN polarity (Kleine-Vehn *et al.*, 2008). PIN polar targeting is based also on orchestrated function of protein kinases and phosphatases interacting with PIN auxin carriers. Three kinases phosphorylating PINs, ACG3 – PID (PINOID) and its homologues WAG1 and 2 are known to target apolarly excreted PIN carriers to apical side of the cell (Friml *et al.*, 2004; Michniewicz *et al.*, 2007). Dephosphorylation of PIN proteins depends on activity of protein phosphatase 2A (PP2A) (Michniewicz *et al.*, 2007). Basal polarity is connected with apolar PIN protein excretion followed by clathrin endocytosis and basal endocytic recycling of unphosphorylated PIN proteins (Friml *et al.*, 2004; Huang *et al.*, 2010; Zhang *et al.*, 2010). To avoid diffusion of PIN proteins in fluid membrane, PIN polarity is maintained in immobile clusters, polar microdomains, probably connected with cellulose compartments of the cell wall (Feraru *et al.*, 2011; Kleine-Vehn *et al.*, 2011). Until now none mechanism directly connecting auxin dependent PIN lateralization process and regulators of PIN polarity is known. In this work we want to describe so far unknown mechanisms by which auxin can modify PIN polarization.

1.1 REFERENCES

- Abas L, Benjamins R, Malenica N, Paciorek T, Wisniewska J, Moulinier-Anzola JC, Sieberer T, Friml J, Luschnig C. 2006. Intracellular trafficking and proteolysis of the Arabidopsis auxin-efflux facilitator PIN2 are involved in root gravitropism. *Nat Cell Biol* **8**(3): 249-256.
- Adamowski M, Friml J. 2015. PIN-dependent auxin transport: action, regulation, and evolution. *Plant Cell* **27**(1): 20-32.
- Balla J, Kalousek P, Reinohl V, Friml J, Prochazka S. 2011. Competitive canalization of PIN-dependent auxin flow from axillary buds controls pea bud outgrowth. *Plant J* **65**(4): 571-577.
- Baster P, Robert S, Kleine-Vehn J, Vanneste S, Kania U, Grunewald W, De Rybel B, Beeckman T, Friml J. 2013. SCF(TIR1/AFB)-auxin signalling regulates PIN vacuolar trafficking and auxin fluxes during root gravitropism. *EMBO J* **32**(2): 260-274.
- Benkova E, Michniewicz M, Sauer M, Teichmann T, Seifertova D, Jurgens G, Friml J. 2003. Local, efflux-dependent auxin gradients as a common module for plant organ formation. *Cell* **115**(5): 591-602.
- Bennett MJ, Marchant A, Green HG, May ST, Ward SP, Millner PA, Walker AR, Schulz B, Feldmann KA. 1996. Arabidopsis AUX1 gene: A permease-like regulator of root gravitropism. *Science* **273**(5277): 948-950.
- Bennett T, Hines G, Leyser O. 2014. Canalization: what the flux? *Trends Genet* **30**(2): 41-48.
- Berleth T, Sachs T. 2001. Plant morphogenesis: long-distance coordination and local patterning. *Curr Opin Plant Biol* **4**(1): 57-62.
- Booker J, Chatfield S, Leyser O. 2003. Auxin acts in xylem-associated or medullary cells to mediate apical dominance. *Plant Cell* **15**(2): 495-507.
- Ding Z, Galvan-Ampudia CS, Demarsy E, Langowski L, Kleine-Vehn J, Fan Y, Morita MT, Tasaka M, Fankhauser C, Offringa R, et al. 2011. Light-mediated polarization of the PIN3 auxin transporter for the phototropic response in Arabidopsis. *Nat Cell Biol* **13**(4): 447-452.
- Donaldson JG, Jackson CL. 2000. Regulators and effectors of the ARF GTPases. *Curr Opin Cell Biol* **12**(4): 475-482.
- Feraru E, Feraru MI, Kleine-Vehn J, Martiniere A, Mouille G, Vanneste S, Vernhettes S, Runions J, Friml J. 2011. PIN polarity maintenance by the cell wall in Arabidopsis. *Curr Biol* **21**(4): 338-343.
- Friml J, Vieten A, Sauer M, Weijers D, Schwarz H, Hamann T, Offringa R, Jurgens G. 2003. Efflux-dependent auxin gradients establish the apical-basal axis of Arabidopsis. *Nature* **426**(6963): 147-153.
- Friml J, Wisniewska J, Benkova E, Mendgen K, Palme K. 2002. Lateral relocation of auxin efflux regulator PIN3 mediates tropism in Arabidopsis. *Nature* **415**(6873): 806-809.
- Friml J, Yang X, Michniewicz M, Weijers D, Quint A, Tietz O, Benjamins R, Ouwerkerk PB, Ljung K, Sandberg G, et al. 2004. A PINOID-dependent binary switch in apical-basal PIN polar targeting directs auxin efflux. *Science* **306**(5697): 862-865.
- Galweiler L, Guan C, Muller A, Wisman E, Mendgen K, Yephremov A, Palme K. 1998. Regulation of polar auxin transport by AtPIN1 in Arabidopsis vascular tissue. *Science* **282**(5397): 2226-2230.
- Geldner N, Friml J, Stierhof YD, Jurgens G, Palme K. 2001. Auxin transport inhibitors block PIN1 cycling and vesicle trafficking. *Nature* **413**(6854): 425-428.

- Goldsmith MH, Cleland RE. 1978.** The contribution of tonoplast and plasma membrane to the electrical properties of a higher-plant cell. *Planta* **143**(3): 261-265.
- Guilfoyle TJ, Hagen G. 2007.** Auxin response factors. *Curr Opin Plant Biol* **10**(5): 453-460.
- Huang F, Zago MK, Abas L, van Marion A, Galvan-Ampudia CS, Offringa R. 2010.** Phosphorylation of conserved PIN motifs directs Arabidopsis PIN1 polarity and auxin transport. *Plant Cell* **22**(4): 1129-1142.
- Jacobs WP. 1955.** Occurrence of diffusible auxin in *Psilotum*. *Science* **122**(3170): 597.
- Jasik J, Bokor B, Stuchlik S, Micieta K, Turna J, Schmelzer E. 2016.** Effects of Auxins on PIN-FORMED2 (PIN2) Dynamics Are Not Mediated by Inhibiting PIN2 Endocytosis. *Plant Physiology* **172**(2): 1019-1031.
- Kleine-Vehn J, Dhonukshe P, Sauer M, Brewer PB, Wisniewska J, Paciorek T, Benkova E, Friml J. 2008.** ARF GEF-dependent transcytosis and polar delivery of PIN auxin carriers in Arabidopsis. *Curr Biol* **18**(7): 526-531.
- Kleine-Vehn J, Ding Z, Jones AR, Tasaka M, Morita MT, Friml J. 2010.** Gravity-induced PIN transcytosis for polarization of auxin fluxes in gravity-sensing root cells. *Proc Natl Acad Sci U S A* **107**(51): 22344-22349.
- Kleine-Vehn J, Wabnik K, Martiniere A, Langowski L, Willig K, Naramoto S, Leitner J, Tanaka H, Jakobs S, Robert S, et al. 2011.** Recycling, clustering, and endocytosis jointly maintain PIN auxin carrier polarity at the plasma membrane. *Mol Syst Biol* **7**: 540.
- Krecek P, Skupa P, Libus J, Naramoto S, Tejos R, Friml J, Zazimalova E. 2009.** The PIN-FORMED (PIN) protein family of auxin transporters. *Genome Biol* **10**(12): 249.
- Mazur E, Benkova E, Friml J. 2016.** Vascular cambium regeneration and vessel formation in wounded inflorescence stems of Arabidopsis. *Sci Rep* **6**: 33754.
- Michniewicz M, Zago MK, Abas L, Weijers D, Schweighofer A, Meskiene I, Heisler MG, Ohno C, Zhang J, Huang F, et al. 2007.** Antagonistic regulation of PIN phosphorylation by PP2A and PINOID directs auxin flux. *Cell* **130**(6): 1044-1056.
- Noh B, Murphy AS, Spalding EP. 2001.** Multidrug resistance-like genes of Arabidopsis required for auxin transport and auxin-mediated development. *Plant Cell* **13**(11): 2441-2454.
- Paciorek T, Zazimalova E, Ruthardt N, Petrasek J, Stierhof YD, Kleine-Vehn J, Morris DA, Emans N, Jurgens G, Geldner N, et al. 2005.** Auxin inhibits endocytosis and promotes its own efflux from cells. *Nature* **435**(7046): 1251-1256.
- Rakusova H, Fendrych M, Friml J. 2015.** Intracellular trafficking and PIN-mediated cell polarity during tropic responses in plants. *Curr Opin Plant Biol* **23**: 116-123.
- Rakusova H, Gallego-Bartolome J, Vanstraelen M, Robert HS, Alabadi D, Blazquez MA, Benkova E, Friml J. 2011.** Polarization of PIN3-dependent auxin transport for hypocotyl gravitropic response in Arabidopsis thaliana. *Plant J* **67**(5): 817-826.
- Raven JA, Smith FA. 1976.** The evolution of chemiosmotic energy coupling. *J Theor Biol* **57**(2): 301-312.
- Robert HS, Grones P, Stepanova AN, Robles LM, Lokerse AS, Alonso JM, Weijers D, Friml J. 2013.** Local auxin sources orient the apical-basal axis in Arabidopsis embryos. *Curr Biol* **23**(24): 2506-2512.
- Robert S, Kleine-Vehn J, Barbez E, Sauer M, Paciorek T, Baster P, Vanneste S, Zhang J, Simon S, Covanova M, et al. 2010.** ABP1 mediates auxin inhibition of clathrin-dependent endocytosis in Arabidopsis. *Cell* **143**(1): 111-121.
- Rubery PH, Sheldrake AR. 1974.** Carrier-mediated auxin transport. *Planta* **118**(2): 101-121.
- Sachs T. 1975.** The induction of transport channels by auxin. *Planta* **127**(3): 201-206.

- Salehin M, Bagchi R, Estelle M. 2015.** SCFTIR1/AFB-based auxin perception: mechanism and role in plant growth and development. *Plant Cell* **27**(1): 9-19.
- Sauer M, Balla J, Luschnig C, Wisniewska J, Reinohl V, Friml J, Benkova E. 2006.** Canalization of auxin flow by Aux/IAA-ARF-dependent feedback regulation of PIN polarity. *Genes Dev* **20**(20): 2902-2911.
- Schrader J, Baba K, May ST, Palme K, Bennett M, Bhalerao RP, Sandberg G. 2003.** Polar auxin transport in the wood-forming tissues of hybrid aspen is under simultaneous control of developmental and environmental signals. *Proc Natl Acad Sci U S A* **100**(17): 10096-10101.
- Sieberer T, Seifert GJ, Hauser MT, Grisafi P, Fink GR, Luschnig C. 2000.** Post-transcriptional control of the Arabidopsis auxin efflux carrier EIR1 requires AXR1. *Curr Biol* **10**(24): 1595-1598.
- Tan X, Calderon-Villalobos LI, Sharon M, Zheng C, Robinson CV, Estelle M, Zheng N. 2007.** Mechanism of auxin perception by the TIR1 ubiquitin ligase. *Nature* **446**(7136): 640-645.
- Vieten A, Vanneste S, Wisniewska J, Benkova E, Benjamins R, Beeckman T, Luschnig C, Friml J. 2005.** Functional redundancy of PIN proteins is accompanied by auxin-dependent cross-regulation of PIN expression. *Development* **132**(20): 4521-4531.
- Wabnik K, Robert HS, Smith RS, Friml J. 2013.** Modeling framework for the establishment of the apical-basal embryonic axis in plants. *Curr Biol* **23**(24): 2513-2518.
- Wisniewska J, Xu J, Seifertova D, Brewer PB, Ruzicka K, Blilou I, Rouquie D, Benkova E, Scheres B, Friml J. 2006.** Polar PIN localization directs auxin flow in plants. *Science* **312**(5775): 883.
- Xu T, Wen M, Nagawa S, Fu Y, Chen JG, Wu MJ, Perrot-Rechenmann C, Friml J, Jones AM, Yang Z. 2010.** Cell surface- and rho GTPase-based auxin signaling controls cellular interdigitation in Arabidopsis. *Cell* **143**(1): 99-110.
- Zazimalova E, Murphy AS, Yang H, Hoyerova K, Hosek P. 2010.** Auxin transporters--why so many? *Cold Spring Harb Perspect Biol* **2**(3): a001552.
- Zhang J, Nodzynski T, Pencik A, Rolcik J, Friml J. 2010.** PIN phosphorylation is sufficient to mediate PIN polarity and direct auxin transport. *Proc Natl Acad Sci U S A* **107**(2): 918-922.

2 **WRKY23 is a component of the transcriptional network mediating auxin feedback on the PIN polarity**

Tomáš Prát, Wim Grunewald, Gergely Molnár, Ricardo Tejos, Markus Schmid, Michael Sauer, and Jiří Friml

2.1 **SUMMARY**

- Auxin is unique among plant hormones due to its ability to move between cells by directional transport, mediated by PIN auxin transporters localized polarly at the plasma membranes. The canalization hypothesis proposes the auxin feed-back on polar PIN localization as a crucial mechanism in mediating multiple developmental processes including vascular tissue formation and regeneration.
- Here, we used the auxin effect on PIN polarity in *Arabidopsis* root meristems as a proxy for canalization and performed microarray experiments to find regulators of this process.
- We identified genes transcriptionally regulated by auxin, which were downstream of SCF^{TIR1}-Aux/IAA-ARF auxin signalling and transcriptionally modulated in an IAA17 (AXR3)- and ARF7/ARF19-dependent manner. Apart from the known molecular players involved in correct PIN polar delivery, we identified and further characterized the *WRKY23* transcription factor as a novel regulator.
- Gain-of-function and dominant-negative mutants revealed that *WRKY23* plays a crucial role in mediating the auxin effect on PIN polarity. In concordance, typical polar auxin transport processes such as gravitropism, organogenesis and leaf vascular pattern formation were disturbed by interfering with *WRKY23* function.
- Our results provide first insights into an auxin transcriptional network targeting PIN localization and regulating plant development mediated by canalization of PIN-dependent auxin transport.

2.2 **INTRODUCTION**

The phytohormone auxin plays a key role in many aspects of a plant's life cycle. A unique attribute of auxin is its polarized, intercellular movement which depends, among other components, on polarly localized PIN auxin exporters (Petrasek *et al.*, 2006; Wisniewska *et*

et al., 2006; Adamowski & Friml, 2015). The so-called canalization hypothesis proposes that auxin acts also as a cue in establishing new polarity axes during the polarization of tissues (Sachs, 1975; Sachs, 1986). Canalization has been proposed *i.e.* to mediate multiple key plant developmental processes including formation of new vasculature (Berleth & Sachs, 2001), its regeneration after wounding (Sauer *et al.*, 2006) and competitive control of apical dominance (Booker *et al.*, 2003; Balla *et al.*, 2011; Bennett *et al.*, 2016). It is likely that the same mechanism plays also a role in the establishment of the embryonic apical-basal axis (Robert *et al.*, 2013; Wabnik *et al.*, 2013) and during organogenesis (Benkova *et al.*, 2003). While the molecular details of auxin-mediated cell- and tissue polarization are largely unknown, one key constituent is feed-back regulation of PIN polarity by auxin signalling (Sachs, 1975; Sauer *et al.*, 2006; Bennett *et al.*, 2014). This auxin feed-back on PIN polarity may be related to a direct auxin effect on clathrin-mediated internalization of PIN proteins (Paciorek *et al.*, 2005; Robert *et al.*, 2010) but the connection is unclear so far (Wabnik *et al.*, 2010).

Auxin feed-back on PIN polarity can be experimentally approximated by PIN polarity re-arrangement following auxin treatment in roots of *Arabidopsis thaliana*. Under standard conditions, PIN1 is localized on the basal sides of endodermal and pericycle cells and cells of the vascular tissue (Friml *et al.*, 2002), whereas PIN2 exhibits basal polarity in the young cells of the cortex but apical polarity in epidermal cells (Muller *et al.*, 1998; Kleine-Vehn *et al.*, 2008). After auxin treatment, both PIN1 and PIN2 appear to be localized also at the lateral cell side. PIN1 changes from predominantly basal to basal and inner-lateral in endodermis and pericycle cells, while PIN2 undergoes a localization shift from the basal to the basal and outer-lateral side of young cortex cells (Sauer *et al.*, 2006). The exact molecular mechanism and biological significance of this effect is unclear but it depends on the transcriptional SCF^{TIR1}-Aux/IAA-ARF auxin signalling pathway (Chapman & Estelle, 2009). In brief, upon auxin binding to the TIR1/AFB receptor family, transcriptional repressors and co-repressors of the Aux/IAA class are degraded, in turn releasing auxin response transcription activators of the ARF family (Salehin *et al.*, 2015).

In a heat-shock (HS) inducible *HS::axr3-1* line expressing a mutated, non-degradable version of the IAA17 transcriptional repressor (Knox *et al.*, 2003; Salehin *et al.*, 2015), as well as in the *arf7 arf19* double mutant defective for these two transcriptional activators expressed in primary root and functionally redundant in organogenic processes (Wilmoth *et al.*, 2005), auxin is no longer effective to mediate PIN polarity re-arrangements in the root

meristem (Sauer *et al.*, 2006). These results suggest that transcriptional auxin signalling regulates the cellular abundance of so far unknown regulators, which in turn modify subcellular sorting or trafficking pathways and other polarity determinants, ultimately leading to changes in polar PIN distribution.

In this work, we performed an expression profiling experiment in *Arabidopsis* roots to identify potential regulators of PIN polarity which are transcriptionally regulated by auxin signalling. We identified several novel regulators and performed a more detailed characterization of the transcription factor WRKY23 and its role in auxin feed-back on PIN polarity.

2.3 MATERIALS AND METHODS

2.3.1 Plant material and growth conditions

All *Arabidopsis thaliana* lines were in Columbia-0 background. The *arf7 arf19* double mutant and *HS::axr3-1* transgenic line have been described previously (Knox *et al.*, 2003; Okushima *et al.*, 2005). For *RPS5A>>WRKY23* analyses, the F1 generation of a *RPS5A::GAL4VP16* (Aida *et al.*, 2004) × *UAS::WRKY23* (Grunewald *et al.*, 2012) cross was analysed and compared with the F1 generations from *UAS::WRKY23* × Wt Col-0 and *RPS5A::GAL4VP16* × Wt Col-0 crosses. *WRKY23::GUS*, *35S::WRKY23-GR*, *WRKY23::WRKY23-SRDX* and *35S::WRKY23-SRDX* were described previously (Grunewald *et al.*, 2008; Grunewald *et al.*, 2012). Seeds were surface sterilized overnight by chlorine gas, sown on solid *Arabidopsis* medium (AM+; half-strength MS basal salts, 1% Sucrose, and 0.8% phytoagar, pH 5.7), and stratified at 4°C for at least 2 days prior to transfer to a growth room with a 16-h-light/8-h-dark regime at 21°C. The seedlings were grown vertically for 4 or 6 days depending on the assay.

2.3.2 Pharmacological treatments

Arabidopsis treatments with auxin or chemicals were done in liquid AM+ medium at 21°C in a growth room using the following concentrations and times: for α -naphthaleneacetic acid (NAA; Sigma Aldrich) at 10 μ M for 4h; dexamethasone (DEX; Sigma Aldrich) 10 μ M for 24h. Mock treatments were performed with equivalent amounts of DMSO.

2.3.3 Microarray Analysis

Wild type Col-0 and *HS::axr3-1* seeds were grown vertically on AM+ plates for 5 days. We applied to the seedlings a 40 minute heat shock at 37°C, allowed 1.5 h to recover at normal growth temperature and subsequently transferred to liquid AM+ medium and treated with 10 µM NAA or DMSO for 4 h. Afterwards, the lower third of 100-130 roots from each treatment was cut off, frozen in liquid N₂, and RNA was extracted with a Quiagen RNAeasy mini kit. Probe preparation and hybridization to *Arabidopsis* ATH1–121501 gene expression array (Affymetrix) was performed as described (Leal Valentim *et al.*, 2015). Expression data for Col-0, *HS::axr3-1*, both NAA and mock treated had been deposited under the ArrayExpress number E-MEXP-3283. Expression data for *arf7 arf19* (ArrayExpress: E-GEOD-627) have been published previously (Okushima *et al.*, 2005). Raw data were pairwise analysed using the logit-t Algorithm (Lemon *et al.*, 2003) with a cutoff of $p=0.05$.

2.3.4 RNA Extraction, cDNA Synthesis and Quantitative RT-PCR and Analysis

RNA extraction, cDNA Synthesis, and quantitative RT-PCR (qRT-PCR) were performed as described (Tejos *et al.*, 2014). Selected candidate gene transcript levels were quantified with qRT-PCR using specific primer pairs designed with Primer-BLAST (<http://www.ncbi.nlm.nih.gov/tools/primer-blast/>). Transcript levels were normalized to *GAMMA-TUBULIN 2 (TUB2; At5g05620)*, which was constitutively expressed and auxin-independent across samples. All PCRs were run in three technical repeats, and the data were processed with a qRT-PCR analysis software (Frederik Coppens; Applied Bioinformatics & Biostatistics group; PSB VIB). Primers used in this study are listed in Supporting Table S2-1.

2.3.5 Whole-mount *in situ* immunolocalization, microscopy and quantitative analysis of PIN relocation

PIN immunolocalizations of primary roots were performed as described (Sauer & Friml, 2010). The antibodies were used in the following dilutions: anti-PIN1, 1:1000 (Paciorek *et al.*, 2005); anti-PIN2, 1:1000 (Abas *et al.*, 2006). In all cases, the secondary goat anti-rabbit antibody coupled to Cy3 (Sigma-Aldrich) was diluted 1:600. Confocal microscopy was performed using a Zeiss LSM 700 confocal microscope. Quantitative analysis of PIN relocation was performed as described (Sauer *et al.*, 2006).

2.3.6 Phenotypic analysis

All measurements were done with ImageJ (<http://rsb.info.nih.gov/ij>). For root length analysis, seedlings were scanned and root lengths were measured. To quantify direction of the root growth, we used vertical growth index (VGI), ratio between the root tip ordinate and the root length (Grabov et al., 2005). Short term root gravistimulation was done by 6 hours of 90 degree induction. The seedlings were scanned and root angles were measured.

2.3.7 Histological analyses and microscopy

To detect β -Glucuronidase (GUS) activity, seedlings were incubated in reaction buffer containing 0.1 M sodium phosphate buffer (pH 7), 1 mM ferricyanide, 1 mM ferrocyanide, 0.1% Triton X-100 and 1 mg/ml X-Gluc for 2 h in dark at 37 °C. Afterwards, chlorophyll was removed by destaining in 70% ethanol and seedlings were cleared.

Clearing of tissues (seedlings, cotyledons) was performed in a solution containing 4% HCl and 20% methanol for 15 min at 65 °C, followed by 15 min incubation in 7% NaOH and 70% ethanol at room temperature. Next, seedlings were rehydrated by successive incubations in 70, 50, 25 and 10% ethanol for 5 min, followed by incubation in a solution containing 25% glycerol and 5% ethanol. Finally, seedlings were mounted in 50% glycerol and monitored by differential interference contrast microscopy DIC (Olympus BX53) or stereomicroscope (Olympus SZX16).

2.4 RESULTS

2.4.1 Identification of components mediating auxin effect on PIN polarity with microarray analysis

The rationale behind the approach was to search for genes which were (i) auxin regulated in roots under conditions when auxin changes PIN polarity and (ii) their auxin regulation is mediated by IAA17 (AXR3) transcriptional repressor. First, to search for auxin induced genes, we matched data from NAA treated and untreated heat shocked wild-type Col-0 control seedlings, resulting in 523 auxin induced genes. Since in *HS::axr3-1* under the same conditions auxin fails to induce PIN polarity changes (**Fig.2-1 A – B**), we compared heat shocked and auxin-treated Col-0 seedlings to similarly handled *HS::axr3-1* seedlings, expressing the auxin

resistant version of the transcriptional repressor IAA17 (AXR3) and we identified 667 genes (**Fig.2-1 C**). The overlap of this set with 523 auxin induced genes yielded 244 genes (**A Appendix Table S1 A – B**), which were induced by auxin and regulated downstream of IAA17. Further comparison with published microarray data on *arf7 arf19* mutant seedlings (Okushima *et al.*, 2005), which are also ineffective to re-arrange PIN polarity (Sauer *et al.*, 2006) yielded a final list of 125 genes (**A Appendix Table S2 A – B**). Some of them were previously shown to be involved in the regulation of PIN polarity. The AGC3 kinase PID (PINOID) and its homologues WAG1 and 2 are known to phosphorylate PINs (Michniewicz *et al.*, 2007) contributing to the control of their polar distribution (Friml *et al.*, 2004; Huang *et al.*, 2010; Zhang *et al.*, 2010). Nevertheless, overexpression of *PID* was shown to be dominant over auxin-induced PIN lateralization (Sauer *et al.*, 2006). Other identified candidate with a known role in PIN polar distribution was the phosphatidylinositol-4-phosphate 5 kinases PIP5K1. This protein, together with and its close homologue PIP5K2, is enriched on basal and apical membrane domains and they are required for PIN trafficking (Mei *et al.*, 2012; Ugalde *et al.*, 2016) and localization (Ischebeck *et al.*, 2013; Tejos *et al.*, 2014). Other candidates for polarity determinants include several previously known players in auxin-mediated plant development, *e.g.* RUL1, a leucine-rich repeat receptor-like kinase regulating cambium formation, a process linked to PIN polarity control (Agusti *et al.*, 2011) (**A Appendix Table S2 B**).

Auxin-dependent PIN lateralization in the root meristem requires a rather prolonged auxin treatment (Sauer *et al.*, 2006) which suggests involvement of a whole cascade of transcriptional processes. Therefore, we looked for transcription factor genes (TFs) induced by auxin in the list of putative polarity regulators as they may be transcriptionally regulating the process of PIN lateralization. The list contains *MIF1* (*MINI ZINC FINGER1*), affecting auxin responses during ectopic meristem formation (Hu *et al.*, 2011) but also *WRKY23* (At2g47260). *WRKY* genes belong to a plant-specific family of 72 transcription factors in *Arabidopsis*, being typically associated with plant defense processes and plant-pathogen interactions (Eulgem & Somssich, 2007). These genes were named by a shared sequence motif of 60 amino acid containing a conserved domain of seven invariant amino acids (WRKYGQK) (Eulgem *et al.*, 2000). The WRKYGQK motif provides high binding preference and contacts a 6 bp DNA sequence element - W-box (/TTGACT/C) contained in target gene promoters (Ulker & Somssich, 2004; Eulgem & Somssich, 2007). Distinct WRKY TFs have distinct selective binding

preferences to certain W-box variants (Ciolkowski *et al.*, 2008). The role of WRKY23 was shown in plant defense processes during plant-nematode interaction but also in regulation of auxin transport by flavonol biosynthesis affecting root- and embryo development. In *Arabidopsis* embryos, WRKY23 expression attenuates both auxin-dependent and auxin-independent signalling pathways towards stem cell specification (Grunewald *et al.*, 2008; Grunewald *et al.*, 2012; Grunewald *et al.*, 2013). Therefore, in this work, we focused on the role of WRKY23-dependent transcriptional regulation in auxin-dependent PIN repolarization.

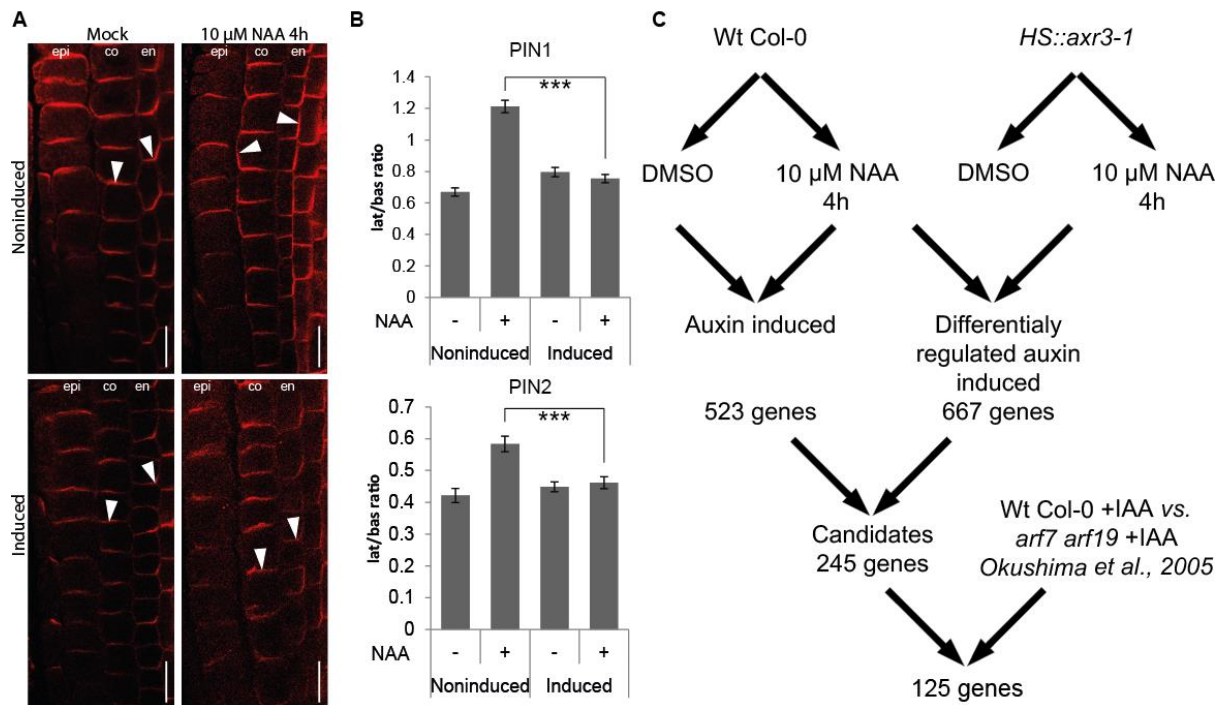


Figure 2-1 Auxin-dependent PIN re-arrangement and scheme of microarray experiment.

A. Immunolocalization of PIN1 and PIN2 proteins in *HS::axr3-1* plants. Lateralization of PIN proteins is dependent on functional SCF^{TIR1}-Aux/IAA-ARF signalling pathway. Heat-shock-induced overexpression of *axr3-1* abolishes lateral PIN relocation after auxin treatment. Arrowheads highlight PIN lateral localization. Bar size 10 μm. B. Quantitative evaluation confirms reduction of auxin-dependent relocation of PIN1 (upper graph) and PIN2 (lower graph), respectively in the induced *HS::axr3-1* line. Graph shows mean ratio of lateral to basal signal intensity of PIN1 in endodermis and PIN2 in cortex cells, error bars indicates standard error. A two-tailed Student's t test compared marked sets of data. (***) $P < 0.0001$. $n > 35$ cells corresponding to roots imaged under comparable conditions. C. Scheme of microarray experiment. A dataset of auxin regulated genes in Wt Col-0 seedlings under conditions where PIN repolarization occurs was overlaid with a second set of genes which are no longer auxin regulated in an induced *HS::axr3-1* background. Experiments in C. were designed by M.Sau., performed by M.Sch. and statistical analysis was performed by M.Sch. and G.M..

2.4.2 ***WRKY23* expression is auxin-dependent and is regulated by auxin signalling**

First, we confirmed and analysed auxin regulation of *WRKY23* expression. Promoters of auxin-inducible genes typically contain tandem localised auxin response elements (AuxREs) which are recognised by auxin response factors (ARFs) (Ulmasov *et al.*, 1997; Boer *et al.*, 2014). ARFs dimerize to act as molecular callipers providing specificity to auxin-dependent gene regulation by measuring the distance of AuxREs in the element pair at the promoter (Boer *et al.*, 2014). Length of the intergenic region between the 3'UTR of the previous gene *UPBEAT* (*UPB*; At2g47270) and the 5'UTR of *WRKY23* (At2g47260) is 4.5 kbp. The predicted 2.4 kbp *WRKY23* promoter by the AGRIS tool (Yilmaz *et al.*, 2011) contains 10 AuxRE and AuxRE-like sites and the extended promoter of 3.2 kbp used for native promoter fusion constructs contains two additional AuxRE sites (Grunewald *et al.*, 2008) (**Fig.2-2 A**). Such density of auxin regulatory sequences in the promoter strongly suggests direct regulation by ARF-dependent auxin signalling (Boer *et al.*, 2014).

In accordance with these findings, we found that *WRKY23* is auxin inducible in a dose- and time-dependent manner. When we treated *Arabidopsis* seedlings with 100 nM NAA for 4 hours, *WRKY23* transcription increased 2-fold, and 1 μ M NAA led to a 6-fold increase (**Fig.2-2 B**). Time response experiments at the consensus concentration of 10 μ M NAA used in PIN lateralization experiments (Sauer *et al.*, 2006) showed that *WRKY23* responds relatively slowly, with an expression increase after 4 hours of auxin treatment (**Fig.2-2 C**). This delay is in accordance with the observed timing of PIN lateralization (Sauer *et al.*, 2006). The dependence on auxin signalling was further supported by compromised *WRKY23* auxin inducibility in *HS::axr3-1* and *arf7 arf19* mutants (**Fig.2-2 D and E**). These results confirm *WRKY23* as a candidate gene arising from our microarray results and show the dependence of *WRKY23* transcription on the SCF^{TIR1} - Aux/IAA - ARF auxin signalling pathway.

A transgenic line harbouring the *uidA* reporter gene (or GUS coding gene) under the control of a 3.2 kb upstream sequence from *WRKY23* showed that auxin induces ectopic expression of *WRKY23* in the root tissues, partly overlapping also with root regions where PIN lateralization can be observed. Without auxin treatment, the expression pattern of *WRKY23* partially overlaps with the *DR5rev* auxin response reporter (**Fig.2-2 F**) (Friml *et al.*, 2003; Grunewald *et al.*, 2008; Grunewald *et al.*, 2012). Previously, we demonstrated that *WRKY23* is expressed in all apical cells of an octant stage embryo and at heart stage the expression of

WRKY23 is detected in both the root and the shoot stem cell niches (**Fig.2-2 G**) (Grunewald *et al.*, 2013). This might indicate that *WRKY23* has - besides its role in root development - also a function in shoot development. We detected *WRKY23* expression in shoot apical meristem as well as at the hydathodes of the cotyledons (**Fig.2-2 H – I**) coinciding with auxin response maxima (Scarpella *et al.*, 2006). Additionally, promoter activity could be detected in the vascular tissue of cotyledons and leaves (**Fig.2-2 I**) again coinciding with auxin response maxima (Scarpella *et al.*, 2006). In both tissues *WRKY23* expression is associated with the vasculature in a patchy pattern and seems to be also higher in the bundle sheath cells surrounding the mature vascular bundles (**Fig.2-2 J**). Moreover, in young leaves *WRKY23* expression precedes differentiation of the vascular strands (**Fig.2-2 K**) and thus might point to a role for *WRKY23* in venation patterning of leaves. GUS staining could be detected in the shoot apical meristem (SAM) (**Fig. S2-1 A – B**). Sectioning the SAM revealed specific *WRKY23* expression in the L1, L2 and L3 layers (**Fig. S2-1 B**). GUS staining could also be observed in the vasculature of flowers and in pollen grains (**Fig. S2-1 C – D**).

The presence of auxin responsive elements in the promoter, the dose- and time dependence of auxin regulation of *WRKY23* expression, its modulation by *AXR3* and dependence on *ARF7* and *ARF19*, together with ectopic expression in specific cell files of root tip following auxin treatment is consistent with a possible involvement of *WRKY23* in the process of auxin-mediated PIN lateralization.

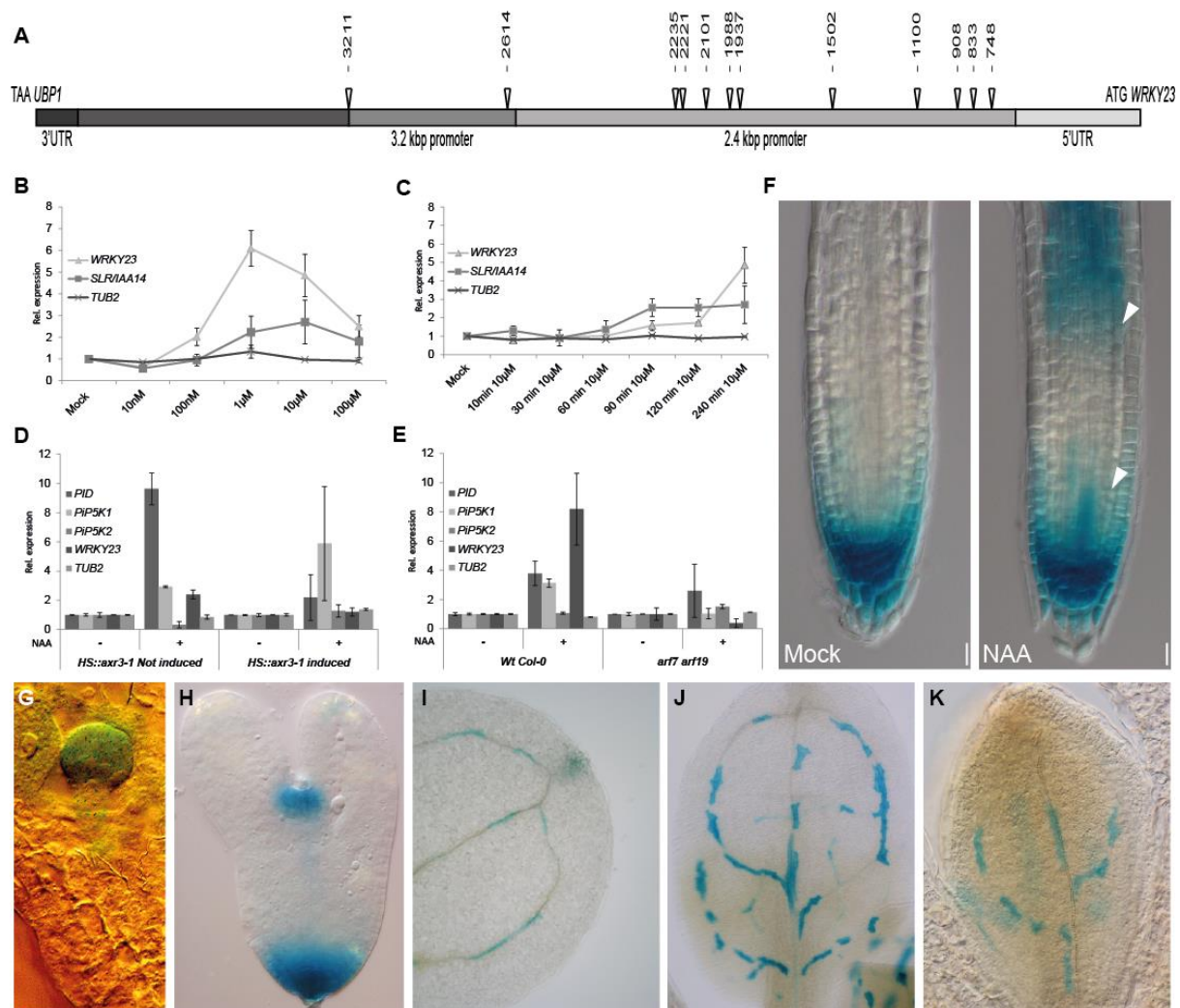


Figure 2-2 *WRKY23* expression is auxin-dependent and is regulated by auxin signalling.

A. Schematic depiction of *WRKY23* promoter; AuxRE and AuxRE-like response elements are shown as triangles. Numbers represent distance from *WRKY23* start codon. B – C. *WRKY23* transcript level is dependent on auxin dose and time of treatment. qRT-PCR analysis of *WRKY23* expression using different concentrations of NAA (B) and treatment time (C). Points represent relative fold change of expression. Error bars represent standard deviation. D. – E. *WRKY23* transcript levels are dependent on auxin SCF^{TIR1}-Aux/IAA-ARF signalling pathway. Data from qRT-PCR confirmation of microarray experiment shows *WRKY23* transcript levels and genes previously connected to PIN polarity in heat-shock-induced and not-induced *HS::arx3-1* plants (D) and in double mutant of *arf7 arf19* compared to Wt Col-0 (E). Bars represent relative fold change of transcript levels. Error bars represent standard deviation. F. *WRKY23* promoter activation by auxin treatment. Expression pattern of *WRKY23::GUS* in the root is changed upon 6 h of auxin treatment. *WRKY23* expression became generally stronger and ectopically expressed in meristematic and transition zone of the root tip (Arrowhead). Bar size 10 µm. G. – H. GUS staining of *WRKY23::GUS* embryos showing promoter activity in all apical cells of an early globular embryo and in SAM and RAM of an early torpedo stage embryo. I. *WRKY23::GUS* cotyledon showing GUS staining at the hydathode and in the vasculature. J. Patchy expression of *WRKY23* in the vasculature of leaves. K. In young leaves, *WRKY23* expression precedes xylem formation. GUS staining in G – K were performed by W.G..

2.4.3 WRKY23 gain-of-function causes PIN2 lateralization

Next, we tested whether altered *WRKY23* expression or activity had effects on the auxin regulation of PIN1 and PIN2 protein localization. We achieved strong constitutive overexpression of *WRKY23* using a GAL4VP16-UAS transactivation system (*RPS5A>>WRKY23*) (Aida *et al.*, 2004; Grunewald *et al.*, 2012; Grunewald *et al.*, 2013), and we also used a dexamethasone-glucocorticoid (DEX/GR) receptor system for inducible gain-of-function as previously described (Grunewald *et al.*, 2012; Grunewald *et al.*, 2013). Strong overexpression of *WRKY23* had a strong effect on PIN polarity by itself. Constitutively active overexpression in *RPS5A>>WRKY23* caused PIN2 lateralization in the root cortex cells, to some extent mimicking the application of auxin (**Fig.2-3 A – B**), while polar PIN1 localization in endodermis cells was not visibly changed (**Fig. S2-2 A – B**). Subsequent treatment with NAA further increased lateralization of PIN2 in cortex cells (**Fig.2-3 A – B**). An inducible *WRKY23* gain-of-function line showed a similar effect on PIN2 polarity: seedlings of a *35S::WRKY23-GR* line treated with dexamethasone to induce *WRKY23-GR* translocation to the nucleus, resulted in PIN2 lateralization in the cortex cells. Again, NAA treatment and DEX had an additive effect in this line (**Fig.2-3 C – D**). Thus, both constitutive and inducible *WRKY23* gain-of-function consistently leads to PIN2 lateralization in cortex cells, and the effect is enhanced by NAA treatment.

2.4.4 Repression of WRKY23 activity abolishes the auxin effect on PIN2 polarization

In complementary experiments, we tested the effect of downregulation of *WRKY23* function. The large *WRKY* family of homologous proteins has extensive functional redundancy among individual members (Schlüttenhofer & Yuan, 2015). Because compensation of loss of *WRKY23* by other members is, given the large size of the *WRKY* gene family, expected, we decided to use a dominant-negative approach with the chimeric repressor silencing technology (Hiratsu *et al.*, 2003). This technology is based on a translational fusion of an activating transcription factor with the repressor domain SRDX, thus inhibiting the expression of target genes. Transactivation activity of *WRKY23*, which is necessary to test before use of chimeric repressor silencing technology, was previously verified in a tobacco transient expression

assay, where the activating or repressing potential of TF fused with GAL4 was tested in presence of a *UAS::Luciferase* construct (Grunewald *et al.*, 2012).

Plants expressing *WRKY23-SRDX* under both the native and constitutive promoters showed a clear insensitivity to auxin in PIN lateralization. Without auxin, plants had an increased basal localization of PIN2 in cortex cells (**Fig. S2-2 C**). Auxin treatment did not lead to PIN2 lateralization as compared to the controls (**Fig.2-3 E – F**).

The observed opposite effects of *WRKY23* gain- and loss-of-function on PIN2 polarity confirmed that *WRKY23* plays an important role in the process of auxin-mediated PIN2 lateralization.

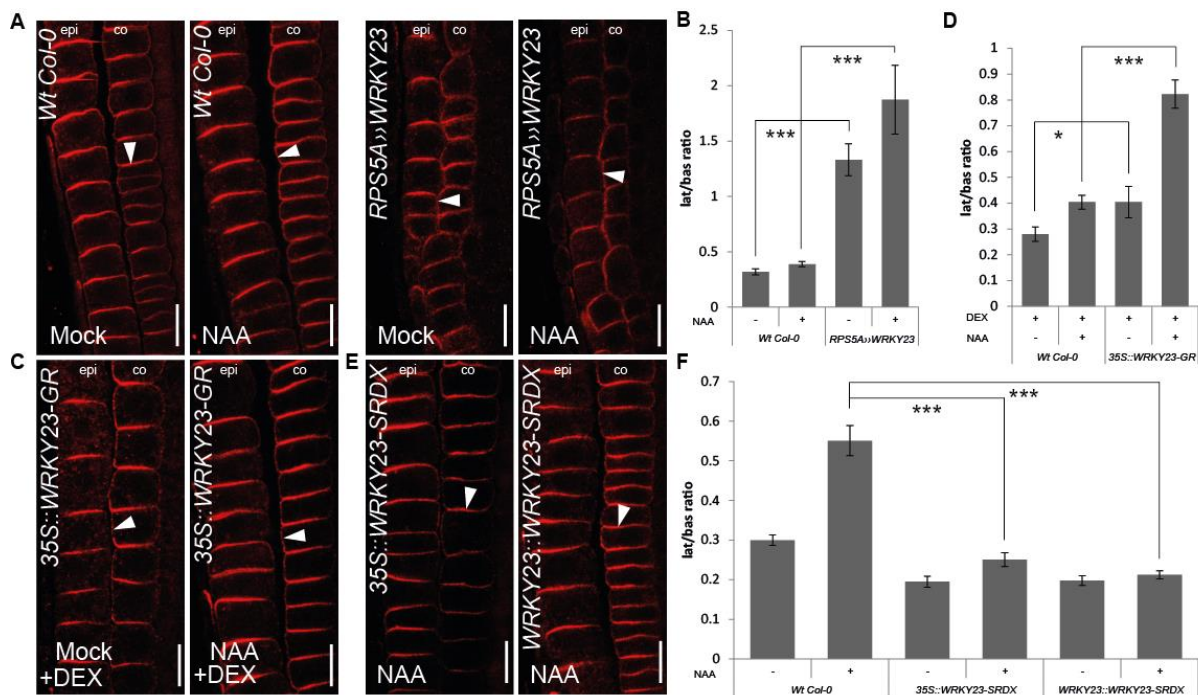


Figure 2-3 *WRKY23* influences auxin-dependent PIN2 re-arrangement.

A. – B. Treatment with NAA increases lateralization of PIN2 in cortex cells of Wt Col-0. Arrowheads highlight PIN polarity. Graph shows mean ratio of lateral to basal signal intensity of PIN2 in cortex cells, error bars indicates standard error. A two-tailed Student’s t test compared marked sets of data. (***) $P < 0.0001$. $n > 35$ cells. C. – D. Inducible gain-of-function of *WRKY23* caused by dexamethasone (DEX) treated 35S::*WRKY23-GR* influence PIN2 polarity. Arrowheads highlight PIN polarity. Graph shows mean ratio of lateral to basal signal intensity of PIN2 in cortex cells, error bars indicates standard error. A two-tailed Student’s t test compared marked sets of data. (*) $P < 0.05$; (***) $P < 0.0001$. $n > 35$ cells. E. – F. Dominant-negative *WRKY23-SRDX* plants driven by native and constitutive promoter abolishes lateral PIN relocation after auxin treatment. Arrowheads highlight PIN polarity. Graph shows mean ratio of lateral to basal signal intensity of PIN2 in cortex cells, error bars indicate standard error. A two-tailed Student’s t test compared marked sets of data. (***) $P < 0.0001$. $n > 28$ cells corresponding to roots imaged under comparable conditions. Bar sizes: 10 μm .

2.4.5 Misregulation of *WRKY23* expression affects growth, responses to environmental stimuli and development in *Arabidopsis*

The importance of tight regulation of PIN polarity for directional auxin fluxes and plant growth and development has previously been shown (Wisniewska *et al.*, 2006; Adamowski & Friml, 2015). Therefore, we analysed PIN polarity- or auxin transport-related phenotypes in transgenic lines with altered expression or activity of *WRKY23*. *RPS5A>>WRKY23* overexpressing plants show growth retardation and collapse of root meristem architecture (**Fig. S2-3 A**) (Grunewald *et al.*, 2012). Epinastic cotyledons of *RPS5A>>WRKY23* (**Fig.2-4 A**) phenocopy external application of auxin or auxin transport inhibitors; additionally, similar phenotypes were observed in the auxin overproducing *yuc1* mutant (Zhao *et al.*, 2001) as well as in auxin transport mutants like *mdr1/abcb1* (Noh *et al.*, 2001). Blocking of *WRKY23* action also led to severe effects on root growth. Plants with native promoter driven dominant-negative *WRKY23-SRDX* as well as strong constitutive promoter driven lines had shortened roots in comparison to Col-0 (**Fig.2-4 B**; **Fig. S2-3 B**).

Another physiological process connected to auxin transport and PIN polarity is root gravitropism. Therefore, we first analysed the direction of root growth relative to the gravity vector. *WRKY23::WRKY23-SRDX* lines showed no or very weak defects, while strong *35S::WRKY23-SRDX* lines phenocopy the defective gravitropism of auxin transport mutants like those observed in *pin2/eir1* (**Fig.2-4 C**) (Luschnig *et al.*, 1998). In a test for gravistimulated reorientation, native promoter-driven *SRDX* lines show a decreased ability to reorient their growth, a defect which is even more pronounced in lines expressing *WRKY23-SRDX* under a strong promoter (**Fig.2-4 D**).

The pattern of leaf venation crucially depends on the auxin feed-back on PIN polarity as proposed by the canalization hypothesis (Scarpella *et al.*, 2006). In plants strongly expressing *WRKY23-SRDX*, we observed vasculature patterning defects in more than 80% of the cotyledons (**Fig.2-4 E**). Most effects were observed in the first and second loops of veins (l1 and l2) which failed to connect to the midvein. In addition to cotyledon venation, we analysed true leaf venation complexity in *WRKY23* dominant-negative and gain-of-function lines. The midvein of *RPS5A>>WRKY23* leaves hardly branched and almost no secondary venation loops could be detected. In some leaves two midveins could be detected and these corresponding leaves were split (**Fig.2-4 F**). *WRKY23-SRDX* leaves revealed a rudimentary venation pattern

compared to wild-type (**Fig.2-4 G**). These results are consistent with compromised PIN-mediated canalization during venation development.

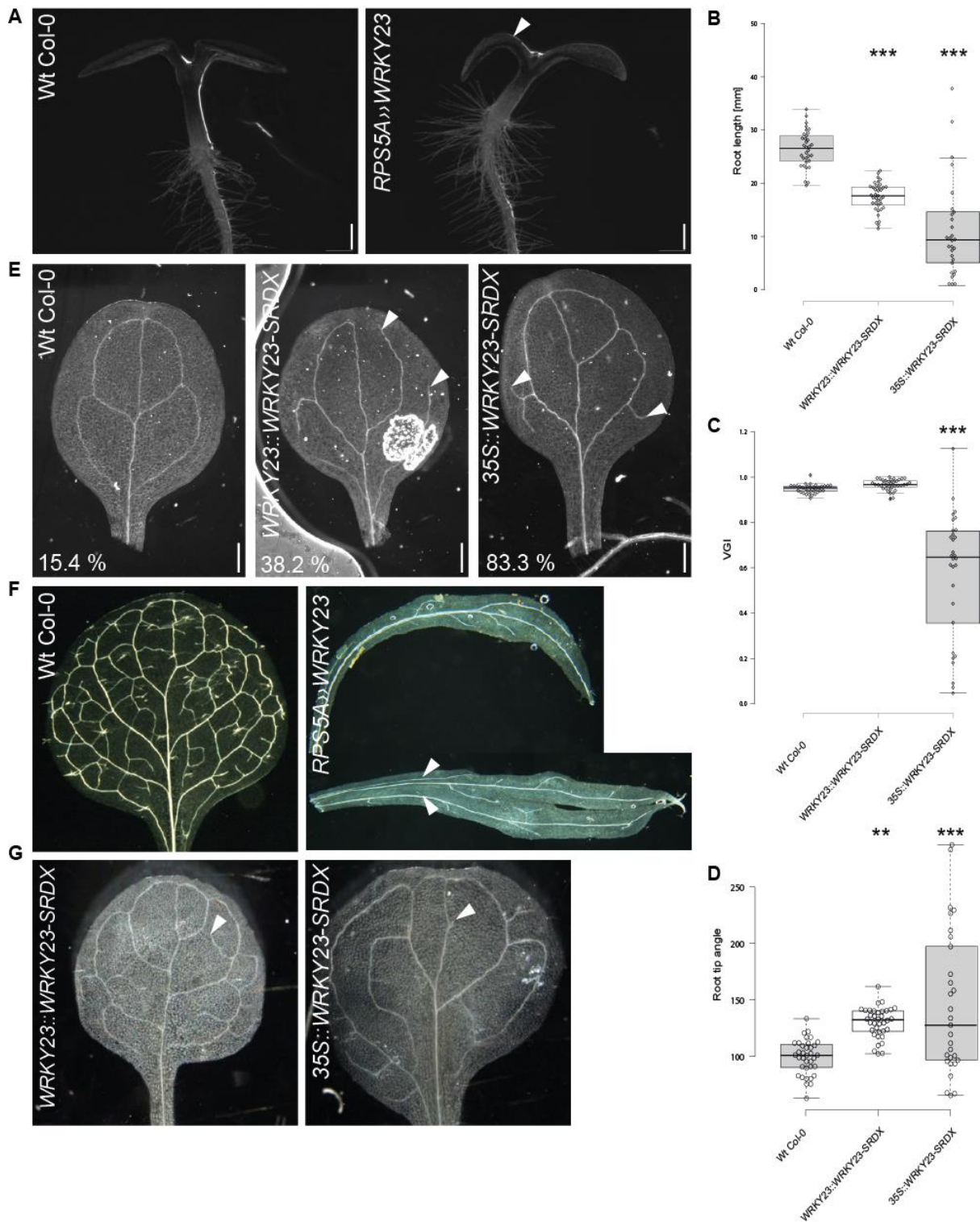


Figure 2-4 Misregulation of WRKY23 expression affects growth, responses to environmental stimuli and development in Arabidopsis.

A. Epinastic cotyledons of *RPS5A>>WRKY23* phenocopy auxin application or auxin transport inhibitors (arrowheads). B. Roots of 6 DAG old plants expressing *WRKY23-SRDX* was significantly shorter than Wt Col-0. Graph show root length, centre lines show the medians; box limits indicate the 25th and 75th percentiles as determined by R software; whiskers extend 1.5 times the interquartile range from the 25th and 75th percentiles; data points are plotted as open circles. A two-tailed Student's t test compared plants expressing *WRKY23-SRDX* and control Wt Col-0. (***) $P < 0.0001$. $n_{\min} = 30$ sample points. C. – D. Gravitropism related phenotypes observed in chimeric repressor silencing *WRKY23-SRDX* lines. Under native *WRKY23* promoter, *SRDX* lines show no or very weak phenotype, while strong *35S::WRKY23-SRDX* lines phenocopy agravitropism of auxin transport mutants. C. Graph show vertical growth index (VGI), ratio between the root tip ordinate and the root length (Grabov *et al.*, 2005). Box-whisker plot parameters as in B. A two-tailed Student's t test compared plants expressing *WRKY23-SRDX* and control Wt Col-0. (***) $P < 0.0001$. $n_{\min} = 30$ sample points. D. Short term gravistimulation by 6 hours of 90 degree induction shows decreased ability of the root to follow new direction of the gravity vector. *WRKY23-SRDX* lines driven by native promoter had weaker effects than lines with strong promoter. Graph show root tip angle. Box-whisker plot parameters as in B. A two-tailed Student's t test compared plants expressing *WRKY23-SRDX* and control Wt Col-0. (**) $P < 0.01$, (***) $P < 0.0001$. $n_{\min} = 30$ sample points. E. Cotyledon venation pattern is severely affected by *WRKY23* misregulation (arrowheads). Percentage represent distribution of primary leaves venation pattern defects. Bar sizes: A, E 1 mm. F. – G. Leaf morphology and venation is affected by *WRKY23* misregulation. F. Cleared leaves of *WRKY23* overexpression. Arrowheads point to the two main veins. G. *WRKY23-SRDX* plants show aberrant leaf morphology and/or venation patterns (Arrowheads). Clearing of primary leaf in F – G were performed by W.G..

2.5 DISCUSSION

Classical experiments led to the formulation of the so called canalization hypothesis, which proposes auxin feed-back on auxin transport as the central element of patterning events (Berleth & Sachs, 2001). In canalization, auxin transport through an initially homogeneous tissue follows a self-organizing pattern leading from initially broad fields of auxin-transporting cells to eventually a narrow transport channel, consequently establishing the position of future vascular veins (Bennett *et al.*, 2014). Sachs's hypothesis is further supported by successful modelling efforts based on the concerted polarization of cells via a feedback mechanism, by which auxin influences the directionality of its own flow (Rolland-Lagan & Prusinkiewicz, 2005; Smith *et al.*, 2006; Wabnik *et al.*, 2010; Wabnik *et al.*, 2011; Bennett *et al.*, 2014; Cieslak *et al.*, 2015). Most of these models rely on hypothetical propositions, such as auxin flux sensors or direct cell-to-cell communication giving testimony to our lack of understanding how canalization mechanistically works. However, canalization has been experimentally proven by visualizing re-arrangement of cellular polarity of PIN auxin

transporters by auxin treatment or local auxin maxima and it has been shown that this effect relies on the transcriptional activation of gene expression through auxin signalling (Sauer *et al.*, 2006).

Our transcriptional profiling experiments provide insight into transcriptional reprogramming during auxin-mediated PIN polarity re-arrangement and identify potential downstream molecular components of this process. Those include *e.g.* established regulators of PIN polarity like PID and PIP5K (Michniewicz *et al.*, 2007; Stenzel *et al.*, 2008; Tejos *et al.*, 2014), which proves that the experimental concept is sound. Among a number of novel components awaiting further characterization, we also found the transcriptional activator WRKY23.

WRKY23 is an auxin responsive gene. The local upregulation of *WRKY23* expression during auxin application is consistent with a possible involvement in the process of PIN repolarization. Auxin induces *WRKY23* transcription in a dose- and time dependent manner and follows the expression pattern of the *DR5rev* auxin signalling reporter. *WRKYs* are traditionally known as genes involved in defensive processes in plants. More and more, this limited functional spectrum is broadened by studies uncovering the involvement of these transcription factors in developmental and other physiological processes than plant defense (Grunewald *et al.*, 2012; Grunewald *et al.*, 2013; Bakshi & Oelmüller, 2014; Guan *et al.*, 2014). In the case of *WRKY23*, apart from a role in plant-nematode interaction with subsequent upregulation of *DR5rev*, participation in auxin transport through flavonol synthesis in the root as well as function in a *mp/bdl* dependent pathway in embryo development have been demonstrated (Grunewald *et al.*, 2008; Grunewald *et al.*, 2012; Grunewald *et al.*, 2013).

We show that *WRKY23* is a crucial factor required for auxin-mediated PIN polarity re-arrangement since gain-of-function and dominant-negative *WRKY23* lines were strongly affected in this process. The observed defects at the cellular level are also developmentally relevant, as we encountered phenotypes in lines with both upregulated and downregulated *WRKY23* function that are typical for altered auxin homeostasis and/or canalization such as changes in the leaf vasculature.

Our results strongly suggest that *WRKY23* is a critical player in auxin feed-back on PIN polar localization. As a transcription factor, a direct mechanistic involvement of *WRKY23* in the localization of transmembrane proteins such as PINs is highly unlikely. Instead, our work opens avenues for future studies revealing the *WRKY23*-dependent transcriptional network

and identifying cellular components executing the auxin effect on PIN polarity. Ultimately, this will provide insights into the canalization-dependent regulation of plant development.

2.6 ACKNOWLEDGEMENTS

This work was supported by the European Research Council (project ERC-2011-StG-20101109-PSDP). WG performed the work as a post-doctoral fellow of the Research Foundation Flanders.

2.7 AUTHOR CONTRIBUTION

T.P., W.G., M.Sau. and J.F. designed the research, T.P., W.G., R.T.,M.Sau. and M.Sch. performed the research, T.P., W.G., R.T.,M.Sau., G.M. and J.F. analyzed the data and T.P.,M.Sau., G.M. and J.F. wrote the paper.

2.8 REFERENCES

- Abas L, Benjamins R, Malenica N, Paciorek T, Wisniewska J, Moulinier-Anzola JC, Sieberer T, Friml J, Luschnig C. 2006. Intracellular trafficking and proteolysis of the Arabidopsis auxin-efflux facilitator PIN2 are involved in root gravitropism. *Nat Cell Biol* 8(3): 249-256.
- Adamowski M, Friml J. 2015. PIN-dependent auxin transport: action, regulation, and evolution. *Plant Cell* 27(1): 20-32.
- Agusti J, Lichtenberger R, Schwarz M, Nehlin L, Greb T. 2011. Characterization of transcriptome remodeling during cambium formation identifies MOL1 and RUL1 as opposing regulators of secondary growth. *PLoS Genet* 7.
- Aida M, Beis D, Heidstra R, Willemsen V, Blilou I, Galinha C, Nussaume L, Noh YS, Amasino R, Scheres B. 2004. The PLETHORA genes mediate patterning of the Arabidopsis root stem cell niche. *Cell* 119(1): 109-120.
- Bakshi M, Oelmuller R. 2014. WRKY transcription factors: Jack of many trades in plants. *Plant Signal Behav* 9(2): e27700.
- Balla J, Kalousek P, Reinohl V, Friml J, Prochazka S. 2011. Competitive canalization of PIN-dependent auxin flow from axillary buds controls pea bud outgrowth. *Plant J* 65(4): 571-577.
- Benkova E, Michniewicz M, Sauer M, Teichmann T, Seifertova D, Jurgens G, Friml J. 2003. Local, efflux-dependent auxin gradients as a common module for plant organ formation. *Cell* 115(5): 591-602.
- Bennett T, Hines G, Leyser O. 2014. Canalization: what the flux? *Trends Genet* 30(2): 41-48.
- Bennett T, Hines G, van Rongen M, Waldie T, Sawchuk MG, Scarpella E, Ljung K, Leyser O. 2016. Connective Auxin Transport in the Shoot Facilitates Communication between Shoot Apices. *PLoS Biol* 14(4): e1002446.
- Berleth T, Sachs T. 2001. Plant morphogenesis: long-distance coordination and local patterning. *Curr Opin Plant Biol* 4(1): 57-62.
- Boer DR, Freire-Rios A, van den Berg WA, Saaki T, Manfield IW, Kepinski S, Lopez-Vidrieo I, Franco-Zorrilla JM, de Vries SC, Solano R, et al. 2014. Structural basis for DNA binding specificity by the auxin-dependent ARF transcription factors. *Cell* 156(3): 577-589.
- Booker J, Chatfield S, Leyser O. 2003. Auxin acts in xylem-associated or medullary cells to mediate apical dominance. *Plant Cell* 15(2): 495-507.
- Chapman EJ, Estelle M. 2009. Mechanism of auxin-regulated gene expression in plants. *Annu Rev Genet* 43: 265-285.
- Cieslak M, Runions A, Prusinkiewicz P. 2015. Auxin-driven patterning with unidirectional fluxes. *J Exp Bot* 66(16): 5083-5102.
- Ciolkowski I, Wanke D, Birkenbihl RP, Somssich IE. 2008. Studies on DNA-binding selectivity of WRKY transcription factors lend structural clues into WRKY-domain function. *Plant Mol Biol* 68(1-2): 81-92.
- Eulgem T, Rushton PJ, Robatzek S, Somssich IE. 2000. The WRKY superfamily of plant transcription factors. *Trends Plant Sci* 5(5): 199-206.
- Eulgem T, Somssich IE. 2007. Networks of WRKY transcription factors in defense signaling. *Curr Opin Plant Biol* 10(4): 366-371.
- Friml J, Benkova E, Blilou I, Wisniewska J, Hamann T, Ljung K, Woody S, Sandberg G, Scheres B, Jurgens G, et al. 2002. AtPIN4 mediates sink-driven auxin gradients and root patterning in Arabidopsis. *Cell* 108(5): 661-673.
- Friml J, Vieten A, Sauer M, Weijers D, Schwarz H, Hamann T, Offringa R, Jurgens G. 2003. Efflux-dependent auxin gradients establish the apical-basal axis of Arabidopsis. *Nature* 426(6963): 147-153.
- Friml J, Yang X, Michniewicz M, Weijers D, Quint A, Tietz O, Benjamins R, Ouwerkerk PB, Ljung K, Sandberg G, et al. 2004. A PINOID-dependent binary switch in apical-basal PIN polar targeting directs auxin efflux. *Science* 306(5697): 862-865.

- Grabov A, Ashley MK, Rigas S, Hatzopoulos P, Dolan L, Vicente-Agullo F. 2005.** Morphometric analysis of root shape. *New Phytol* **165**(2): 641-651.
- Grunewald W, De Smet I, De Rybel B, Robert HS, van de Cotte B, Willemsen V, Gheysen G, Weijers D, Friml J, Beeckman T. 2013.** Tightly controlled WRKY23 expression mediates Arabidopsis embryo development. *EMBO Rep* **14**(12): 1136-1142.
- Grunewald W, De Smet I, Lewis DR, Lofke C, Jansen L, Goeminne G, Vanden Bossche R, Karimi M, De Rybel B, Vanholme B, et al. 2012.** Transcription factor WRKY23 assists auxin distribution patterns during Arabidopsis root development through local control on flavonol biosynthesis. *Proc Natl Acad Sci U S A* **109**(5): 1554-1559.
- Grunewald W, Karimi M, Wieczorek K, Van de Cappelle E, Wischnitzki E, Grundler F, Inze D, Beeckman T, Gheysen G. 2008.** A role for AtWRKY23 in feeding site establishment of plant-parasitic nematodes. *Plant Physiology* **148**(1): 358-368.
- Guan Y, Meng X, Khanna R, LaMontagne E, Liu Y, Zhang S. 2014.** Phosphorylation of a WRKY transcription factor by MAPKs is required for pollen development and function in Arabidopsis. *PLoS Genet* **10**(5): e1004384.
- Hiratsu K, Matsui K, Koyama T, Ohme-Takagi M. 2003.** Dominant repression of target genes by chimeric repressors that include the EAR motif, a repression domain, in Arabidopsis. *Plant J* **34**(5): 733-739.
- Hu W, Feng B, Ma H. 2011.** Ectopic expression of the Arabidopsis MINI ZINC FINGER1 and MIF3 genes induces shoot meristems on leaf margins. *Plant Mol Biol* **76**(1-2): 57-68.
- Huang F, Zago MK, Abas L, van Marion A, Galvan-Ampudia CS, Offringa R. 2010.** Phosphorylation of conserved PIN motifs directs Arabidopsis PIN1 polarity and auxin transport. *Plant Cell* **22**(4): 1129-1142.
- Ischebeck T, Werner S, Krishnamoorthy P, Lerche J, Meijon M, Stenzel I, Lofke C, Wiessner T, Im YJ, Perera IY, et al. 2013.** Phosphatidylinositol 4,5-bisphosphate influences PIN polarization by controlling clathrin-mediated membrane trafficking in Arabidopsis. *Plant Cell* **25**(12): 4894-4911.
- Kleine-Vehn J, Leitner J, Zwiewka M, Sauer M, Abas L, Luschnig C, Friml J. 2008.** Differential degradation of PIN2 auxin efflux carrier by retromer-dependent vacuolar targeting. *Proc Natl Acad Sci U S A* **105**(46): 17812-17817.
- Knox K, Grierson CS, Leyser O. 2003.** AXR3 and SHY2 interact to regulate root hair development. *Development* **130**(23): 5769-5777.
- Leal Valentim F, Mourik S, Pose D, Kim MC, Schmid M, van Ham RC, Busscher M, Sanchez-Perez GF, Molenaar J, Angenent GC, et al. 2015.** A quantitative and dynamic model of the Arabidopsis flowering time gene regulatory network. *PLoS One* **10**(2): e0116973.
- Lemon WJ, Liyanarachchi S, You M. 2003.** A high performance test of differential gene expression for oligonucleotide arrays. *Genome Biol* **4**(10): R67.
- Luschnig C, Gaxiola RA, Grisafi P, Fink GR. 1998.** EIR1, a root-specific protein involved in auxin transport, is required for gravitropism in Arabidopsis thaliana. *Genes Dev* **12**(14): 2175-2187.
- Mei Y, Jia WJ, Chu YJ, Xue HW. 2012.** Arabidopsis phosphatidylinositol monophosphate 5-kinase 2 is involved in root gravitropism through regulation of polar auxin transport by affecting the cycling of PIN proteins. *Cell Res* **22**(3): 581-597.
- Michniewicz M, Zago MK, Abas L, Weijers D, Schweighofer A, Meskiene I, Heisler MG, Ohno C, Zhang J, Huang F, et al. 2007.** Antagonistic regulation of PIN phosphorylation by PP2A and PINOID directs auxin flux. *Cell* **130**(6): 1044-1056.
- Muller A, Guan C, Galweiler L, Tanzler P, Huijser P, Marchant A, Parry G, Bennett M, Wisman E, Palme K. 1998.** AtPIN2 defines a locus of Arabidopsis for root gravitropism control. *EMBO J* **17**(23): 6903-6911.
- Noh B, Murphy AS, Spalding EP. 2001.** Multidrug resistance-like genes of Arabidopsis required for auxin transport and auxin-mediated development. *Plant Cell* **13**(11): 2441-2454.

- Okushima Y, Overvoorde PJ, Arima K, Alonso JM, Chan A, Chang C, Ecker JR, Hughes B, Lui A, Nguyen D, et al. 2005.** Functional genomic analysis of the AUXIN RESPONSE FACTOR gene family members in *Arabidopsis thaliana*: unique and overlapping functions of ARF7 and ARF19. *Plant Cell* **17**(2): 444-463.
- Paciorek T, Zazimalova E, Ruthardt N, Petrasek J, Stierhof YD, Kleine-Vehn J, Morris DA, Emans N, Jurgens G, Geldner N, et al. 2005.** Auxin inhibits endocytosis and promotes its own efflux from cells. *Nature* **435**(7046): 1251-1256.
- Petrasek J, Mravec J, Bouchard R, Blakeslee JJ, Abas M, Seifertova D, Wisniewska J, Tadele Z, Kubes M, Covanova M, et al. 2006.** PIN proteins perform a rate-limiting function in cellular auxin efflux. *Science* **312**(5775): 914-918.
- Robert HS, Grones P, Stepanova AN, Robles LM, Lokerse AS, Alonso JM, Weijers D, Friml J. 2013.** Local auxin sources orient the apical-basal axis in *Arabidopsis* embryos. *Curr Biol* **23**(24): 2506-2512.
- Robert S, Kleine-Vehn J, Barbez E, Sauer M, Paciorek T, Baster P, Vanneste S, Zhang J, Simon S, Covanova M, et al. 2010.** ABP1 mediates auxin inhibition of clathrin-dependent endocytosis in *Arabidopsis*. *Cell* **143**(1): 111-121.
- Rolland-Lagan AG, Prusinkiewicz P. 2005.** Reviewing models of auxin canalization in the context of leaf vein pattern formation in *Arabidopsis*. *Plant J* **44**(5): 854-865.
- Sachs T. 1975.** The induction of transport channels by auxin. *Planta* **127**(3): 201-206.
- Sachs T. 1986.** Cellular interactions in tissue and organ development. *Symp Soc Exp Biol* **40**: 181-210.
- Salehin M, Bagchi R, Estelle M. 2015.** SCFTIR1/AFB-based auxin perception: mechanism and role in plant growth and development. *Plant Cell* **27**(1): 9-19.
- Sauer M, Balla J, Luschnig C, Wisniewska J, Reinohl V, Friml J, Benkova E. 2006.** Canalization of auxin flow by Aux/IAA-ARF-dependent feedback regulation of PIN polarity. *Genes Dev* **20**(20): 2902-2911.
- Sauer M, Friml J. 2010.** Immunolocalization of proteins in plants. *Methods Mol Biol* **655**: 253-263.
- Scarpella E, Marcos D, Friml J, Berleth T. 2006.** Control of leaf vascular patterning by polar auxin transport. *Genes Dev* **20**(8): 1015-1027.
- Schluttenhofer C, Yuan L. 2015.** Regulation of specialized metabolism by WRKY transcription factors. *Plant Physiology* **167**(2): 295-306.
- Smith RS, Guyomarc'h S, Mandel T, Reinhardt D, Kuhlemeier C, Prusinkiewicz P. 2006.** A plausible model of phyllotaxis. *Proc Natl Acad Sci U S A* **103**(5): 1301-1306.
- Stenzel I, Ischebeck T, Konig S, Holubowska A, Sporysz M, Hause B, Heilmann I. 2008.** The type B phosphatidylinositol-4-phosphate 5-kinase 3 is essential for root hair formation in *Arabidopsis thaliana*. *Plant Cell* **20**(1): 124-141.
- Tejos R, Sauer M, Vanneste S, Palacios-Gomez M, Li H, Heilmann M, van Wijk R, Vermeer JE, Heilmann I, Munnik T, et al. 2014.** Bipolar Plasma Membrane Distribution of Phosphoinositides and Their Requirement for Auxin-Mediated Cell Polarity and Patterning in *Arabidopsis*. *Plant Cell* **26**(5): 2114-2128.
- Ugalde JM, Rodriguez-Furlan C, Rycke RD, Norambuena L, Friml J, Leon G, Tejos R. 2016.** Phosphatidylinositol 4-phosphate 5-kinases 1 and 2 are involved in the regulation of vacuole morphology during *Arabidopsis thaliana* pollen development. *Plant Sci* **250**: 10-19.
- Ulker B, Somssich IE. 2004.** WRKY transcription factors: from DNA binding towards biological function. *Curr Opin Plant Biol* **7**(5): 491-498.
- Ulmasov T, Hagen G, Guilfoyle TJ. 1997.** ARF1, a transcription factor that binds to auxin response elements. *Science* **276**(5320): 1865-1868.
- Wabnik K, Kleine-Vehn J, Balla J, Sauer M, Naramoto S, Reinohl V, Merks RM, Govaerts W, Friml J. 2010.** Emergence of tissue polarization from synergy of intracellular and extracellular auxin signaling. *Mol Syst Biol* **6**: 447.
- Wabnik K, Kleine-Vehn J, Govaerts W, Friml J. 2011.** Prototype cell-to-cell auxin transport mechanism by intracellular auxin compartmentalization. *Trends Plant Sci* **16**(9): 468-475.

- Wabnik K, Robert HS, Smith RS, Friml J. 2013.** Modeling framework for the establishment of the apical-basal embryonic axis in plants. *Curr Biol* **23**(24): 2513-2518.
- Wilmoth JC, Wang S, Tiwari SB, Joshi AD, Hagen G, Guilfoyle TJ, Alonso JM, Ecker JR, Reed JW. 2005.** NPH4/ARF7 and ARF19 promote leaf expansion and auxin-induced lateral root formation. *Plant J* **43**(1): 118-130.
- Wisniewska J, Xu J, Seifertova D, Brewer PB, Ruzicka K, Blilou I, Rouquie D, Benkova E, Scheres B, Friml J. 2006.** Polar PIN localization directs auxin flow in plants. *Science* **312**(5775): 883.
- Yilmaz A, Mejia-Guerra MK, Kurz K, Liang X, Welch L, Grotewold E. 2011.** AGRIS: the Arabidopsis Gene Regulatory Information Server, an update. *Nucleic Acids Res* **39**(Database issue): D1118-1122.
- Zhang J, Nodzynski T, Pencik A, Rolcik J, Friml J. 2010.** PIN phosphorylation is sufficient to mediate PIN polarity and direct auxin transport. *Proc Natl Acad Sci U S A* **107**(2): 918-922.
- Zhao Y, Christensen SK, Fankhauser C, Cashman JR, Cohen JD, Weigel D, Chory J. 2001.** A role for flavin monooxygenase-like enzymes in auxin biosynthesis. *Science* **291**(5502): 306-309.

2.9 SUPPORTING INFORMATION

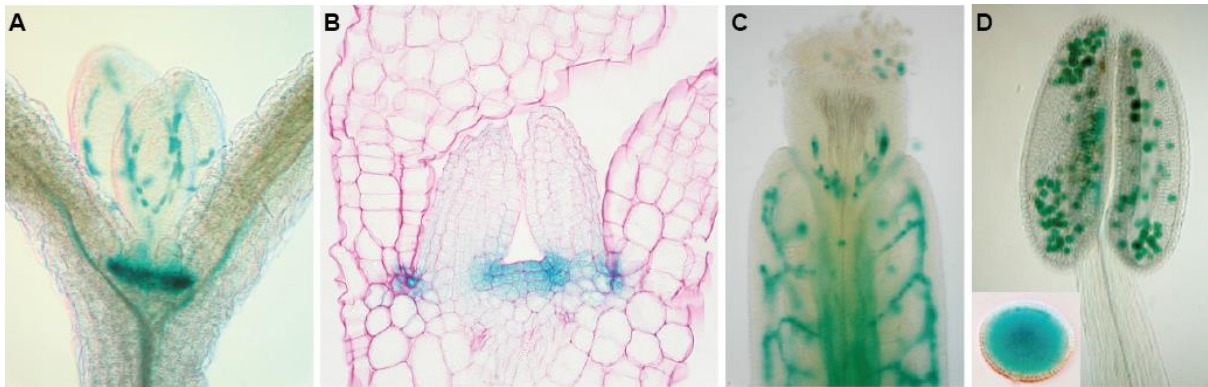


Figure S 2-1 Expression pattern of WRKY23.

A. Expression of *WRKY23* in shoot apical meristem (SAM) and in the vasculature of leaves. B. Section of a GUS stained SAM shows specific *WRKY23* expression in the L1, L2 and L3 layers. C. *WRKY23* expression in the vasculature of the pistil. D. *WRKY23::GUS* anther showing *WRKY23* promoter activity in pollen (inset). GUS staining in Figure S 2-1 were performed by W.G..

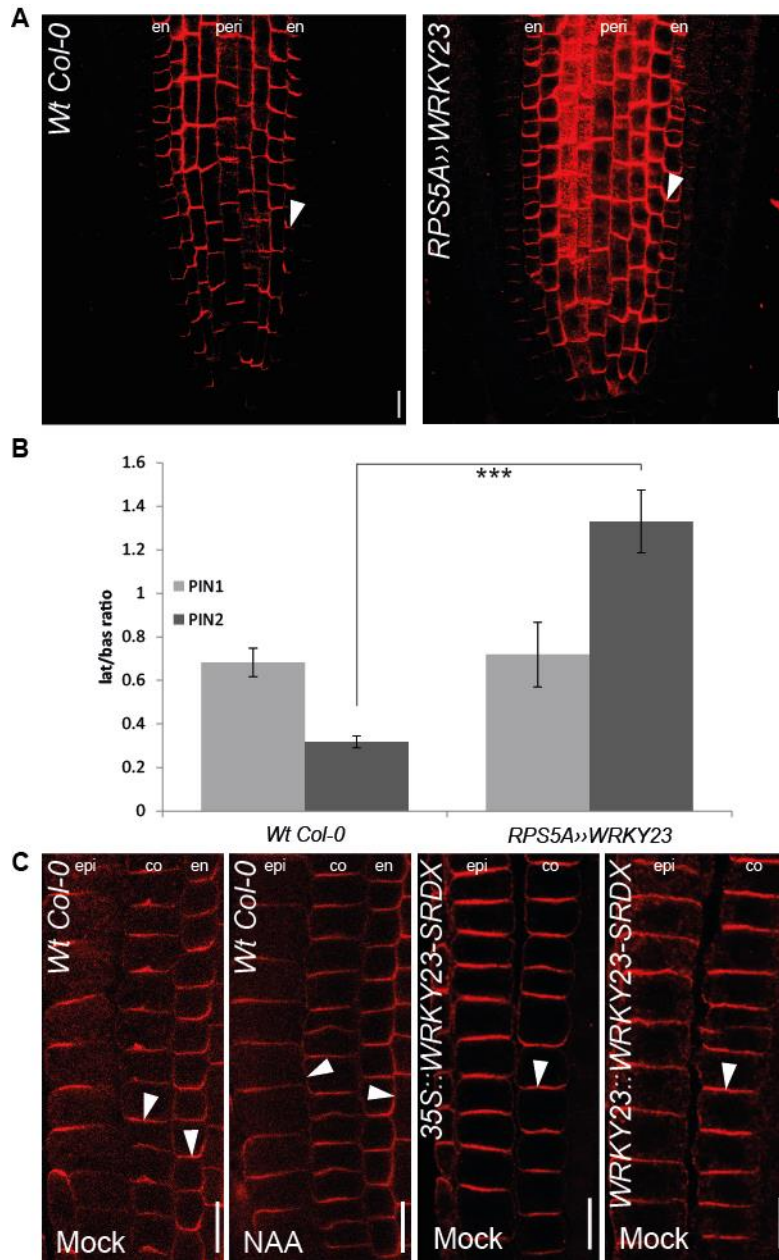


Figure S 2-2 *WRKY23* influences auxin-dependent *PIN2* re-arrangement.

A – B. Immunolocalization of PIN1 and PIN2 proteins in *RPS5A>>WRKY23* overexpression lines changes polarity of PIN2 but not PIN1. Arrowheads highlight PIN polarity. Graph shows mean ratio of lateral to basal signal intensity of PIN1 in endodermis and PIN2 in cortex cells in *RPS5A>>WRKY23*, error bars indicates standard error. A two-tailed Student’s t test compared marked sets of data. (***) $P < 0.0001$. $n > 35$ cells corresponding to roots imaged under comparable conditions. C. Immunolocalization of PIN2 in dominant-negative *WRKY23-SRDX* plants driven by native and constitutive promoter. Without auxin, plants have increased basal localization of PIN2 on their membranes in cortex.

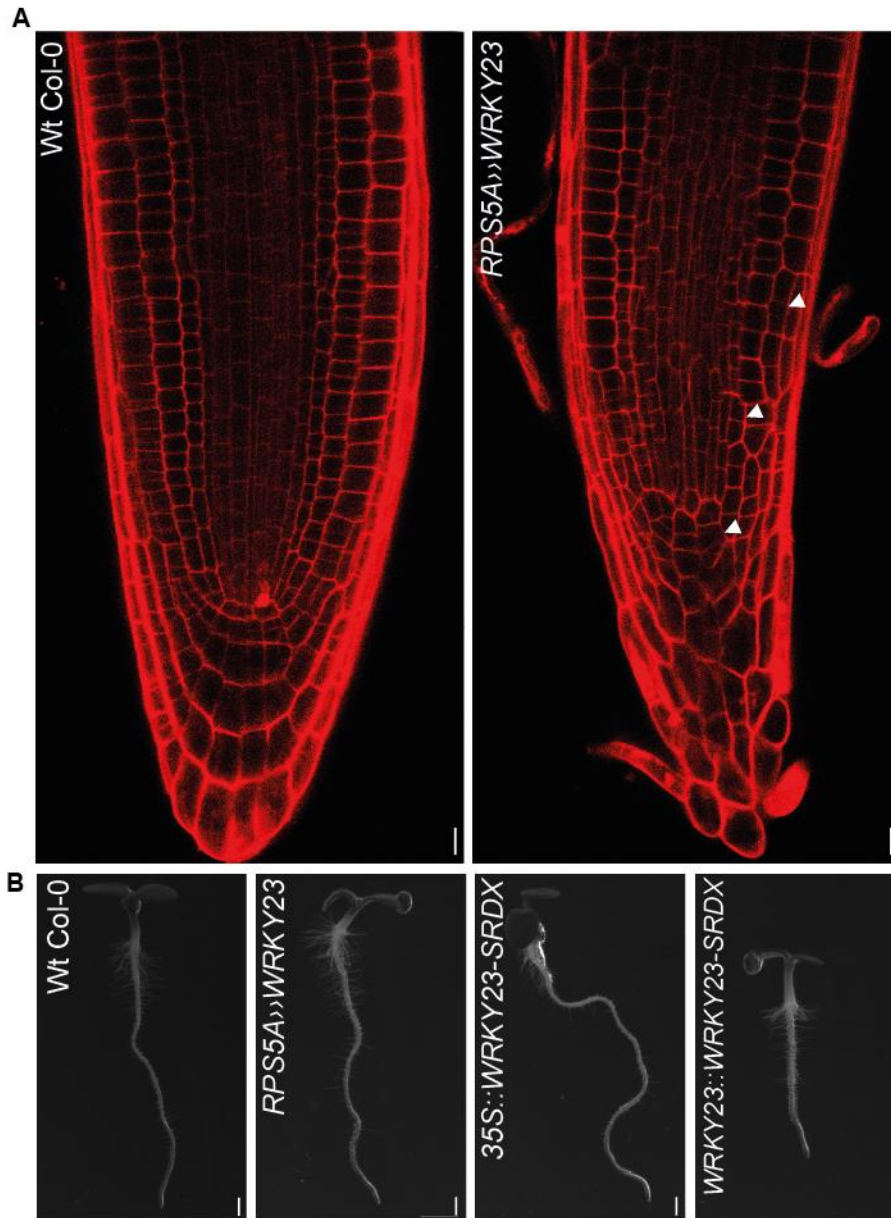


Figure S 2-3 Morphological phenotypes of *WRKY23* misregulation.

A. Collapse of root meristem architecture of *RPS5A::WRKY23* (arrowheads) (Grunewald et al., 2012). B. Overall phenotype of *WRKY23* overexpressor and dominant-negative line seedlings. Bar sizes: A 10 μ m, B 1 mm.

The list of qRT PCR primers used in this study:

PID_FOR 5'-TGCCGACTCTTTACGCTGAG-3'
PID_REV 5'-CTTCGGCGGCATAAAATCTGG-3'

Grunewald et al., 2013

WRKY23_FOR 5'-AGTCTCGGTAATGGTTGCTTTGG-3'
WRKY23_REV 5'-TGTTGCTGCTGTTGGTGATGG-3'
TUB-2_FOR 5'-ACTCGTTGGGAGGAGGAACT-3'
TUB-2_REV 5'-ACACCAGACATAGTAGCAGAAATCAAG-3'

Shkolnik-Inbar and Bar-Zvi, 2010

IAA14_FOR 5'-CCTTCTAAGCCTCCTGCTAAAGC-3'
IAA14_REV 5'-CCGCTCTTCTGATTAGCCATAAC-3'

Tejos et al., 2014

PIP5K1_FOR 5'-GGAACATTGTGAATCGAGGACTG-3'
PIP5K1_REV 5'-CCGTCTCGTCTCTCTACTTCTT-3'
PIP5K2_FOR 5'-ATGATGCGTGAACCGCTTG-3'
PIP5K2_REV 5'-TTCCATGCTGCAGGTTGAGCA-3'

Table S 2-1 List of primers used in this study.

3 WRKY23 downstream target LHT1 transporter mediates auxin-dependent PIN polarization

Tomáš Prát, Wim Grunewald, Gergely Molnár, and Jiří Friml

3.1 SUMMARY

- Different lifestyle of plants lead to unique cell biology and physiology strategies in comparison with animals, *e.g.* in plant cell polarity regulations. This process is tightly connected with self-organizing pattern of auxin transport proposed by canalization hypothesis.
- Here we used the auxin effect on PIN polarity in *Arabidopsis* root meristems as a proxy for canalization and performed microarray experiments to find regulators of the auxin effect on PIN polarity. Recently, we identified WRKY23 TF transcriptionally regulated by auxin downstream of SCF^{TIR1}-Aux/IAA-ARF auxin signalling in an IAA17 (AXR3)- and ARF7/ARF19-dependent manner in the process of auxin-dependent PIN repolarization.
- In order to identify direct targets of WRKY23, we performed expression profiling experiments using an inducible *WRKY23* overexpression and auxin-treated dominant-negative *WRKY23* line. The obtained gene list was further filtered with publicly available expression datasets. We identified 14 possible regulators of auxin-dependent PIN repolarization.
- Based on polarity-related phenotypes we selected LYSINE-HISTIDINE TRANSPORTER 1 (LHT1; At5g40780), a small amino acid permease.
- We characterised the role of LHT1 in auxin feedback on PIN repolarization, identified its transcriptional regulation, we proposed a potential mechanism of its action. Our results highlighted WRKY23 transcriptional network targeting PIN with a consequence of regulation of plant development via PIN-dependent auxin transport processes.

3.2 INTRODUCTION

Plants evolved a unique developmental program in comparison with animals. Absence of cell movement in a scaffold of a rigid cell wall results in and leads to an utterly different concept of cell polarization and on site determined cell fate. How plants achieve the adaptability and self-organizing properties of their development is still not sufficiently understood but in many

of these aspects, the plant hormone auxin and its directional transport between cells plays a central role.

A classic example of patterning process in plants is canalization. Canalization is a self-organizing pattern of auxin transport leading from an initially broad domain of auxin-transporting cells to narrow channel, consequently establishing *e.g.* the position of future vascular veins (Bennett *et al.*, 2014). This hypothesis came as an outcome from pioneer experiments of Tsvi Sachs who proposed auxin feedback on auxin transport as the main mechanism during canalization (Sachs, 1975; Sachs, 1986). Sachs's hypotheses were further supported by successful modelling efforts assuming a coordination between polarizing cells via a feedback mechanism by which auxin influences the directionality of its own flow (Rolland-Lagan & Prusinkiewicz, 2005; Smith *et al.*, 2006; Heisler *et al.*, 2010; Wabnik *et al.*, 2010; Wabnik *et al.*, 2011; Bennett *et al.*, 2014; Cieslak *et al.*, 2015). Most of these models rely on hypothetical assumptions such as flux sensors or direct cell-to-cell communication; however, there is no experimental evidence for their existence. Canalization has been experimentally shown by visualizing the re-arrangement of cellular polarity of PIN auxin transporters by auxin treatment or local auxin maxima. It also has been shown that this repolarization relies on activation of gene expression through auxin signalling (Sauer *et al.*, 2006).

We aim to identify the molecular players behind the auxin-dependent PIN repolarization. PIN1 is localized on the basal sides of endodermal and pericycle cells and cells of the vascular tissue in the root (Friml *et al.*, 2002a) whereas PIN2 has basal polarity in the cells of young cortex but apical polarity in epidermis (Kleine-Vehn *et al.*, 2008). After auxin treatment, the localization of PIN1 changes from basal to inner-lateral in endodermis- and pericycle cells, while PIN2 undergoes a basal – outer lateral localization shift in young cortex cells (Sauer *et al.*, 2006). The molecular mechanism of this effect is unclear but it depends on the transcriptional SCF^{TIR1}-Aux/IAA-ARF signalling pathway (Sauer *et al.*, 2006; Salehin *et al.*, 2015). Expression profiling on mutants in the SCF^{TIR1}-Aux/IAA-ARF pathway in *Arabidopsis* roots identified *WRKY23*, a transcription factor as an auxin-dependent regulator of PIN polarity (Prat *et al.*, unpublished data). *WRKY23* belongs to plant-specific family of transcription factors in *Arabidopsis*, being typically but not exclusively associated with plant defense processes and plant-pathogen interactions (Eulgem & Somssich, 2007). We previously described a role of *WRKY23* in plant-nematode interactions, in regulating auxin

transport by flavonol biosynthesis affecting root development, in *Arabidopsis* embryo development by attenuation of both auxin-dependent and -independent signalling pathways towards stem cell specification and recently, in the auxin feedback regulation of PIN polarity (Grunewald *et al.*, 2008; Grunewald *et al.*, 2012; Grunewald *et al.*, 2013; Prat *et al.*, unpublished data). We demonstrated that transcriptional auxin signalling control cellular abundance of WRKY23 and thus mediate so far unknown regulators which change the subcellular polarity sorting or trafficking pathways ultimately re-arranging the polar PIN distribution (Prat *et al.*, unpublished data).

In order to identify direct targets of WRKY23, we performed expression profiling experiments using an inducible gain-of-function line (*35S::WRKY23-GR*; (Grunewald *et al.*, 2012)). To sort out WRKY23-independent auxin-induced genes, we used an auxin-treated dominant-negative WRKY23 line (*35S::WRKY23-SRDX*; (Grunewald *et al.*, 2012)) that is defunct in PIN re-arrangement. The obtained gene list was further filtered with publicly available expression datasets. Among several genes mostly related to the groups of cell wall and defense process regulators, we identified *LYSINE-HISTIDINE TRANSPORTER 1 (LHT1; At5g40780)*, a small amino acid permease gene from the amino acid/auxin permease family (AAP). Here, we present its detailed characterization in auxin feedback on PIN repolarization and we propose a potential mechanism of its action.

3.3 MATERIALS AND METHODS

3.3.1 Plant material and growth conditions

All *Arabidopsis thaliana* lines were in Columbia-0 background. T-DNA mutants were acquired from the Nottingham Arabidopsis Stock Centre (NASC; <http://www.arabidopsis.info>). T-DNA mutants used in this study are SALK_062169 (*exp20-1*), SALK_124968 (*exl3-1*), SALK_048655 (*pmei1-1*), SALK_092291 (*chr1-1*), SAIL_761_D09 (*chr2-1*) and SALK_034566 (*lht1-1*). Primers used in genotyping are listed in Supporting information (Table S3-1). The *arf7 arf19* double mutant (Okushima *et al.*, 2005), *HS::axr3-1* (Knox *et al.*, 2003), *35S::WRKY23-GR* and *35S::WRKY23-SRDX* (Grunewald *et al.*, 2008; Grunewald *et al.*, 2012), *Col-0::EARLI1 RNAi [1-1]* (Cecchini *et al.*, 2015) and *LHT1::ΔLHT1-GUS* (Hirner *et al.*, 2006) have been described previously. Seeds were sterilized overnight by chlorine gas, sown on solid *Arabidopsis* medium (AM+: half-strength MS basal salts, 1% Sucrose, and 0.8% phyto-agar, pH 5.7), and stratified

at 4°C for at least 2 days prior to transfer to a growth room with a 16-h-light/8-h-dark illumination regime at 21°C. Seedlings were grown vertically for 4 or 6 days, depending on the assay.

3.3.2 Construction of transgenic lines

DNA constructs was created with the Gateway cloning technology (Karimi *et al.*, 2007) (Invitrogen). For the *RPS5A::LHT1* construct, a 3260-bp-long LHT1-specific fragment was amplified from a genomic DNA template with iProof High-Fidelity DNA Polymerase (BioRad) with primer LHT1_attB1_Fw (5'-GGGGACAAGTTTGTACAAAAAAGCAGGCTTCATGGTAGCTCAAGCTCCTCA-3') and primer LHT1_attB2_Rv (5'-GGGGACCACTTTGTACAAGAAAGCTGGGTTTTATGAGTAAACTTGTATC-3') and recombined by BP reaction with pDONR221 to yield pEN-L1-LHT1-R2. Latter vector was then recombined by LR MultiSite reaction with pEN_L4_RPS5A_R1, pEN-L1-LHT1-R2 and the binary gateway vector pB7m24GW,3. The obtained vectors were transformed to *Agrobacterium tumefaciens* strain C58C1 (pMP90), which was used in a floral dip transformation of *Arabidopsis thaliana* (L.) Heyhn Columbia-0 (Col-0) (Clough & Bent, 1998). At least two independent transgenic lines were examined. Overexpression of these lines was confirmed by qRT-PCR, primers are included in Supporting Table S3-1.

3.3.3 Phenotypic analysis

All measurements were done with ImageJ (<http://rsb.info.nih.gov/ij>). For root length analysis, seedlings were scanned and root lengths were measured. To quantify direction of the root growth, we used vertical growth index (VGI), ratio between the root tip ordinate and the root length (Grabov *et al.*, 2005). Short term root gravistimulation was done by 6 hours of 90 degree induction. The seedlings were scanned and root angles were measured. For hypocotyl length and gravitropism were seeds stratified for 2 days at 4°C, exposed to light for 5-6 h at 21°C, and cultivated in the dark at 21°C. Four days old etiolated seedlings were scanned for length measurements or plates with seedlings were rotated 90° and measured after 24 h.

3.3.4 Pharmacological treatments

Arabidopsis treatments with auxin or chemicals were done in liquid AM+ medium at 21°C in a growth room. For auxin treatment, plants were incubated with 10 µM α-naphthaleneacetic acid (NAA; Sigma Aldrich) for 4h or 6h; while dexamethasone (DEX; Sigma Aldrich) was applied in 10 µM concentration for 6h or 24h. Mock treatments were performed with equivalent amounts of DMSO.

3.3.5 Microarray analysis

Roots of 5-day-old *35S::WRKY23-GR* were treated with 10 µM DEX for 6 hours or DMSO, respectively. Wt Col-0 and *35S::WRKY23-SRDX* plants were treated with 10 µM NAA or DMSO for 6 hours. The roots were subsequently collected for RNA isolation. All points were sampled in three independent experiments. Total RNA (200 µg per array) was used to hybridize ATH1 Affymetrix *Arabidopsis* arrays in accordance with standard procedures at VIB Nucleomics Core. Data files containing the probe level intensities (.cel files) were used for background correction and normalization using the log₂ scale RMA procedure (Irizarry *et al.*, 2003) with R (<http://www.r-project.org>) and the Bioconductor package affyImGUI (<http://bioinf.wehi.edu.au/affyImGUI/>). Genes with the same or contrasting *WRKY23* expression profiles were selected by Pavlidis template matching in TMeV 4.0 (TIGR) (Saeed *et al.*, 2003). Finally, genes with a significant P value (< 0.001), denoting expression above background, with minimum 2-fold change compared to the respective control, were retained for further analysis.

3.3.6 RNA extraction, cDNA synthesis, and quantitative RT-PCR and analysis

RNA extraction, cDNA Synthesis, and quantitative RT-PCR was performed as described by Tejos *et al.* (2014). Targets were quantified with specific primer pairs designed with Primer-BLAST (<http://www.ncbi.nlm.nih.gov/tools/primer-blast/>). Expression levels were normalized to *GAMMA-TUBULIN 2 (TUB2; At5g05620)* which was constitutively expressed across samples. All PCRs were run in three technical repeats and the data were processed with qRT PCR analysis software (Frederik Coppens; Applied Bioinformatics & Biostatistics group; PSB VIB, Belgium). Primers used in the study are listed in Supporting information (Table S3-1).

3.3.7 Whole-mount *in situ* Immunolocalization, microscopy and quantitative analysis of PIN relocalization

PIN immunolocalizations in primary root were performed as described by Sauer and Friml (2010). The antibodies were used in the following dilutions: anti-PIN1, 1:1000 (Paciorek *et al.*, 2005) and anti-PIN2, 1:1000 (Abas *et al.*, 2006). In all cases, the secondary goat anti-rabbit antibody coupled to Cy3 (Sigma-Aldrich) was diluted 1:600. Confocal microscopy was performed using a Zeiss LSM 700 confocal microscope. Quantitative analysis of PIN relocalization was performed as described by Sauer *et al.* (2006).

3.3.8 Histological analyses and microscopy

To detect β -Glucuronidase (GUS) activity, seedlings were incubated in reaction buffer containing 0.1 M sodium phosphate buffer (pH 7), 1 mM ferricyanide, 1 mM ferrocyanide, 0.1% Triton X-100 and 1 mg/ml X-Gluc for 2 h in dark at 37 °C. Afterwards, chlorophyll was removed by destaining in 70% ethanol and seedlings were cleared.

Clearing of tissues (seedlings, cotyledons) was performed in a solution containing 4% HCl and 20% methanol for 15 min at 65 °C, followed by 15 min incubation in 7% NaOH and 70% ethanol at room temperature. Next, seedlings were rehydrated by successive incubations in 70, 50, 25 and 10% ethanol for 5 min, followed by incubation in a solution containing 25% glycerol and 5% ethanol. Finally, seedlings were mounted in 50% glycerol and monitored by differential interference contrast microscopy DIC (Olympus BX53) or stereomicroscope (Olympus SZX16).

3.3.9 Basipetal auxin transport assay

Seeds were sown on AM+ plates, stratified for 2 days at 4°C, exposed to light for 5-6 h at 21°C, and grown in the dark at 21°C for 5 days. Etiolated hypocotyls were decapitated to avoid the effect of cotyledon auxin biosynthesis. A droplet of AM+-agar (1.25%) with 1 μ M ³H-IAA (American Radiolabeled Chemicals, Inc.) and DMSO, or 1 μ M ³H-IAA and 50 μ M IAA was applied to the apical part of the hypocotyls, respectively. After 6 hours, hypocotyls were collected, homogenized in liquid nitrogen and incubated overnight in Opti-Fluor scintillation cocktail (Perkin Elmer). Content of transported ³H-IAA was then measured in a scintillation counter (Hidex 300SL) for 120 s with three technical repetitions.

3.4 RESULTS AND DISCUSSION

3.4.1 Identification of WRKY23 downstream targets by microarray analysis

To identify downstream targets of WRKY23, *i.e.* genes potentially regulating PIN repolarization, we designed a microarray experiment using lines where WRKY23 is either inducibly nuclear targeted (*35S::WRKY23-GR*) or where WRKY23 is turned into a transcriptional repressor (*35S::WRKY23-SRDX*) (Grunewald *et al.*, 2012) (**Fig.3-1 A**). First, we obtained a gene set by comparing *35S::WRKY23-GR* seedlings with and without Dexamethasone (Dex) treatment. A total of 111 genes, which were up-regulated in dexamethasone treated seedlings are targets of WRKY23. Next, we identified WRKY23-dependent genes in their auxin response. We found 950 genes which lost responsiveness to auxin treatment in *35S::WRKY23-SRDX* compared to control. The overlap between two gene sets identified a list of 61 genes. The list was confronted with previously published microarray data on auxin-treated seedlings of *solitary root1 (slr-1)* mutant (Vanneste *et al.*, 2005) because WRKY23 acts downstream of the SLR/IAA14 transcriptional repressor (**Fig.3-1 B**) (Grunewald *et al.*, 2008). Genes, which were up-regulated in Wt Col-0 but not in *slr-1* seedlings after auxin treatment, were used to filter the set of genes from our microarray experiment. Using this approach, we identified 14 genes as putative polarity determinants (**Fig.3-1 C**). Obtained data from expression profiling were further verified by qRT-PCR measurement of transcript levels (**Fig. S3-1 A – B**).

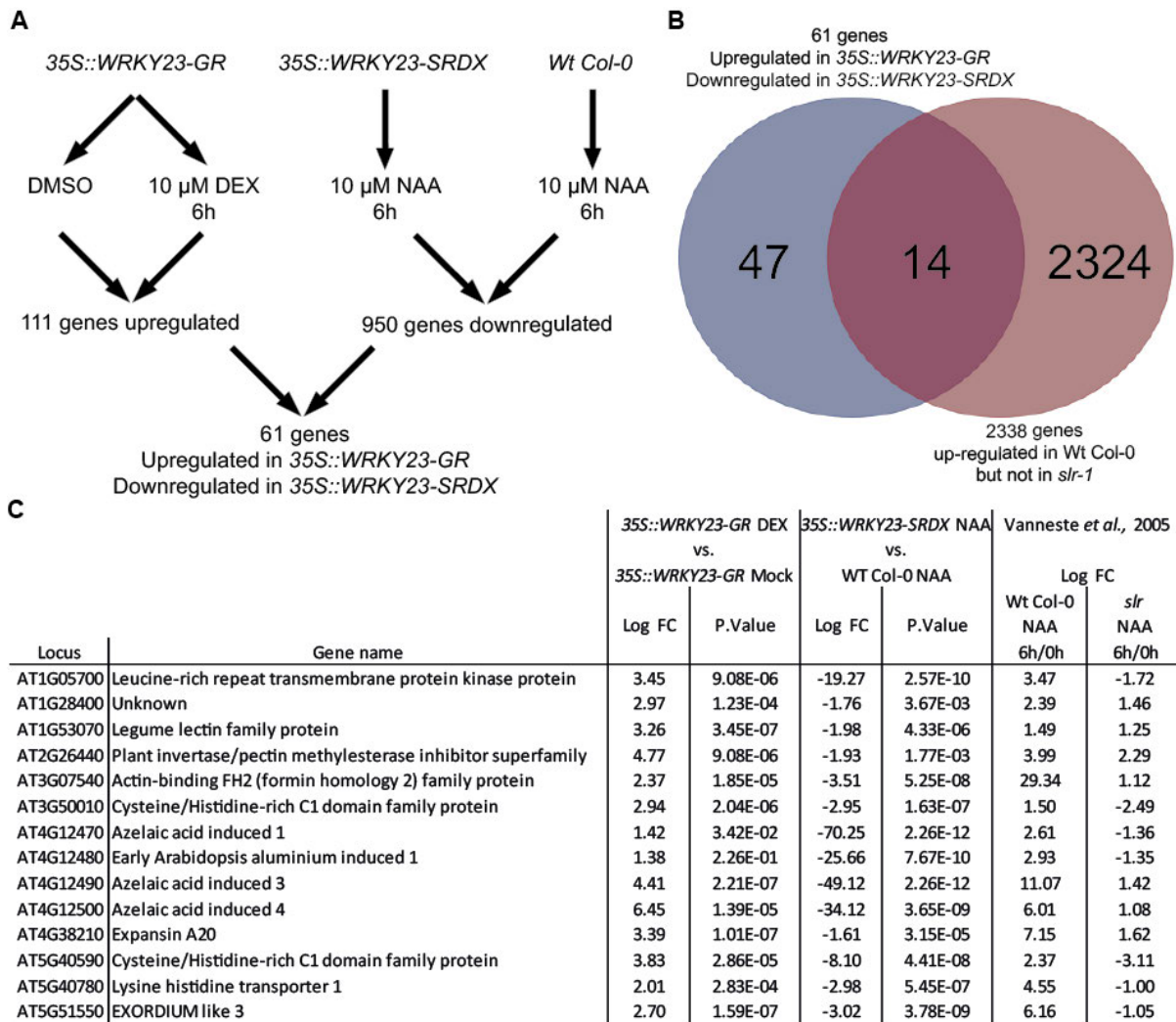


Figure 3-1 Expression profiling experiments to identify WRKY23-downstream regulators of PIN repolarization.

A. Scheme of the microarray experiments and filtering strategy. Selected genes in each filtering step show a minimum 2-fold change compared to the respective control with a p value lower than 0,001. B. Candidate list overlap with auxin-inducible genes in an SLR1-dependent manner (Vanneste *et al.*, 2005). C. Final list of putative polarity determinants identified in the microarray experiments. Experiments in Figure 3-1 were designed and statistical analysis was performed by W.G..

3.4.2 Defense and stress related genes

The highest fold changes of the expression were observed in the group of bifunctional inhibitor/lipid-transfer protein/seed storage 2S albumin superfamily proteins commonly termed as *AZI1-like* genes or *EARLI1-like* genes (*AZI1*, *EARLI1*, *AZI3*, *AZI4*; *At4g12470* to *At4g12500*) (**Fig.3-1 C and Fig. S3-1 A – B**). *EARLI1-like* genes belong to a superfamily of proteins containing 8 cysteine residues, so called eight-cysteine-motif (8CM), and they are further sub-grouped into the HyPRP family of hybrid proline-rich proteins by the presence of a proline-rich domain (PRD) before the 8CM motif in their amino acid sequence (Jose-Estanyol

et al., 2004). The *EARLI1-like* gene group forms a cluster on the chromosome 4 of *Arabidopsis*. Paralogous genes within this cluster share high sequence similarity and therefore they have probably similar functions (Jose-Estanyol *et al.*, 2004). The AZI1 protein (AZELAIC ACID INDUCED 1; At4g12470) is a component of both systemic acquired resistance (SAR) and induced systemic resistance. These processes act through mobile priming signal by uptake of lipid-derived azelaic acid (Jung *et al.*, 2009; Cecchini *et al.*, 2015). Together with EARLI1 (EARLY ARABIDOPSIS ALUMINUM INDUCED 1; At4g12480) they contain a putative signal sequence followed by a hydrophilic PRD similar to HyPRPs and to the N-terminus of extensins located in the plant cell wall. The C-terminal hydrophobic 8CM motif was suggested to have a functional connection to the cell membrane (Zhang & Schlappi, 2007). Microsomal fractionation experiments demonstrated that AZI1 and its close paralogue EARLI1 have strong association with membranes while the SAR induction targets EARLI1-like proteins associate with plastids (Cecchini *et al.*, 2015). It was suggested that EARLI1 is secreted to the cell wall but its 8CM motif anchors it to the cell membrane. EARLI1, classified as a putative lipid-transfer protein, has been thought to be involved in maintenance of membrane- or cell wall stability (Bubier & Schlappi, 2004) where it forms high order complexes and/or aggregates in the extracellular space to protect the cell from damage (Zhang & Schlappi, 2007).

Our microarray selection contains also a pair of genes encoding Cysteine/Histidine-rich C1 domain proteins (hereby named as CHR1; At3g50010 and CHR2; At5g40590) (**Fig. 3-1 C and Fig. S3-1 A – B**). These genes belong to the family of tandem CCCH-zinc finger proteins characterized by three cysteines followed by one histidine (Blackshear, 2002). Some of the members of this plant-unique family were shown to mediate plant growth, development and stress responses by regulation of gene expression at both transcriptional and post-transcriptional levels (Pomeranz *et al.*, 2010; Pomeranz *et al.*, 2011). As an example, CaDC1 proteins bind RNA and DNA and are required for plant defense responses to microbial pathogens in pepper (Hwang *et al.*, 2014).

3.4.3 Cell wall related genes

Another group of candidate genes that could be generalized by functional similarity, being commonly involved in defense processes in the cell wall, are members of the expansin-, and exordium-like families (*EXP20*; At4g38210 and *EXL3*; At5t51550, respectively), together with

a plant invertase/pectin methylesterase inhibitor superfamily protein gene (*PMEI*; At2g26440) (**Fig. 3-1 C and Fig. S3-1 A – B**). Expansins are proteins mediating cell wall loosening: they enable the local sliding of polymers by reducing adhesion between adjacent cell wall polysaccharides. They act *e.g.* in cell wall remodelling after cytokinesis or during syncytium formation by parasitic nematodes (Wieczorek *et al.*, 2006; Marowa *et al.*, 2016). Dynamics of the cell wall determines cell shape and function during development (Fukuda, 2014). Expansins have the ability to trigger non-enzymatically pH-dependent relaxation of the cell wall and thus to allow cell expansion, a phenomenon called acid growth (Rayle & Cleland, 1992; Cosgrove, 2000). Expansins can be influenced by various environmental factors but also by plant hormones including auxin (McQueen-Mason *et al.*, 1992; Zhao *et al.*, 2012).

EXORDIUM and *EXORDIUM-LIKE* genes (*EXO*; *EXL*) were identified as brassinosteroid (BR) induced genes. The function of *EXO* genes is essential for cell expansion in leaves; they potentially coordinate responses of BR with environmental and developmental signals and adaptation to low nutrition stress (Schroder *et al.*, 2009; Schroder *et al.*, 2011). *EXO* proteins are conserved, both topologically and in their sequence, in evolutionary distinct green plants (Schroder *et al.*, 2009). *EXO*, *EXL* and other members of the family carry an N-terminal signal peptide. *In silico* analyses as well as experimental evidence indicate an extracellular localization of these proteins as a part of cell wall proteome (Jamet *et al.*, 2006; Schroder *et al.*, 2011).

Plant invertase/pectin methylesterase inhibitor superfamily proteins (*PMEi*) are regulators of plant methylesterases (*PMEs*) either during growth and development (Reca *et al.*, 2012; Rocchi *et al.*, 2012) or during plant-pathogen interactions (Lionetti *et al.*, 2012). *PMEs* remove methyl esters from pectin and thus make the cell wall susceptible for the action of microbial polygalacturonases and pectin lyases (Arancibia & Motsenbocker, 2006). Overexpression of *PMEi*s reduces *PME* activity, leading to a higher level of pectin esterification and to a concomitant increase in resistance to fungal and bacterial pathogens (Lionetti *et al.*, 2007; Raiola *et al.*, 2011). The sugar beet cyst nematode *Heterodera schachtii* infects *Arabidopsis* roots and exploits the host-encoded *PME3*. Overexpression of *PME3* causes increased susceptibility to the nematode. It was proposed that *PME3* locally reduces the pectin esterification and improves the cell wall loosening of pre-syncytial cells during early stages of syncytium formation (Hewezi *et al.*, 2008). Interestingly, *WRKY23* is expressed during the early stages of feeding site establishment (Grunewald *et al.*, 2008).

3.4.4 Residual candidates

From the rest of the candidates in our list, attention was focused on an actin-binding FH2 (*FORMIN HOMOLOGY 2; FH2; At3g07540*) family protein (**Fig. 3-1 C, Fig. S3-1 A – B**). Formins (FH2 domain-containing proteins) are key eukaryotic cytoskeletal regulators (Blanchoin & Staiger, 2010). In some plants, formin interacts with microtubules (Wang *et al.*, 2012). Angiosperm formins can be divided into two clades (Class I and Class II) exhibiting characteristic domain organisation. Class I formins are often transmembrane proteins (Cvrckova *et al.*, 2004). The most abundant Class I formin, FH1 (Hruz *et al.*, 2008) can nucleate and bundle actin (Michelot *et al.*, 2005; Michelot *et al.*, 2006). Mutation of *FH1* causes stabilization of the actin cytoskeleton and increases microtubule end dynamics possibly as result of microtubule-actin cross-talk (Rosero *et al.*, 2013).

We identified also previously not described genes *i.e.* a gene encoding an unknown protein (*UNK1; At1g28400*) (**Fig.3-1 C, Fig. S3-1 A – B**). The gene has a very close homolog (*UNK2; At2g33850*). However, their biological function is currently not known and no T-DNA mutants are available. The *LEGUME LECTIN FAMILY PROTEIN (LLP; At1g53070)* is not very well-described protein, either. Legume lectins are known to bind carbohydrates in the cell wall but further characterisation of this particular protein has never been done due to missing T-DNA mutant lines in public databases.

3.4.5 LHT1 transporter

WRKY23 also regulates *LYSINE-HISTIDINE TRANSPORTER 1 (LHT1; At5g40780)* (**Fig.3-1 C, Fig. S3-1 A – B**). LHT1 is a transport protein from the AAAP (amino acid/auxin permease) superfamily, consisting of lysine-histidine transporters (LHTs), amino acid permeases (AAPs), proline transporters (ProTs), γ -aminobutyric acid transporters (GATs), ANT1-like aromatic and neutral amino acid transporters and auxin transporters (AUXs (Bennett *et al.*, 1996; Wipf *et al.*, 2002; Rentsch *et al.*, 2007)). The LHT family consists of 10 members (LHT1 to 10) in *Arabidopsis* (Tegeger & Ward, 2012). LHT1 was originally described as a lysine and histidine selective transporter (Chen & Bush, 1997). Subsequent studies on LHT1 and LHT2 suggest that LHTs preferentially transport neutral and acidic amino acids with high affinity (Lee & Tegeger, 2004; Hirner *et al.*, 2006; Svennerstam *et al.*, 2007; Svennerstam *et al.*, 2008). Functional analysis proved that LHT1 has much higher affinity to amino acids than the transporters of

the related AAP subfamily (Hirner *et al.*, 2006). LHT1 is a CM-localised transmembrane protein that is expressed in the root epidermis and leaf mesophyll cells and has been suggested to be involved in import of organic nitrogen in the amino acid form from the soil solution (Hirner *et al.*, 2006). Homologous genes to *LHT1* exhibit distinct and partially overlapping spatio-temporal expression patterns (Hirner *et al.*, 2006; Forsum *et al.*, 2008). A forward genetic screen revealed that a mutation in *LHT1* caused resistance to ACC (1-aminocyclopropane-1-carboxylic acid), an ethylene precursor (Shin *et al.*, 2015). Several nitrate/peptide transporter family members have been shown to transport plant hormones (Krouk *et al.*, 2010; Kanno *et al.*, 2012). For example, NRT1.1 has dual transport specificity for the endogenous hormone auxin and for the exogenous nutrient nitrate. The two substrates seem to compete for NRT1.1 transport activity: at low nitrate concentrations, auxin-transport capacity of NRT1.1 is high, whereas at high nitrate concentrations, the auxin uptake into cells is low (Krouk *et al.*, 2010).

3.4.6 Polarity related phenotype analysis narrows down the list of putative regulators

To narrow down the list of genes from our microarray experiment, we decided to employ thorough analysis of the PIN polarity/auxin transport-related phenotypes. The importance of tight regulation of PIN polarity for growth and development has previously been shown (Wisniewska *et al.*, 2006 reviewed in Adamowski & Friml, 2015).

At first, we decided to study leaf venation pattern in mutant lines. Leaf venation crucially depends on the polarity of PIN proteins and in particular on the auxin feedback on PIN polarity as proposed by the canalization hypothesis (Scarpella *et al.*, 2006). As we have shown previously, dominant-negative downregulation of *WRKY23* causes venation defects and morphological changes in cotyledons (Prat *et al.*, unpublished data). Therefore, we looked for uniquely appeared or enriched abnormal patterns in available mutants and transgenic lines. In Wt Col-0 cotyledons, veins form closed circles, at the beginning two and then four lobes (**Fig.3-2 A**). This almost unvarying pattern is formed by the self-regulatory auxin canalization mechanism, depending on correct PIN1 polarity (Scarpella *et al.*, 2006). We screened a set of publicly available T-DNA mutants; nevertheless, no T-DNA insertion lines could be found for *FH2* (At3g07540), *LLP* (At1g53070) and *UNK1* and *UNK2* (At1g28400; At2g33850). First, we checked venation patterning in knock-out mutants in our cell wall-

related candidates. We observed no or very little abnormalities in cotyledon vascularization (*exp20-1*: 15%; *exl3-1*: 14%; and *pmei1-1*: 20.3%) (**Fig.3-2 A**). Similarly, the defense- and stress-related *chr1-1* and *chr2-1* mutants did not show any obvious venation phenotype, neither in single nor in double homozygous form (**Fig.3-2 A**). Since *EARLI1-like* genes form a gene cluster and they share a high sequence similarity (Jose-Estanyol *et al.*, 2004), analysis of single mutants is useless and formation of multiple mutants is impossible due to tight linkage. Therefore, we used RNAi targeting all members of this group (*Col-0::EARLI1 RNAi [1-1]*) (Cecchini *et al.*, 2015) (**Fig.3-2 A**). Although transcript levels of each targeted *EARLI1-like* homologues was substantially diminished (**Fig. S3-1 C**), we observed only very mild changes in vascularization pattern with slightly increased frequency (25%) in comparison with control. On the other hand, we observed strong venation patterning defects in *lht1-1*, a loss-of-function T-DNA mutant of *LHT1* (**Fig.3-2 A**, **Fig. S3-1 D**). In more than 41% of cotyledons, vascularization was not connected to the midvein and loops were not finished. To gain further insight, we overexpressed *LHT1* under the constitutive *RPS5A* promoter (**Fig. S3-1 E**). Interestingly, a similar effect as of null-mutant was observed in the *LHT1* overexpressors (48%) (**Fig. 3-2 A**). Taken together, a combination of results from gain-of-function and loss-of-function lines demonstrated the effect of *LHT1* in leaf venation patterning.

As was previously demonstrated, regulation of root growth is fundamentally connected with auxin transport. For that reason, we checked root length in our promising candidates characterized as having deviated cotyledon vascularization (**Fig.3-2 B**). While *pmei1-1* and *Col-0::EARLI1 RNAi [1-1]* had no or very little effect on root length, astonishingly, roots of *lht1-1* plants grew longer than *Col-0*. Oppositely, *RPS5A::LHT1* plants had shorter roots (**Fig.3-2 B**). As was previously shown, vertical growth of the root in accordance to gravity vector depends on correct auxin transport and PIN polarity (Wisniewska *et al.*, 2006), unfortunately, vertical root growth observed in mutants of candidate gene lines shows no or very weak phenotypes (**Fig. S3-3**).

We noticed that *RPS5A::LHT1* had a normal closed apical hook but shortened hypocotyl in comparison with control (**Fig.3-2 C**). PIN polarity is also very important in hypocotyl negative gravitropism (Rakusova *et al.*, 2011; Rakusova *et al.*, 2015). Hypocotyl negative gravitropism is caused by asymmetric growth due to unequal auxin distribution that is generated by mainly PIN3-mediated lateral transport. Gravity stimulation polarizes PIN3 to the bottom side of endodermal cells resulting in auxin accumulation in adjacent tissues at the

lower side of the stimulated organ where auxin induces cell elongation and eventually hypocotyl bending (Friml *et al.*, 2002b; Rakusova *et al.*, 2011; Rakusova *et al.*, 2015). We found in stimulated etiolated hypocotyls that *lht1-1* hypocotyls were hypersensitive to gravity, while overexpression of *LHT1* caused inability to react to gravity direction (**Fig.3-2 D**).

Altogether, we found in our physiological tests that expression of *LHT1* affected leaf venation pattern, root growth and hypocotyl gravitropism. Therefore we conclude that *LHT1* may regulate auxin transport and/or PIN protein polarity.

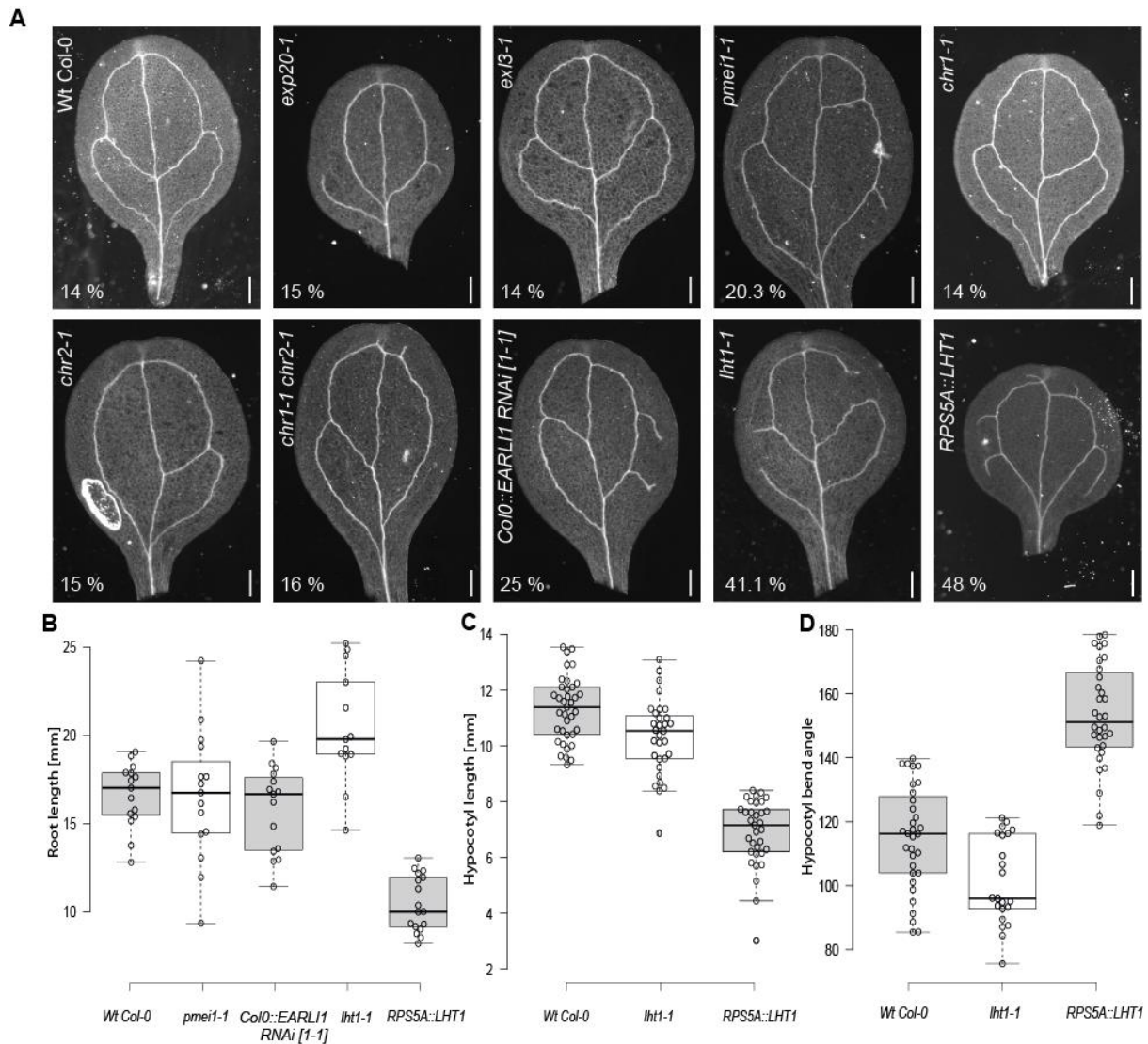


Figure 3-2 Polarity-related phenotype analysis of mutants in putative regulators.

A. Cotyledon venation pattern analysis of mutants in putative regulators. Percentages represent quantity of defect cotyledons. Bar size 1 mm. B. Root length analysis of mutants in putative regulators. Centre lines show the medians; box limits indicate the 25th and 75th percentiles as determined by the R software; whiskers extend 1.5 times the interquartile range from the 25th to 75th percentiles; data points are plotted as open circles. $n_{\min} = 20$ sample points. C. Hypocotyl length analysis of mutants in putative regulators. Box-whisker plot

parameters are as in B. $n_{\min} = 30$ sample points. D. Hypocotyl response to gravistimulation of mutants in putative regulators. Box-whisker plot parameters are as in B. $n_{\min} = 30$ sample points.

3.4.7 Effect of *LHT1* gene expression on PIN2 lateralization

Expression profiling experiments were focused on identification of molecular players responsible for auxin-dependent PIN repolarization. Therefore we tested the effect of auxin on PIN2 polarity in the root tip of *lht1-1* and *RPS5A::LHT1* lines.

We analysed PIN2 abundance at basal and outer lateral membrane domains of cortex cells by immunolocalization. NAA treatment increased PIN2 lateralization in cortex cells of Wt Col-0 (**Fig.3-3 A**). In contrast, *lht1-1* showed lower ability to auxin-dependent PIN repolarization. Without auxin application, PIN2 polarity was not affected (**Fig.3-3 B and D**). In contrast to the observed lateralization defect in *lht1-1*, we observed increased PIN2 lateralization in *RPS5A::LHT1* plants without hormone application. Interestingly, plants responded to NAA similar to Wt Col-0 and no difference in the PIN2 polarity index could be detected (**Fig.3-3 C and E**). These results showed that correct expression level of *LHT1* is necessary for successful repolarization of PIN2 but *LHT1* itself is not indispensable for polarity establishment.

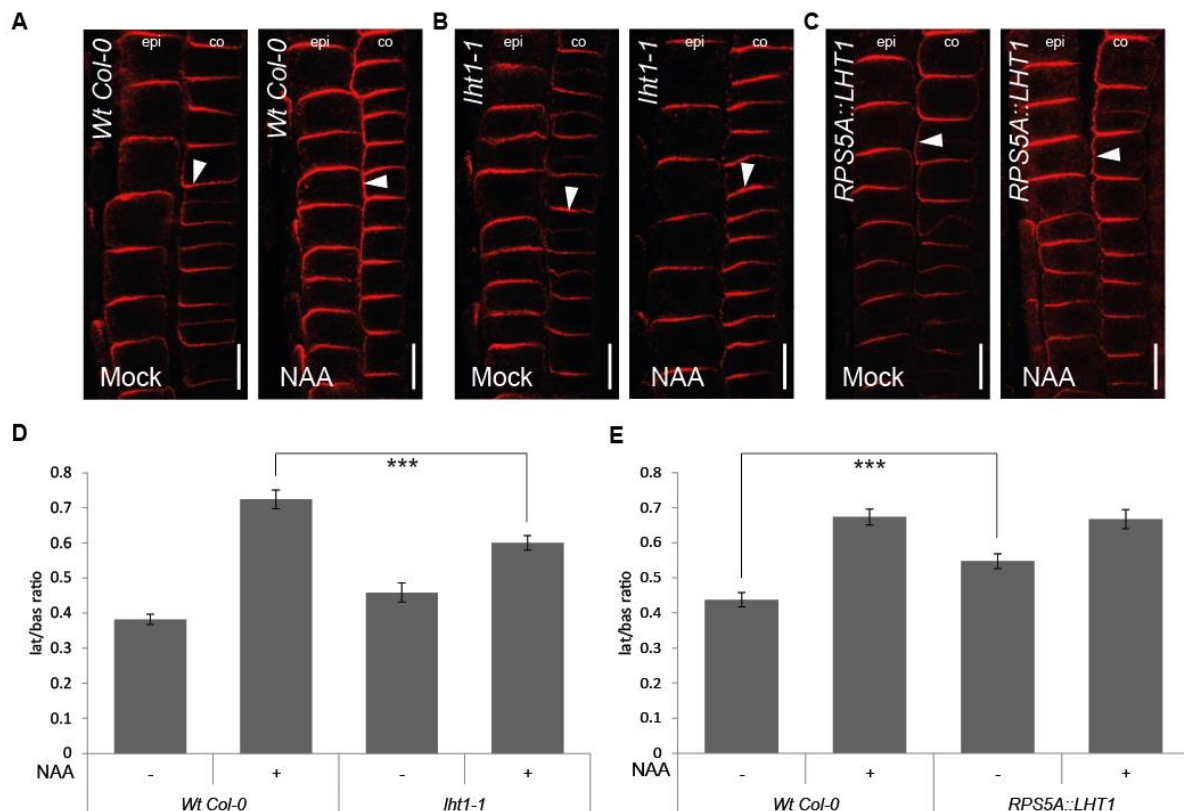


Figure 3-3 Immunolocalization of PIN2 protein in root of *LHT1* loss- and gain-of-function lines.

A. Cortex cells of Wt Col-0 treated with Mock/NAA. Arrowheads highlight PIN polarity. B. Cortex cells of *lht1-1* treated with Mock/NAA. Arrowheads highlight PIN polarity. C. Cortex cells of *RPS5A::LHT1* treated with Mock/NAA. Arrowheads highlight PIN polarity. D. Visualization of mean ratio of lateral to basal signal intensity of PIN2 in cortex cells in Wt Col-0 and *lht1-1* treated plants with 10 μ M NAA for 4 hours. Error bars indicates standard error. A two-tailed Student's t test compared marked sets of data. (***) $P < 0.0001$. $n > 50$ cells corresponding to roots imaged under comparable conditions. E. Visualization of mean ratio of lateral to basal signal intensity of PIN2 in cortex cells in *RPS5A::LHT1* plants treated with 10 μ M NAA for 4 hours. Error bars indicates standard error. A two-tailed Student's t test compared marked sets of data. (***) $P < 0.0001$. $n > 50$ cells corresponding to roots imaged under comparable conditions.

3.4.8 Expression of *LHT1* is regulated by *WRKY23* and depends on auxin signalling pathway

Next, we investigated the expression regulation of *LHT1*. In our previous study, we demonstrated that dexamethasone-induced nuclear localization of *WRKY23*-GR increased PIN2 lateralization in the cortex, comparably to NAA treatment (Prat *et al.*, unpublished data). Therefore, we tested whether *LHT1* expression is *WRKY23*-dependent. Indeed, *LHT1* showed increased expression levels after activation of *WRKY23*-GR. From the other side of microarray selection criteria, we confirmed that *LHT1* is auxin inducible. After NAA application, expression of *LHT1* increased, while after the same auxin treatment in dominant-negative *35S::WRKY23-SRDX* line *LHT1* expression was downregulated in comparison with control Wt-Col0 (**Fig.3-4 A**).

As it was shown previously, auxin is unable to mediate PIN polarity re-arrangements in induced *HS::axr3-1* and in *arf7 arf19* double mutant backgrounds (Sauer *et al.*, 2006). We also showed *WRKY23* expression dependence on auxin signalling. According to our results, expression of *LHT1* gene follows the logic of gene regulation involved in PIN repolarization (**Fig.3-4 B**). Auxin acts through its signalling pathway to activate expression of the *WRKY23* transcription factor. *WRKY23* transactivation then regulates expression of *LHT1*, in agreement with our microarray results. Whether the not on/off-like effect of *LHT1* on PIN repolarization is due to its extensive redundancy or to a rather modulator than effector function, remains to be elucidated.

Next, we analysed auxin-dependence of *LHT1* expression in more detail. Similar to *WRKY23* (Prat *et al.*, unpublished data), expression of *LHT1* depends on the concentration of applied auxin. In comparison with *WRKY23*, after 4 hours of 10 nM NAA treatment, we

observed mRNA levels had increased three times (**Fig.3-4 C**). This sensitivity to auxin application lead to hypothesis that this gene is also directly activated by auxin signalling and WRKY23 acts as fine tuner of this process. This hypothesis is further supported with time regulation of the *LHT1* expression. We observed that already 60 minutes of 10 μ M NAA increased expression of *LHT1* (**Fig.3-4 D**). In contrast, 10 μ M NAA used in PIN lateralization experiments increased expression of *WRKY23* between 120 and 240 minutes of auxin treatment.

Auxin application expanded the expression domain of *LHT1*. We applied effective amount of NAA to reporter lines expressing transcription fusion of *LHT1* with *GUS*. *LHT1:: Δ LHT1-GUS* (Hirner *et al.*, 2006) is expressed in the root tip including the columella, lateral root cap, epidermis and probably also cortex and endodermis. Six hours of NAA treatment generally increased *LHT1* expression and expanded the expression pattern to the entire root tip (**Fig.3-4 E**).

The observed transcriptional behaviour demonstrated dual dependency of *LHT1* expression on both auxin signalling and on WRKY23. On the one hand, *LHT1* expression was activated in Dex-induced *35S::WRKY23-GR* plants, while *LHT1* lost its auxin-inducibility in *35S::WRKY23-SRDX* background. Furthermore, *LHT1* is more sensitive to auxin application than *WRKY23*, both in time as well as in concentration dependence. This could be understood that *LHT1* plays a role in complex regulation network with consequence of increasing modulation variety. Unambiguous PIN polarity regulation as was shown *e.g.* in PID overexpression cannot explain very tiny polarity oscillation during plant growth and development. Involvement of additional step in regulatory process, *e.g.* in modulation of auxin signalling or transport in cells undergoing PIN repolarization remained to be clarified.

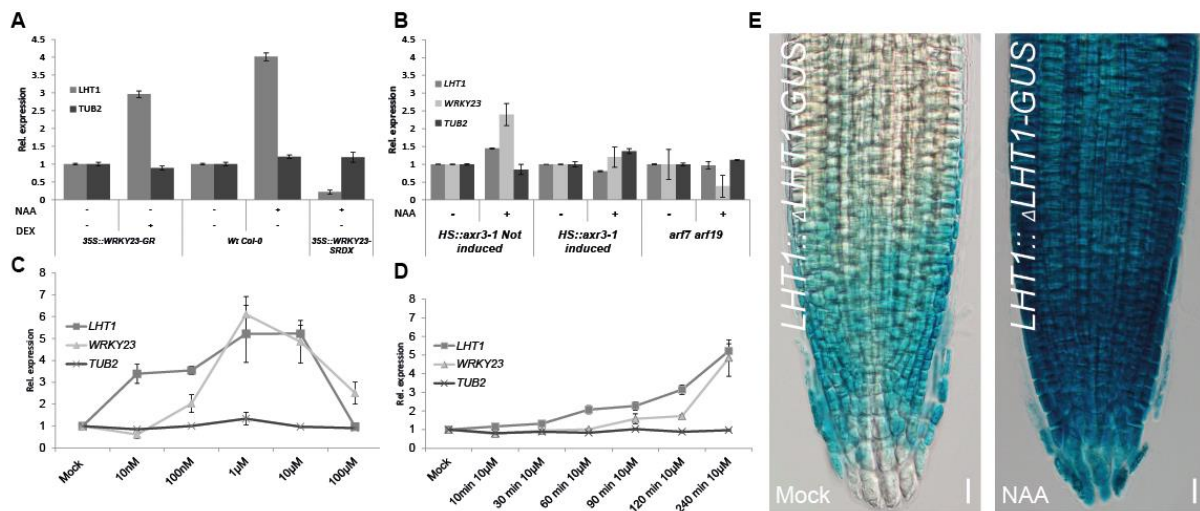


Figure 3-4 Transcript levels and expression of LHT1 during auxin treatments.

A. *LHT1* transcript level depends on WRKY23. qRT-PCR experiment showed dependence of *LHT1* transcript levels, normalized to mRNA levels in controls. Bars represent relative fold change of expression. Error bars represent standard deviation (see Materials and Methods for detailed description). B. *LHT1* transcript level is dependent on auxin through the SCF^{TIR1}-Aux/IAA-ARF signalling pathway. qRT-PCR experiment showed transcript levels of *LHT1* in auxin signalling mutants *HS::axr3-1* and *arf7 arf19*. Bars represent relative fold change of expression. Error bars represent standard deviation (see Materials and Methods for detailed description). C. – D. *LHT1* expression is auxin dose and time dependent. qRT-PCR experiment showed transcript levels of *LHT1* in Wt Col-0 seedlings treated with respective concentration of NAA for respective time. Points represent relative fold change of expression. Error bars represent standard deviation (see Materials and Methods for detailed description). E. *LHT1* promoter activation after auxin treatment. Expression pattern of *LHT1::ΔLHT1-GUS* (Hirner et al., 2006) in cleared root tips was visualized with a DIC microscope (see Materials and Methods for detailed description). Bar size 10 µm.

3.4.9 *LHT1* expression regulates auxin abundance/signalling in the root tip

To analyse the function of *LHT1* during repolarization, we crossed *RPS5A::LHT1* with the auxin reporters DR5rev and R2D2 (Benkova et al., 2003; Liao et al., 2015). We observed defects in local auxin maxima formation in the root tip. *DR5rev::GFP* signal spread to the outer tiers in columella cells and lateral root cap suggesting that auxin transport was affected (Fig.3-5 A). Therefore, we further analysed auxin response in the root tip by quantitative measurement of ratiometric auxin reporter R2D2 (Fig.3-5 B). In R2D2, the DII auxin degradable domain is fused to n3×Venus and a stabilised mDII domain fused to ntdTomato on a single transgene. Reduction of yellow relative to red signal measures auxin accumulation in this system (Liao et al., 2015). In control R2D2 plants, average ratio between fluorescent channels was equal to 1, while in the crossed gain-of-function lines of *LHT1* to R2D2 the fluorescent ratio was shifted

in favour of the stabilised mDII domain represented by the red channel (**Fig.3-5 C**). These results indicate a possible change in auxin transport with a consequence of increased level of auxin in the cells of the root tip.

To date, several permeases were shown to exhibit dual transport activity for structurally different substrates (Krouk *et al.*, 2010; Kanno *et al.*, 2012). Since *LHT1* is expressed in the hypocotyl too (**Fig.3-5 D – E**), we tested auxin transport ability in hypocotyls by radioactively labelled basipetal auxin transport assay. We observed a significant decrease in transported ^3H -IAA in *lht1-1* null-mutant. In contrast, hypocotyls of gain-of-function lines transported three times more radioactively labelled IAA than the control line did. In a complementary experiment, we added excessive amounts of non-labelled IAA to the drop of ^3H -IAA in order to check substrate competitiveness of auxin transport. In all of the cases, in control, null-mutant, and gain-of-function lines, we detected decreased levels of ^3H -IAA suggesting that non-labelled IAA is competing for active transport with ^3H -IAA (**Fig.3-5 F**). All these results proposed a hypothesis, that *LHT1* has a role in cellular auxin transport important for auxin-dependent PIN repolarization.

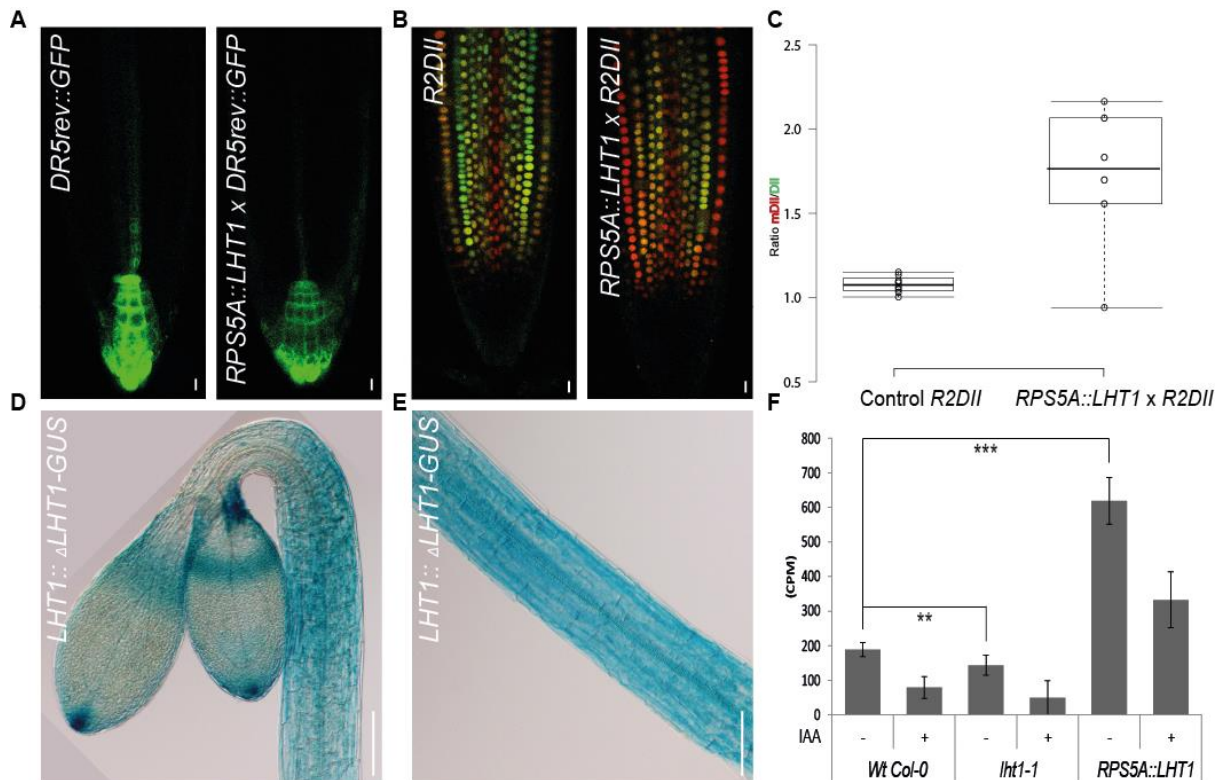


Figure 3-5 Auxin abundance/signalling in the root tip of *LHT1* loss- and gain-of-function lines.

A. Defects in formation of local auxin maxima in the root tip. Note the GFP signal spread to the outer tiers in columella cells and lateral root cap in the *LHT1* overexpressor. B. – C. *LHT1* overexpression caused shift of fluorescent ratio in root cells of ratiometric *R2D2* auxin reporter in favour of the stabilised mDII domain. Chart represents quantification of fluorescent channel measurements of the *R2D2*. D. – E. GUS staining of etiolated hypocotyl of *LHT1::ΔLHT1-GUS* (Hirner *et al.*, 2006). *LHT1* promoter is active in cotyledons, apical hook and also in etiolated hypocotyls. F. Measurement of basipetal transport of radioactively labelled auxin in *LHT1* loss- and gain-of-function etiolated hypocotyls. Adding of non-labelled auxin decreased transport activity due to substrate inhibition. Graph shows counts per minutes (CPM) of radioactivity in hypocotyls of Col-0 and *lht1-1* and *RPS5A::LHT1* treated with ^3H -IAA for 6 hours. Error bars indicates standard deviation. A two-tailed Student's t test compared marked sets of data. (**) $P < 0.01$ (***) $P < 0.0001$.

Observed mechanism of *LHT1* function opens a question about physiological relevance of auxin transport and/or auxin levels in the cells during auxin-dependent PIN repolarization. In transgenic lines with ectopic expression of PIN1 and PIN2 proteins, lateralization was cell type-specific but not affected. Strong constitutive expression of PIN1 in *35S::PIN1* transgenic line did not change character of PIN1 lateralization to outer-lateral side either was PIN1 ectopically expressed in cortex cells (Sauer *et al.*, 2006). We can speculate that auxin levels decreased inside the cells ectopically expressing PIN efflux carriers. Similarly, in mutants of auxin influx carriers, intracellular auxin levels should be affected. Protein family of influx carriers consists of four genes in *Arabidopsis*: *AUX1*, *LAX1*, *LAX2*, and *LAX3*, which are non-polarly localized on the CM. They play a role in keeping auxin in the transporting cells, thereby overcoming its leakage from the transport channels (Petrasek & Friml, 2009). Mutations in auxin influx carriers result in developmental defects. In *aux1* mutants root gravitropism is severely affected and have a decreased number of lateral roots. *lax3* mutants show postponed lateral root emergence. Double mutants *aux1 lax3* act alongside to regulate lateral root development by regulating the emergence and initiation (Marchant *et al.*, 2002; Swarup *et al.*, 2008). Mutations in multiple members of the AUX/LAX family cause irregular divergence angles between successive primordia and thus affect phyllotactic patterning in aerial parts of *Arabidopsis* (Bainbridge *et al.*, 2008). These findings highlight the effect of auxin intake in developmental processes. Nevertheless, PIN re-arrangement in roots of *aux1-21 lax1 lax2 lax3* quadruple mutant was not affected (**Fig. S3-4**).

However, we demonstrated that *LHT1* mediated auxin-dependent PIN polarity re-arrangement since gain-of-function and loss-of-function *LHT1* lines were affected in this

process. The phenotypes on cellular level were also developmentally relevant, as we observed defects typical for altered auxin homeostasis and/or canalization such as changes in the leaf vasculature and hypocotyl gravitropism. Phenotypes in root, with exception of PIN rearrangement, were rather mild. Whether the causative effect of *LHT1* is due to its extensive redundancy among members of AAAPs or to a rather modulator than effector function, remains unclear. Therefore, characterisation of auxin and its conjugates content and experimental evidence of auxin transport also in heterologous systems would be necessary for understanding of *LHT1* action. Physiological function of plant permeases with dual transport activity for structurally different substrates may represent missing part in regulation of complex developmental processes, *e.g.* auxin-nitrate competition moderated by *NRT1.1* in lateral root initiation (Krouk *et al.*, 2010). Hence we propose that integrative mathematical models of self-regulatory auxin feedback on canalization should take in account also these dual substrate transporters.

3.5 ACKNOWLEDGEMENTS

We thank Friederike Wanke and Michael R. Schläppi for providing published material and Matouš Glanc for help with auxin transport assay. This work was supported by the European Research Council (project ERC-2011-StG-20101109-PSDP). WG performed the work as a post-doctoral fellow of the Research Foundation Flanders.

3.6 AUTHOR CONTRIBUTION

T.P., W.G., and J.F. designed the research, T.P. and W.G., performed the research, T.P., W.G., G.M. and J.F. analyzed the data and T.P., G.M. and J.F. wrote the paper.

3.7 REFERENCES

- Abas L, Benjamins R, Malenica N, Paciorek T, Wisniewska J, Moulinier-Anzola JC, Sieberer T, Friml J, Luschnig C. 2006. Intracellular trafficking and proteolysis of the Arabidopsis auxin-efflux facilitator PIN2 are involved in root gravitropism. *Nat Cell Biol* **8**(3): 249-256.
- Adamowski M, Friml J. 2015. PIN-dependent auxin transport: action, regulation, and evolution. *Plant Cell* **27**(1): 20-32.
- Arancibia RA, Motsenbocker CE. 2006. Pectin methylesterase activity in vivo differs from activity in vitro and enhances polygalacturonase-mediated pectin degradation in tabasco pepper. *J Plant Physiol* **163**(5): 488-496.
- Bainbridge K, Guyomarc'h S, Bayer E, Swarup R, Bennett M, Mandel T, Kuhlemeier C. 2008. Auxin influx carriers stabilize phyllotactic patterning. *Genes Dev* **22**(6): 810-823.
- Benkova E, Michniewicz M, Sauer M, Teichmann T, Seifertova D, Jurgens G, Friml J. 2003. Local, efflux-dependent auxin gradients as a common module for plant organ formation. *Cell* **115**(5): 591-602.
- Bennett MJ, Marchant A, Green HG, May ST, Ward SP, Millner PA, Walker AR, Schulz B, Feldmann KA. 1996. Arabidopsis AUX1 gene: A permease-like regulator of root gravitropism. *Science* **273**(5277): 948-950.
- Bennett T, Hines G, Leyser O. 2014. Canalization: what the flux? *Trends Genet* **30**(2): 41-48.
- Blackshear PJ. 2002. Tristetraprolin and other CCCH tandem zinc-finger proteins in the regulation of mRNA turnover. *Biochem Soc Trans* **30**(Pt 6): 945-952.
- Blanchoin L, Staiger CJ. 2010. Plant formins: diverse isoforms and unique molecular mechanism. *Biochim Biophys Acta* **1803**(2): 201-206.
- Bubier J, Schlappi M. 2004. Cold induction of EARL1, a putative Arabidopsis lipid transfer protein, is light and calcium dependent. *Plant, Cell & Environment* **27**(7): 929-936.
- Cecchini NM, Steffes K, Schlappi MR, Gifford AN, Greenberg JT. 2015. Arabidopsis AZI1 family proteins mediate signal mobilization for systemic defence priming. *Nat Commun* **6**: 7658.
- Chen L, Bush DR. 1997. LHT1, a lysine- and histidine-specific amino acid transporter in Arabidopsis. *Plant Physiology* **115**(3): 1127-1134.
- Cieslak M, Runions A, Prusinkiewicz P. 2015. Auxin-driven patterning with unidirectional fluxes. *J Exp Bot* **66**(16): 5083-5102.
- Clough SJ, Bent AF. 1998. Floral dip: a simplified method for Agrobacterium-mediated transformation of Arabidopsis thaliana. *Plant J* **16**(6): 735-743.
- Cosgrove DJ. 2000. Loosening of plant cell walls by expansins. *Nature* **407**(6802): 321-326.
- Cvrckova F, Novotny M, Pickova D, Zarsky V. 2004. Formin homology 2 domains occur in multiple contexts in angiosperms. *BMC Genomics* **5**(1): 44.
- Eulgem T, Somssich IE. 2007. Networks of WRKY transcription factors in defense signaling. *Curr Opin Plant Biol* **10**(4): 366-371.
- Forsum O, Svennerstam H, Ganeteg U, Nasholm T. 2008. Capacities and constraints of amino acid utilization in Arabidopsis. *New Phytol* **179**(4): 1058-1069.
- Friml J, Benkova E, Blilou I, Wisniewska J, Hamann T, Ljung K, Woody S, Sandberg G, Scheres B, Jurgens G, et al. 2002a. AtPIN4 mediates sink-driven auxin gradients and root patterning in Arabidopsis. *Cell* **108**(5): 661-673.
- Friml J, Wisniewska J, Benkova E, Mendgen K, Palme K. 2002b. Lateral relocation of auxin efflux regulator PIN3 mediates tropism in Arabidopsis. *Nature* **415**(6873): 806-809.
- Fukuda H. 2014. *Plant Cell Wall Patterning and Cell Shape*: John Wiley & Sons, Inc, Hoboken, NJ, USA.
- Grabov A, Ashley MK, Rigas S, Hatzopoulos P, Dolan L, Vicente-Agullo F. 2005. Morphometric analysis of root shape. *New Phytol* **165**(2): 641-651.
- Grunewald W, De Smet I, De Rybel B, Robert HS, van de Cotte B, Willemsen V, Gheysen G, Weijers D, Friml J, Beeckman T. 2013. Tightly controlled WRKY23 expression mediates Arabidopsis embryo development. *EMBO Rep* **14**(12): 1136-1142.

- Grunewald W, De Smet I, Lewis DR, Lofke C, Jansen L, Goeminne G, Vanden Bossche R, Karimi M, De Rybel B, Vanholme B, et al. 2012.** Transcription factor WRKY23 assists auxin distribution patterns during Arabidopsis root development through local control on flavonol biosynthesis. *Proc Natl Acad Sci U S A* **109**(5): 1554-1559.
- Grunewald W, Karimi M, Wieczorek K, Van de Cappelle E, Wischnitzki E, Grundler F, Inze D, Beeckman T, Gheysen G. 2008.** A role for AtWRKY23 in feeding site establishment of plant-parasitic nematodes. *Plant Physiology* **148**(1): 358-368.
- Heisler MG, Hamant O, Krupinski P, Uyttewaal M, Ohno C, Jonsson H, Traas J, Meyerowitz EM. 2010.** Alignment between PIN1 polarity and microtubule orientation in the shoot apical meristem reveals a tight coupling between morphogenesis and auxin transport. *PLoS Biol* **8**(10): e1000516.
- Hewezi T, Howe P, Maier TR, Hussey RS, Mitchum MG, Davis EL, Baum TJ. 2008.** Cellulose binding protein from the parasitic nematode *Heterodera schachtii* interacts with Arabidopsis pectin methylesterase: cooperative cell wall modification during parasitism. *Plant Cell* **20**(11): 3080-3093.
- Hirner A, Ladwig F, Stransky H, Okumoto S, Keinath M, Harms A, Frommer WB, Koch W. 2006.** Arabidopsis LHT1 is a high-affinity transporter for cellular amino acid uptake in both root epidermis and leaf mesophyll. *Plant Cell* **18**(8): 1931-1946.
- Hruz T, Laule O, Szabo G, Wessendorp F, Bleuler S, Oertle L, Widmayer P, Gruissem W, Zimmermann P. 2008.** Genevestigator v3: a reference expression database for the meta-analysis of transcriptomes. *Adv Bioinformatics* **2008**: 420747.
- Hwang IS, Choi DS, Kim NH, Kim DS, Hwang BK. 2014.** The pepper cysteine/histidine-rich DC1 domain protein CaDC1 binds both RNA and DNA and is required for plant cell death and defense response. *New Phytol* **201**(2): 518-530.
- Irizarry RA, Hobbs B, Collin F, Beazer-Barclay YD, Antonellis KJ, Scherf U, Speed TP. 2003.** Exploration, normalization, and summaries of high density oligonucleotide array probe level data. *Biostatistics* **4**(2): 249-264.
- Jamet E, Canut H, Boudart G, Pont-Lezica RF. 2006.** Cell wall proteins: a new insight through proteomics. *Trends Plant Sci* **11**(1): 33-39.
- Jose-Estanyol M, Gomis-Ruth FX, Puigdomenech P. 2004.** The eight-cysteine motif, a versatile structure in plant proteins. *Plant Physiol Biochem* **42**(5): 355-365.
- Jung HW, Tschaplinski TJ, Wang L, Glazebrook J, Greenberg JT. 2009.** Priming in systemic plant immunity. *Science* **324**(5923): 89-91.
- Kanno Y, Hanada A, Chiba Y, Ichikawa T, Nakazawa M, Matsui M, Koshiba T, Kamiya Y, Seo M. 2012.** Identification of an abscisic acid transporter by functional screening using the receptor complex as a sensor. *Proc Natl Acad Sci U S A* **109**(24): 9653-9658.
- Karimi M, Depicker A, Hilson P. 2007.** Recombinational cloning with plant gateway vectors. *Plant Physiology* **145**(4): 1144-1154.
- Kleine-Vehn J, Leitner J, Zwiewka M, Sauer M, Abas L, Luschig C, Friml J. 2008.** Differential degradation of PIN2 auxin efflux carrier by retromer-dependent vacuolar targeting. *Proc Natl Acad Sci U S A* **105**(46): 17812-17817.
- Knox K, Grierson CS, Leyser O. 2003.** AXR3 and SHY2 interact to regulate root hair development. *Development* **130**(23): 5769-5777.
- Krouk G, Lacombe B, Bielach A, Perrine-Walker F, Malinska K, Mounier E, Hoyerova K, Tillard P, Leon S, Ljung K, et al. 2010.** Nitrate-regulated auxin transport by NRT1.1 defines a mechanism for nutrient sensing in plants. *Dev Cell* **18**(6): 927-937.
- Lee YH, Tegeder M. 2004.** Selective expression of a novel high-affinity transport system for acidic and neutral amino acids in the tapetum cells of Arabidopsis flowers. *Plant J* **40**(1): 60-74.
- Liao CY, Smet W, Brunoud G, Yoshida S, Vernoux T, Weijers D. 2015.** Reporters for sensitive and quantitative measurement of auxin response. *Nat Methods* **12**(3): 207-210, 202 p following 210.

- Lionetti V, Cervone F, Bellincampi D. 2012.** Methyl esterification of pectin plays a role during plant-pathogen interactions and affects plant resistance to diseases. *J Plant Physiol* **169**(16): 1623-1630.
- Lionetti V, Raiola A, Camardella L, Giovane A, Obel N, Pauly M, Favaron F, Cervone F, Bellincampi D. 2007.** Overexpression of pectin methylesterase inhibitors in Arabidopsis restricts fungal infection by Botrytis cinerea. *Plant Physiology* **143**(4): 1871-1880.
- Marchant A, Bhalerao R, Casimiro I, Eklof J, Casero PJ, Bennett M, Sandberg G. 2002.** AUX1 promotes lateral root formation by facilitating indole-3-acetic acid distribution between sink and source tissues in the Arabidopsis seedling. *Plant Cell* **14**(3): 589-597.
- Marowa P, Ding A, Kong Y. 2016.** Expansins: roles in plant growth and potential applications in crop improvement. *Plant Cell Rep* **35**(5): 949-965.
- McQueen-Mason S, Durachko DM, Cosgrove DJ. 1992.** Two endogenous proteins that induce cell wall extension in plants. *Plant Cell* **4**: 1425-1433.
- Michelot A, Derivery E, Paterski-Boujemaa R, Guerin C, Huang S, Parcy F, Staiger CJ, Blanchoin L. 2006.** A novel mechanism for the formation of actin-filament bundles by a nonprocessive formin. *Curr Biol* **16**(19): 1924-1930.
- Michelot A, Guerin C, Huang S, Ingouff M, Richard S, Rodiuc N, Staiger CJ, Blanchoin L. 2005.** The formin homology 1 domain modulates the actin nucleation and bundling activity of Arabidopsis FORMIN1. *Plant Cell* **17**(8): 2296-2313.
- Okushima Y, Overvoorde PJ, Arima K, Alonso JM, Chan A, Chang C, Ecker JR, Hughes B, Lui A, Nguyen D, et al. 2005.** Functional genomic analysis of the AUXIN RESPONSE FACTOR gene family members in Arabidopsis thaliana: unique and overlapping functions of ARF7 and ARF19. *Plant Cell* **17**(2): 444-463.
- Paciorek T, Zazimalova E, Ruthardt N, Petrasek J, Stierhof YD, Kleine-Vehn J, Morris DA, Emans N, Jurgens G, Geldner N, et al. 2005.** Auxin inhibits endocytosis and promotes its own efflux from cells. *Nature* **435**(7046): 1251-1256.
- Petrasek J, Friml J. 2009.** Auxin transport routes in plant development. *Development* **136**(16): 2675-2688.
- Pomeranz M, Finer J, Jang JC. 2011.** Putative molecular mechanisms underlying tandem CCCH zinc finger protein mediated plant growth, stress, and gene expression responses. *Plant Signal Behav* **6**(5): 647-651.
- Pomeranz M, Lin PC, Finer J, Jang JC. 2010.** AtTZF gene family localizes to cytoplasmic foci. *Plant Signal Behav* **5**(2): 190-192.
- Raiola A, Lionetti V, Elmaghraby I, Immerzeel P, Mellerowicz EJ, Salvi G, Cervone F, Bellincampi D. 2011.** Pectin methylesterase is induced in Arabidopsis upon infection and is necessary for a successful colonization by necrotrophic pathogens. *Mol Plant Microbe Interact* **24**(4): 432-440.
- Rakusova H, Fendrych M, Friml J. 2015.** Intracellular trafficking and PIN-mediated cell polarity during tropic responses in plants. *Curr Opin Plant Biol* **23**: 116-123.
- Rakusova H, Gallego-Bartolome J, Vanstraelen M, Robert HS, Alabadi D, Blazquez MA, Benkova E, Friml J. 2011.** Polarization of PIN3-dependent auxin transport for hypocotyl gravitropic response in Arabidopsis thaliana. *Plant J* **67**(5): 817-826.
- Rayle DL, Cleland RE. 1992.** The Acid Growth Theory of auxin-induced cell elongation is alive and well. *Plant Physiology* **99**(4): 1271-1274.
- Reca IB, Lionetti V, Camardella L, D'Avino R, Giardina T, Cervone F, Bellincampi D. 2012.** A functional pectin methylesterase inhibitor protein (SolyPMEI) is expressed during tomato fruit ripening and interacts with PME-1. *Plant Mol Biol* **79**(4-5): 429-442.
- Rentsch D, Schmidt S, Tegeder M. 2007.** Transporters for uptake and allocation of organic nitrogen compounds in plants. *FEBS Lett* **581**(12): 2281-2289.
- Rocchi V, Janni M, Bellincampi D, Giardina T, D'Ovidio R. 2012.** Intron retention regulates the expression of pectin methyl esterase inhibitor (Pmei) genes during wheat growth and development. *Plant Biol (Stuttg)* **14**(2): 365-373.

- Rolland-Lagan AG, Prusinkiewicz P. 2005.** Reviewing models of auxin canalization in the context of leaf vein pattern formation in Arabidopsis. *Plant J* **44**(5): 854-865.
- Rosero A, Zarsky V, Cvrckova F. 2013.** AtFH1 formin mutation affects actin filament and microtubule dynamics in Arabidopsis thaliana. *J Exp Bot* **64**(2): 585-597.
- Sachs T. 1975.** The induction of transport channels by auxin. *Planta* **127**(3): 201-206.
- Sachs T. 1986.** Cellular interactions in tissue and organ development. *Symp Soc Exp Biol* **40**: 181-210.
- Saeed AI, Sharov V, White J, Li J, Liang W, Bhagabati N, Braisted J, Klapa M, Currier T, Thiagarajan M, et al. 2003.** TM4: a free, open-source system for microarray data management and analysis. *Biotechniques* **34**(2): 374-378.
- Salehin M, Bagchi R, Estelle M. 2015.** SCFTIR1/AFB-based auxin perception: mechanism and role in plant growth and development. *Plant Cell* **27**(1): 9-19.
- Sauer M, Balla J, Luschnig C, Wisniewska J, Reinohl V, Friml J, Benkova E. 2006.** Canalization of auxin flow by Aux/IAA-ARF-dependent feedback regulation of PIN polarity. *Genes Dev* **20**(20): 2902-2911.
- Sauer M, Friml J. 2010.** Immunolocalization of proteins in plants. *Methods Mol Biol* **655**: 253-263.
- Scarpella E, Marcos D, Friml J, Berleth T. 2006.** Control of leaf vascular patterning by polar auxin transport. *Genes Dev* **20**(8): 1015-1027.
- Schroder F, Lisso J, Lange P, Mussig C. 2009.** The extracellular EXO protein mediates cell expansion in Arabidopsis leaves. *BMC Plant Biol* **9**: 20.
- Schroder F, Lisso J, Mussig C. 2011.** EXORDIUM-LIKE1 promotes growth during low carbon availability in Arabidopsis. *Plant Physiology* **156**(3): 1620-1630.
- Shin K, Lee S, Song WY, Lee RA, Lee I, Ha K, Koo JC, Park SK, Nam HG, Lee Y, et al. 2015.** Genetic identification of ACC-RESISTANT2 reveals involvement of LYSINE HISTIDINE TRANSPORTER1 in the uptake of 1-aminocyclopropane-1-carboxylic acid in Arabidopsis thaliana. *Plant and Cell Physiology* **56**(3): 572-582.
- Smith RS, Guyomarc'h S, Mandel T, Reinhardt D, Kuhlemeier C, Prusinkiewicz P. 2006.** A plausible model of phyllotaxis. *Proc Natl Acad Sci U S A* **103**(5): 1301-1306.
- Svennerstam H, Ganeteg U, Bellini C, Nasholm T. 2007.** Comprehensive screening of Arabidopsis mutants suggests the lysine histidine transporter 1 to be involved in plant uptake of amino acids. *Plant Physiology* **143**(4): 1853-1860.
- Svennerstam H, Ganeteg U, Nasholm T. 2008.** Root uptake of cationic amino acids by Arabidopsis depends on functional expression of amino acid permease 5. *New Phytol* **180**(3): 620-630.
- Swarup K, Benkova E, Swarup R, Casimiro I, Peret B, Yang Y, Parry G, Nielsen E, De Smet I, Vanneste S, et al. 2008.** The auxin influx carrier LAX3 promotes lateral root emergence. *Nat Cell Biol* **10**(8): 946-954.
- Tegeder M, Ward JM. 2012.** Molecular Evolution of Plant AAP and LHT Amino Acid Transporters. *Front Plant Sci* **3**: 21.
- Vanneste S, De Rybel B, Beemster GT, Ljung K, De Smet I, Van Isterdael G, Naudts M, Iida R, Gruitsem W, Tasaka M, et al. 2005.** Cell cycle progression in the pericycle is not sufficient for SOLITARY ROOT/IAA14-mediated lateral root initiation in Arabidopsis thaliana. *Plant Cell* **17**(11): 3035-3050.
- Wabnik K, Govaerts W, Friml J, Kleine-Vehn J. 2011.** Feedback models for polarized auxin transport: an emerging trend. *Mol Biosyst* **7**(8): 2352-2359.
- Wabnik K, Kleine-Vehn J, Balla J, Sauer M, Naramoto S, Reinohl V, Merks RM, Govaerts W, Friml J. 2010.** Emergence of tissue polarization from synergy of intracellular and extracellular auxin signaling. *Mol Syst Biol* **6**: 447.
- Wang J, Xue X, Ren H. 2012.** New insights into the role of plant formins: regulating the organization of the actin and microtubule cytoskeleton. *Protoplasma* **249** Suppl 2: S101-107.
- Wieczorek K, Golecki B, Gerdes L, Heinen P, Szakasits D, Durachko DM, Cosgrove DJ, Kreil DP, Puzio PS, Bohlmann H, et al. 2006.** Expansins are involved in the formation of nematode-induced syncytia in roots of Arabidopsis thaliana. *Plant J* **48**(1): 98-112.

- Wipf D, Ludewig U, Tegeder M, Rentsch D, Koch W, Frommer WB. 2002.** Conservation of amino acid transporters in fungi, plants and animals. *Trends Biochem Sci* **27**(3): 139-147.
- Wisniewska J, Xu J, Seifertova D, Brewer PB, Ruzicka K, Blilou I, Rouquie D, Benkova E, Scheres B, Friml J. 2006.** Polar PIN localization directs auxin flow in plants. *Science* **312**(5775): 883.
- Zhang Y, Schlappi M. 2007.** Cold responsive EARLI1 type HyPRPs improve freezing survival of yeast cells and form higher order complexes in plants. *Planta* **227**(1): 233-243.
- Zhao MR, Han YY, Feng YN, Li F, Wang W. 2012.** Expansins are involved in cell growth mediated by abscisic acid and indole-3-acetic acid under drought stress in wheat. *Plant Cell Rep* **31**(4): 671-685.

3.8 SUPPORTING INFORMATION

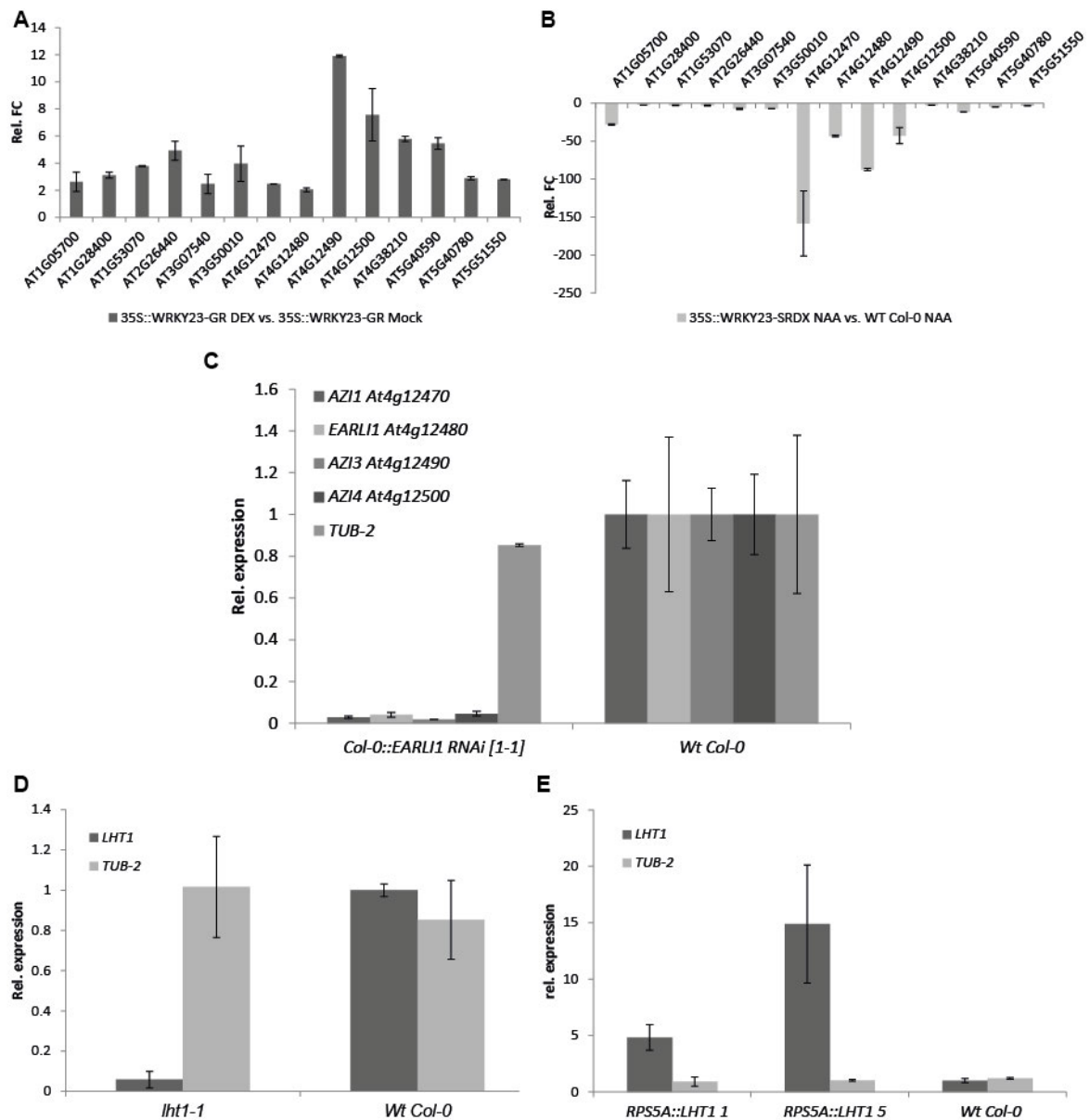


Figure S 3-1 Transcript level confirmation of microarray experiment.

A. Candidate genes are upregulated by WRKY23-GR DEX induction. Bars represent relative fold change of expression. Error bars represent standard deviation B. Candidate genes are downregulated in auxin treated dominant-negative *WRKY23-SRDX* line compared with auxin treated Wt Col-0. Bars represent relative fold change of expression. Error bars represent standard deviation C. *EARL1-like* gene transcript level was decreased in *Col-0::EARL1 RNAi [1-1]* (Cecchini *et al.*, 2015). Bars represent relative fold change of expression. Error bars represent standard deviation D. *LHT1* transcript was almost absent in *lht1-1* T-DNA mutant line. Bars represent relative fold change of expression. Error bars represent standard deviation (see Materials and Methods for detailed description). E. *LHT1* was overexpressed in transgenic lines under control of constitutive RPS5A promoter. Bars represent relative fold change of expression. Error bars represent standard deviation (see Materials and Methods for detailed description).

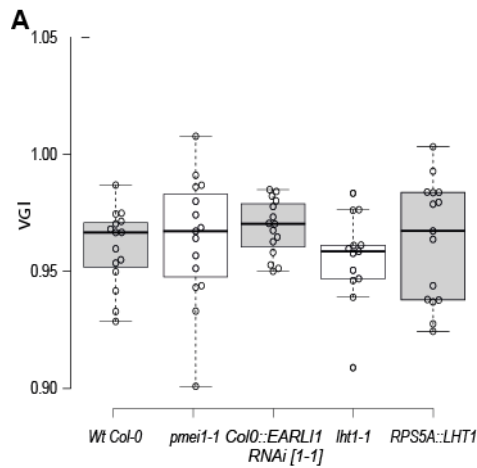


Figure S 3-2 Vertical root growth in accordance to gravity vector observed in mutants of candidate gene line.

A. Vertical root growth in accordance to gravity vector observed in mutants of candidate gene lines shows no or very weak phenotype. Graph shows vertical growth index (VGI), the ratio between the root tip ordinate and the root length (Grabov *et al.*, 2005). Box-whisker plot parameters are as in Fig. 2 B. $n_{\min} = 20$ sample points.

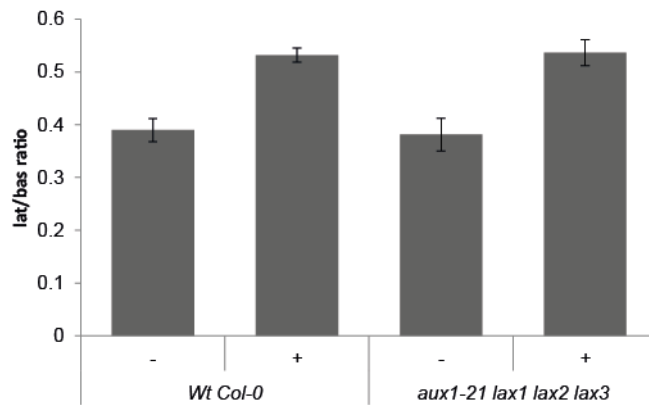


Figure S 3-3 PIN2 re-arrangement in cortex cells in Wt Col-0 and aux1-21 lax1 lax2 lax3.

Graph shows mean ratio of lateral to basal signal intensity of PIN2 in cortex cells in Wt Col-0 and *aux1-21 lax1 lax2 lax3* treated plants with 10 μ M NAA for 4 hours. Error bars indicates standard error.

List of primers used in this study

T-DNA genotyping primers:

Line	Name	Sequence
<i>exp20-1</i>	SALK_062169C_FOR	AAGACAAAGATGAGCCACTCG
<i>exp20-1</i>	SALK_062169C_REV	GTCAGAGCAATCTTTTGTGCGC
<i>exl3-1</i>	SALK_124968C_FOR	GCAATCATTAGGCAAAAGCTG
<i>exl3-1</i>	SALK_124968C_REV	TCAGCCGTTGGATCTAAACAC
<i>pmei1-1</i>	SALK_048655_FOR	TACTTGCTCCAAGCCTTCAAC
<i>pmei1-1</i>	SALK_048655_REV	TGCCCAAATAACCCTTG
<i>chr1-1</i>	SALK_092291C_FOR	TGCGTTGTTGTTTTGTTTTTTC
<i>chr1-1</i>	SALK_092291C_REV	ACAAACATCGCATTGGAAC
<i>chr2-1</i>	SAIL_761_D09_FOR	ATAATCTCCACGAAACATGCG
<i>chr2-1</i>	SAIL_761_D09_REV	CTCCCTCCGTTTCTTAAAG
<i>lht1-1</i>	SALK_034566_FOR	CTGTACATCCCCAAAATCATG
<i>lht1-1</i>	SALK_034566_REV	ACCTGAGAGACATAACGGCAG
T-DNA	SALK_LBa1	TGGTTCACGTAGTGGGCCATCG
T-DNA	SAIL_LB1	CAGAAATGGATAAATAGCCTTGC

qRT-PCR primers:

Gene	Name	Sequence
<i>TUB2</i>	TUB-2_FOR	ACTCGTTGGGAGGAGGAACT
<i>TUB2</i>	TUB-2_REV	ACACCAGACATAGTAGCAGAAATCAAG
<i>WRKY23</i>	WRKY23_FOR	AGTCTCGGTAATGGTTGCTTTGG
<i>WRKY23</i>	WRKY23_REV	TGTTGCTGCTGTTGGTGATGG
<i>AT1G05700</i>	AT1G05700_FOR	TCAAACCAGTCCAATGGCGA
<i>AT1G05700</i>	AT1G05700_REV	TCCTTTGCCGAGGACTTGAC
<i>AT1G28400</i>	AT1G28400_FOR	CGACCGAGACTAACTACGAACAG
<i>AT1G28400</i>	AT1G28400_REV	CTTGCTCCTCAACAACTCTTCAG
<i>AT1G53070</i>	AT1G53070_FOR	AAGTAGTCTCTGTTACGATTG
<i>AT1G53070</i>	AT1G53070_REV	CGAACCAAACCAAACCTG
<i>AT2G26440</i>	AT2G26440_FOR	ATGCCAGGACAATTCACGGT
<i>AT2G26440</i>	AT2G26440_REV	ACGCAAGGATGGAGCAGTTT
<i>AT3G07540</i>	AT3G07540_FOR	GAGGTTCTGCGACTGTGTGA
<i>AT3G07540</i>	AT3G07540_REV	CTCCTCAGCAGCAGTTTCCA
<i>AT3G50010</i>	AT3G50010_FOR	GGACTCGGAAGCCACAAC
<i>AT3G50010</i>	AT3G50010_REV	GAGTATCTCTGGATGAGTAACAC
<i>AZI1</i>	AT4G12470_FOR	ACCCTTACAACACCGAATATAAC
<i>AZI1</i>	AT4G12470_REV	GTGGAGGAGGACATTGGAC
<i>EARL11</i>	AT4G12480_FOR	GTGATGCCCGTGCACAAATA
<i>EARL11</i>	AT4G12480_REV	AGTCTCACTCTCACACATTGGT
<i>AZI3</i>	AT4G12490_FOR	ACACATACGACGCACACAGT
<i>AZI3</i>	AT4G12490_REV	TGCGCGGAAAAAGATAACGC
<i>AZI4</i>	AT4G12500_FOR	CTTAACCACTGCTACTGATTGTC
<i>AZI4</i>	AT4G12500_REV	GGACCGAAGGACTTGAATC
<i>EXP20</i>	AT4G38210_FOR	AAGTGGTTGGTGTGAAAG
<i>EXP20</i>	AT4G38210_REV	TTCCTTGGTATGTCATTCC
<i>AT5G40590</i>	AT5G40590_FOR	CGGTTTAGTTTCAAATGCGATG
<i>AT5G40590</i>	AT5G40590_REV	TCTTTCTTTGCCTCTTCTTTTC
<i>LHT1</i>	AT5G40780_FOR	GCCATCTACAAACCAAGAAATAC
<i>LHT1</i>	AT5G40780_REV	TGCTTGAATAACGATTGTCCTTAG
<i>AT5G51550</i>	AT5G51550_FOR	CACCGCCGATGATGTCTAC
<i>AT5G51550</i>	AT5G51550_REV	CGAACGGATAAGCACAAACTC

Table S 3-1 List of primers used in this study for T-DNA genotyping and qRT-PCR.

4 LRRK1, a leucine-rich repeat receptor-like kinase and its role in auxin-dependent PIN re-arrangement

Tomáš Prát, Wim Grunewald, Gergely Molnár, Elwira Smakowska, Youssef Belkhadir, Bert De Rybel, and Jiří Friml

4.1 INTRODUCTION

The auxin feed-back on polar PIN localization was proposed by canalization hypothesis as a crucial mechanism in mediating multiple developmental processes. We used the auxin effect on PIN polarity in *Arabidopsis* root meristems as a proxy for canalization and performed microarray experiments to find regulators of this process. Recently, we identified a novel regulator downstream of SCF^{TIR1}-Aux/IAA-ARF auxin signalling pathway, transcription factor WRKY23, and demonstrated its crucial role in mediating the auxin effect on PIN polarity (Prat et al., unpublished data). To describe WRKY23 transcriptional network targeting PIN localization and thus regulating plant development, we performed expression profiling experiments using an inducible gain-of-function line (*35S::WRKY23-GR*; Grunewald et al., 2012) and an auxin-treated dominant-negative WRKY23 line (*35S::WRKY23-SRDX*; Grunewald et al., 2012) that is defunct in PIN re-arrangement. Acquired list of putative polarity determinants was further narrowed down by polarity-related phenotype analysis of insertional mutants. We identified *LYSINE-HISTIDINE TRANSPORTER 1* (*LHT1*; *At5g40780*), a small amino acid/auxin permease affecting auxin-dependent PIN repolarization. Nevertheless, observed imperfect phenotypes of gain- and loss-of-function line in *LHT1* gene suggest involvement also other putative players accomplishing regulatory pathway of auxin-dependent PIN repolarization.

Besides other candidates, our microarray focused on identification of putative PIN polarity determinants revealed also a member of leucine-rich repeat receptor-like protein kinase (LRR-RLK) (hereby named as *LRRK1*; *LEUCINE-RICH REPEAT TRANSMEMBRANE PROTEIN KINASE PROTEIN 1*; *At1g05700*). Some *Eukaryotes*, like yeast or animals, use to sense extracellular signals, they activate intracellular signalling pathways and regulate cellular responses via transmembrane G-protein-coupled receptors (GPCRs). However, the existence of GPCRs has never been sufficiently demonstrated in plants (Taddese et al., 2014). Instead, there are 610 RLKs and related receptor-like cytoplasmic kinases in *Arabidopsis* (Shiu &

Bleecker, 2001). Based on extracellular domain structures, RLKs are divided into 21 subfamilies. The most abundant and studied subfamily, leucine-rich repeat LRR-RLKs, contains 223 members in *Arabidopsis*. LRR-RLKs are further grouped into 14 subfamilies (I – XIV) based on protein sequence similarity. Even though LRR-RLKs are best-characterized RLKs, only 89 LRR-RLKs have been described based on their biological function, expression profiles, protein-protein interaction or sequence similarity to known LRR-RLKs and only about 60 of them have been functionally characterized (Wu *et al.*, 2016). LRR-RLKs are cell surface receptors carrying an extracellular LRR domain, a transmembrane domain, and a cytoplasmic kinase domain. The LRRs are involved in ligand binding, whereas the kinase domain can be involved in auto- and/or trans-phosphorylation and is potentially able to initiate a signal transduction cascade (Liebrand *et al.*, 2014). LRR-RLKs play a fundamental role in cell-to-cell and plant-environment communications in plant development and defense responses (Li & Tax, 2013). The best described LRR-RLKs are BR receptor BRASSINOSTEROID INSENSITIVE 1 (BRI1) and coreceptor BRI1-ASSOCIATED RECEPTOR KINASE 1 (BAK1) (Li & Chory, 1997; Hothorn *et al.*, 2011; Santiago *et al.*, 2013). BAK1 belongs to subfamily II of LRR-RLK containing signal peptide at the N-terminus followed by four leucine zippers, five LRRs, a proline-rich region, a single transmembrane domain, and serine/threonine protein kinase domain (Li *et al.*, 2002). In contrast, BRI1 is a member of distinct subfamily X with 25 LRRs separated by unique 70 amino acid loop-out “island” between 21st and 22nd LRR, a single transmembrane domain, and an intracellular serine/threonine protein kinase domain (Li & Chory, 1997). A combination of receptor with numerous repeats of LRRs and rather short BAK1 is also present in signalling pathways regulating plant innate immunity. BAK1 acts as coreceptor interacting with LRR-RLKs FLAGELLIN SENSITIVE 2 (FLS2) flagellin receptor (Chinchilla *et al.*, 2007b; Sun *et al.*, 2013), EF-Tu RECEPTOR (EFR) EF-Tu peptide receptor, PEPTIDE RECEPTOR 1 and 2 (PEPR1 and PEPR2) endogenous Pep peptides receptors in defense processes (Heese *et al.*, 2007; Postel *et al.*, 2010; Roux *et al.*, 2011). Extracellular LRRs conformation suggest that the ligands of receptors may be likely peptides either from plant cells or pathogens, with exception of the BR receptor complex BRI1-BAK1 mediated BR signalling pathway (Wu *et al.*, 2016). Spectra of potential ligands could be extended by interaction with leucine-rich repeat-receptor-like proteins (LRR-RLPs) that carry an extracellular LRR ligand-binding domain but lack any obvious cytoplasmic signalling competent moiety, as was shown in case of SUPPRESSOR OF BIR1-1 (SOBIR1) LRR-RLK interacting with RLP30 (Zhang *et al.*, 2013; Liebrand *et al.*, 2014).

Identified LRR-RLK belongs to subfamily I of LRR-RLK. Amino acid sequence analysis revealed a predicted signal peptide at its N-terminus followed by relatively long extracellular domain containing three LRR repeats, a single helical transmembrane domain, and intracellular serine/threonine protein kinase domain. Sequence alignment of extracellular domain of LRRK1 showed very low identity (max. 50 – 52.9%; E-value: 24E-168 - 120E-156) to other LRR-RLKs, neighbor-joining phylogenetic tree visualizes an isolated position within subfamily I of LRR-RLKs (**Fig. S4-1 A**). LRRK1 is topologically analogous to LIGHT-REPRESSIBLE RECEPTOR PROTEIN KINASE (LRRPK; At3g21340) (Deeken & Kaldenhoff, 1997), even though they are sequentially different (**Fig. S4-1 B**).

In this work, we characterized the role of LRRK1 in auxin-dependent PIN re-arrangement. We described its transcriptional behaviour, subcellular localization and studied its role in PIN protein recycling. Based on global expression data, we tried to identify ligand responsible for mechanism of signalling and suggested plausible signalling partners.

4.2 MATERIALS AND METHODS

4.2.1 Plant material and growth conditions

All *Arabidopsis thaliana* lines were in Columbia-0 background. T-DNA mutants were acquired from the Nottingham *Arabidopsis* Stock Centre (NASC; <http://www.arabidopsis.info>). T-DNA mutants used in this study are SALK_025603C (*lrrk1-1*), SALK_055351C (*pxc2-1*) and SALK_018730C (*pxc2-2*). Primers used in genotyping are listed in Supporting information (Table S4-1). The *arf7 arf19* double mutant (Okushima *et al.*, 2005), *HS::axr3-1* (Knox *et al.*, 2003), *35S::WRKY23-GR* and *35S::WRKY23-SRDX* (Grunewald *et al.*, 2008; Grunewald *et al.*, 2012), *LRRK1::GUS*, *PXC2::GUS* and *RHS16::GUS* (Wu *et al.*, 2016) have been described previously. Seeds were sterilized overnight by chlorine gas, sown on solid *Arabidopsis* medium (AM+: half-strength MS basal salts, 1% Sucrose, and 0.8% phyto-agar, pH 5.7), and stratified at 4°C for at least 2 days prior to transfer to a growth room with a 16-h-light/8-h-dark illumination regime at 21°C. Seedlings were grown vertically for 4 or 6 days, depending on the assay.

4.2.2 Construction of transgenic lines

DNA constructs were created with the Gateway cloning technology (Karimi *et al.*, 2007) (Invitrogen). For the *RPS5A::LRRK1* construct, a 3450-bp-long LRRK1-specific fragment was amplified from a genomic DNA template with iProof High-Fidelity DNA Polymerase (BioRad) with primer LRRK1_attB1_Fw (5'-GGGGACAAGTTTGTACAAAAAAGCAGGCTTCATGGAAGAGTTTCGTTTTCTC-3') and primer LRRK1_attB2_Rv (5'-GGGGACCACTTTGTACAAGAAAGCTGGGTTTCAATAGTTCTTGTTACTCTCTTC-3') and recombined by BP reaction with pDONR221 to yield pEN-L1-LRRK1-R2. Latter vector was then recombined by LR MultiSite reaction with pEN_L4_RPS5A_R1, pEN-L1-LRRK1-R2 and the binary gateway vector pB7m24GW,3. For the *35S::LRRK1-GFP* construct a 3459-bp-long LRRK1-specific fragment was amplified from a genomic DNA template with primer LRRK1_attB1_Fw mentioned above and stop codon was substituted by three amino acid linker (Trp; Asp; Pro) with primer LRRK1ns_attB2_Rv (5'-GGGGACCACTTTGTACAAGAAAGCTGGGTTTGGTTCCCAATAGTTCTTGTTACTCTCTTC-3') and recombined by BP reaction with pDONR221 to yield pEN-L1-LRRK1ns-R2. Latter vector was then recombined by LR reaction with the binary gateway vector pB7FWG2.0. The obtained vectors were transformed to *Agrobacterium tumefaciens* strain C58C1 (pMP90), which was used in a floral dip transformation of *Arabidopsis thaliana* (L.) Heyhn Columbia-0 (Col-0) (Clough & Bent, 1998). At least two independent transgenic lines were examined. Overexpression of these lines was confirmed by qRT-PCR, primers are included in Supporting information (Table S4-1).

4.2.3 Pharmacological treatments

Arabidopsis treatments with auxin or chemicals were done in liquid AM+ medium at 21°C in a growth room. For auxin treatment, plants were incubated with 10 µM α-naphthaleneacetic acid (NAA; Sigma Aldrich) for 4h or 6h; while dexamethasone (DEX; Sigma Aldrich) was applied in 10 µM concentration for 6h or 24h. For BFA and NAA/BFA experiments, seedlings were incubated in 25 µM of Brefeldin A (BFA; Sigma Aldrich) for 90 min, 10 µM NAA for 30 min for pre-treatments and with 25 µM BFA/10 µM NAA for 90 min for co-treatments. For flg22 application, seedlings were treated with 10 µM of flg22 peptide by 5min vacuum infiltration

and then observed after 30 min. Mock treatments were performed with equivalent amounts of DMSO.

4.2.4 IP and MS

IP experiments were performed as described previously (Zwiewka *et al.*, 2011) using 3 g of seedlings of *35S::LRRK1-GFP* transgenic line in Col-0 background. Interacting proteins were isolated by applying a total protein extracts to anti-GFP-coupled magnetic beads (Milteny Biotech). Three biological replicates of each sample were compared with three nontransgenic Col-0 samples. MS and statistical analysis using MaxQuant and Perseus software were performed as described previously (Hubner *et al.*, 2010; Lu *et al.*, 2011) with minor modifications.

4.2.5 RNA extraction, cDNA synthesis, and quantitative RT-PCR and analysis

RNA extraction, cDNA Synthesis, and quantitative RT-PCR was performed as described by Tejos *et al.* (2014). Targets were quantified with specific primer pairs designed with Primer-BLAST (<http://www.ncbi.nlm.nih.gov/tools/primer-blast/>). Expression levels were normalized to *GAMMA-TUBULIN 2 (TUB2; At5g05620)* which was constitutively expressed across samples. All PCRs were run in three technical repeats and the data were processed with qRT PCR analysis software (Frederik Coppens; Applied Bioinformatics & Biostatistics group; PSB VIB, Belgium). Primers used in the study are listed in Supporting information (Table S4-1).

4.2.6 Whole-mount *in situ* Immunolocalization, microscopy and quantitative analysis of PIN relocation

PIN immunolocalizations in primary root were performed as described by Sauer and Friml (2010). The antibodies were used in the following dilutions: anti-PIN1, 1:1000 (Paciorek *et al.*, 2005) and anti-PIN2, 1:1000 (Abas *et al.*, 2006). In all cases, the secondary goat anti-rabbit antibody coupled to Cy3 (Sigma-Aldrich) was diluted 1:600. Confocal microscopy was performed using a Zeiss LSM 700 confocal microscope. Quantitative analysis of PIN relocation was performed as described by Sauer *et al.* (2006).

4.2.7 Transient expression in *Arabidopsis* mesophyll protoplasts

Mesophyll protoplasts were isolated from rosette leaves of 4-week-old *Arabidopsis* plants grown in soil under controlled environmental conditions in a 16:8 h light/dark cycle or under continuous light at 21 °C. Protoplasts were isolated and transient expression assays were carried out as described (Wu *et al.*, 2009) with minor modifications. Protoplasts were transfected with 10 or 20 µg of a reporter plasmid DNA of the binary gateway vector pB7FWG2.0 that contained *LRRK1-GFP* under the control of the 35S promoter. Protoplasts were overnight dark incubated at room temperature in glucose-mannitol GM medium. Next day protoplasts were observed using Zeiss LSM 700 confocal microscope.

4.2.8 Histological analyses and microscopy

To detect β-Glucuronidase (GUS) activity, seedlings were incubated in reaction buffer containing 0.1 M sodium phosphate buffer (pH 7), 1 mM ferricyanide, 1 mM ferrocyanide, 0.1% Triton X-100 and 1 mg/ml X-Gluc for 2 h in dark at 37 °C. Afterwards, chlorophyll was removed by destaining in 70% ethanol and seedlings were cleared.

Propidium iodide staining was performed by incubating roots samples in 10 µg/ml propidium iodide (PI; Sigma Aldrich) solution for 5 min. For FM6-64 staining, seedlings were stained in 2 µM of FM4-64 (FM4-64; Sigma Aldrich) solution for 1 min at room temperature.

Clearing of tissues (seedlings, cotyledons) was performed in a solution containing 4% HCl and 20% methanol for 15 min at 65 °C, followed by 15 min incubation in 7% NaOH and 70% ethanol at room temperature. Next, seedlings were rehydrated by successive incubations in 70, 50, 25 and 10% ethanol for 5 min, followed by incubation in a solution containing 25% glycerol and 5% ethanol. Finally, seedlings were mounted in 50% glycerol and monitored by differential interference contrast microscopy DIC (Olympus BX53) or stereomicroscope (Olympus SZX16).

4.3 RESULTS AND DISCUSSION

4.3.1 *LRRK1* gain-of-function causes PIN2 lateralization

LRRK1 gain-of-function caused increased lateralization of PIN2 protein in young cortex cells of root. To confirm involvement of *LRRK1*, we cloned genomic DNA and expressed under constitutive promoter *RPS5A* to get strong overexpression (**Fig. S4-2**). In young cortex cells,

application of NAA changed localization of PIN2 from basal to outer lateral side (**Fig.4-1 A**). PIN2 proteins in gain-of-function lines were immunolocalised and fluorescent signal on basal and lateral membrane of cortex cells was measured. We observed increase in lateral localization of PIN2 proteins in plants overexpressing *LRRK1* (**Fig.4-1 B, D**). Treatment of auxin further increased laterality of PIN2 proteins to levels similar in auxin treated Wt Col-0 (**Fig.4-1 B, D**). In contrast to observed lateralization in gain-of-function plants, T-DNA knock-out mutant *Irrk1-1* (**Fig. S4- 2**) showed lower ability of auxin-dependent PIN repolarization (**Fig.4-1 C, E**). Mutation in candidate gene *LRRK1* had consequence in less pronounced lateralization of the PIN2 protein in cortex cell. Without auxin application, PIN2 polarity was not altered (**Fig.4-1 C, E**). These results showed that *LRRK1* gene is necessary for successful repolarization of the PIN proteins but polarity establishment is not affected.

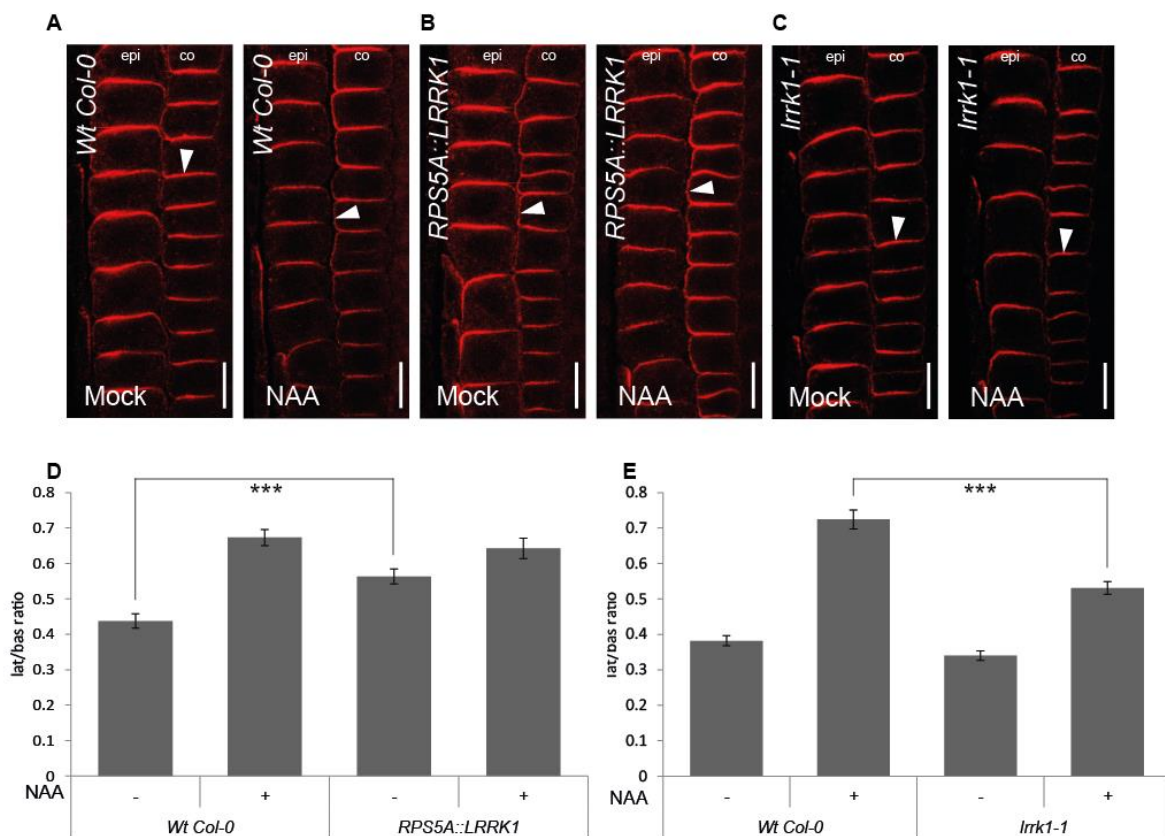


Figure 4-1 Immunolocalization of PIN2 protein in root of *LRRK1* gain- and loss-of-function lines.

A. Cortex cells of Wt Col-0 treated with Mock/NAA. Arrowheads highlight PIN polarity. B. Cortex cells of *Irrk1-1* treated with Mock/NAA. Arrowheads highlight PIN polarity. C. Cortex cells of *LRRK1* gain-of-function line treated with Mock/NAA. Arrowheads highlight PIN polarity. D. Visualization of mean ratio of lateral to basal signal intensity of PIN2 in cortex cells in Wt Col-0 and *Irrk1-1* treated plants with 10 μ M NAA for 4 hours. Error bars indicates standard error. A two-tailed Student's t test compared marked sets of data. (***) $P < 0.0001$. $n > 50$

cells corresponding to roots imaged under comparable conditions. E. Visualization of mean ratio of lateral to basal signal intensity of PIN2 in cortex cells in *RPS5A::LRRK1* plants treated with 10 μ M NAA for 4 hours. Error bars indicates standard error. A two-tailed Student's t test compared marked sets of data. (***) $P < 0.0001$. $n > 50$ cells corresponding to roots imaged under comparable conditions.

4.3.2 **WRKY23 influences auxin signalling-dependent transcription regulation of *LRRK1***

In our previous study, we demonstrated that dexamethasone-inducible gain-of-function *35S::WRKY23-GR* increased re-arrangement of PIN2 in the young cortex cells of the root comparably to auxin NAA treatment (Prat et al., unpublished data). Therefore, we checked expression of *LRRK1* in this line. *LRRK1* gene has increased expression level after activation of dexamethasone inducible gain-of-function *35S::WRKY23-GR* (**Fig.4-2 A**). After NAA application, transcript level of *LRRK1* increased, while after the same auxin treatment in dominant-negative *35S::WRKY23-SRDX* line, mRNA level of *LRRK1* decreased in comparison with the control line Wt-Col0 (**Fig.4-2 A**). These results suggested that *WRKY23* TF regulates transcription of *LRRK1*.

As was previously shown, in the inducible *HS::axr3-1* mutant line expressing a non-degradable version of the IAA17 transcriptional repressor, as well as in the *arf7 arf19* double mutant defective in these two transcriptional activators, auxin was ineffective to mediate PIN polarity re-arrangements (Sauer et al., 2006). We also showed *WRKY23* dependence on auxin signalling that was supported by a compromised *WRKY23* auxin inducibility in these auxin signalling mutants. In auxin signalling mutants, activated *HS::axr3-1* and *arf7 arf19*, application of NAA was not able to increase transcript level of *LRRK1* (**Fig.4-2 B**). Based on these results, auxin acts through its signalling pathway to activate expression of *WRKY23* transcriptional factor and subsequently, *WRKY23* transactivation regulates expression of effector, *LRRK1*, identified in the microarray experiment (**Fig.4-2 B**).

We used the same approach to describe transcriptional regulation of candidate genes as in the previous study of *WRKY23* action in PIN repolarization. As well as *WRKY23*, *LRRK1* expression depended on concentration of applied auxin. Four hours of 10 nM NAA already increased *LRRK1* mRNA amount three times while *WRKY23* gene had higher expression in 100 nM NAA (**Fig.4-2 C**). This sensitivity to auxin application lead to hypothesis that expression of these genes is also directly activated by auxin signalling and *WRKY23* acts as a tight regulator. This is further supported by temporal regulation of the *LRRK1* expression. We observed that

30 minutes of 10 μ M NAA already increased *LRRK1* gene expression while *WRKY23* gene had higher expression in 10 μ M NAA between 120 and 240 minutes of auxin treatment (Fig.4-2 D). Therefore, we suppose that expression of *LRRK1* is tightly regulated by auxin.

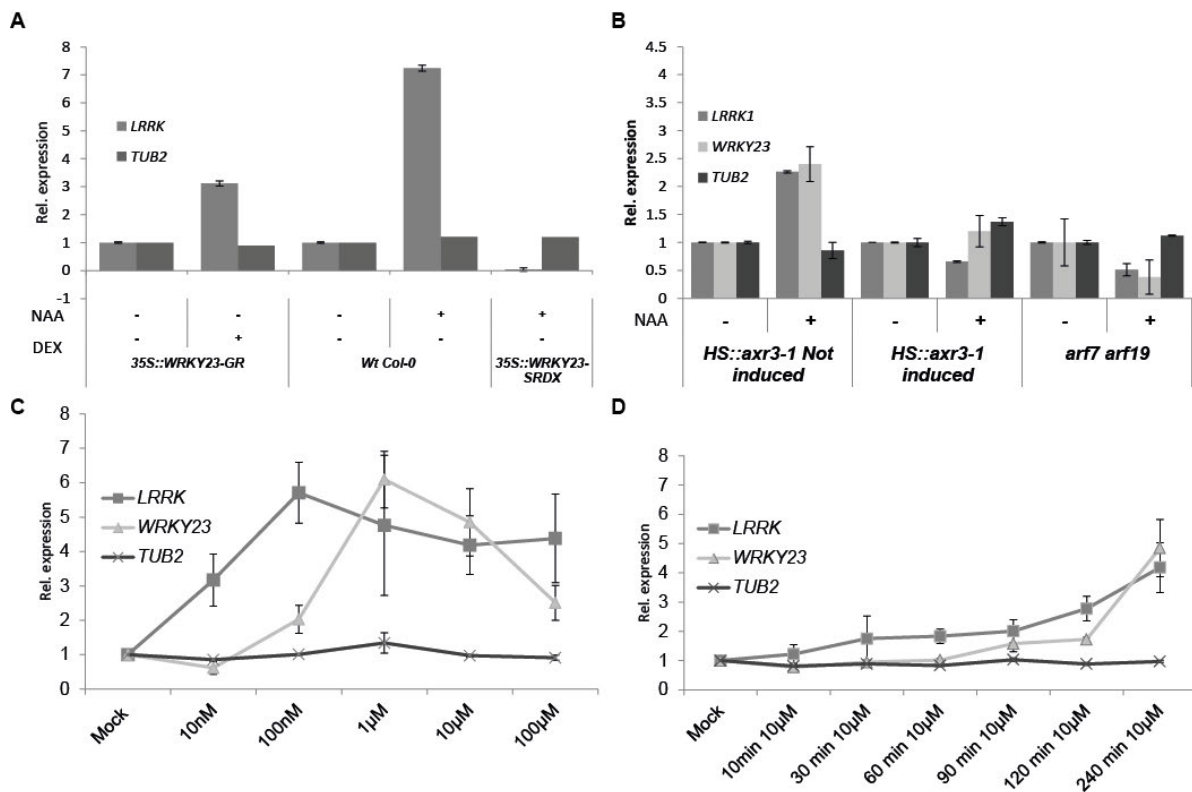


Figure 4-2 Transcript levels of *LRRK1* during auxin treatments.

A. *LRRK1* transcript level depends on *WRKY23*. qRT-PCR experiment showed dependence of *LRRK1* transcript levels on *WRKY23* normalized to mRNA levels in controls. Bars represent relative fold change of expression. Error bars represent standard deviation (see Materials and Methods for detailed description). B. *LRRK1* transcript level is dependent on auxin through the SCF^{TIR1}-Aux/IAA-ARF signalling pathway. qRT-PCR experiment showed transcript levels of *LRRK1* in auxin signalling mutants *HS::axr3-1* and *arf7 arf19*. Bars represent relative fold change of expression. Error bars represent standard deviation (see Materials and Methods for detailed description). C. – D. *LRRK1* expression is auxin dose- and time-dependent. qRT-PCR experiment showed transcript levels of *LRRK1* in Wt Col-0 seedlings treated with respective concentration of NAA for respective time. Points represent relative fold change of expression. Error bars represent standard deviation (see Materials and Methods for detailed description).

4.3.3 Subcellular localization of LRRK1 and its function in constitutive PIN cycling

To address how LRRK1 influences PIN polarity, we created reporter fusion of LRRK1 and fluorescent marker eGFP to the C-terminus by replacing *LRRK1* stop codon with three amino acid linker Trp-Asp-Pro like in another LRR-RLK *BRI1* (Friedrichsen *et al.*, 2000). Predicted structure of LRRK1 proposes presence of single span helical transmembrane domain at position 511 – 531. First, we checked subcellular localization of LRRK1 in *Arabidopsis* protoplast transient expression system. Observed fluorescent signal tightly colocalized with CM of *Arabidopsis* mesophyll protoplast (**Fig.4-3 A**). This was further confirmed by short application of FM4-64 staining CM or propidium iodide staining cell wall on roots with stable expression of *LRRK1-GFP* (**Fig.4-3 B, C**). Immunolocalization of PIN2 in *LRRK1-GFP* reporter line demonstrated that both proteins colocalized on cell membrane. In comparison with rigorous presence of PIN2 on apical domain of root epidermal cells, localization of LRRK1 was apolar (**Fig.4-3 D**). Similarly, colocalization of *LRRK1-GFP* and immunolocalized PIN1 in cortex cells is only at basal and inner lateral sides while *LRRK1-GFP* signal is present also on apical and outer lateral sides of cortex cells (**Fig.4-3 E, F**).

Auxin was for long time evidenced to block endocytosis of PIN proteins from CM. Nevertheless, recent publication of Jasik and collaborators disprove this auxin effect on endocytosis (Paciorek *et al.*, 2005; Jasik *et al.*, 2016). Application of fungal toxin Brefeldin A (BFA) on *LRRK1-GFP* reporter led to formation of so-called BFA bodies that were shared with PIN2 proteins (**Fig.4-3 G, H**). Interestingly, pre-treatment with auxin analogue NAA did not lead to inhibition of BFA bodies formation of LRRK1-GFP as robustly as was described in case of PIN2 proteins (**Fig.4-3 G – I**) (Paciorek *et al.*, 2005; Jasik *et al.*, 2016). Moreover, strong constitutive overexpression of *LRRK1* caused decreased ability of PIN1 and PIN2 to form BFA bodies (Data not shown).

Altogether, described subcellular localization LRRK1 to CM, ability to cycle between endomembrane systems, and effect on BFA bodies formation guided us to hypothesis, that LRRK1 protein sense an unknown extracellular ligand that influences polarity of PIN proteins.

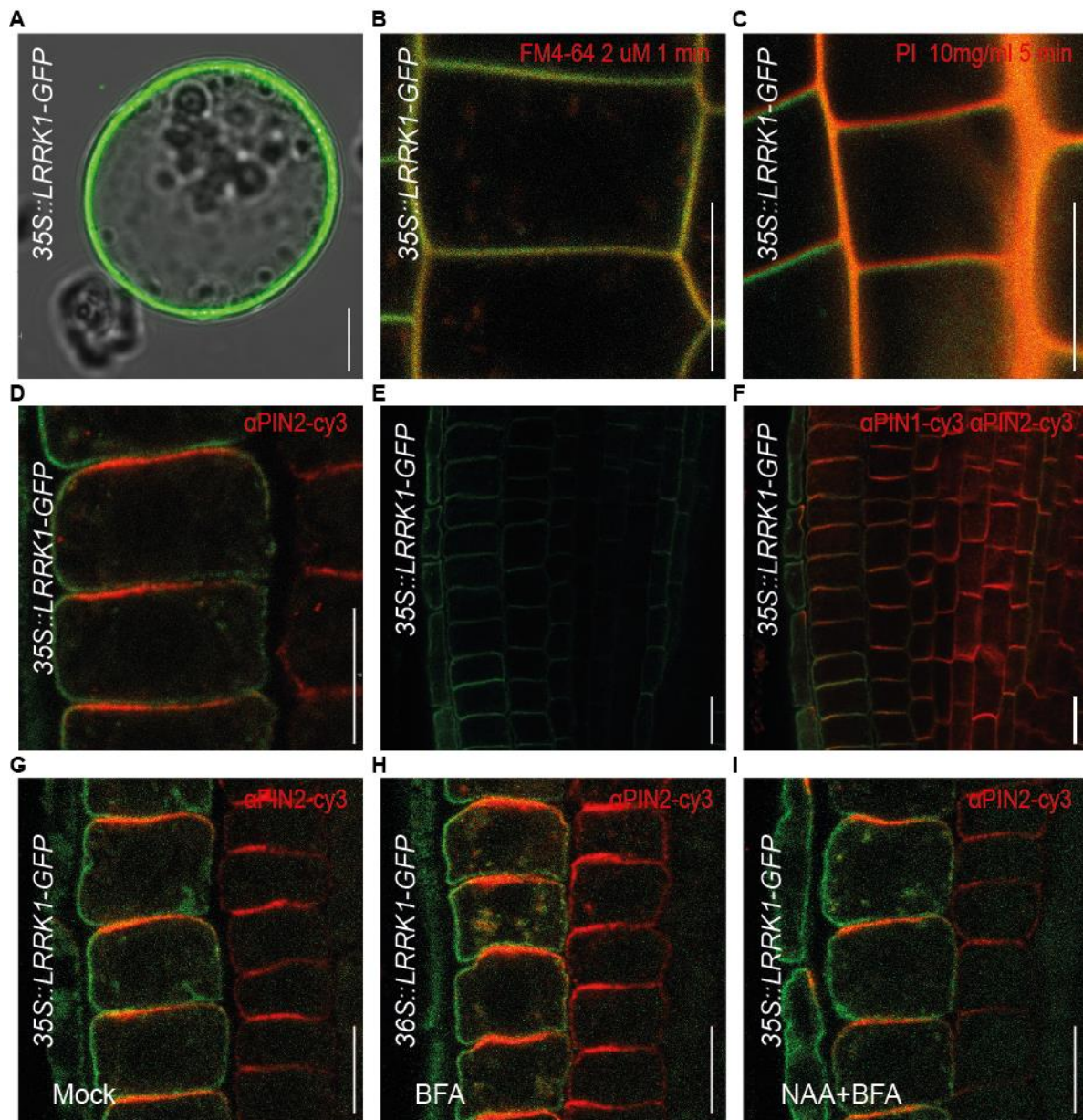


Figure 4-3 Subcellular localization of LRRK1.

A. Transient expression of 35S::LRRK1-GFP in *Arabidopsis* protoplasts. Protoplasts were isolated from rosette leaves and transfected with vector containing 35S::LRRK1-GFP construct. B. Short FM4-64 (2 μM) staining of *Arabidopsis* root. Red dye tightly colocalized with 35S::LRRK1-GFP. C. Propidium iodine staining of *Arabidopsis* root. Likewise, red dye tightly colocalized with 35S::LRRK1-GFP. D. PIN2 immunolocalization of root epidermal cells in 35S::LRRK1-GFP. Colocalization of 35S::LRRK1-GFP with PIN2 on CM. PIN2 is localized on apical side of cells whereas LRRK1-GFP localization is apolar. E. – F. PIN1 and PIN2 immunolocalization of root of 35S::LRRK1-GFP. G. – I. BFA and NAA/BFA treatments of 35S::LRRK1-GFP root cells. Bar size 10 μm.

4.3.4 Application of auxin and flg22 does not lead to LRRK1 internalization

LRR-RLKs are known as receptors of various extracellular signals. Thus, first we tried to identify ligand of LRRK1. We searched for transcriptional regulators of LRRK1 by application of condition search tool in GENEVESTIGATOR® (Nebion AG) global library of expression data (Zimmermann *et al.*, 2004). We found that the strongest perturbations of LRRK1 expression data were caused by bacterial peptides (EF-Tu and flg22), auxin IAA, and NAA (**Fig. S4-3**). Moreover, upregulation of *LRRK1* by defense-related WRKY23 TF suggests that original function of this LRR-RLK is in plant immunity by its interaction with, *e.g.* FLS2 receptor of bacterial flagellin, as was shown for FLS2-BAK1 (Chinchilla *et al.*, 2007b; Sun *et al.*, 2013). FLS2 underwent ligand induced endocytosis (**Fig.4-4 A**) (Robatzek *et al.*, 2006). As part of the immune response, cell membrane FLS2 is activated by flg22 and recruited to ARABIDOPSIS RAB GTPase ARA7/RabF2b- and ARA6/RabF1-positive endosomes which are compartments of the late endosomal trafficking pathway (Robatzek *et al.*, 2006; Beck *et al.*, 2012). This process depends on BAK1/SERK3 (Chinchilla *et al.*, 2007b; Beck *et al.*, 2012), which itself undergoes constitutive endocytosis (Rusinova *et al.*, 2004). We applied flg22 peptide to seedlings expressing LRRK1-GFP and FLS2-GFP. We observed fluorescent endocytic vesicles 30 minutes after application of flg22 in FLS2-GFP fluorescent marker line, the same application to LRRK1-GFP did not lead to internalization (**Fig.4-4 B**). We did not observe any changes in subcellular localization of LRRK1 even after prolonged treatment (Data not shown).

Second group of possible ligands suggested by GENEVESTIGATOR® database was auxin; we therefore tested auxin action on *LRRK1* reporter fusion. Auxin application had effect neither on polarity, nor subcellular localization of LRRK1. We measured ratio of lateral to basal fluorescent signal of LRRK1, similarly to lateral index of PIN proteins (**Fig. 4 C**) (Sauer *et al.*, 2006). We did not observe any significant change from original apolar localization of LRRK1, however, only very mild increase of inner lateral fluorescent signal in cells of epidermis was observed (**Fig.4-4 D**). Auxin application also caused non-significant decrease of intracellular to membrane fluorescence ratio (**Fig.4-4 E**). Overall fluorescence was only marginally lower (**Fig.4-4 F**). Observed non-significant difference in fluorescence, subcellular localization, and membrane polarity of LRRK1 imply no effect of auxin on these processes. On other hand, ligands are not always affecting these processes on its receptors as was shown on BR receptor BRI1 (Santiago *et al.*, 2013). Our survey on ligand was not successful; hence we focused our attention on identification of interactors of LRRK1.

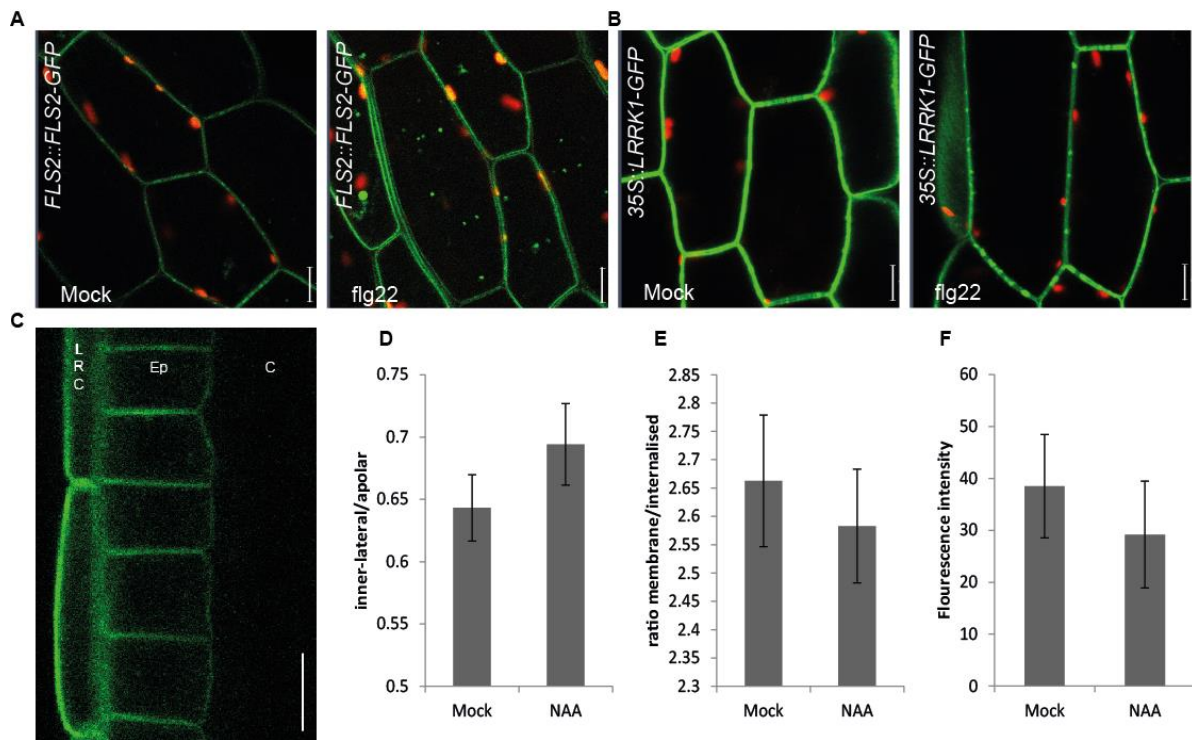


Figure 4-4 Effect of suggested ligands on LRRK1 subcellular localization.

A. Ligand-induced endocytosis of FLS2 by flg22. Hypocotyl epidermal cells of FLS2 reporter line underwent ligand-induced endocytosis upon application of bacterial peptide flg22. B. flg22 application on hypocotyl epidermal cells of LRRK1-GFP line. C. Auxin application on root cells of LRRK1-GFP line. Bar size 10 μ m. D. Graph shows mean ratio of inner-lateral to apolar signal intensity of LRRK1-GFP in epidermal cells treated with 10 μ M NAA for 4 hours or DMSO. E. Graph shows mean ratio of signal on membrane to intracellular signal intensity of LRRK1-GFP epidermal cells treated with 10 μ M NAA for 4 hours or DMSO. F. Graph shows mean value of signal intensity of LRRK1-GFP epidermal cells treated with 10 μ M NAA for 4 hours or DMSO.

4.3.5 Signalling interactors of LRRK1

LRR-RLKs act in complexes with other RLKs to increase specificity of ligand binding and sensing. Previously identified receptor complexes suggested that LRR-LRKs need a ligand binding receptor and co-receptor. Ligand binding with the receptor creates a new binding surface to a co-receptor, signalling cascades can be then initiated only when the receptor-ligand-co-receptor complex is formed (Wu *et al.*, 2016). Generally, these complexes are created from interaction of high order LRR receptors and rather short co-receptor LRR-RLKs. Most thoroughly studied LRR-RLKs, BRI1 and FLS2, share common signalling component and have slightly different activation mechanisms (Belkhadir *et al.*, 2014). The best example of these complexes is BRI1 LRR-RLK. Activated by brassinosteroid BRI1 phosphorylates negative

regulator BRASSINOSTEROID KINASE INHIBITOR 1 (BKI1) leading to displacement from membrane to cytosol where it become inactive (Jaillais *et al.*, 2011). Then, a co-receptor LRR-RLK BAK1 can create complex with BRI1 associated with transphosphorylation of kinase domains (Bajwa *et al.*, 2013). In parallel, activated BRI1 kinase phosphorylates BR SIGNALING KINASE 1 (BSK1), receptor-like cytoplasmic kinase (Tang *et al.*, 2008; Sreeramulu *et al.*, 2013). BSK1 positively regulates BR signalling by relaying BRI1 signals to downstream signalling components, *e.g.* BRASSINOSTEROID INSENSITIVE 2 (BIN2) glycogen synthase kinase 3 (GSK3)-type kinase (Li *et al.*, 2001), or negatively regulates the pathway by phosphorylating downstream transcription factors BRASSINAZOLE RESISTANT 1 (BZR1) and BRI1-EMS suppressor1 (BES1) at multiple sites (Kim *et al.*, 2009).

We checked possible interactors of LRRK1 in testbed of other LRR-RLKs on insect cell expression system *in vitro*. Genome-scale interaction assay developed for high throughput identification of extracellular domain association uses phosphorylation of protein bait with a result of substrate colour change upon reaction with the enzyme (Belkhadir and Smakowska, personal communication). Based on *in vitro* interaction screen on extracellular domains of LRR-RLKs, two potential interactors with high confidence were identified: PXY/TDR CORRELATED 2 (*PXC2*; At5g01890) type VII and ROOT HAIR SPECIFIC 16 (*RHS16*; At4g29180) type I LRR-RLK. *PXC2* is classified to a small group of three LRR-RLKs based on *in silico* co-expression and functional clustering analyses with similar transcript profile like *PXY/TDR* (Wang *et al.*, 2013). PHLOEM INTERCALATED WITH XYLEM (PXY) is a member of XI LRR-RLK subfamily and acts as receptor of TDIF (Tracheary element differentiation factor), or known as CLAVATA3/ENDOSPERM SURROUNDING REGION41/44 (CLE41/44) (Fisher & Turner, 2007; Hirakawa *et al.*, 2008). CLE peptides usually contain 12 - 13 amino acids. They are essential for regulation of proliferation and differentiation of the shoot apical meristems, root apical meristem, and procambium (Fukuda, 2016). CLE44/41 was shown to inhibit xylem cell differentiation and to promote procambial cell proliferation (Ito *et al.*, 2006). CLE peptides are expressed in phloem cells, then transferred to procambial zone where mature and are immediately sensed by PXY (Etchells & Turner, 2010). Activated complex of CLE peptide ligand and PXY receptor promotes procambial cell proliferation by triggering WUS homologs, *WOX4* and *WOX14* (Hirakawa *et al.*, 2010; Etchells *et al.*, 2013). CLE-PXY complex also influences expression of *BES1*, a downstream TF of BRI1 signalling cascade to suppress tracheary element differentiation (Kondo *et al.*, 2014). Structural study of CLE-PXY complex revealed

conserved recognition mechanism. Comparison of other XI LRR-RLK subfamily receptors showed conserved Arg-x-Arg motif important for recognition of their peptide ligands (Song *et al.*, 2016; Zhang *et al.*, 2016b). To regulate procambial cell proliferation, PXY receptor uses to sense TDIFs interaction with co-receptor SOMATIC EMBRYOGENETIC RECEPTOR KINASE (SERK1/SERK2/BAK1/BAK1-LIKE) (Zhang *et al.*, 2016a). Family of LRR-RLKs commonly acts as co-receptors of *e.g.* BR (BRI1-BAK1) or immune signalling (FLS2-BAK1) and therefore, they are involved in wide spectrum of processes like plant development and defense (Li *et al.*, 2002; Nam & Li, 2002; Chinchilla *et al.*, 2007a).

Expression pattern of suggested interactor *PCX2* correlates with *PXC3* and with *REVOLUTA* class III HD-ZIP transcriptional regulator important in vascular differentiation (Etchells & Turner, 2010). *PXC2* was, in contrast to *PXY*, expressed in the root tip while *PXY* expression begins in elongation zone (Wang *et al.*, 2013). *PXC2* belongs to subfamily VII with 18 extracellular LRRs whereas *PXY* is a member of subfamily XI with 21 LRRs. Moreover, alignment of extracellular domains of *PXY* and *PXC2* revealed only 32% identity of amino acid sequence.

RHS16 belongs to subfamily I of LRR-RLKs. *RHS16* was originally identified in a screen of root hair specific genes based on presence of conserved RHE (root hair element) cis-element in promoter (Won *et al.*, 2009). The same cis-element is present in all known morphogenetic H genes (Kim *et al.*, 2006). Core RHE consists of 16 or 17 nucleotides with incomplete palindromic structure. Composite consensus of RHE elements of WHHDTGNNN(N)KCACGWH within 1000 bp upstream of start codons were used to obtain fundamental overview on genes expressed in root hairs. A list of genes was further filtered using expression profiling experiments, promoter assays, *etc.*, to final set of 24 genes, containing also *RHS16* (Won *et al.*, 2009). Similarly, *RHS16* was identified in computational screen of microarrays and virtual *Arabidopsis* root hair proteome (Cvrckova *et al.*, 2010).

First, we checked spatio-temporal expression patterns of potential interactors to find out whether interaction is physically possible. Then, we used transcriptional reporter fusions (Wu *et al.*, 2016) to test effect of auxin application on expression pattern. *LRRK1::GUS* reporter was expressed in the cells of elongation zone of the root (**Fig.4-5 A**) (Wu *et al.*, 2016). Auxin application expanded expression pattern of *LRRK1*. We applied effective amount of NAA to transcription fusion of *LRRK1* promoter with GUS. After 6 hours of auxin application, expression pattern was shifted to the younger cells of epidermis and cortex where a PIN

repolarization event happens (**Fig.4-5 A**). *PXC2::GUS* reporter expression pattern in the root tip comprises LRC, cells close to QC, young cortex and endodermis cells, and cells of two procambial poles (**Fig. 4-5 B**). Auxin application led to diffusion of expression pattern to meristematic zone of the root where it can meet expression pattern of *LRRK1*. Expression pattern of *RHS16* was exclusively localised in root hairs and did not overlap with any of potential interactors (**Fig.4-5 C**).

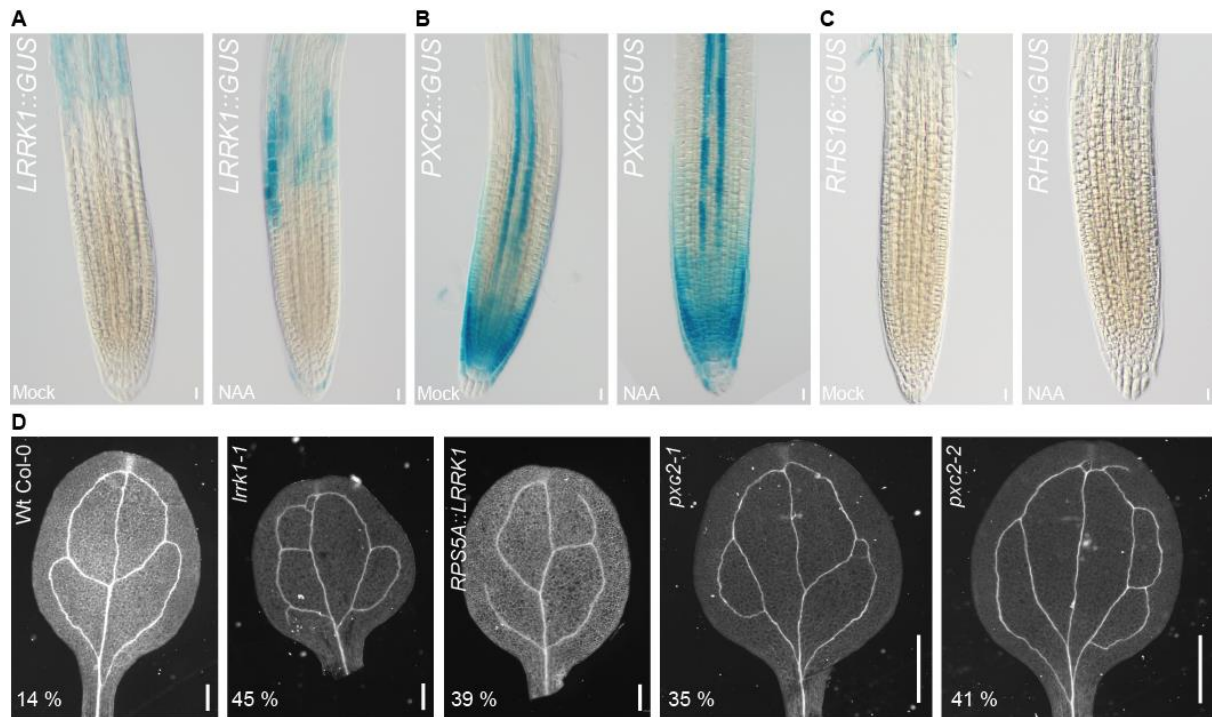


Figure 4-5 Expression patterns of *LRRK1*, *PXC2*, and *RHS16* and *LRRK1* and *PXC2* mutant venation defects.

A. Expression pattern of *LRRK1::GUS* (Wu *et al.*, 2016). B. Expression pattern of *PXC2::GUS* (Wu *et al.*, 2016) C. Expression pattern of *RHS16::GUS*. Cleared root tips were visualized with a DIC microscope (see Materials and Methods for detailed description). D. Cotyledon venation pattern in *lrrk1-1* mutant, lines overexpressing *LRRK1*, *pxc2-1*, and *pxc2-2* mutants. Percentages represent quantity of defect cotyledons. Bar size A – C 10 μ m.; D. 1 mm.

As we have shown previously, *WRKY23* loss-of-function causes venation defects and morphological changes in cotyledons (Prat *et al.*, unpublished data). Leaf venation crucially depends on polarity of PIN proteins and in particular on the auxin feed-back on PIN polarity as proposed by canalization hypothesis (Scarpella *et al.*, 2006). Therefore, we looked for abnormal venation patterns in *LRRK1* and *PXC2* mutants which were not present in control or were present significantly more often than in Wt Col-0 (max. 15% of defects). In control Wt

Col-0 cotyledons, venation pattern formed closed circles at the beginning two and then four lobes. This almost unvarying pattern is formed by self-regulatory mechanism of auxin canalization dependent on correct PIN1 polarity (Scarpella *et al.*, 2006). Almost half of cotyledons of knock-out mutant *lrrk1-1* had severe defects in venation presenting mainly additional loops on I2 or dead-end unconnected veins to midvein (**Fig.4-5 D**). Similarly, overexpression of *LRRK1* caused defective vascularization in cotyledons. Moreover, loss-of-function lines of *PXC2* - *pxc2-1* and *pxc2-2* contained several defective venation patterns reminiscent of *lrrk1-1* mutants (**Fig.4-5 D**). These results suggest involvement of *LRRK1* and *PXC2* in auxin canalization, a process dependent on auxin feed-back on PIN polarity.

4.3.6 Target interactors of LRRK1

To identify broad interactome of LRRK1, we performed immunoprecipitation experiment. As a bait protein we used whole translation fusion of LRRK1 protein sequence of 94.9798 kDa with eGFP (32.7 kDa). Interacting complex proteins were pulled-down and analysed on MS device. We observed large numbers of CM transporters within a list of probable interactors. The most important groups were further studied (**B Appendix Table S1**).

At the top of the list, complexes of PIP (PLASMA MEMBRANE INTRINSIC PROTEINS) PIP1A-E and PIP2 were found. PIPs are one of the group of aquaporins, the main gateways of cell membrane for water exchange. These multifunctional channels facilitate passive diffusion of water and/or small neutral solutes across biological membranes (Bienert & Chaumont, 2014). PIPs are organised as highly conserved tetramers in which each subunit forms functional channel (Tornroth-Horsefield *et al.*, 2007). The monomers are constituted of six transmembrane domains (TM1-TM6) which are linked by five loops (A-E). The N- and C-termini lengths are the main structural difference among members of PIPs and together with B and D loops are cytosolic (Chevalier & Chaumont, 2015). PIPs are clustered into three clusters, one cluster for PIP1 group and two clusters for PIP2 group (Soto *et al.*, 2012). These two groups potentially form heterotetramers or heterooligomers and thereby modify characteristics of both subfamilies in terms of activity, trafficking, and gating (Zelazny *et al.*, 2007). Controversially, PIP proteins are commonly found in IP experiments on CM proteins. Therefore it is very probable that interaction between LRRK1 and PIPs is due to its so-called “stickiness” and MS results may have been false positive (**B Appendix Table S1**).

Second group, more related to background of LRRK1 identification, were proteins related to auxin transport (**B Appendix Table S1**). In complexes probably interacting with LRRK1, two ABCB transporters PGP2/ABCB2 and PGP19/ABCB19, and ABCG transporter PEN3/ABCG36, and two PIN proteins PIN4 and PIN7 were present. ATP binding cassette (ABC) superfamily of transporters is of the largest and most ubiquitous transporter families, ABC transporters share a high degree of structural conservation between bacteria and eukaryotes (Becker *et al.*, 2009). The most important plant-specific subgroup of 22 members in *Arabidopsis* is ABCB transporter family [B-type: ABCB/multidrug resistance (MDR)/phosphoglycoprotein (PGP)]. ABCB1, ABCB4, ABCB14, ABCB15, ABCB19, and ABCB21 are associated with auxin transport, although not exclusively (Geisler & Murphy, 2006; Titapiwatanakun *et al.*, 2009; Kaneda *et al.*, 2011; Kamimoto *et al.*, 2012; Cho & Cho, 2013). ABCB1, ABCB4, and ABCB19 function in auxin driven root development and require activity of the immunophilin TWISTED DWARF1 (TWD1/FKBP42) to be correctly inserted on the CM where have stable and mostly apolar localization (Wu *et al.*, 2010). ABCB19 stabilizes PIN1 on microdomains and enhances substrate specificity of the overall transport and regulates root and cotyledon development and tropic bending response (Mravec *et al.*, 2008; Titapiwatanakun *et al.*, 2009; Christie *et al.*, 2011). Type G ABC transporter ABCG36/PDR8/PEN3 was identified to regulate pathogen responses (Stein *et al.*, 2006), heavy metal transport (Kim *et al.*, 2007), and also participate in regulation of IBA sensitivity and IAA homeostasis (Strader & Bartel, 2009). ABCG36 and a redundant homologue ABCB37 shows a strictly polar localization at the outer sides of epidermal and root cap cells (Langowski *et al.*, 2010; Ruzicka *et al.*, 2010).

PIN (PIN-FORMED) proteins belong to a plant-specific family of probable proton gradient-driven secondary transporters lacking ATP-binding domain (Zazimalova *et al.*, 2010). According to the length of central hydrophilic domain, eight members of PIN proteins are divided into two groups: (i) shorter intracellular PINs with partially or entirely reduced central domain and (ii) long canonical PINs with long hydrophilic domain localized in the CM (Krecek *et al.*, 2009). The polar localization of PIN proteins is established by cycling between the CM and endosomal compartments such as the trans-Golgi network/early endosomes (TGN/EE). PIN recycling occurs via clathrin-mediated endocytosis and depends on phosphorylation and ubiquitination (Kleine-Vehn *et al.*, 2011; Lofke *et al.*, 2013). Phosphorylation of PIN proteins is mediated by protein kinase PINOID (PID). Phosphorylation of PINs results in their GNOM-

independent recycling back to the CM on apical side of the cell (Friml *et al.*, 2004; Dhonukshe *et al.*, 2010). Another kinase D6 PROTEIN KINASE (D6PK) has been recently demonstrated to regulate PIN phosphorylation and, together with PID, D6PK promotes PINs-mediated auxin transport through the CM by maintaining PIN phosphorylation status. D6PK CM localization is essential to establish and maintain PIN phosphorylation (Zourelidou *et al.*, 2009; Willige *et al.*, 2013; Barbosa *et al.*, 2014). Unphosphorylated PINs or those dephosphorylated by the PP2A phosphatase (Michniewicz *et al.*, 2007) are recycled back to the CM via BFA-sensitive ADP-ribosylation factor-guanine nucleotide exchange factor (ARF-GEF) GNOM. Monoubiquitination and subsequent polyubiquitination of PIN proteins induce their endocytosis followed by trafficking from the TGN/EE to late endosomes where the SNX1/BLOC-1 complex mediates transfer to multivesicular bodies (MVBs) for vacuolar degradation (Habets & Offringa, 2014).

In all these complex processes, diverse mechanisms of phosphorylation/dephosphorylation provided by kinases/phosphatases have been identified to date. Phosphorylation mainly controls PINs by directly acting on either their transport activity or their intracellular trafficking. Subsequently, phosphorylation impacts the polarity, degradation, and CM accumulation of PIN proteins. Despite the fact that interactions of PIN proteins were exhaustively investigated in past decades, still many of the regulatory parts are missing. We identified receptor-like protein kinase LRRK1 affecting auxin-dependent PIN repolarization in transcription profiling experiments. Post-transcriptional mechanism of LRRK1 action remains unclear but first insights into subcellular localization and LRRK1 role in PIN protein recycling were performed. Based on global expression data, we tried to identify a ligand responsible for signalling and furthermore, we suggested plausible signalling partners. Our work continues revealing WRKY23-dependent transcriptional network and WRKY23 role in executing auxin effect on PIN polarity in canalization-dependent regulation of plant development.

Deciphering of LRRK1 function still remains incomplete. The most important step will be to sort out the list of possible interactors and to perform direct interaction assays to confirm protein-protein interactions. If these experiments confirm interaction of LRRK1 and PIN proteins, description, how differential phosphorylation of PIN proteins acts on polarity and/or their activity, will be interesting. This can move forward our understanding how PIN polarity is both stable in some processes but highly dynamic and variable in others.

4.4 ACKNOWLEDGEMENTS

We thank Yunzhe Wu and Jia Li for providing published material. This work was supported by the European Research Council (project ERC-2011-StG-20101109-PSDP).

4.5 AUTHOR CONTRIBUTION

T.P., and J.F. designed the research, T.P., E.S., and B.d.R. performed the research, T.P., G.M., and J.F. analyzed the data, and T.P., G.M., and J.F. wrote the paper.

4.6 REFERENCES

- Abas L, Benjamins R, Malenica N, Paciorek T, Wisniewska J, Moulinier-Anzola JC, Sieberer T, Friml J, Luschnig C. 2006. Intracellular trafficking and proteolysis of the Arabidopsis auxin-efflux facilitator PIN2 are involved in root gravitropism. *Nat Cell Biol* **8**(3): 249-256.
- Bajwa VS, Wang X, Blackburn RK, Goshe MB, Mitra SK, Williams EL, Bishop GJ, Krasnyanski S, Allen G, Huber SC, et al. 2013. Identification and functional analysis of tomato BRI1 and BAK1 receptor kinase phosphorylation sites. *Plant Physiology* **163**(1): 30-42.
- Barbosa IC, Zourelidou M, Willige BC, Weller B, Schwechheimer C. 2014. D6 PROTEIN KINASE activates auxin transport-dependent growth and PIN-FORMED phosphorylation at the plasma membrane. *Dev Cell* **29**(6): 674-685.
- Beck M, Zhou J, Faulkner C, MacLean D, Robatzek S. 2012. Spatio-temporal cellular dynamics of the Arabidopsis flagellin receptor reveal activation status-dependent endosomal sorting. *Plant Cell* **24**(10): 4205-4219.
- Becker P, Hakenbeck R, Henrich B. 2009. An ABC transporter of *Streptococcus pneumoniae* involved in susceptibility to vancomycin and bacitracin. *Antimicrob Agents Chemother* **53**(5): 2034-2041.
- Belkhadir Y, Yang L, Hetzel J, Dangl JL, Chory J. 2014. The growth-defense pivot: crisis management in plants mediated by LRR-RK surface receptors. *Trends Biochem Sci* **39**(10): 447-456.
- Bienert GP, Chaumont F. 2014. Aquaporin-facilitated transmembrane diffusion of hydrogen peroxide. *Biochim Biophys Acta* **1840**(5): 1596-1604.
- Chevalier AS, Chaumont F. 2015. Trafficking of plant plasma membrane aquaporins: multiple regulation levels and complex sorting signals. *Plant and Cell Physiology* **56**(5): 819-829.
- Chinchilla D, Boller T, Robatzek S. 2007a. Flagellin signalling in plant immunity. *Adv Exp Med Biol* **598**: 358-371.
- Chinchilla D, Zipfel C, Robatzek S, Kemmerling B, Nurnberger T, Jones JD, Felix G, Boller T. 2007b. A flagellin-induced complex of the receptor FLS2 and BAK1 initiates plant defence. *Nature* **448**(7152): 497-500.
- Cho M, Cho HT. 2013. The function of ABCB transporters in auxin transport. *Plant Signal Behav* **8**(2): e22990.
- Christie JM, Yang H, Richter GL, Sullivan S, Thomson CE, Lin J, Titapiwatanakun B, Ennis M, Kaiserli E, Lee OR, et al. 2011. phot1 inhibition of ABCB19 primes lateral auxin fluxes in the shoot apex required for phototropism. *PLoS Biol* **9**(6): e1001076.
- Clough SJ, Bent AF. 1998. Floral dip: a simplified method for *Agrobacterium*-mediated transformation of *Arabidopsis thaliana*. *Plant J* **16**(6): 735-743.
- Cvrckova F, Bezvoda R, Zarsky V. 2010. Computational identification of root hair-specific genes in *Arabidopsis*. *Plant Signal Behav* **5**(11): 1407-1418.
- Deeken R, Kaldenhoff R. 1997. Light-repressible receptor protein kinase: a novel photo-regulated gene from *Arabidopsis thaliana*. *Planta* **202**(4): 479-486.
- Dhonukshe P, Huang F, Galvan-Ampudia CS, Mahonen AP, Kleine-Vehn J, Xu J, Quint A, Prasad K, Friml J, Scheres B, et al. 2010. Plasma membrane-bound AGC3 kinases phosphorylate PIN auxin carriers at TPRXS(N/S) motifs to direct apical PIN recycling. *Development* **137**(19): 3245-3255.
- Etchells JP, Provost CM, Mishra L, Turner SR. 2013. WOX4 and WOX14 act downstream of the PXY receptor kinase to regulate plant vascular proliferation independently of any role in vascular organisation. *Development* **140**(10): 2224-2234.
- Etchells JP, Turner SR. 2010. The PXY-CLE41 receptor ligand pair defines a multifunctional pathway that controls the rate and orientation of vascular cell division. *Development* **137**.
- Fisher K, Turner S. 2007. PXY, a receptor-like kinase essential for maintaining polarity during plant vascular-tissue development. *Curr Biol* **17**.

- Friedrichsen DM, Joazeiro CA, Li J, Hunter T, Chory J. 2000.** Brassinosteroid-insensitive-1 is a ubiquitously expressed leucine-rich repeat receptor serine/threonine kinase. *Plant Physiology* **123**(4): 1247-1256.
- Friml J, Yang X, Michniewicz M, Weijers D, Quint A, Tietz O, Benjamins R, Ouwerkerk PB, Ljung K, Sandberg G, et al. 2004.** A PINOID-dependent binary switch in apical-basal PIN polar targeting directs auxin efflux. *Science* **306**(5697): 862-865.
- Fukuda H. 2016.** Signaling, transcriptional regulation, and asynchronous pattern formation governing plant xylem development. *Proc Jpn Acad Ser B Phys Biol Sci* **92**(3): 98-107.
- Geisler M, Murphy AS. 2006.** The ABC of auxin transport: the role of p-glycoproteins in plant development. *FEBS Lett* **580**(4): 1094-1102.
- Grunewald W, De Smet I, Lewis DR, Lofke C, Jansen L, Goeminne G, Vanden Bossche R, Karimi M, De Rybel B, Vanholme B, et al. 2012.** Transcription factor WRKY23 assists auxin distribution patterns during Arabidopsis root development through local control on flavonol biosynthesis. *Proc Natl Acad Sci U S A* **109**(5): 1554-1559.
- Grunewald W, Karimi M, Wieczorek K, Van de Cappelle E, Wischnitzki E, Grundler F, Inze D, Beeckman T, Gheysen G. 2008.** A role for AtWRKY23 in feeding site establishment of plant-parasitic nematodes. *Plant Physiology* **148**(1): 358-368.
- Habets ME, Offringa R. 2014.** PIN-driven polar auxin transport in plant developmental plasticity: a key target for environmental and endogenous signals. *New Phytol* **203**(2): 362-377.
- Heese A, Hann DR, Gimenez-Ibanez S, Jones AM, He K, Li J, Schroeder JI, Peck SC, Rathjen JP. 2007.** The receptor-like kinase SERK3/BAK1 is a central regulator of innate immunity in plants. *Proc Natl Acad Sci U S A* **104**(29): 12217-12222.
- Hirakawa Y, Kondo Y, Fukuda H. 2010.** TDIF peptide signaling regulates vascular stem cell proliferation via the WOX4 homeobox gene in Arabidopsis. *Plant Cell* **22**.
- Hirakawa Y, Shinohara H, Kondo Y, Inoue A, Nakanomyo I, Ogawa M, Sawa S, Ohashi-Ito K, Matsubayashi Y, Fukuda H. 2008.** Non-cell-autonomous control of vascular stem cell fate by a CLE peptide/receptor system. *Proc Natl Acad Sci USA* **105**.
- Hothorn M, Belkadir Y, Dreux M, Dabi T, Noel JP, Wilson IA, Chory J. 2011.** Structural basis of steroid hormone perception by the receptor kinase BRI1. *Nature* **474**(7352): 467-471.
- Hubner NC, Bird AW, Cox J, Splettstoesser B, Bandilla P, Poser I, Hyman A, Mann M. 2010.** Quantitative proteomics combined with BAC TransgeneOmics reveals in vivo protein interactions. *J Cell Biol* **189**(4): 739-754.
- Ito Y, Nakanomyo I, Motose H, Iwamoto K, Sawa S, Dohmae N, Fukuda H. 2006.** Dodeca-CLE peptides as suppressors of plant stem cell differentiation. *Science* **313**(5788): 842-845.
- Jaillais Y, Hothorn M, Belkadir Y, Dabi T, Nimchuk ZL, Meyerowitz EM, Chory J. 2011.** Tyrosine phosphorylation controls brassinosteroid receptor activation by triggering membrane release of its kinase inhibitor. *Genes Dev* **25**(3): 232-237.
- Jasik J, Bokor B, Stuchlik S, Micieta K, Turna J, Schmelzer E. 2016.** Effects of Auxins on PIN-FORMED2 (PIN2) Dynamics Are Not Mediated by Inhibiting PIN2 Endocytosis. *Plant Physiology* **172**(2): 1019-1031.
- Kamimoto Y, Terasaka K, Hamamoto M, Takanashi K, Fukuda S, Shitan N, Sugiyama A, Suzuki H, Shibata D, Wang B, et al. 2012.** Arabidopsis ABCB21 is a facultative auxin importer/exporter regulated by cytoplasmic auxin concentration. *Plant and Cell Physiology* **53**(12): 2090-2100.
- Kaneda M, Schuetz M, Lin BS, Chanis C, Hamberger B, Western TL, Ehling J, Samuels AL. 2011.** ABC transporters coordinately expressed during lignification of Arabidopsis stems include a set of ABCBs associated with auxin transport. *J Exp Bot* **62**(6): 2063-2077.
- Karimi M, Depicker A, Hilson P. 2007.** Recombinational cloning with plant gateway vectors. *Plant Physiology* **145**(4): 1144-1154.
- Kim DW, Lee SH, Choi SB, Won SK, Heo YK, Cho M, Park YI, Cho HT. 2006.** Functional conservation of a root hair cell-specific cis-element in angiosperms with different root hair distribution patterns. *Plant Cell* **18**(11): 2958-2970.

- Kim DY, Bovet L, Maeshima M, Martinoia E, Lee Y. 2007.** The ABC transporter AtPDR8 is a cadmium extrusion pump conferring heavy metal resistance. *Plant J* **50**(2): 207-218.
- Kim TW, Guan S, Sun Y, Deng Z, Tang W, Shang JX, Sun Y, Burlingame AL, Wang ZY. 2009.** Brassinosteroid signal transduction from cell-surface receptor kinases to nuclear transcription factors. *Nat Cell Biol* **11**(10): 1254-1260.
- Kleine-Vehn J, Wabnik K, Martiniere A, Langowski L, Willig K, Naramoto S, Leitner J, Tanaka H, Jakobs S, Robert S, et al. 2011.** Recycling, clustering, and endocytosis jointly maintain PIN auxin carrier polarity at the plasma membrane. *Mol Syst Biol* **7**: 540.
- Knox K, Grierson CS, Leyser O. 2003.** AXR3 and SHY2 interact to regulate root hair development. *Development* **130**(23): 5769-5777.
- Kondo Y, Ito T, Nakagami H, Hirakawa Y, Saito M, Tamaki T, Shirasu K, Fukuda H. 2014.** Plant GSK3 proteins regulate xylem cell differentiation downstream of TDIF-TDR signalling. *Nat Commun* **5**: 3504.
- Krecek P, Skupa P, Libus J, Naramoto S, Tejos R, Friml J, Zazimalova E. 2009.** The PIN-FORMED (PIN) protein family of auxin transporters. *Genome Biol* **10**(12): 249.
- Langowski L, Ruzicka K, Naramoto S, Kleine-Vehn J, Friml J. 2010.** Trafficking to the outer polar domain defines the root-soil interface. *Curr Biol* **20**(10): 904-908.
- Li J, Chory J. 1997.** A putative leucine-rich repeat receptor kinase involved in brassinosteroid signal transduction. *Cell* **90**(5): 929-938.
- Li J, Nam KH, Vafeados D, Chory J. 2001.** BIN2, a new brassinosteroid-insensitive locus in Arabidopsis. *Plant Physiology* **127**(1): 14-22.
- Li J, Tax FE. 2013.** Receptor-like kinases: key regulators of plant development and defense. *J Integr Plant Biol* **55**(12): 1184-1187.
- Li J, Wen J, Lease KA, Doke JT, Tax FE, Walker JC. 2002.** BAK1, an Arabidopsis LRR receptor-like protein kinase, interacts with BRI1 and modulates brassinosteroid signaling. *Cell* **110**(2): 213-222.
- Liebrand TW, van den Burg HA, Joosten MH. 2014.** Two for all: receptor-associated kinases SOBIR1 and BAK1. *Trends Plant Sci* **19**(2): 123-132.
- Lofke C, Luschig C, Kleine-Vehn J. 2013.** Posttranslational modification and trafficking of PIN auxin efflux carriers. *Mech Dev* **130**(1): 82-94.
- Lu J, Boeren S, de Vries SC, van Valenberg HJ, Vervoort J, Hettinga K. 2011.** Filter-aided sample preparation with dimethyl labeling to identify and quantify milk fat globule membrane proteins. *J Proteomics* **75**(1): 34-43.
- Michniewicz M, Zago MK, Abas L, Weijers D, Schweighofer A, Meskiene I, Heisler MG, Ohno C, Zhang J, Huang F, et al. 2007.** Antagonistic regulation of PIN phosphorylation by PP2A and PINOID directs auxin flux. *Cell* **130**(6): 1044-1056.
- Mravec J, Kubes M, Bielach A, Gaykova V, Petrasek J, Skupa P, Chand S, Benkova E, Zazimalova E, Friml J. 2008.** Interaction of PIN and PGP transport mechanisms in auxin distribution-dependent development. *Development* **135**(20): 3345-3354.
- Nam KH, Li J. 2002.** BRI1/BAK1, a receptor kinase pair mediating brassinosteroid signaling. *Cell* **110**(2): 203-212.
- Okushima Y, Overvoorde PJ, Arima K, Alonso JM, Chan A, Chang C, Ecker JR, Hughes B, Lui A, Nguyen D, et al. 2005.** Functional genomic analysis of the AUXIN RESPONSE FACTOR gene family members in Arabidopsis thaliana: unique and overlapping functions of ARF7 and ARF19. *Plant Cell* **17**(2): 444-463.
- Paciorek T, Zazimalova E, Ruthardt N, Petrasek J, Stierhof YD, Kleine-Vehn J, Morris DA, Emans N, Jurgens G, Geldner N, et al. 2005.** Auxin inhibits endocytosis and promotes its own efflux from cells. *Nature* **435**(7046): 1251-1256.
- Postel S, Kufner I, Beuter C, Mazzotta S, Schwedt A, Borlotti A, Halter T, Kemmerling B, Nurnberger T. 2010.** The multifunctional leucine-rich repeat receptor kinase BAK1 is implicated in Arabidopsis development and immunity. *Eur J Cell Biol* **89**(2-3): 169-174.

- Robatzek S, Chinchilla D, Boller T. 2006.** Ligand-induced endocytosis of the pattern recognition receptor FLS2 in Arabidopsis. *Genes Dev* **20**(5): 537-542.
- Roux M, Schwessinger B, Albrecht C, Chinchilla D, Jones A, Holton N, Malinovsky FG, Tor M, de Vries S, Zipfel C. 2011.** The Arabidopsis leucine-rich repeat receptor-like kinases BAK1/SERK3 and BKK1/SERK4 are required for innate immunity to hemibiotrophic and biotrophic pathogens. *Plant Cell* **23**(6): 2440-2455.
- Russinova E, Borst JW, Kwaaitaal M, Cano-Delgado A, Yin Y, Chory J, de Vries SC. 2004.** Heterodimerization and endocytosis of Arabidopsis brassinosteroid receptors BRI1 and AtSERK3 (BAK1). *Plant Cell* **16**(12): 3216-3229.
- Ruzicka K, Strader LC, Bailly A, Yang H, Blakeslee J, Langowski L, Nejedla E, Fujita H, Itoh H, Syono K, et al. 2010.** Arabidopsis PIS1 encodes the ABCG37 transporter of auxinic compounds including the auxin precursor indole-3-butyric acid. *Proc Natl Acad Sci U S A* **107**(23): 10749-10753.
- Santiago J, Henzler C, Hothorn M. 2013.** Molecular mechanism for plant steroid receptor activation by somatic embryogenesis co-receptor kinases. *Science* **341**(6148): 889-892.
- Sauer M, Balla J, Luschnig C, Wisniewska J, Reinohl V, Friml J, Benkova E. 2006.** Canalization of auxin flow by Aux/IAA-ARF-dependent feedback regulation of PIN polarity. *Genes Dev* **20**(20): 2902-2911.
- Sauer M, Friml J. 2010.** Immunolocalization of proteins in plants. *Methods Mol Biol* **655**: 253-263.
- Scarpella E, Marcos D, Friml J, Berleth T. 2006.** Control of leaf vascular patterning by polar auxin transport. *Genes Dev* **20**(8): 1015-1027.
- Shiu SH, Bleecker AB. 2001.** Receptor-like kinases from Arabidopsis form a monophyletic gene family related to animal receptor kinases. *Proc Natl Acad Sci USA* **98**.
- Song W, Liu L, Wang J, Wu Z, Zhang H, Tang J, Lin G, Wang Y, Wen X, Li W, et al. 2016.** Signature motif-guided identification of receptors for peptide hormones essential for root meristem growth. *Cell Res* **26**(6): 674-685.
- Soto G, Alleva K, Amodeo G, Muschietti J, Ayub ND. 2012.** New insight into the evolution of aquaporins from flowering plants and vertebrates: orthologous identification and functional transfer is possible. *Gene* **503**(1): 165-176.
- Sreeramulu S, Mostizky Y, Sunitha S, Shani E, Nahum H, Salomon D, Hayun LB, Gruetter C, Rauh D, Ori N, et al. 2013.** BSKs are partially redundant positive regulators of brassinosteroid signaling in Arabidopsis. *Plant J* **74**(6): 905-919.
- Stein M, Dittgen J, Sanchez-Rodriguez C, Hou BH, Molina A, Schulze-Lefert P, Lipka V, Somerville S. 2006.** Arabidopsis PEN3/PDR8, an ATP binding cassette transporter, contributes to nonhost resistance to inappropriate pathogens that enter by direct penetration. *Plant Cell* **18**(3): 731-746.
- Strader LC, Bartel B. 2009.** The Arabidopsis PLEIOTROPIC DRUG RESISTANCE8/ABCG36 ATP binding cassette transporter modulates sensitivity to the auxin precursor indole-3-butyric acid. *Plant Cell* **21**(7): 1992-2007.
- Sun Y, Li L, Macho AP, Han Z, Hu Z, Zipfel C, Zhou JM, Chai J. 2013.** Structural basis for flg22-induced activation of the Arabidopsis FLS2-BAK1 immune complex. *Science* **342**(6158): 624-628.
- Taddese B, Upton GJ, Bailey GR, Jordan SR, Abdulla NY, Reeves PJ, Reynolds CA. 2014.** Do plants contain g protein-coupled receptors? *Plant Physiology* **164**(1): 287-307.
- Tang W, Kim TW, Osés-Prieto JA, Sun Y, Deng Z, Zhu S, Wang R, Burlingame AL, Wang ZY. 2008.** BSKs mediate signal transduction from the receptor kinase BRI1 in Arabidopsis. *Science* **321**(5888): 557-560.
- Tejos R, Sauer M, Vanneste S, Palacios-Gomez M, Li H, Heilmann M, van Wijk R, Vermeer JE, Heilmann I, Munnik T, et al. 2014.** Bipolar Plasma Membrane Distribution of Phosphoinositides and Their Requirement for Auxin-Mediated Cell Polarity and Patterning in Arabidopsis. *Plant Cell* **26**(5): 2114-2128.

- Titapiwatanakun B, Blakeslee JJ, Bandyopadhyay A, Yang H, Mravec J, Sauer M, Cheng Y, Adamec J, Nagashima A, Geisler M, et al. 2009.** ABCB19/PGP19 stabilises PIN1 in membrane microdomains in Arabidopsis. *Plant J* **57**(1): 27-44.
- Tornroth-Horsefield S, Gourdon P, Horsefield R, Brive L, Yamamoto N, Mori H, Snijder A, Neutze R. 2007.** Crystal structure of AcrB in complex with a single transmembrane subunit reveals another twist. *Structure* **15**(12): 1663-1673.
- Wang J, Kucukoglu M, Zhang L, Chen P, Decker D, Nilsson O, Jones B, Sandberg G, Zheng B. 2013.** The Arabidopsis LRR-RLK, PXC1, is a regulator of secondary wall formation correlated with the TDIF-PXY/TDR-WOX4 signaling pathway. *BMC Plant Biol* **13**(1): 1-11.
- Willige BC, Ahlers S, Zourelidou M, Barbosa IC, Demarsy E, Trevisan M, Davis PA, Roelfsema MR, Hangarter R, Fankhauser C, et al. 2013.** D6PK AGCVIII kinases are required for auxin transport and phototropic hypocotyl bending in Arabidopsis. *Plant Cell* **25**(5): 1674-1688.
- Won SK, Lee YJ, Lee HY, Heo YK, Cho M, Cho HT. 2009.** Cis-element- and transcriptome-based screening of root hair-specific genes and their functional characterization in Arabidopsis. *Plant Physiology* **150**(3): 1459-1473.
- Wu FH, Shen SC, Lee LY, Lee SH, Chan MT, Lin CS. 2009.** Tape-Arabidopsis Sandwich - a simpler Arabidopsis protoplast isolation method. *Plant Methods* **5**: 16.
- Wu G, Otegui MS, Spalding EP. 2010.** The ER-localized TWD1 immunophilin is necessary for localization of multidrug resistance-like proteins required for polar auxin transport in Arabidopsis roots. *Plant Cell* **22**(10): 3295-3304.
- Wu Y, Xun Q, Guo Y, Zhang J, Cheng K, Shi T, He K, Hou S, Gou X, Li J. 2016.** Genome-Wide Expression Pattern Analyses of the Arabidopsis Leucine-Rich Repeat Receptor-Like Kinases. *Mol Plant* **9**(2): 289-300.
- Zazimalova E, Murphy AS, Yang H, Hoyerova K, Hosek P. 2010.** Auxin transporters--why so many? *Cold Spring Harb Perspect Biol* **2**(3): a001552.
- Zelazny E, Borst JW, Muylaert M, Batoko H, Hemminga MA, Chaumont F. 2007.** FRET imaging in living maize cells reveals that plasma membrane aquaporins interact to regulate their subcellular localization. *Proc Natl Acad Sci U S A* **104**(30): 12359-12364.
- Zhang H, Lin X, Han Z, Qu LJ, Chai J. 2016a.** Crystal structure of PXY-TDIF complex reveals a conserved recognition mechanism among CLE peptide-receptor pairs. *Cell Res* **26**(5): 543-555.
- Zhang H, Lin X, Han Z, Wang J, Qu LJ, Chai J. 2016b.** SERK Family Receptor-like Kinases Function as Co-receptors with PXY for Plant Vascular Development. *Mol Plant* **9**(10): 1406-1414.
- Zhang W, Fraiture M, Kolb D, Loffelhardt B, Desaki Y, Boutrot FF, Tor M, Zipfel C, Gust AA, Brunner F. 2013.** Arabidopsis receptor-like protein30 and receptor-like kinase suppressor of BIR1-1/EVERSHED mediate innate immunity to necrotrophic fungi. *Plant Cell* **25**(10): 4227-4241.
- Zimmermann P, Hirsch-Hoffmann M, Hennig L, Gruissem W. 2004.** GENEVESTIGATOR. Arabidopsis microarray database and analysis toolbox. *Plant Physiology* **136**.
- Zourelidou M, Muller I, Willige BC, Nill C, Jikumaru Y, Li H, Schwechheimer C. 2009.** The polarly localized D6 PROTEIN KINASE is required for efficient auxin transport in Arabidopsis thaliana. *Development* **136**(4): 627-636.
- Zwiewka M, Feraru E, Moller B, Hwang I, Feraru MI, Kleine-Vehn J, Weijers D, Friml J. 2011.** The AP-3 adaptor complex is required for vacuolar function in Arabidopsis. *Cell Res* **21**(12): 1711-1722.

4.7 SUPPORTING INFORMATION

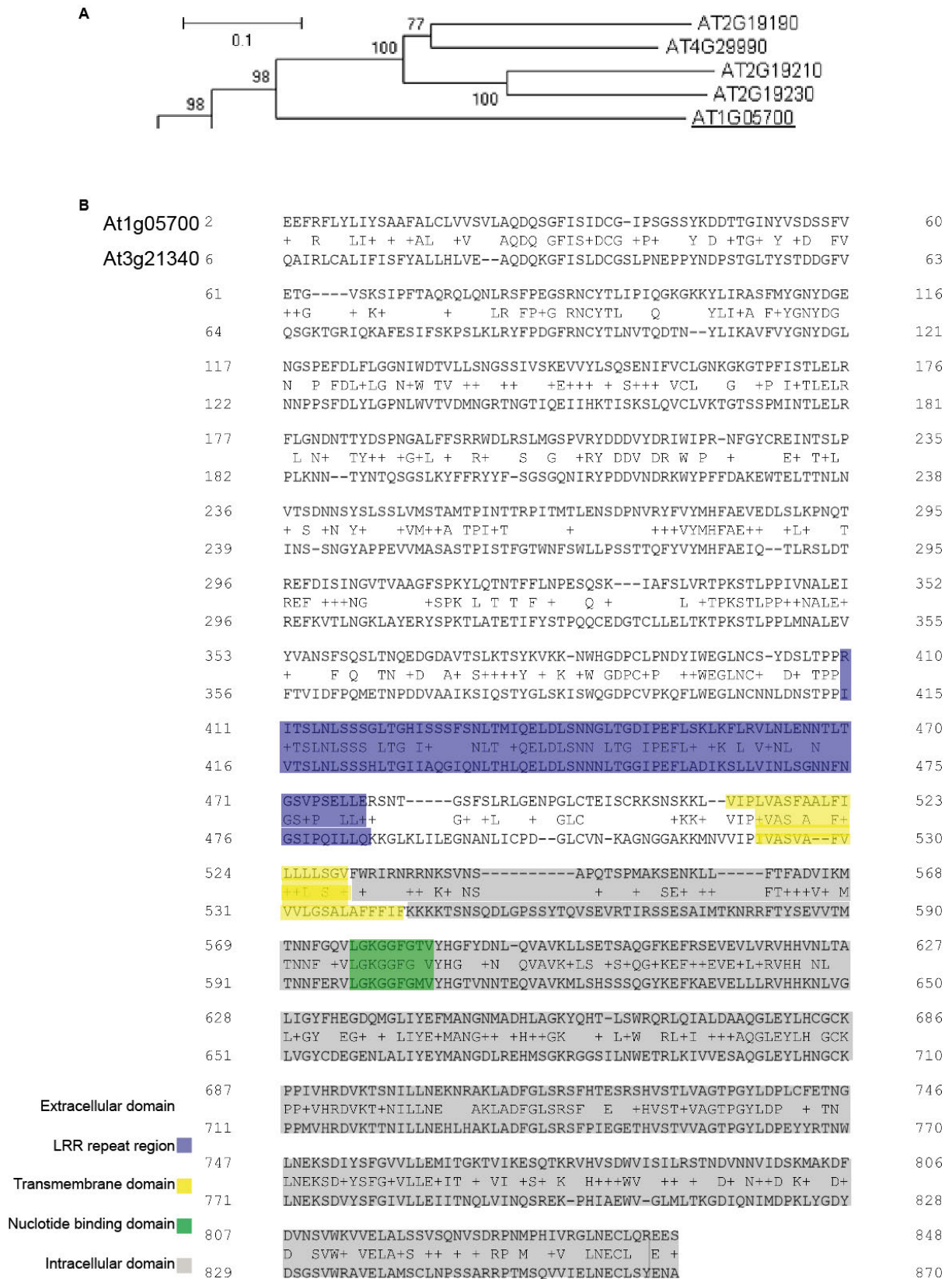


Figure S 4-1 Sequence alignment of extracellular domain of LRRK1 show very low identity to other LRR-RLK.

A. Neighbour-joining phylogenetic tree visualize isolated position of *LRRK1* within I subfamily of LRR-RLKs. B. Amino acid sequence alignment of LRRK1 with topologically analogous to LIGHT-REPRESSIBLE RECEPTOR PROTEIN KINASE (LRRPK; At3g21340) (Deeken & Kaldenhoff, 1997).

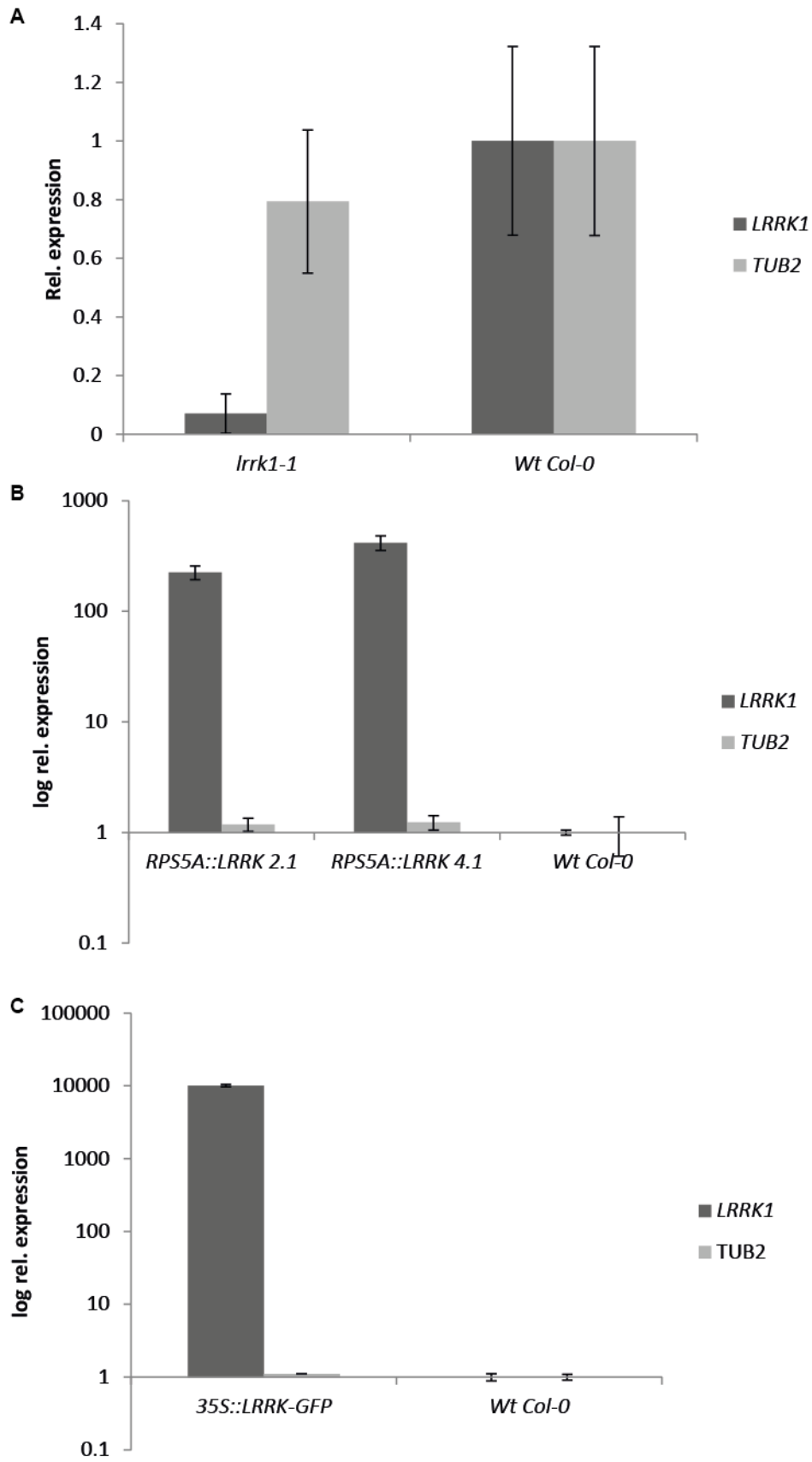


Figure S 4-2 Transcript level confirmation of mutant and transgenic plant lines.

A. *LRRK1* transcript was almost absent in *Irrk1-1* T-DNA mutant line. Bars represent relative fold change of expression. Error bars represent standard deviation (see Materials and Methods for detailed description). B. *LRRK1* was overexpressed in transgenic lines under control of constitutive RPS5A promoter. Bars represent relative fold change of expression. Y axis is represented in logarithmic scale \log_{10} . Error bars represent standard deviation (see Materials and Methods for detailed description). C. *LRRK1-GFP* was overexpressed in transgenic lines under control of constitutive 35S promoter. Bars represent relative fold change of expression. Y axis is represented in logarithmic scale \log_{10} . Error bars represent standard deviation (see Materials and Methods for detailed description).

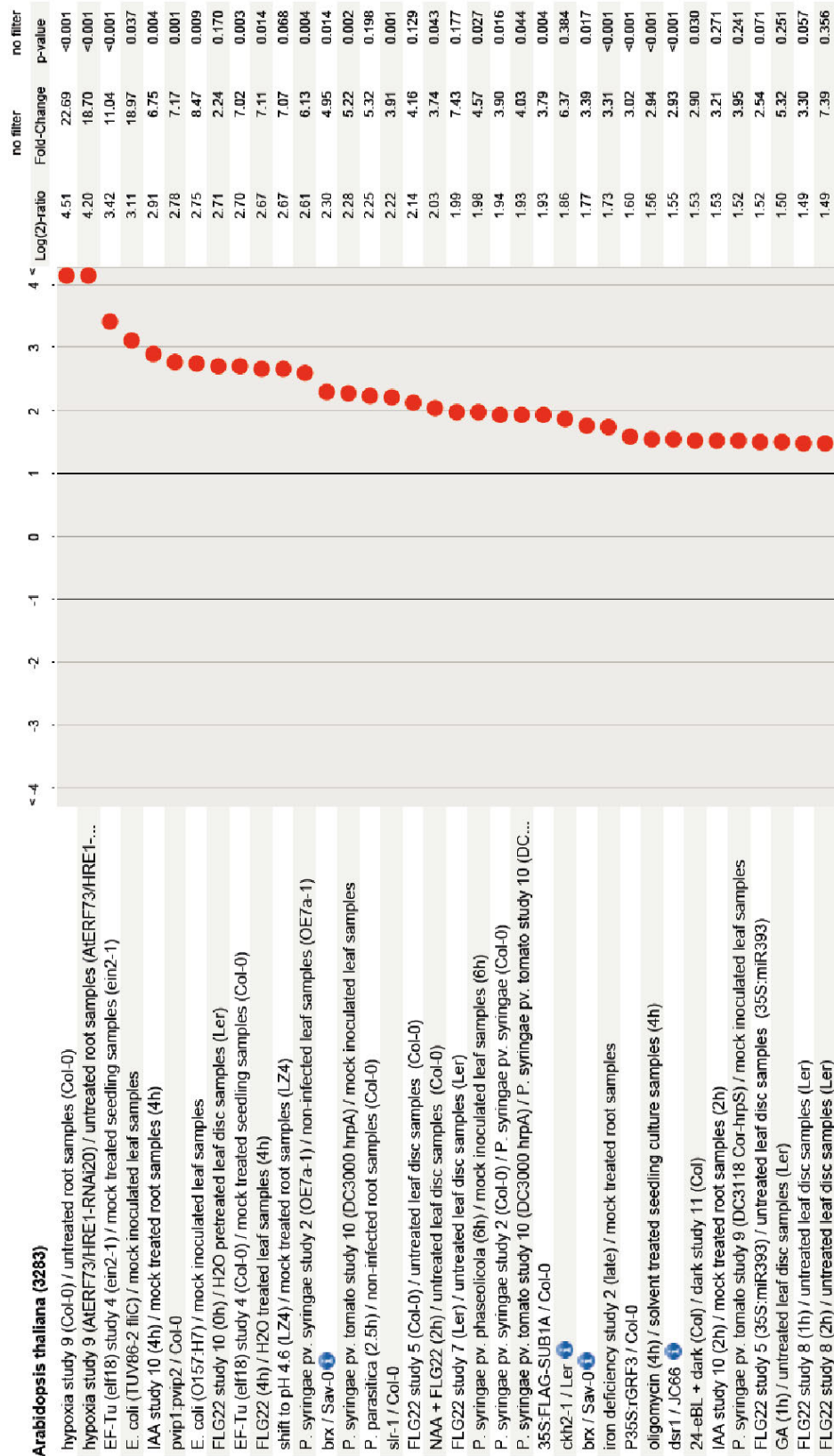


Figure S 4-3 Output from GENEVESTIGATOR® (Nebion AG) global library of expression data.

We found that LRRK1 strongest perturbations of expression data were caused by bacterial peptides (EF-Tu and flg22) and by auxin IAA and NAA. Based on Zimmermann *et al.*, 2004.

List of primers used in this study

T-DNA genotyping primers:

Line	Name	Sequence
<i>lrrk1-1</i>	SALK_025603C_FOR	ATATATGACCCGTTAACCCGC
<i>lrrk1-1</i>	SALK_025603C_REV	CTTAGGTTTCTCGGGAACGAC
<i>pxc2-1</i>	SALK_055351_FOR	CAATCTCTCGGGAAGTCTTCC
<i>pxc2-1</i>	SALK_055351_REV	CCTTCTCTCACCGTCTCACAC
<i>pxc2-2</i>	SALK_018730_FOR	TGGACCCTTTGTGACTTTCAC
<i>pxc2-2</i>	SALK_018730_REV	GCGGAAGCTTGTACAGACATC
<i>T-DNA</i>	SALK_LBa1	TGGTTCACGTAGTGGGCCATCG

qRT-PCR primers:

Gene	Name	Sequence
<i>TUB2</i>	TUB-2_FOR	ACTCGTTGGGAGGAGGAACT
<i>TUB2</i>	TUB-2_REV	ACACCAGACATAGTAGCAGAAATCAAG
<i>WRKY23</i>	WRKY23_FOR	AGTCTCGGTAATGGTTGCTTTGG
<i>WRKY23</i>	WRKY23_REV	TGTTGCTGCTGTTGGTGATGG
<i>LRRK1</i>	AT1G05700_FOR	TCAAACCAGTCCAATGGCGA
<i>LRRK1</i>	AT1G05700_REV	TCCTTTGCCGAGGACTTGAC

Table S 4-1 List of primers used in this study for T-DNA genotyping and qRT-PCR

5 Strigolactone interfere auxin-dependent PIN re-arrangement in *Arabidopsis*

Jing Zhang, Zuzana Medvedova, Ewa Mazur, Tomáš Prát, Jozef Balla, Vilem Reinöhl, Elizabeth A. Dun, Saiko Yoshida, Phillip B. Brewer, and Jiří Friml

5.1 INTRODUCTION

Phytohormones play an essential role in regulation of plant development and architecture in response to variable environmental conditions. In many developmental processes, the crosstalk of several hormones is implicated, thus, coordination of their overlapping activities is crucial for correct plant development. Hormone auxin is unique among other known plant hormones by its strictly controlled transport in a directional manner which is mediated by polarly localized PIN-FORMED (PIN) auxin transporters. Recently, strigolactone, a newly described plant hormone, was suggested to crosstalk with auxin in plant development.

Developmental role of strigolactone lies in regulation of shoot architecture by inhibition of branching (Gomez-Roldan *et al.*, 2008; Umehara *et al.*, 2008; Kohlen *et al.*, 2011). Strigolactone biosynthesis is derived from the carotenoid pathway (Matusova *et al.*, 2005) via the activity of various oxygenases (Gomez-Roldan *et al.*, 2008; Umehara *et al.*, 2008). In *Arabidopsis*, the cytochrome P450 (MAX1; AtCyp711A1), the carotenoid dioxygenases MORE AXILLARY GROWTH3 (MAX3; AtCCD7), and MAX4 (AtCCD8) are involved in the biosynthesis of strigolactone (Turnbull *et al.*, 2002; Sorefan *et al.*, 2003; Booker *et al.*, 2005) whereas the MAX2 protein containing F-box and leucine-rich repeats likely takes part in signal perception or transduction pathway (Booker *et al.*, 2005; Stirnberg *et al.*, 2007). Plants mutated in any of the MAX genes display increased numbers of shoot branches. This mutant phenotype can be rescued by the application of the synthetic strigolactone analog GR24 (Gomez-Roldan *et al.*, 2008) in MAX2-dependent manner.

Recent publications demonstrate strong evidence showing connections between strigolactone and auxin. Exogenous application of GR24 reduces basipetal auxin transport in isolated stem segments (Crawford *et al.*, 2010). Furthermore, GR24 treatment has effects in auxin-related processes observed in mutants with defective auxin transport (Benkova *et al.*,

2003) like primary root elongation, lateral root initiation and development, and root hair formation in tomato and *Arabidopsis* (Koltai *et al.*, 2010; Ruyter-Spira *et al.*, 2011).

However, the underlying molecular mechanism remains elusive. Here, we show that strigolactone modulates auxin-dependent PIN proteins re-arrangement.

5.2 MATERIALS

The following transgenic plants, mutants, and constructs have been described previously: Seeds of *DEX>>MAX1* (Crawford *et al.*, 2010) and *max2-3* were kindly gifted by Ottoline Leyser, University of York, UK.

5.3 RESULTS

We tested strigolactone role in a feed-back between auxin and PIN polarity (Adamowski & Friml, 2015) by the auxin-mediated polarity re-arrangements of the PIN auxin transporters in *Arabidopsis* roots (Sauer *et al.*, 2006). In primary roots, PIN2 localizes to the apical cell side in epidermis and preferentially to the basal cell side in young cortex cells (Kleine-Vehn *et al.*, 2008). Auxin treatment leads to PIN2 re-arrangements in cortex to the outer lateral sides (Sauer *et al.*, 2006). We used treatments with active strigolactone analogue GR24 (Gomez-Roldan *et al.*, 2008; Umehara *et al.*, 2008) and *DEX>>MAX1* line conditional expressing strigolactone biosynthetic enzyme MAX1 (Crawford *et al.*, 2010).

This auxin effect was consistently inhibited by co-treatment with GR24 (**Fig.5-1 A**) in a MAX2-dependent manner because strigolactone effect was not observed in signalling mutant *max2-3* (**Fig.5-1 B**). Results of auxin-dependent PIN re-arrangement in *DEX>>MAX1* line with induction of endogenous strigolactone biosynthesis confirmed effect of externally applied strigolactone analogue GR24 (**Fig.5-1 C - D**).

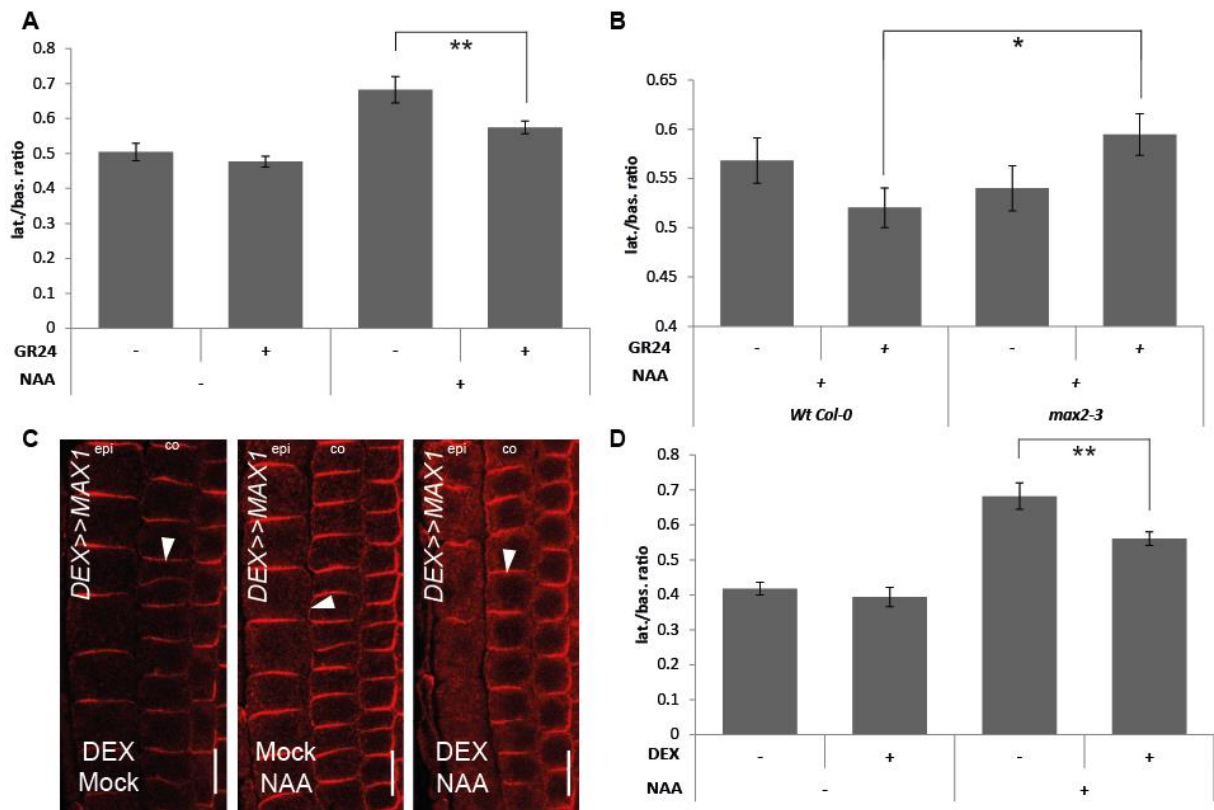


Figure 5-1 Role of strigolactone in the regulation of PIN polarity.

A. Graph shows mean ratio of lateral to basal signal intensity of PIN2 in cortex cells in Wt Col-0 1h pre-treated plants by 50 μ M GR24 and subsequently treated with 10 μ M NAA for 4 hours. Error bars indicate standard error. A two-tailed Student's t-test compared marked sets of data. (**) $P < 0.01$. $n > 50$ cells corresponding to roots imaged under comparable conditions. B. Graph shows mean ratio of lateral to basal signal intensity of PIN2 in cortex cells in Wt Col-0 and *max2-3* mutant after 1h pre-treated plants by 50 μ M GR24 and subsequently treated with 10 μ M NAA for 4 hours. Error bars indicate standard error. A two-tailed Student's t-test compared marked sets of data. (*) $P < 0.05$. $n > 35$ cells corresponding to roots imaged under comparable conditions. C. Cortex cells of *DEX>>MAX1* plant line induced by DEX/Mock treated with NAA/Mock. Arrowheads highlight PIN polarity. D. Graph shows mean ratio of lateral to basal signal intensity of PIN2 in cortex cells pre-treated by 50 μ M DEX *DEX>>MAX1* plants induced for 24h and treated with 10 μ M NAA for 4 hours. Error bars indicate standard error. A two-tailed Student's t-test compared marked sets of data. (**) $P < 0.01$. $n > 42$ cells corresponding to roots imaged under comparable conditions.

5.4 REFERENCES

- Adamowski M, Friml J. 2015. PIN-dependent auxin transport: action, regulation, and evolution. *Plant Cell* **27**(1): 20-32.
- Benkova E, Michniewicz M, Sauer M, Teichmann T, Seifertova D, Jurgens G, Friml J. 2003. Local, efflux-dependent auxin gradients as a common module for plant organ formation. *Cell* **115**(5): 591-602.
- Booker J, Sieberer T, Wright W, Williamson L, Willett B, Stirnberg P, Turnbull C, Srinivasan M, Goddard P, Leyser O. 2005. MAX1 encodes a cytochrome P450 family member that acts downstream of MAX3/4 to produce a carotenoid-derived branch-inhibiting hormone. *Dev Cell* **8**(3): 443-449.
- Crawford S, Shinohara N, Sieberer T, Williamson L, George G, Hepworth J, Muller D, Domagalska MA, Leyser O. 2010. Strigolactones enhance competition between shoot branches by dampening auxin transport. *Development* **137**(17): 2905-2913.
- Gomez-Roldan V, Fermas S, Brewer PB, Puech-Pages V, Dun EA, Pillot JP, Letisse F, Matusova R, Danoun S, Portais JC, et al. 2008. Strigolactone inhibition of shoot branching. *Nature* **455**(7210): 189-194.
- Kleine-Vehn J, Dhonukshe P, Sauer M, Brewer PB, Wisniewska J, Paciorek T, Benkova E, Friml J. 2008. ARF GEF-dependent transcytosis and polar delivery of PIN auxin carriers in Arabidopsis. *Curr Biol* **18**(7): 526-531.
- Kohlen W, Charnikhova T, Liu Q, Bours R, Domagalska MA, Beguerie S, Verstappen F, Leyser O, Bouwmeester H, Ruyter-Spira C. 2011. Strigolactones are transported through the xylem and play a key role in shoot architectural response to phosphate deficiency in nonarbuscular mycorrhizal host Arabidopsis. *Plant Physiology* **155**(2): 974-987.
- Koltai H, LekKala SP, Bhattacharya C, Mayzlish-Gati E, Resnick N, Winger S, Dor E, Yoneyama K, Yoneyama K, Hershenhorn J, et al. 2010. A tomato strigolactone-impaired mutant displays aberrant shoot morphology and plant interactions. *J Exp Bot* **61**(6): 1739-1749.
- Matusova R, Rani K, Verstappen FW, Franssen MC, Beale MH, Bouwmeester HJ. 2005. The strigolactone germination stimulants of the plant-parasitic *Striga* and *Orobanche* spp. are derived from the carotenoid pathway. *Plant Physiology* **139**(2): 920-934.
- Ruyter-Spira C, Kohlen W, Charnikhova T, van Zeijl A, van Bezouwen L, de Ruijter N, Cardoso C, Lopez-Raez JA, Matusova R, Bours R, et al. 2011. Physiological effects of the synthetic strigolactone analog GR24 on root system architecture in Arabidopsis: another belowground role for strigolactones? *Plant Physiology* **155**(2): 721-734.
- Sauer M, Balla J, Luschnig C, Wisniewska J, Reinohl V, Friml J, Benkova E. 2006. Canalization of auxin flow by Aux/IAA-ARF-dependent feedback regulation of PIN polarity. *Genes Dev* **20**(20): 2902-2911.
- Sorefan K, Booker J, Haurogne K, Goussot M, Bainbridge K, Foo E, Chatfield S, Ward S, Beveridge C, Rameau C, et al. 2003. MAX4 and RMS1 are orthologous dioxygenase-like genes that regulate shoot branching in Arabidopsis and pea. *Genes Dev* **17**(12): 1469-1474.
- Stirnberg P, Furner IJ, Ottoline Leyser HM. 2007. MAX2 participates in an SCF complex which acts locally at the node to suppress shoot branching. *Plant J* **50**(1): 80-94.
- Turnbull CG, Booker JP, Leyser HM. 2002. Micrografting techniques for testing long-distance signalling in Arabidopsis. *Plant J* **32**(2): 255-262.

Umehara M, Hanada A, Yoshida S, Akiyama K, Arite T, Takeda-Kamiya N, Magome H, Kamiya Y, Shirasu K, Yoneyama K, et al. 2008. Inhibition of shoot branching by new terpenoid plant hormones. *Nature* **455**(7210): 195-200.

6 Development of novel auxin sensor

Tomáš Prát, Inmaculada Sanchez Romero, and Harald Lukas Janovjak

6.1 INTRODUCTION

Modern, advanced research in auxin-related plant science requires proper identification of auxin transport, distribution and accumulation. We are reliant on sensors, reporters and other indicators, basic tools for description of physiological processes as well as in every other biological science. Our knowledge of auxin biology is crucially dependent on limitations of these instruments.

Auxin sensors are usually based on SCF^{TIR1}-Aux/IAA-ARF auxin signalling pathway. The *IAA2::uidA* reporter gene was constructed by fusing the *uidA*-coding sequence to the *IAA2* promoter sequence (Luschnig *et al.*, 1998). The most commonly used reporter of auxin - DR5, is based on binding preference of ARF factors of SCF^{TIR1}-Aux/IAA-ARF auxin signalling pathway to specific DNA sequence 5'-TGTCtC-3' in gene promoters, AuxRE elements (auxin response elements). Sensor DR5 was constructed by fusion of minimal constitutive promoter 35S followed by nine repetition of AuxRE motif (5'-TGTCTC-3'), together expressing *uidA* (GUS) (Ulmasov *et al.*, 1997), different fluorescent proteins (Friml *et al.*, 2003), or luciferase (Moreno-Risueno *et al.*, 2010). DR5 based sensor was recently upgraded to DR5v2. Analysis of crystal structure of two functionally divergent ARFs and protein binding microarray experiments revealed, that AuxRE motif used in original DR5 is not high-affinity binding site (Boer *et al.*, 2014; Liao *et al.*, 2015). Instead, nine high affinity AuxRE sites (5'-TGTCGG-3') was used to create novel DR5v2 reporter (Liao *et al.*, 2015). DR5v2 exhibit broader expression pattern than original line, *e.g.* during embryogenesis more distinctly mark cells in incipient cotyledon and in the root tip DR5v2 has high response also in adjacent cells of QC, in columella (Liao *et al.*, 2015). Although both markers respond to low concentration of auxin, neither DR5 nor DR5v2 show linear response to auxin concentration or treatment duration, and hence these cannot be used to infer actual auxin level (Liao *et al.*, 2015).

Position of ARF and AuxRE interaction at the end of the signalling pathway determine, that DR5 and DR5v2 reporters sense output of auxin signalling, resulting in delay of reporter activity (Vernoux *et al.*, 2011). To overcome that was developed auxin sensor *DII* using process at the beginning of auxin signalling. In comparison to DR5, *DII* is a negative reporter, indicates

auxin signalling input. Interacting Domain II of Aux/IAA protein is fused with fast maturing version of YFP fluorescent protein (VENUS). Binding of auxin between TIR1 protein and DII domain triggers ubiquitination of *DII* reporter and its degradation in proteasome. Moreover, fusion with fast maturing fluorescent marker, decrease signals appearance from 3 hours in case of *DR5::GFP* to less than 30 minutes (Brunoud *et al.*, 2012). Comparison with control line expressing mDII-Venus, that lack auxin-dependent degradation, allows semiquantitative measurement of auxin input. Unfortunately, handling with multiple controls as well as 35S promoter, not active at early steps of embryogenesis, used to drive *DII/mDII-Venus* limit experimental applications (Liao *et al.*, 2015). A single reporter *R2D2* was designed recently to overcome these issues. Ratiometric version of two DIIs combines DII domain fused with n3xVenus yellow fluorophore and mDII fused with ndtTomato red fluorophore, both constructs driven by two RPS5A promoters on single transgene. A simple image analysis of yellow/red ratio allows semiquantitative measurement of auxin accumulation at cellular level (Liao *et al.*, 2015). Different philosophy partially based on SCF^{TIR1}-Aux/IAA-ARF auxin signalling pathway auxin uses ratiometric luminescent biosensor (Wend *et al.*, 2013). Sensor construct comprises two components: a sensor module (SM), fused to firefly luciferase, and renilla luciferase. Both components are linked by a 2A peptide. 13-amino-acid minimal degradation sequences of three selected Aux/IAA family members (IAA17, IAA28, and IAA31) that confer auxin-dependent degradation were used as sensor modules. The 2A peptide allows for the stoichiometrical co-expression of SM-firefly and renilla luciferase. Auxin concentration-dependent degradation of the sensor could be monitored as a decrease in firefly relative to renilla luminescence (F/R) (Wend *et al.*, 2013).

These auxin sensors share fundamental disadvantage: They are not sensing auxin directly but through SCF^{TIR1}-Aux/IAA-ARF auxin signalling pathway. That is preventing usage of them in auxin signalling mutants. Moreover was suggested that DR5 sensor is activated also by brassinolides as well as IAA (Nakamura *et al.*, 2003). The potential method for direct auxin sensing, immunolocalization of free IAA with monoclonal anti-IAA antibodies, does not allow *in vivo* assays (Nishimura *et al.*, 2011). Therefore, we would like to develop direct auxin sensor with rapid response, spatiotemporal resolution, sensitive and selective, providing dose response signal (ratiometric), which will be easy to use.

6.1.1 Fluorescent sensors – probes as alternative in monitoring receptor-dependent signalling

To overcome disadvantages of the native receptor-dependent sensors, we would like to use an alternative method of introduction artificial probe for specific ligand. Till today, three different kinds of fluorescent probes were published: FRET probes, sensors with circularly permuted fluorescent protein and thiol-derived sensor.

Genetically-encoded Foerster Resonance Energy Transfer (FRET) nanosensors have been developed for quantification of the dynamic changes in concentration of several biologically active ligands with improved spatiotemporal resolution. FRET sensors are fusion proteins composed of a ligand-binding moiety and a fluorescent pair, donor and acceptor fluorophores, with overlapping emission and excitation spectra, typically CFP and YFP (Hou *et al.*, 2011). Binding of the ligand causes a conformational change that affects the relative distance and/or orientation between the fluorescent proteins, resulting in increase or a decrease of FRET efficiency (Marvin *et al.*, 2013).

An alternative strategy for creating genetically-encoded sensors is the allosteric modulation of the fluorescence properties of a single fluorophore. These sensors have a number of advantages: their ligand-bound states may be nearly as bright as the parental fluorophore, while their ligand-free states may be arbitrarily dim, providing broad range of fluorescence intensity. Therefore, single fluorophore sensors have increased signal-to-noise ratio (SNR) and are more resistant to photobleaching artifacts, than the FRET sensors (Tian *et al.*, 2009). Circularly permuted YFP (cpYFP) has been successfully used as a reporter fluorophore of sensors for H₂O₂ (HyPer), cGMP (FlnG), ATP:ADP ratio (Perceval) or other circularly permuted fluorophore cpGFP has been used in iGluSnFr sensor of glutamate (Belousov *et al.*, 2006; Nausch *et al.*, 2008; Berg *et al.*, 2009; Marvin *et al.*, 2011). In each case, the emission intensity was at least doubled upon ligand binding (Marvin *et al.*, 2013).

The third type of fluorescent probe, glutamate (E) optical sensor (EOS), is a hybrid sensor made from the alpha-amino-3-hydroxy-5-methyl-4-isoxazolepropionic acid (AMPA) receptor. EOS contains glutamate-binding core and a small thiol-reactive fluorescent dye, that change fluorescence intensity upon binding of glutamate *e.g.* in mouse somatosensory cortical neurons (Namiki *et al.*, 2007).

These three possible methods of sensor creation are based on small binding cores which have to fulfill crucial attribute: change of structural conformation upon binding of the ligand.

6.2 RESULTS

6.2.1 Identification of binding cores for auxin

Essential step of sensor creation is identification of binding core with known structure, which undergoes conformational change transferred to fluorescent part of the sensor. As well as in every kind of protein design, two strategies, rational and irrational, are possible. Irrational strategy of protein engineering is based on adjustment of scaffold, known flexible binding core for different ligand, to bind ligand of interest resulting in specific sensor for that compound. For creation of sensors is usually used mutation, *in vitro* directed evolution of PBP (Periplasmic binding proteins), transporters for glutamate and aspartate in bacteria (Alicea *et al.*, 2011; Marvin *et al.*, 2013). The rational strategy, use opposite way, the knowledge of specific binding of the ligand to binding core, from which the sensor is created. We decided to follow rational strategy, based on ligand dependent survey.

Firstly, we tried to identify auxin binding pockets in proteins with known preference to auxin. Not surprisingly at the beginning we were focused on auxin receptor, TIR1 and protein ABP1 (AUXIN BINDING PROTEIN 1). However was ABP1 protein the first discovered auxin receptor, mechanism of its signalling function remains unknown (Chen *et al.*, 2001). Recently, the significance of the ABP1 pathway has been undermined by the lack of any obvious developmental phenotypes of the *abp1* knockout mutants (Gao *et al.*, 2015; Grones *et al.*, 2015; Michalko *et al.*, 2015; Michalko *et al.*, 2016). ABP1 protein contains KDEL sequence determining its localization to endoplasmatic reticulum but small fraction is secreted to apoplast with ideal pH for binding of auxin (Henderson *et al.*, 1997). Unfortunately, auxin receptor and ABP1 do not undergo change of conformation necessary for establishment of sensor. Therefore, we did *in silico* survey of other auxin binding protein. We suggested that members of auxin biosynthesis, conjugation, degradation and transport should contain auxin binding pocket but in none of them is the structure known. After unsuccessful survey of plant proteins, we decided to expand area of the search.

We presumed that some of the other chemical compounds could share structural and chemical attributes with to auxin. Therefore, we perform ligand-dependent survey in

databases of published space structures of proteins (PDB – protein databank) with compounds similar to auxin. We identified two possible binding cores. The first of them is PPAR γ (PEROXISOME PROLIFERATOR_ACTIVATED RECEPTOR γ). This protein is a ligand-dependent transcription factor. Its function is correlated with glucose homeostasis and insulin sensitization in animals (Schupp *et al.*, 2009). PPAR γ contains two binding pockets recognize distinct ligands, one for trans-fatty acids and the second for serotonin-like molecules. Serotonin metabolites, 5-methoxy-indole acetate (MIA) and 5-hydroxy-indole acetate (HIA) contain indole acetate ring function as a common moiety for the recognition in the sub-pocket near helix H12 of protein PPAR γ . Chemical structure of MIA and HIA is almost similar to IAA. Conformation structure of PPAR γ undergoes change upon binding (Waku *et al.*, 2010), therefore we decided to use this protein as binding pocket for sensor creation. The second protein which we identified is HCPTP-A/ACP1 (ACID PHOSPHATASE LOCUS 1). ACP1 is a low molecular weight phosphotyrosine phosphatase (LMW-PTP), which presents two main enzymatic activities: phosphoprotein tyrosine phosphatase and flavin mononucleotide phosphatase (Bottini *et al.*, 2002). ACP1 are present in two isoenzyme states, having different molecular and catalytic properties, suggesting that they may be implicated in different biological functions in the human cells, like regulation of many growth factors, such as platelet-derived growth factor receptor (Chiarugi *et al.*, 1996), fibroblast growth factor receptor (Rigacci *et al.*, 1999), insulin receptor (Pandey *et al.*, 2007) and ephrin receptor, a peptide ligand that binds to the ephrin receptor family of tyrosine kinase receptors (Kikawa *et al.*, 2002). ACP1 has been cocrystallized with synthetic auxin NAA and change structural conformation upon binding, so we presumed the possibility of use this protein as binding core of sensor.

6.2.2 Cloning of selected binding cores, creation of the sensor

As a template for amplification of selected genes PPAR γ and ACP1 we were using cDNA isolated from HEK293 cells (Human embryonic kidney 293). Based on the results of public available microarray experiments on HEK293 cells, is the gene expression of both genes up-regulated. We amplified the genes using gene specific primers containing restriction site for *SapI* (*Lgul*) non-palindromic restriction endonuclease (RE) and unique linker, which allows insertion of DNA sequence in proper direction into plasmids called GoldenGate cloning

system. We cloned PCR product following GoldenGate “one pot” periodic ligation and digestion protocol.

The next step after binding core cloning was the establishment of sensor based on type. In a case of cpGFP sensor, the crucial step was introduction of fluorophore into part of the protein undergoing a conformational change upon binding. We were using digestion and ligation using RE but because of there was none unique restriction site in the sequence, we introduce it through primers containing nucleotide substitution causes *in vitro* synonymous mutation in the binding core sequence to make recognition site for *Bam*HI RE. Then we ligated cpGFP sequence specifically into this site by *Bam*HI RE. The second sensor we made was the FRET probe, therefore we cloned binding core between two fluorophores, acceptor CFP and emitter VENUS (YFP). Because of the sequence of binding core contained stop codon Amber, we removed it by substitution of nucleotides, similarly like in cpGFP insertion but we changed Amber stop codon to codon for tyrosine amino acid. Then all three parts, CFP, binding core and YFP are expressed together as one protein. The third sensor EOS-like, were cloned for testing of functionality of sensors and elucidation of spatiotemporal conformational change (Namiki *et al.*, 2007). For that was necessary to introduce cysteine amino acid to flexible loop of our binding core. The mechanism of signal emission of this kind of sensor is based on chemical reaction between cysteine and maleimide joined with small fluorescent dye, in our case AlexaFluor488 (Alexa488). After adding of reducing agent tris(2-carboxyethyl)phosphine (TCEP), that can keep the cysteines from forming di-sulphide bonds, will not react as readily with the maleimide. Insertion of artificial cysteine in the loop that undergoes change of conformation upon binding of the ligand, on exposed part of the protein to space, deviate the observed fluorescence signal.

6.2.3 Testing of the sensor

The important step in sensor creation is a validation of function. We developed high throughput method for testing of the sensor *in vitro*, using streptavidin-biotin binding assay on 96-well plate (Winkler *et al.*, 1997). The sensor was cloned with biotin tag, the site providing strong biotinylation. The ELISA 96-well plate with transparent bottom was coated with streptavidin solution at final concentration 10 µg/mL. Then the isolated protein fractions, supernatant or pellet, was applied to each well. After multiple washing, to get rid of unbound proteins, only protein with a biotin tag is present in the well. We were using Biotek plate

reader H1 with injectors for rapid testing of fluorescence changes of our sensor. We performed pilot experiment to verify usability of streptavidin-biotin assay. We were using biotinylated Alexa488 in comparison to free Alexa488. To test suitability for protein testing, we applied eGFP protein with biotin tag and without, respectively. Results show the sensitivity of our method, for Alexa488 we could distinguish concentration with threshold between 10 nM and 1nM and for proteins dilutions to 1:20 in blocking solution.

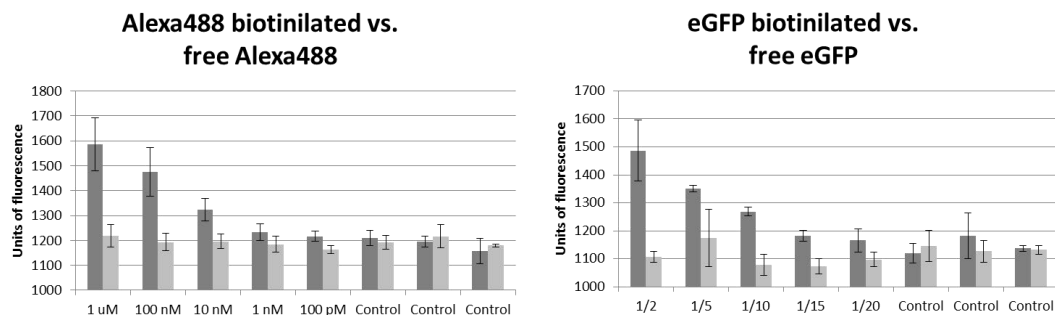


Figure 6-1 Pilot experiments to verify usability of streptavidin-biotin assay.

6.2.4 EOS-like sensor

The first experiments with sensors were performed. We expressed EOS-like sensor containing ACP1 binding core in IPTG inducible heat-shock competent cell line BL21. We defined expression condition, the concentration of IPTG as 0.1 – 0.4 μ M, temperature 18 deg. C in overnight cultivation. Then we isolated whole protein content, divided to soluble supernatant fraction and insoluble pellet. We applied protein fractions to our streptavidin coated 96-well plate, performed maleimide reaction with TCEP, cultivated overnight with 0.125 mM solution of Alexa488-C5-maleimide fluorescent dye and after extensive washing we added auxin NAA or IAA in final concentration of 1.25 mM. We made six triplicates for each supernatant, pellet, NAA and IAA together with controls without protein fractions or with protein but without fluorescent dye. Before adding of auxin, we have measured background fluorescence, which then was deducted from obtained fluorescence signal.

The results from measurement of fluorescent signal in activated EOS-like sensor showed not robust, random changes of the signal. Therefore, we can't claim that the binding core of ACP1 is functional for binding of auxin and could be used for sensor. Since we were not sure if these negative results are caused by experiment design or method, we decide anyway to continue with other fluorescent sensor types.

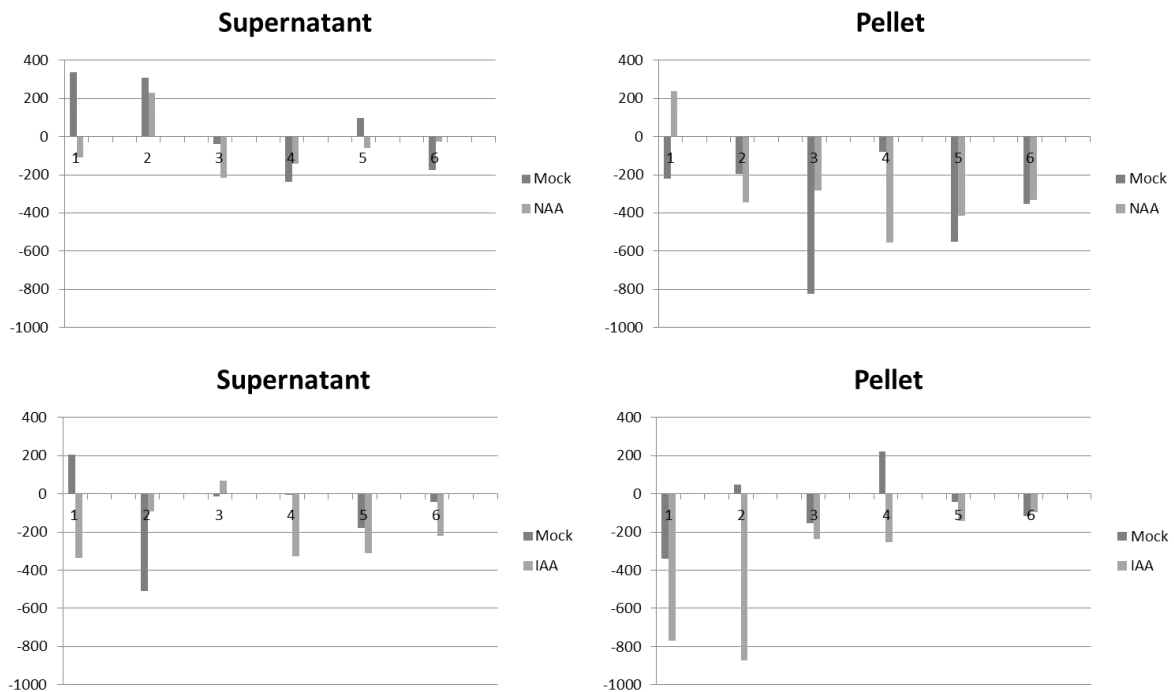


Figure 6-2 Results of maleimide reaction on EOS-like sensor with ACP1 binding core.

6.2.5 FRET based sensor

We expressed EOS-like sensor containing ACP1 binding core in IPTG inducible heat-shock competent cell line BL21. We used defined expression condition like in EOS sensor, the concentration of IPTG as 0.1 – 0.4 μ M, temperature 18 deg. C in overnight cultivation. Unfortunately, no increase in expression was observed, maybe because of cell toxicity of produced transgene induced by IPTG.

Therefore, we used ZYM-5052 autoinduction medium for BL21 cells. Protein extract of sonicated cells was then purified on Ni-NTA His GraviTrap column (GE Healthcare), with binding buffer containing 20 mM imidazole and elution buffer of 500 mM imidazole. Purified protein was desalted by PD-10 desalting column (GE Healthcare). From 600 mL of bacterial culture we got 3.5 mL of purified ACP1-flipe FRET probe of concentration about 2 mg/mL.

Protein was diluted in sodium phosphate monobasic buffer concentration 0.25 or 0.5 mg/mL. We measured fluorescence properties of ACP1-flipe probe in spectrophotometer (Spectramax M2e microplate/cuvette reader) at excitation wavelength 433 nm, with cut off 455 nm in emission spectrum of 460 – 560 nm with step per 2 nm and 3 technical repeats. As a control we used benzoic acid (BA) with pK_a = 4.19, that is very close to pK_a of IAA (pK_a = 4.7 - 4.84). As secondary control, we used structurally similar compound to IAA, its precursor tryptophan (Trp) amino acid with pK_a =9.4. We tested three different concentrations

1 nM, 10 nM and 100 nM of IAA, BA and 10 nM and 100 nM for Trp. Mock treatments were performed with equivalent amounts of the respective solvents. Moreover, we tested also NAA of 10 nM. For analysis we used ratio of fluorescent intensity of CFP emission wavelength 470 nm to YFP emission wavelength 534 nm.

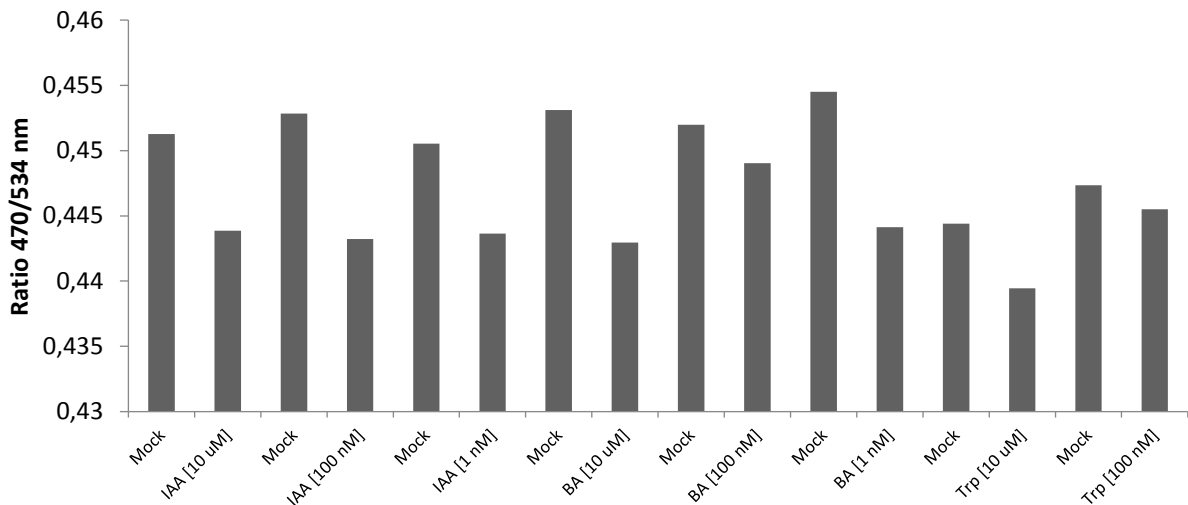


Figure 6-3 Results of FRET sensor with ACP1 binding core.

Unfortunately, we observed FRET process ongoing also by mock treated ACP1-fluorophore sensor. Emission spectra were not dramatically shifted in favor of YFP neither by application of different concentration of native auxin IAA, nor NAA auxin analogue. Control treatments, as well as auxins caused not stable and robust random change of fluorescent intensity. FRET ongoing without application of ligand could be simply caused by fact, that binding core of ACP1 is too small, by absence of longer linker separating both fluorophores and spatial conformation of whole artificial protein. Theoretically, these issues could be solved by use of probe with single fluorescent protein, circularly permuted GFP.

6.2.6 cpGFP sensor

For expression and extraction of ACP1-cpGFP probe we used similar experimental procedure as in case of genetically encoded, high-signal-to-noise maltose sensor (Marvin et al., 2011). Protein was extracted by freeze-thaw lysis and rapid shaking in 800 μ L phosphate-buffered saline in 2 mL Eppendorf tube. Crude lysate was clarified by centrifugation at 4000g for 30 min. Clarified lysate was diluted and transferred to cuvette for spectrophotometry and mixed with IAA or BA or Trp to final concentration of ligand 10 nM 100 nM. We measured spectral properties of mixture in spectrophotometer (Spectramax M2e microplate/cuvette reader) at excitation wavelength 485 nm, with cut off 495 nm in emission spectrum

of 500 - 560 nm with step per 2 nm and 3 technical repeats. For analysis we used ratio of fluorescent intensities $\Delta F/F_0$ where ΔF is difference between fluorescent intensity after adding ligand and initial fluorescence at wavelength of 514 nm ($\Delta F = F_{\text{ligand}} - F_0$; $F_{514 \text{ nm}}$) and F_0 is initial fluorescence (Marvin et al., 2011).

We performed two independent experiments with similar trend for 100 nM concentration of compounds, interestingly 10 nM concentration of BA caused opposite change of ratio. These not robust, random changes of the fluorescent signal are in line with two previous strategies for sensor design. Therefore, we cannot claim that the binding core of ACP1 is functional for binding of auxin and could be used for sensor.

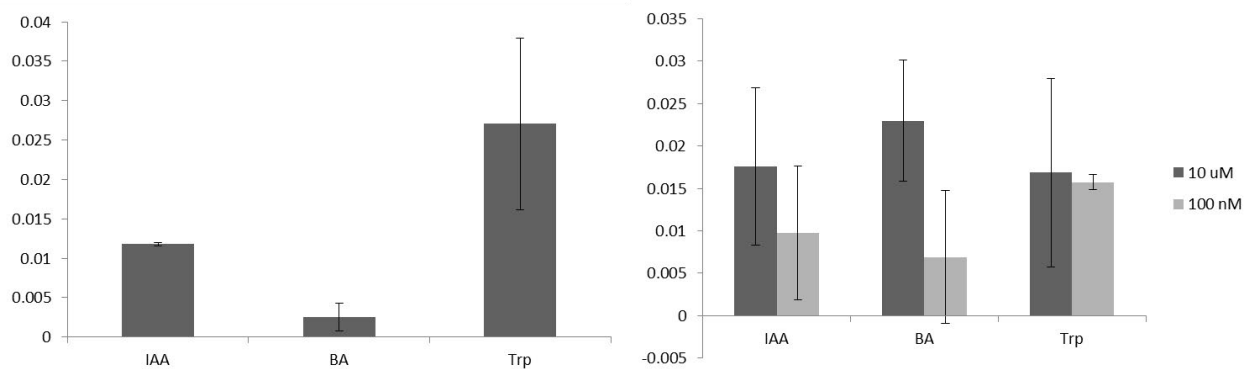


Figure 6-4 Results of two independent experiments with cpGFP sensor containing ACP1 binding core.

6.3 DISCUSSION

Due to time constrains, PPAR γ binding core was not cloned to check binding core capabilities but all cloning plasmids were done and method procedures were optimized. If none of the identified binding core will be successful, irrational design approach in sensor creation is possible to use. It means *e.g. in vitro* directed evolution of PBP (Periplasmic binding proteins) to develop sensitivity for auxin (Alicea et al., 2011; Marvin et al., 2013). Fundamental issue in this approach will be cope structural similarity of IAA to common compound in plant cells – Tryptophan.

Recently, direct interaction of ETTIN (ETT/ARF3) auxin response factor and basic helix-loop-helix (bHLH) transcription factor INDEHISCENT (IND) upon presence of auxin was suggested (Østergaard, personal communication). *ETT* encodes an auxin response factor (ARF3) and mutants show pleiotropic phenotypes that include ectopic sepals and petals and fewer stamens in the abaxial domain (Nemhauser et al., 2000). IND is responsible for the formation of an auxin minimum in the dehiscence zone of the fruit. This auxin minimum is

required for separation layer specification (Sorefan *et al.*, 2009). Overexpression of IND in seedlings was found to lead to PIN1 and PIN3 polarity loss. IND and the bHLH transcription factor SPATULA (SPT) were found to bind the promoters of the AGC kinase genes PINOID (PID) and WAG2 and to repress the expression of PID and upregulate the expression of WAG2 in seedlings and developing fruits (Sorefan *et al.*, 2009; Girin *et al.*, 2011). Protein-protein interaction of ETT and IND was thoroughly tested by FRET assay (Weijers, personal communication). We proposed model of possible FRET probe using interaction of ETT and IND.

Substantial amount of questions is still not answered. One of the first is connected to phenotypes caused by gain-of-function of IND and loss-of-function *ett* respectively. Biosensor cannot change phenotype. Possible way is a deletion study inspired *e.g.* on *spt* mutant but still sensitive to auxin-dependent interaction. Other questions are how does proposed sensor affect auxin signalling? What if sensor switches on auxin responsive genes *e.g.* PID? How does sensor affect pool of intracellular auxin? Does interaction of IND and ETT need other putative regulators/interactors? Does interaction happen without DNA binding (that is relevant for sensors of apoplastic auxin levels)?

From practical point of view is relevant which terminus shall be used for CFP/YFP for ETT and IND, what are necessary molecular properties of flexible linker “hinge” between IND and ETT and how to perform fast turnover of sensor.

Although, we were not successful with experimental auxin sensor design we identified possible ways for future investigation on field of plant hormone auxin biosensors.

6.4 REFERENCES

- Alicea I, Marvin JS, Miklos AE, Ellington AD, Looger LL, Schreiter ER. 2011. Structure of the Escherichia coli phosphonate binding protein PhnD and rationally optimized phosphonate biosensors. *J Mol Biol* **414**(3): 356-369.
- Belousov VV, Fradkov AF, Lukyanov KA, Staroverov DB, Shakhbazov KS, Terskikh AV, Lukyanov S. 2006. Genetically encoded fluorescent indicator for intracellular hydrogen peroxide. *Nat Methods* **3**(4): 281-286.
- Berg J, Hung YP, Yellen G. 2009. A genetically encoded fluorescent reporter of ATP:ADP ratio. *Nat Methods* **6**(2): 161-166.
- Boer DR, Freire-Rios A, van den Berg WA, Saaki T, Manfield IW, Kepinski S, Lopez-Vidrieo I, Franco-Zorrilla JM, de Vries SC, Solano R, et al. 2014. Structural basis for DNA binding specificity by the auxin-dependent ARF transcription factors. *Cell* **156**(3): 577-589.
- Bottini N, Ammendola M, Gloria-Bottini F. 2002. ACP1 is associated with allergy. *Allergy* **57**(7): 651-652.
- Brunoud G, Wells DM, Oliva M, Larrieu A, Mirabet V, Burrow AH, Beeckman T, Kepinski S, Traas J, Bennett MJ, et al. 2012. A novel sensor to map auxin response and distribution at high spatio-temporal resolution. *Nature* **482**(7383): 103-106.
- Chen JG, Ullah H, Young JC, Sussman MR, Jones AM. 2001. ABP1 is required for organized cell elongation and division in Arabidopsis embryogenesis. *Genes Dev* **15**(7): 902-911.
- Chiarugi P, Cirri P, Raugei G, Manao G, Taddei L, Ramponi G. 1996. Low M(r) phosphotyrosine protein phosphatase interacts with the PDGF receptor directly via its catalytic site. *Biochem Biophys Res Commun* **219**(1): 21-25.
- Friml J, Vieten A, Sauer M, Weijers D, Schwarz H, Hamann T, Offringa R, Jurgens G. 2003. Efflux-dependent auxin gradients establish the apical-basal axis of Arabidopsis. *Nature* **426**(6963): 147-153.
- Gao Y, Zhang Y, Zhang D, Dai X, Estelle M, Zhao Y. 2015. Auxin binding protein 1 (ABP1) is not required for either auxin signaling or Arabidopsis development. *Proc Natl Acad Sci U S A* **112**(7): 2275-2280.
- Girin T, Paicu T, Stephenson P, Fuentes S, Korner E, O'Brien M, Sorefan K, Wood TA, Balanza V, Ferrandiz C, et al. 2011. INDEHISCENT and SPATULA interact to specify carpel and valve margin tissue and thus promote seed dispersal in Arabidopsis. *Plant Cell* **23**(10): 3641-3653.
- Grones P, Chen X, Simon S, Kaufmann WA, De Rycke R, Nodzynski T, Zazimalova E, Friml J. 2015. Auxin-binding pocket of ABP1 is crucial for its gain-of-function cellular and developmental roles. *J Exp Bot* **66**(16): 5055-5065.
- Henderson J, Baulry JM, Ashford DA, Oliver SC, Hawes CR, Lazarus CM, Venis MA, Napier RM. 1997. Retention of maize auxin-binding protein in the endoplasmic reticulum: quantifying escape and the role of auxin. *Planta* **202**(3): 313-323.
- Hou BH, Takanaga H, Grossmann G, Chen LQ, Qu XQ, Jones AM, Lalonde S, Schweissgut O, Wiechert W, Frommer WB. 2011. Optical sensors for monitoring dynamic changes of intracellular metabolite levels in mammalian cells. *Nat Protoc* **6**(11): 1818-1833.
- Kikawa KD, Vidale DR, Van Etten RL, Kinch MS. 2002. Regulation of the EphA2 kinase by the low molecular weight tyrosine phosphatase induces transformation. *J Biol Chem* **277**(42): 39274-39279.
- Liao CY, Smet W, Brunoud G, Yoshida S, Vernoux T, Weijers D. 2015. Reporters for sensitive and quantitative measurement of auxin response. *Nat Methods* **12**(3): 207-210, 202 p following 210.

- Luschign C, Gaxiola RA, Grisafi P, Fink GR. 1998.** EIR1, a root-specific protein involved in auxin transport, is required for gravitropism in *Arabidopsis thaliana*. *Genes Dev* **12**(14): 2175-2187.
- Marvin JS, Borghuis BG, Tian L, Cichon J, Harnett MT, Akerboom J, Gordus A, Renninger SL, Chen TW, Bargmann CI, et al. 2013.** An optimized fluorescent probe for visualizing glutamate neurotransmission. *Nat Methods* **10**(2): 162-170.
- Marvin JS, Schreiter ER, Echevarria IM, Looger LL. 2011.** A genetically encoded, high-signal-to-noise maltose sensor. *Proteins* **79**(11): 3025-3036.
- Michalko J, Dravecka M, Bollenbach T, Friml J. 2015.** Embryo-lethal phenotypes in early *abp1* mutants are due to disruption of the neighboring *BSM* gene. *F1000Res* **4**: 1104.
- Michalko J, Glanc M, Perrot-Rechenmann C, Friml J. 2016.** Strong morphological defects in conditional *Arabidopsis abp1* knock-down mutants generated in absence of functional *ABP1* protein. *F1000Res* **5**: 86.
- Moreno-Risueno MA, Van Norman JM, Moreno A, Zhang J, Ahnert SE, Benfey PN. 2010.** Oscillating gene expression determines competence for periodic *Arabidopsis* root branching. *Science* **329**(5997): 1306-1311.
- Nakamura A, Higuchi K, Goda H, Fujiwara MT, Sawa S, Koshiba T, Shimada Y, Yoshida S. 2003.** Brassinolide induces *IAA5*, *IAA19*, and *DR5*, a synthetic auxin response element in *Arabidopsis*, implying a cross talk point of brassinosteroid and auxin signaling. *Plant Physiology* **133**(4): 1843-1853.
- Namiki S, Sakamoto H, Iinuma S, Iino M, Hirose K. 2007.** Optical glutamate sensor for spatiotemporal analysis of synaptic transmission. *Eur J Neurosci* **25**(8): 2249-2259.
- Nausch LW, Ledoux J, Bonev AD, Nelson MT, Dostmann WR. 2008.** Differential patterning of cGMP in vascular smooth muscle cells revealed by single GFP-linked biosensors. *Proc Natl Acad Sci U S A* **105**(1): 365-370.
- Nemhauser JL, Feldman LJ, Zambryski PC. 2000.** Auxin and *ETTIN* in *Arabidopsis* gynoecium morphogenesis. *Development* **127**(18): 3877-3888.
- Nishimura T, Toyooka K, Sato M, Matsumoto S, Lucas MM, Strnad M, Baluska F, Koshiba T. 2011.** Immunohistochemical observation of indole-3-acetic acid at the *IAA* synthetic maize coleoptile tips. *Plant Signal Behav* **6**(12): 2013-2022.
- Pandey SK, Yu XX, Watts LM, Michael MD, Sloop KW, Rivard AR, Leedom TA, Mancham VP, Samadzadeh L, McKay RA, et al. 2007.** Reduction of low molecular weight protein-tyrosine phosphatase expression improves hyperglycemia and insulin sensitivity in obese mice. *J Biol Chem* **282**(19): 14291-14299.
- Rigacci S, Rovida E, Bagnoli S, Dello Sbarba P, Berti A. 1999.** Low M(r) phosphotyrosine protein phosphatase activity on fibroblast growth factor receptor is not associated with enzyme translocation. *FEBS Lett* **459**(2): 191-194.
- Schupp M, Cristancho AG, Lefterova MI, Hanniman EA, Briggs ER, Steger DJ, Qatanani M, Curtin JC, Schug J, Ochsner SA, et al. 2009.** Re-expression of *GATA2* cooperates with peroxisome proliferator-activated receptor- γ depletion to revert the adipocyte phenotype. *J Biol Chem* **284**(14): 9458-9464.
- Sorefan K, Girin T, Liljegren SJ, Ljung K, Robles P, Galvan-Ampudia CS, Offringa R, Friml J, Yanofsky MF, Ostergaard L. 2009.** A regulated auxin minimum is required for seed dispersal in *Arabidopsis*. *Nature* **459**(7246): 583-586.
- Ulmasov T, Murfett J, Hagen G, Guilfoyle TJ. 1997.** Aux/*IAA* proteins repress expression of reporter genes containing natural and highly active synthetic auxin response elements. *Plant Cell* **9**(11): 1963-1971.

- Vernoux T, Brunoud G, Farcot E, Morin V, Van den Daele H, Legrand J, Oliva M, Das P, Larrieu A, Wells D, et al. 2011.** The auxin signalling network translates dynamic input into robust patterning at the shoot apex. *Mol Syst Biol* **7**: 508.
- Waku T, Shiraki T, Oyama T, Maebara K, Nakamori R, Morikawa K. 2010.** The nuclear receptor PPARgamma individually responds to serotonin- and fatty acid-metabolites. *EMBO J* **29**(19): 3395-3407.
- Wend S, Dal Bosco C, Kampf MM, Ren F, Palme K, Weber W, Dovzhenko A, Zurbriggen MD. 2013.** A quantitative ratiometric sensor for time-resolved analysis of auxin dynamics. *Sci Rep* **3**: 2052.
- Winkler IG, Lochelt M, Levesque JP, Bodem J, Flugel RM, Flower RL. 1997.** A rapid streptavidin-capture ELISA specific for the detection of antibodies to feline foamy virus. *J Immunol Methods* **207**(1): 69-77.

7 Conclusions

The auxin feed-back on polar PIN localization was proposed by canalization hypothesis as a crucial mechanism in mediating multiple developmental processes. Here, we used the auxin effect on PIN polarity in *Arabidopsis* root meristems as a proxy for canalization and performed microarray experiments to find regulators of this process.

We described novel regulator downstream of SCF^{TIR1}-Aux/IAA-ARF auxin signalling pathway, transcription factor *WRKY23* (At2g47260), and demonstrate its crucial role in mediating the auxin effect on PIN polarity. In order to identify transcriptional targets of *WRKY23*, we performed consequential expression profiling experiments. Among several genes mostly related to the groups of cell wall and defense process regulators, we identified *LYSINE-HISTIDINE TRANSPORTER 1* (*LHT1*; At5g40780), a small amino acid permease gene and member of receptor-like protein kinase LRR-RLK (*LEUCINE-RICH REPEAT TRANSMEMBRANE PROTEIN KINASE PROTEIN 1*; *LRRK1*; At1g05700), which also affects auxin-dependent PIN re-arrangement. Additionally, we described role of novel phytohormone group, strigolactone, in auxin-dependent PIN re-arrangement, that could be a fundament for future studies in this field.

Our results provide first insights into an auxin transcriptional network targeting PIN localization and thus regulating plant development. This work provides unique comprehensive treatise on regulation property of auxin signalling on PIN polarity re-arrangement which is not been reported so far.

A. Appendix – WRKY23 is a component of the transcriptional network mediating auxin feedback on the PIN polarity

Table S1.

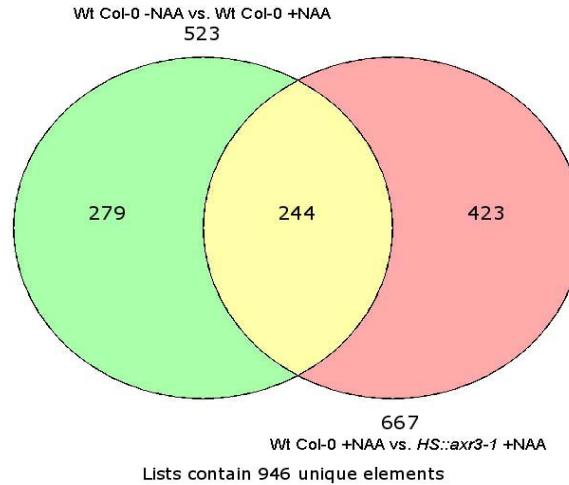
A. Venn diagram representing gene overlay of microarray experiments. Dataset of auxin regulated genes in Wt Col-0 seedlings was overlaid with a second set of acquired from comparison of auxin treated Wt Col-0 and heat-shock induced auxin treated *HS::axr3-1*. Overlap of these genes yielded a list of 244 candidate genes list. B. The gene model description is depicted as it appears in TAIR database. Experiments were designed by M.Sau., performed by M.Sch. and statistical analysis was performed by M.Sch. and G.M..

Table S2.

A. Venn diagram representing gene overlay of microarray experiments. Datasets of genes differentially regulated in *HS::axr3-1* compared to auxin-regulated genes in wild were overlaid with a third set of genes which are no longer auxin regulated in *arf7 arf19* background (Okushima *et al.*, 2005). B. Candidate genes from microarray experiments yielded 125 genes containing also putative polarity regulators. The gene model description is depicted as it appears in TAIR database. Experiments were designed by M.Sau., performed by M.Sch. and statistical analysis was performed by M.Sch. and G.M..

Table S1.

A



B

Locus identifier	Primary Gene Symbol	Gene Model Description
AT1G02400	GIBBERELLIN 2-OXIDASE 6 (GA2OX6)	Encodes a gibberellin 2-oxidase that acts on C19 gibberellins but not C20 gibberellins.
AT1G02850	BETA GLUCOSIDASE 11 (BGLU11)	beta glucosidase 11 (BGLU11)
AT1G03820		unknown protein
AT1G03870	FASCICLIN-LIKE ARABINOOGALACTAN 9 (FLA9)	fasciclin-like arabinogalactan-protein 9 (Fla9)
AT1G04040		HAD superfamily, subfamily IIB acid phosphatase
AT1G05530	UDP-GLUCOSYL TRANSFERASE 75B2 (UGT75B2)	Encodes a protein with glucosyltransferase activity with high sequence homology to UGT1 (AT1G05560). It belongs to an UGT subfamily that binds UDP-glucose but not UDP-glucuronate, UDP-galactose, or UDP-rhamnose as the glycosyl donor. UGT2 was shown to be able to use abscisic acid as glycosylation substrate in the presence of UDP-glucose.
AT1G08500	EARLY NODULIN-LIKE PROTEIN 18 (ENODL18)	early-nodulin-like protein 18 (ENODL18); FUNCTIONS IN: electron carrier activity, copper ion binding; LOCATED IN: anchored to membrane;
AT1G14350	FOUR LIPS (FLP)	Encodes a putative MYB transcription factor involved in stomata development, loss of FLP activity results in a failure of guard mother cells (GMCs) to adopt the guard cell fate, thus they continue to divide resulting in abnormal stomata consisting of clusters of numerous guard cell-like cells. This phenotype is enhanced in double mutants with MYB88.
AT1G14540		Peroxidase superfamily protein
AT1G15210	ATP-BINDING CASSETTE G35 (ABCG35)	pleiotropic drug resistance 7 (PDR7)
AT1G15580	INDOLE-3-ACETIC ACID INDUCIBLE 5 (IAA5)	auxin induced protein
AT1G19220	AUXIN RESPONSE FACTOR 19 (ARF19)	Encodes an auxin response factor that contains the conserved VP1-B3 DNA-binding domain at its N-terminus and the Aux/IAA-like domains III and IV present in most ARFs at its C-terminus. The protein interacts with IAA1 (yeast two hybrid) and other auxin response elements such as ER7 and ER9 (yeast one hybrid). ARF19 protein can complement many aspects of the ar7 mutant phenotype and , together with ARF7, is involved in the response to ethylene. In the ar7 arf19 double mutant, several auxin- responsive genes (e.g. IAA5, LBD16, LBD29 and LBD33) are no longer upregulated by auxin.
AT1G21980	PHOSPHATIDYLINOSITOL 1-4-PHOSPHATE 5-KINASE 1 (PIP5K1)	Type I phosphatidylinositol-4-phosphate 5-kinase. Preferentially phosphorylates PtdIns4P. Induced by water stress and abscisic acid in Arabidopsis thaliana. Expressed in procambial cells of leaves, flowers and roots. A N-terminal Membrane Occupation and Recognition Nexus (MORN) affects enzyme activity and distribution.
AT1G22330		RNA-binding (RRM/RBD/RNP motifs) family protein
AT1G22530	PATELLIN 2 (PATL2)	PATELLIN 2 (PATL2)
AT1G23080	PIN-FORMED 7 (PIN7)	Encodes a novel component of auxin efflux that is located apically in the basal cell and is involved during embryogenesis in setting up the apical-basal axis in the embryo. It is also involved in pattern specification during root development. In roots, it is expressed at lateral and basal membranes of provascular cells in the meristem and elongation zone, whereas in the columella cells it coincides with the PIN3 domain. Plasma membrane-localized PIN proteins mediate a saturable efflux of auxin. PINs mediate auxin efflux from mammalian and yeast cells without needing additional plant-specific factors. The action of PINs in auxin efflux is distinct from PGP, rate-limiting, specific to auxins and sensitive to auxin transport inhibitors. PINs are directly involved of in catalyzing cellular auxin efflux.
AT1G25230		Calcineurin-like metallo-phosphoesterase superfamily protein;
AT1G25450	3-KETOACYL-COA SYNTHASE 5 (KCS5)	Encodes KCS5, a member of the 3-ketoacyl-CoA synthase family involved in the biosynthesis of VLCFA (very long chain fatty acids).
AT1G28370	ERF DOMAIN PROTEIN 11 (ERF11)	encodes a member of the ERF (ethylene response factor) subfamily B-1 of ERF/AP2 transcription factor family. The protein contains one AP2 domain. There are 15 members in this subfamily including ATERF-3, ATERF-4, ATERF-7, and leafy petiole.
AT1G28380	NECROTIC SPOTTED LESIONS 1 (NSL1)	This gene is predicted to encode a protein involved in negatively regulating salicylic acid-related defense responses and cell death programs.
AT1G28680		HXXXD-type acyl-transferase family protein
AT1G29500		SAUR-like auxin-responsive protein family
AT1G29510	SMALL AUXIN UPREGULATED 68 (SAUR68)	SMALL AUXIN UPREGULATED 68 (SAUR68);
AT1G33590		Leucine-rich repeat (LRR) family protein
AT1G33790		jacalin lectin family protein;
AT1G50660		unknown protein;
AT1G52050		Mannose-binding lectin superfamily protein;
AT1G52830	INDOLE-3-ACETIC ACID 6 (IAA6)	An extragenic dominant suppressor of the hy2 mutant phenotype. Also exhibits aspects of constitutive photomorphogenic phenotype in the absence of hy2. Mutants have dominant leaf curling phenotype shortened hypocotyls and reduced apical hook. Induced by indole-3-acetic acid.
AT1G55330	ARABINOOGALACTAN PROTEIN 21 (AGP21)	Encodes a putative arabinogalactan-protein (AGP21).

Locus identifier	Primary Gene Symbol	Gene Model Description
AT1G55740	SEED IMBIBITION 1 (SIP1)	seed imbibition 1 (SIP1)
AT1G56020		unknown protein
AT1G60000		RNA-binding (RRM/RBD/RNP motifs) family protein
AT1G60010		unknown protein
AT1G62770		Plant invertase/pectin methylesterase inhibitor superfamily protein
AT1G63830		PLAC8 family protein;
AT1G64390	GLYCOSYL HYDROLASE 9C2 (GH9C2)	glycosyl hydrolase 9C2 (GH9C2)
AT1G64405		unknown protein
AT1G69530	EXPANSIN A1 (EXPA1)	Member of Alpha-Expansin Gene Family. Naming convention from the Expansin Working Group (Kende et al. Plant Mol Bio). Involved in the formation of nematode-induced syncytia in roots of Arabidopsis thaliana.
AT1G70230	TRICHOME BIREFRINGENCE-LIKE 27 (TBL27)	Encodes a member of the TBL (TRICHOME BIREFRINGENCE-LIKE) gene family containing a plant-specific DUF231 (domain of unknown function) domain. TBL gene family has 46 members, two of which (TBR/AT5G06700 and TBL3/AT5G01360) have been shown to be involved in the synthesis and deposition of secondary wall cellulose, presumably by influencing the esterification state of pectic polymers. A nomenclature for this gene family has been proposed (Volker Bischoff & Wolf Scheible, 2010, personal communication).
AT1G70560	TRYPTOPHAN AMINOTRANSFERASE OF ARABIDOPSIS 1 (TAA1)	TAA1 is involved in the shade-induced production of indole-3-pyruvate (IPA), a precursor to IAA, a biologically active auxin. It is also involved in regulating many aspects of plant growth and development from embryogenesis to flower formation and plays a role in ethylene-mediated signaling. This enzyme can catalyze the formation of IPA from L-tryptophan. Though L-Trp is expected to be the preferred substrate <i>in vivo</i> , TAA1 also acts as an aminotransferase using L-Phe, L-Tyr, L-Leu, L-Ala, L-Met, and L-Gln.
AT1G70940	PIN-FORMED 3 (PIN3)	A regulator of auxin efflux and involved in differential growth. PIN3 is expressed in gravity-sensing tissues, with PIN3 protein accumulating predominantly at the lateral cell surface. PIN3 localizes to the plasma membrane and to vesicles. In roots, PIN3 is expressed without pronounced polarity in tiers two and three of the columella cells, at the basal side of vascular cells, and to the lateral side of pericycle cells of the elongation zone. PIN3 overexpression inhibits root cell growth. Protein phosphorylation plays a role in PIN3 trafficking to the plasma membrane.
AT1G72900		Toll-Interleukin-Resistance (TIR) domain-containing protein;
AT1G73590	PIN-FORMED 1 (PIN1)	Encodes an auxin efflux carrier involved in shoot and root development. It is involved in the maintenance of embryonic auxin gradients. Loss of function severely affects organ initiation, pin1 mutants are characterised by an inflorescence meristem that does not initiate any flowers, resulting in the formation of a naked inflorescence stem. PIN1 is involved in the determination of leaf shape by actively promoting development of leaf margin serrations. In roots, the protein mainly resides at the basal end of the vascular cells, but weak signals can be detected in the epidermis and the cortex. Expression levels and polarity of this auxin efflux carrier change during primordium development suggesting that cycles of auxin build-up and depletion accompany, and may direct, different stages of primordium development. PIN1 action on plant development does not strictly require function of PGP1 and PGP19 proteins.
AT1G73620		Pathogenesis-related thaumatin superfamily protein
AT1G73780		Bifunctional inhibitor/lipid-transfer protein/seed storage 2S albumin superfamily protein;
AT1G74660	MINI ZINC FINGER 1 (MIF1)	Encodes MINI ZINC FINGER 1 (MIF1) which has a zinc finger domain but lacks other protein motifs normally present in transcription factors. MIF1 physically interact with a group of zinc finger-homeodomain (ZHD) transcription factors, such as ZHD5 (AT1G75240), that regulate floral architecture and leaf development. Gel mobility shift assays revealed that MIF1 blocks the DNA binding activity of ZHD5 homodimers by competitively forming MIF1-ZHD5 heterodimers. Constitutive overexpression of MIF1 caused dramatic developmental defects, seedlings were non-responsive to gibberellin (GA) for cell elongation, hypersensitive to the GA synthesis inhibitor paclobutrazol (PAC) and abscisic acid (ABA), and hypersensitive to auxin, brassinosteroid and cytokinin, but normally responsive to ethylene.
AT1G74790		catalytics
AT1G75500	WALLS ARE THIN 1 (WAT1)	An Arabidopsis thaliana homolog of Medicago truncatula NODULIN21 (MtN21). The gene encodes a plant-specific, predicted integral membrane protein and is a member of the Plant-Drug/Metabolite Exporter (P-DME) family (Transporter Classification number: TC 2.A.7.3).
AT1G77280		Protein kinase protein with adenine nucleotide alpha hydrolases-like domain
AT1G78100		F-box family protein;
AT1G78420		RING/U-box superfamily protein
AT2G01430	HOMEBOX-LEUCINE ZIPPER PROTEIN 17 (HB17)	homeobox-leucine zipper protein 17 (HB17);
AT2G01910	(ATMAP65-6)	Binds microtubules. Induces a crisscross mesh of microtubules, not bundles. Not involved in microtubule polymerization nor nucleation. Localizes to mitochondria.
AT2G02620		Cysteine/Histidine-rich C1 domain family protein
AT2G03730	ACT DOMAIN REPEAT 5 (ACR5)	Member of a small family of ACT domain containing proteins. ACT domains are thought to be involved in amino acid binding.
AT2G03830	ROOT MERISTEM GROWTH FACTOR 8 (RGF8)	Encodes a root meristem growth factor (RGF). Belongs to a family of functionally redundant homologous peptides that are secreted, tyrosine-sulfated, and expressed mainly in the stem cell area and the innermost layer of central columella cells. RGFs are required for maintenance of the root stem cell niche and transit amplifying cell proliferation. Members of this family include: At5g60810 (RGF1), At1g13620 (RGF2), At2g04025 (RGF3), At3g30350 (RGF4), At5g51451 (RGF5), At4g16515 (RGF6), At3g02240 (RGF7), At2g03830 (RGF8) and At5g64770 (RGF9).
AT2G05940		Protein kinase superfamily protein;
AT2G14960	(GH3.1)	encodes a protein similar to IAA-amido synthases. Lines carrying an insertion in this gene are hypersensitive to auxin.
AT2G18690		unknown protein;
AT2G18800	XYLOGLUCAN ENDOTRANSGLUCOSYLASE/HYDROLASE 21 (XTH21)	xyloglucan endotransglucosylase/hydrolase 21 (XTH21);
AT2G18980		Peroxidase superfamily protein
AT2G22500	UNCOUPLING PROTEIN 5 (UCP5)	Encodes one of the mitochondrial dicarboxylate carriers (DIC): DIC1 (AT2G22500), DIC2 (AT4G24570), DIC3 (AT5G09470).
AT2G23170	(GH3.3)	encodes an IAA-amido synthase that conjugates Asp and other amino acids to auxin <i>in vitro</i> .
AT2G25790		Leucine-rich receptor-like protein kinase family protein;
AT2G28400		Protein of unknown function, DUF584;
AT2G29460	GLUTATHIONE S-TRANSFERASE TAU 4 (GSTU4)	Encodes glutathione transferase belonging to the tau class of GSTs. Naming convention according to Wagner et al. (2002).
AT2G30040	MITOGEN-ACTIVATED PROTEIN KINASE KINASE 14 (MAPKKK14)	member of MEKK subfamily
AT2G30140		UDP-Glycosyltransferase superfamily protein
AT2G30930		unknown protein
AT2G33310	AUXIN-INDUCED PROTEIN 13 (IAA13)	Auxin induced gene, IAA13 (IAA13).
AT2G34650	PINOID (PID)	Encodes a protein serine/threonine kinase that may act as a positive regulator of cellular auxin efflux, as a binary switch for PIN polarity, and as a negative regulator of auxin signaling. Recessive mutants exhibit similar phenotypes as pin-formed mutants in flowers and inflorescence but distinct phenotypes in cotyledons and leaves. Expressed in the vascular tissue proximal to root and shoot meristems, shoot apex, and embryos. Expression is induced by auxin. Overexpression of the gene results in phenotypes in the root and shoot similar to those found in auxin-insensitive mutants. The protein physically interacts with TCH3 (TOUCH3) and PID-BINDING PROTEIN 1 (PBP1), a previously uncharacterized protein containing putative EF-hand calcium-binding motifs. Acts together with ENP (ENHANCER OF PINOID) to instruct precursor cells to elaborate cotyledons in the transition stage embryo. Interacts with PDK1. PID autophosphorylation is required for the ability of PID to phosphorylate an exogenous substrate. PID activation loop is required for PDK1-dependent PID phosphorylation and requires the PIF domain. Negative regulator of root hair growth. PID kinase activity is critical for the inhibition of root hair growth and for maintaining the proper subcellular localization of PID.
AT2G35930	PLANT U-BOX 23 (PUB23)	Encodes a cytoplasmically localized U-box domain containing E3 ubiquitin ligase that is involved in the response to water stress and acts as a negative regulator of PAMP-triggered immunity.

Locus identifier	Primary Gene Symbol	Gene Model Description
AT2G35980	YELLOW-LEAF-SPECIFIC GENE 9 (YLS9)	Encodes a protein whose sequence is similar to tobacco hairpin-induced gene (HIN1) and Arabidopsis non-race specific disease resistance gene (NDR1). Expression of this gene is induced by cucumber mosaic virus, spermine and during senescence. The gene product is localized to the chloroplast.
AT2G36220		unknown protein
AT2G39350	ATP-BINDING CASSETTE G1 (ABCG1)	ABC-2 type transporter family protein
AT2G39370		unknown protein;
AT2G39700	EXPANSIN A4 (EXPA4)	putative expansin.
AT2G40540	POTASSIUM TRANSPORTER 2 (KT2)	putative potassium transporter AtKT2p (AtKT2) mRNA.
AT2G41100	TOUCH 3 (TCH3)	encodes a calmodulin-like protein, with six potential calcium binding domains. Calcium binding shown by Ca(2+)-specific shift in electrophoretic mobility. Expression induced by touch and darkness. Expression may also be developmentally controlled. Expression in growing regions of roots, vascular tissue, root/shoot junctions, trichomes, branch points of the shoot, and regions of siliques and flowers.
AT2G41380		S-adenosyl-L-methionine-dependent methyltransferases superfamily protein;
AT2G41810		_ unknown
AT2G42430	LATERAL ORGAN BOUNDARIES-DOMAIN 16 (LBD16)	LOB-domain protein gene LBD16. This gene contains one auxin-responsive element (AuxRE).
AT2G42440		Lateral organ boundaries (LOB) domain family protein; CONTAINS InterPro DOMAIN/s: Lateral organ boundaries, LOB (InterPro:IPR004883)
AT2G42570	TRICHOME BIREFRINGENCE-LIKE 39 (TBL39)	Encodes a member of the TBL (TRICHOME BIREFRINGENCE-LIKE) gene family containing a plant-specific DUF231 (domain of unknown function) domain. TBL gene family has 46 members, two of which (TBR/AT5G06700 and TBL3/AT5G01360) have been shown to be involved in the synthesis and deposition of secondary wall cellulose, presumably by influencing the esterification state of pectic polymers. A nomenclature for this gene family has been proposed (Volker Bischoff & Wolf Scheible, 2010, personal communication).
AT2G42870	PHY RAPIDLY REGULATED 1 (PAR1)	Encodes PHYTOCHROME RAPIDLY REGULATED1 (PAR1), an atypical basic helix-loop-helix (bHLP) protein. Closely related to PAR2 (At3g58850). Up regulated after simulated shade perception. Acts in the nucleus to control plant development and as a negative regulator of shade avoidance response. Functions as transcriptional repressor of auxin-responsive genes SAUR15 (AT4G38850) and SAUR68 (AT1G29510).
AT2G43290	MULTICOPY SUPPRESSORS OF SNF4 DEFICIENCY IN YEAST 3 (MSS3)	Encodes calmodulin-like MSS3.
AT2G43590		Chitinase family protein
AT2G43880		Pectin lyase-like superfamily protein;
AT2G45400	(BEN1)	involved in the regulation of brassinosteroid metabolic pathway
AT2G45420	LOB DOMAIN-CONTAINING PROTEIN 18 (LBD18)	LOB domain-containing protein 18 (LBD18)
AT2G47130		NAD(P)-binding Rossmann-fold superfamily protein
AT2G47140		NAD(P)-binding Rossmann-fold superfamily protein
AT2G47260	WRKY DNA-BINDING PROTEIN 23 (WRKY23)	Encodes a member of WRKY Transcription Factor; Group I. Involved in nematode feeding site establishment.
AT2G47440		Tetratricopeptide repeat (TPR)-like superfamily protein Eukaryotes - 33 (source: NCBI BLINK).
AT3G01190		Peroxidase superfamily protein
AT3G02850	STELAR K+ OUTWARD RECTIFIER (SKOR)	Encodes SKOR, a member of Shaker family potassium ion (K+) channel. This family includes five groups based on phylogenetic analysis (FEBS Letters (2007) 581: 2357): I (inward rectifying channel): AKT1 (AT2G26650), AKT5 (AT4G32500) and SPIK (also known as AKT6, AT2G25600); II (inward rectifying channel): KAT1 (AT5G46240) and KAT2 (AT4G18290); III (weakly inward rectifying channel): AKT2 (AT4G22200); IV (regulatory subunit involved in inwardly rectifying conductance formation): KAT3 (also known as AtKC1, AT4G32650); V (outward rectifying channel): SKOR (AT3G02850) and GORK (AT5G37500). Mediates the delivery of K+ from stellar cells to the xylem in the roots towards the shoot. mRNA accumulation is modulated by abscisic acid. K+ gating activity is modulated by external and internal K+.
AT3G02885	GAST1 PROTEIN HOMOLOG 5 (GASA5)	GAST1 protein homolog 5 (GASA5); INVOLVED IN: response to gibberellin stimulus;
AT3G06460		GNS1/SUR4 membrane protein family;
AT3G07010		Pectin lyase-like superfamily protein
AT3G07390	AUXIN-INDUCED IN ROOT CULTURES 12 (AIR12)	isolated from differential screening of a cDNA library from auxin-treated root culture. sequence does not show homology to any known proteins and is predicted to be extracellular.
AT3G09280		unknown protein
AT3G12700		Eukaryotic aspartyl protease family protein;
AT3G13380	BRI1-LIKE 3 (BRL3)	Similar to BRI, brassinosteroid receptor protein.
AT3G14690	CYTOCHROME P450, FAMILY 72, SUBFAMILY A, POLYPEPTIDE 15 (CYP72A15)	putative cytochrome P450
AT3G15540	INDOLE-3-ACETIC ACID INDUCIBLE 19 (IAA19)	Primary auxin-responsive gene. Involved in the regulation stamen filaments development.
AT3G16180		Major facilitator superfamily protein
AT3G16570	RAPID ALKALINIZATION FACTOR 23 (RALF23)	Encodes RALF23, a member of a diversely expressed predicted peptide family showing sequence similarity to tobacco Rapid Alkalinization Factor (RALF), and is believed to play an essential role in the physiology of Arabidopsis. Consists of a single exon and is characterized by a conserved C-terminal motif and N-terminal signal peptide. RALF23 is significantly downregulated by brassinolide treatment of seedlings. Overexpression of AtRALF23 impairs brassinolide-induced hypocotyls elongation, and mature overexpressing plants are shorter and bushier. RALF23 overexpression produces slower growing seedlings with roots that have reduced capacity to acidify the rhizosphere.
AT3G18280		Bifunctional inhibitor/lipid-transfer protein/seed storage 2S albumin superfamily protein;
AT3G18560		unknown protein;
AT3G19200		unknown protein;
AT3G19320		Leucine-rich repeat (LRR) family protein
AT3G20015		Eukaryotic aspartyl protease family protein
AT3G20830		AGC (cAMP-dependent, cGMP-dependent and protein kinase C) kinase family protein;
AT3G21250	ATP-BINDING CASSETTE C8 (ABCC8)	member of MRP subfamily
AT3G21700	(SGP2)	Monomeric G protein. Expressed in root epidermal cells that are destined to become atrichoblasts. Also expressed during pollen development and in the pollen tube tip.
AT3G23030	INDOLE-3-ACETIC ACID INDUCIBLE 2 (IAA2)	auxin inducible gene expressed in the nucleus
AT3G23730	XYLOGLUCAN ENDOTRANSGLUCOSYLASE/HYDROLASE 16 (XTH16)	xyloglucan endotransglucosylase/hydrolase 16 (XTH16); FUNCTIONS IN: hydrolase activity, acting on glycosyl bonds, hydrolase activity, hydrolyzing O-glycosyl compounds, xyloglucan:xyloglucosyl transferase activity; INVOLVED IN: carbohydrate metabolic process, cellular glucan metabolic process
AT3G24750		unknown protein
AT3G26610		Pectin lyase-like superfamily protein

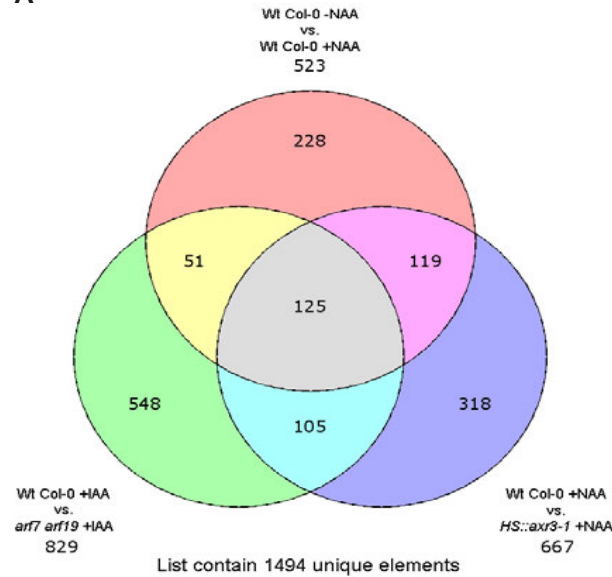
Locus identifier	Primary Gene Symbol	Gene Model Description
AT3G26760		NAD(P)-binding Rossmann-fold superfamily protein
AT3G28850		Glutaredoxin family protein
AT3G42800		unknown protein
AT3G43800	GLUTATHIONE S-TRANSFERASE TAU 27 (GSTU27)	Encodes glutathione transferase belonging to the tau class of GSTs. Naming convention according to Wagner et al. (2002).
AT3G44990	XYLOGLUCAN ENDO-TRANSGLYCOSYLASE-RELATED 8 (XTR8)	xyloglucan endo-transglycosylase
AT3G48520	CYTOCHROME P450, FAMILY 94, SUBFAMILY B, POLYPEPTIDE 3 (CYP94B3)	CYP94B3 is a jasmonoyl-isoleucine-12-hydroxylase that catalyzes the formation of 12-OH-JA-Ile from JA-Ile. By reducing the levels of this the biologically active phytohormone, CYP94B3 attenuates the jasmonic acid signaling cascade. CYP94B3 transcript levels rise in response to wounding.
AT3G49350		Ypt/Rab-GAP domain of gyp1p superfamily protein
AT3G49360	6-PHOSPHOGLUCONOLACTONASE 2 (PGL2)	6-phosphogluconolactonase 2 (PGL2)
AT3G49700	1-AMINOCYCLOPROPANE-1-CARBOXYLATE SYNTHASE 9 (ACS9)	encodes a member of the 1-aminocyclopropane-1-carboxylate (ACC) synthase (S-adenosyl-L-methionine methylthioadenosine-lyase, EC 4.4.1.14) gene family. Mutants produce elevated levels of ethylene as etiolated seedlings.
AT3G50660	DWARF 4 (DWF4)	Encodes a 22kD#945; hydroxylase whose reaction is a rate-limiting step in brassinosteroid biosynthetic pathway. The protein is a member of CYP90B gene family. CLM is an epi-allele with small, compressed rosette, reduced internode length, and reduced fertility, appears in selfed ddm mutant plants possibly due to loss of cytosine methylation. Transcripts accumulate in actively growing tissues, and GUS expression is negatively regulated by brassinosteroids. Localized in the endoplasmic reticulum. The in vitro expressed protein can perform the C-22 hydroxylation of a variety of C27-, C28- and C29-sterols. Cholesterol was the best substrate, followed by campesterol. Sitosterol was a poor substrate.
AT3G51410		Arabidopsis protein of unknown function (DUF241)
AT3G51670	PATL6	SEC14 cytosolic factor family protein / phosphoglyceride transfer family protein
AT3G54000		Uncharacterised conserved protein UCP022260
AT3G54770		RNA-binding (RRM/RBD/RNP motifs) family protein
AT3G54950	PATATIN-RELATED PHOSPHOLIPASE IIIBETA (pPLAIIIBeta)	Encodes pPLAIIIBeta, a member of the Group 3 patatin-related phospholipases. pPLAIIIBeta hydrolyzes phospholipids and galactolipids and additionally has acyl-CoA thioesterase activity. Alterations of pPLAIIIBeta result in changes in lipid levels and composition.
AT3G55690		unknown protein;
AT3G55720		Protein of unknown function (DUF620)
AT3G56230		BTB/POZ domain-containing protein
AT3G56880		VQ motif-containing protein
AT3G58190	LATERAL ORGAN BOUNDARIES-DOMAIN 29 (LBD29)	This gene contains two auxin-responsive element (AuxRE).
AT3G60550	CYCLIN P3;2 (CYCP3;2)	cyclin p3;2 (CYCP3;2);
AT3G60630	HAIRY MERISTEM 2 (HAM2)	Belongs to one of the LOM (LOST MERISTEMS) genes: AT2G45160 (LOM1), AT3G60630 (LOM2) and AT4G00150 (LOM3). LOM1 and LOM2 promote cell differentiation at the periphery of shoot meristems and help to maintain their polar organization.
AT3G60640	AUTOPHAGY 8G (ATG8G)	AUTOPHAGY 8G (ATG8G)
AT3G61490		Pectin lyase-like superfamily protein;
AT3G62100	INDOLE-3-ACETIC ACID INDUCIBLE 30 (IAA30)	Encodes a member of the Aux/IAA family of proteins implicated in auxin signaling. IAA30 lacks the conserved degron (domain II) found in many family members. IAA30 transcripts are induced by auxin treatment and accumulate preferentially in the quiescent center cells of the root meristem. Overexpression of IAA30 leads to defects in gravitropism, root development, root meristem maintenance, and cotyledon vascular development. Target of LEC2 and AGL15. Promotes somatic embryogenesis.
AT3G63440	CYTOKININ OXIDASE/DEHYDROGENASE 6 (CKX6)	This gene used to be called AtCKX7. It encodes a protein whose sequence is similar to cytokinin oxidase/dehydrogenase, which catalyzes the degradation of cytokinins.
AT4G00080	UNFERTILIZED EMBRYO SAC 11 (UNE11)	unfertilized embryo sac 11 (UNE11)
AT4G01870		tolB protein-related
AT4G03820		Protein of unknown function (DUF3537)
AT4G08040	1-AMINOCYCLOPROPANE-1-CARBOXYLATE SYNTHASE 11 (ACS11)	encodes an aminotransferase that belongs to ACC synthase gene family structurally
AT4G09570	CALCIUM-DEPENDENT PROTEIN KINASE 4 (CPK4)	Encodes a member of Calcium Dependent Protein Kinase (CDPK) gene family. Positive regulator of ABA signaling. Phosphorylates ABA responsive transcription factors ABF1 and ABF4.
AT4G11280	1-AMINOCYCLOPROPANE-1-CARBOXYLIC ACID (ACC) SYNTHASE 6 (ACS6)	encodes a member of the 1-aminocyclopropane-1-carboxylate (ACC) synthase (S-adenosyl-L-methionine methylthioadenosine-lyase, EC 4.4.1.14) gene family
AT4G12110	STEROL-4ALPHA-METHYL OXIDASE 1-1 (SMO1-1)	Encodes a member of the SMO1 family of sterol 4alpha-methyl oxidases. More specifically functions as a 4,4-dimethyl-9beta,19-cyclopropylsterol-4alpha-methyl oxidase.
AT4G12410		SAUR-like auxin-responsive protein family; CONTAINS InterPro DOMAIN/s: Auxin responsive SAUR protein (InterPro:IPR003676); BEST Arabidopsis thaliana protein match is: SAUR-like auxin-responsive protein family (TAIR:AT4G22620.1); Has 1137 Blast hits to 1128 proteins in 26 species: Archae - 0; Bacteria - 0; Metazoa - 0; Fungi - 0; Plants - 1136; Viruses - 0; Other Eukarvotes - 1 (source: NCBI BLINK).
AT4G12720	(NUDT7)	Encodes a protein with ADP-ribose hydrolase activity. Negatively regulates EDS1-conditioned plant defense and programmed cell death.
AT4G12730	FASCICLIN-LIKE ARABINOGALACTAN 2 (FLA2)	AF333971 Arabidopsis thaliana fasciclin-like arabinogalactan-protein 2 (Fla2) mRNA, complete cds
AT4G12880	EARLY NODULIN-LIKE PROTEIN 19 (ENODL19)	early nodulin-like protein 19 (ENODL19)
AT4G13180		NAD(P)-binding Rossmann-fold superfamily protein).
AT4G13195	CLAVATA3/ESR-RELATED 44 (CLE44)	Belongs to a large gene family, called CLE for CLAVATA3/ESR-related, encoding small peptides with conserved carboxyl termini. The C-terminal 12 amino acid sequence of CLE44 is identical to that of a duodeca peptide (TDIF, tracheary element differentiation inhibitory factor) isolated from Arabidopsis and functions as a suppressor of plant stem cell differentiation. TDIF sequence is also identical to the C-terminal 12 amino acids of CLE41 (At3g24770).
AT4G14130	XYLOGLUCAN ENDOTRANSGLUCOSYLASE E/HYDROLASE 15 (XTH15)	xyloglucan endotransglycosylase-related protein (XTR7)
AT4G14560	INDOLE-3-ACETIC ACID INDUCIBLE (IAA1)	auxin (indole-3-acetic acid) induced gene (IAA1) encoding a short-lived nuclear-localized transcriptional regulator protein.

Locus identifier	Primary Gene Symbol	Gene Model Description
AT4G14750	IQ-DOMAIN 19 (IQD19)	IQ-domain 19 (IQD19); CONTAINS InterPro DOMAIN/s: IQ calmodulin-binding region (InterPro:IPR000048)
AT4G17350		DOMAIN/s: Pleckstrin-like, plant (InterPro:IPR013666), Protein of unknown function DUF828 (InterPro:IPR008546), Pleckstrin homology (InterPro:IPR001849)
AT4G17490	ETHYLENE RESPONSIVE ELEMENT BINDING FACTOR 6 (ERF6)	Encodes a member of the ERF (ethylene response factor) subfamily B-3 of ERF/AP2 transcription factor family (ATERF-6). The protein contains one AP2 domain. There are 18 members in this subfamily including ATERF-1, ATERF-2, AND ATERF-5.
AT4G17870	PYRABACTIN RESISTANCE 1 (PYR1)	Encodes a member of the PYR (pyrabactin resistance)/PYL(PYR1-like)/RCAR (regulatory components of ABA receptor) family proteins with 14 members. PYR/PYL/RCAR family proteins function as abscisic acid sensors. Mediate ABA-dependent regulation of protein phosphatase 2Cs ABI1 and ABI2.
AT4G20460		NAD(P)-binding Rossmann-fold superfamily protein
AT4G21200	GIBBERELLIN 2-OXIDASE 8 (GA2OX8)	Encodes a protein with gibberellin 2-oxidase activity which acts specifically on C-20 gibberellins.
AT4G21850	METHIONINE SULFOXIDE REDUCTASE B9 (MSRB9)	methionine sulfoxide reductase B9 (MSRB9);
AT4G21870		HSP20-like chaperones superfamily protein
AT4G22530		S-adenosyl-L-methionine-dependent methyltransferases superfamily protein
AT4G22620		SAUR-like auxin-responsive protein family
AT4G22780	ACT DOMAIN REPEAT 7 (ACR7)	Member of a family of ACT domain containing proteins . ACT domains are involved in amino acid binding .
AT4G24160		Encodes a soluble lysophosphatidic acid acyltransferase with additional triacylglycerol lipase and phosphatidylcholine hydrolyzing enzymatic activities. Plays a pivotal role in maintaining the lipid homeostasis by regulating both phospholipid and neutral lipid levels.
AT4G25250		Plant invertase/pectin methyltransferase inhibitor superfamily protein
AT4G26320	ARABINOGLACTAN PROTEIN 13 (AGP13)	arabinogalactan protein 13 (AGP13);
AT4G27260	(WES1)	encodes an IAA-amido synthase that conjugates Asp and other amino acids to auxin in vitro. Lines carrying insertions in this gene are hypersensitive to auxin.
AT4G27280		Calcium-binding EF-hand family protein;
AT4G27290		S-locus lectin protein kinase family protein
AT4G28640	INDOLE-3-ACETIC ACID INDUCIBLE 11 (IAA11)	Auxin induced gene, IAA11 (IAA11).
AT4G29900	AUTOINHIBITED CA(2+)-ATPASE 10 (ACA10)	one of the type IIB calcium pump isoforms. encodes an autoinhibited Ca(2+)-ATPase that contains an N-terminal calmodulin binding autoinhibitory domain.
AT4G30170		Peroxidase family protein
AT4G30420		nodulin MtN21 /EamA-like transporter family protein
AT4G30450		glycine-rich protein
AT4G31320		SAUR-like auxin-responsive protein family
AT4G31910		HXXXD-type acyl-transferase family protein
AT4G32280	INDOLE-3-ACETIC ACID INDUCIBLE 29 (IAA29)	Auxin inducible protein.
AT4G34150		Calcium-dependent lipid-binding (CaLB domain) family protein;
AT4G34710	ARGININE DECARBOXYLASE 2 (ADC2)	encodes a arginine decarboxylase (ADC), a rate-limiting enzyme that catalyzes the first step of polyamine (PA) biosynthesis via ADC pathway in Arabidopsis thaliana. Arabidopsis genome has two ADC paralogs, ADC1 and ADC2. ADC2 is stress-inducible (osmotic stress). Double mutant analysis showed that ADC genes are essential for the production of PA, and are required for normal seed development. Overexpression causes phenotypes similar to GA-deficient plants and these plants show reduced levels of GA due to lower expression levels of AtGA20ox1, AtGA3ox3 and AtGA3ox1.
AT4G35210		Arabidopsis protein of unknown function (DUF241);
AT4G35320		unknown protein
AT4G37290		unknown protein
AT4G37295		unknown protein
AT4G37590	NAKED PINS IN YUC MUTANTS 5 (NPY5)	A member of the NPY gene family (NPY1/AT4G31820, NPY2/AT2G14820, NPY3/AT5G67440, NPY4/AT2G23050, NPY5/AT4G37590). Involved in auxin-mediated organogenesis.
AT5G01750		Protein of unknown function (DUF567)
AT5G01840	OVATE FAMILY PROTEIN 1 (OPF1)	Encodes a member of the plant specific ovate protein family. Members of this family have been shown to bind to KNOX and BELL-like TALE class homeodomain proteins. This interaction may mediate relocalization of the TALE homeodomain from the nucleus to the cytoplasm. Functions as a transcriptional repressor that suppresses cell elongation.
AT5G02760		Protein phosphatase 2C family protein
AT5G03960	IQ-DOMAIN 12 (IQD12)	IQ-domain 12 (IQD12)
AT5G04980		DNase I-like superfamily protein
AT5G05160	REDUCED IN LATERAL GROWTH1 (RUL1)	Encodes a receptor-like kinase that activates secondary growth, the production of secondary vascular tissues.
AT5G06080	LOB DOMAIN-CONTAINING PROTEIN 33 (LBD33)	LOB domain-containing protein 33 (LBD33)
AT5G10210		C2 calcium-dependent membrane targeting
AT5G10430	ARABINOGLACTAN PROTEIN 4 (AGP4)	Encodes arabinogalactan-protein (AGP4).
AT5G12050		unknown protein;
AT5G13910	LEAFY PETIOLE (LEP)	Encodes a member of the ERF (ethylene response factor) subfamily B-1 of ERF/AP2 transcription factor family (LEAFY PETIOLE). The protein contains one AP2 domain. There are 15 members in this subfamily including ATERF-3, ATERF-4, ATERF-7, and LEAFY PETIOLE. Acts as a positive regulator of gibberellic acid-induced germination.
AT5G15890	TRICHOME BIREFRINGENCE-LIKE 21 (TBL21)	Encodes a member of the TBL (TRICHOME BIREFRINGENCE-LIKE) gene family containing a plant-specific DUF231 (domain of unknown function) domain. TBL gene family has 46 members, two of which (TBR/AT5G06700 and TBL3/AT5G01360) have been shown to be involved in the synthesis and deposition of secondary wall cellulose, presumably by influencing the esterification state of pectic polymers. A nomenclature for this gene family has been proposed (Volker Bischoff & Wolf Scheible, 2010, personal communication).
AT5G16110		unknown protein
AT5G16120		alpha/beta-Hydrolases superfamily protein
AT5G17340		Putative membrane lipoprotein
AT5G18560	(PUCHI)	Encodes PUCHI, a member of the ERF (ethylene response factor) subfamily B-1 of ERF/AP2 transcription factor family. The protein contains one AP2 domain. There are 15 members in this subfamily including ATERF-3, ATERF-4, ATERF-7, and leafy petiole. PUCHI is required for morphogenesis in the early lateral root primordium of Arabidopsis. Expressed in early floral meristem (stage 1 to 2). Required for early floral meristem growth and for bract suppression. Triple mutant with bop1 and bop2 displays a strong defect in the determination of floral meristem identity with reduced LFY expression and the lack of AP1 expression.
AT5G19530	ACAULIS 5 (ACL5)	Encodes a spermine synthase. Required for internode elongation and vascular development, specifically in the mechanism that defines the boundaries between veins and nonvein regions. This mechanism may be mediated by polar auxin transport. Though ACL5 has been shown to function as a spermine synthase in E. coli, an ACL5 knockout has no effect on the endogenous levels of free and conjugated polyamines in Arabidopsis, suggesting that ACL5 may have a very specific or altogether different in vivo function.

Locus identifier	Primary Gene Symbol	Gene Model Description
AT5G20230	BLUE-COPPER-BINDING PROTEIN (BCB)	Al-stress-induced gene
AT5G24100		Leucine-rich repeat protein kinase family protein
AT5G26930	GATA TRANSCRIPTION FACTOR 23 (GATA23)	Encodes a member of the GATA factor family of zinc finger transcription factors. Controls lateral root founder cell specification.
AT5G27000	KINESIN 4 (ATK4)	Encodes a kinesin-like protein that binds microtubules in an ATP-dependent manner.
AT5G39670		Calcium-binding EF-hand family protein;
AT5G40540		Protein kinase superfamily protein
AT5G42050		DCD (Development and Cell Death) domain protein
AT5G43700	AUXIN INDUCIBLE 2-11 (ATAUX2-11)	Auxin inducible protein similar to transcription factors.
AT5G47250		LRR and NB-ARC domains-containing disease resistance protein;
AT5G47370	(HAT2)	homeobox-leucine zipper genes induced by auxin, but not by other phytohormones. Plays opposite roles in the shoot and root tissues in regulating auxin-mediated morphogenesis.
AT5G47440		CONTAINS InterPro DOMAIN/s: Pleckstrin-like, plant (InterPro:IPR013666), Protein of unknown function DUF828 (InterPro:IPR008546), Pleckstrin homology (InterPro:IPR001849)
AT5G48150	PHYTOCHROME A SIGNAL TRANSDUCTION 1 (PAT1)	Member of GRAS gene family. Semi-dominant mutant has a reduced response to far-red light and appears to act early in the phytochrome A signaling pathway.
AT5G49360	BETA-XYLOSIDASE 1 (BXL1)	Encodes a bifunctional [beta]-D-xylosidase/[alpha]-L-arabinofuranosidase required for pectic arabinan modification. Located in the extracellular matrix. Gene is expressed specifically in tissues undergoing secondary wall thickening. This is a member of glycosyl hydrolase family 3 and has six other closely related members.
AT5G49450	BASIC LEUCINE-ZIPPER 1 (bZIP1)	basic leucine-zipper 1 (bZIP1)
AT5G51670		Protein of unknown function (DUF668)
AT5G52450		MATE efflux family protein
AT5G52900		unknown protein
AT5G53250	ARABINOGALACTAN PROTEIN 22 (AGP22)	arabinogalactan protein 22 (AGP22)
AT5G54130		Calcium-binding endonuclease/exonuclease/phosphatase family
AT5G54380	THESEUS1 (THE1)	Encodes THESEUS1 (THE1), a receptor kinase regulated by Brassinosteroids and required for cell elongation during vegetative growth.
AT5G54490	PINOID-BINDING PROTEIN 1 (PBP1)	Encodes a PINOID (PID)-binding protein containing putative EF-hand calcium-binding motifs. The interaction is dependent on the presence of calcium. mRNA expression is up-regulated by auxin. Not a phosphorylation target of PID, likely acts upstream of PID to regulate the activity of this protein in response to changes in calcium levels.
AT5G54500	FLAVODOXIN-LIKE QUINONE REDUCTASE 1 (FQR1)	Encodes a flavin mononucleotide-binding flavodoxin-like quinone reductase that is a primary auxin-response gene.
AT5G54510	DWARF IN LIGHT 1 (DFL1)	Encodes an IAA-amido synthase that conjugates Ala, Asp, Phe, and Trp to auxin. Lines overexpressing this gene accumulate IAA-ASP and are hypersensitive to several auxins. Identified as a dominant mutation that displays shorter hypocotyls in light grown plants when compared to wild type siblings. Protein is similar to auxin inducible gene from pea (GH3).
AT5G57100		Nucleotide/sugar transporter family protein
AT5G57520	ZINC FINGER PROTEIN 2 (ZFP2)	Encodes a zinc finger protein containing only a single zinc finger.
AT5G60450	AUXIN RESPONSE FACTOR 4 (ARF4)	Encodes a member of the ARF family of transcription factors which mediate auxin responses. ARF4 appears to have redundant function with ETT(ARF3) in specifying abaxial cell identity.
AT5G60520		Late embryogenesis abundant (LEA) protein-related;
AT5G60660	PLASMA MEMBRANE INTRINSIC PROTEIN 2;4 (PIP2;4)	A member of the plasma membrane intrinsic protein subfamily PIP2. When expressed in yeast cells can conduct hydrogen peroxide into those cells. Mutants exhibit longer root hairs.
AT5G62280		Protein of unknown function (DUF1442)
AT5G64250		Aldolase-type TIM barrel family protein
AT5G65390	ARABINOGALACTAN PROTEIN 7 (AGP7)	arabinogalactan protein 7 (AGP7)
AT5G65670	INDOLE-3-ACETIC ACID INDUCIBLE 9 (IAA9)	auxin (indole-3-acetic acid) induced gene
AT5G67430		Acyl-CoA N-acyltransferases (NAT) superfamily protein

Table S2.

A



B

Locus identifier	Primary Gene Symbol	Gene Model Description
AT1G02400	GIBBERELLIN 2-OXIDASE 6 (GA2OX6)	Encodes a gibberellin 2-oxidase that acts on C19 gibberellins but not C20 gibberellins.
AT1G03870	FASCICLIN-LIKE ARABINOOGALACTAN 9 (FLA9)	fasciclin-like arabinogalactan-protein 9 (Fla9)
AT1G08500	EARLY NODULIN-LIKE PROTEIN 18 (ENODL18)	early nodulin-like protein 18 (ENODL18); FUNCTIONS IN: electron carrier activity, copper ion binding; LOCATED IN: anchored to membrane;
AT1G15580	INDOLE-3-ACETIC ACID INDUCIBLE 5 (IAA5)	auxin induced protein
AT1G19220	AUXIN RESPONSE FACTOR19 (ARF19)	Encodes an auxin response factor that contains the conserved VP1-B3 DNA-binding domain at its N-terminus and the Aux/IAA-like domains III and IV present in most ARFs at its C-terminus. The protein interacts with IAA1 (yeast two hybrid) and other auxin response elements such as ER7 and ER9 (yeast one hybrid). ARF19 protein can complement many aspects of the <i>arf7</i> mutant phenotype and, together with ARF7, is involved in the response to ethylene. In the <i>arf7 arf19</i> double mutant, several auxin-responsive genes (e.g. IAA5, LBD16, LBD29 and LBD33) are no longer upregulated by auxin.
AT1G21980	PHOSPHATIDYLINOSITOL 4-PHOSPHATE 5-KINASE 1 (PIP5K1)	Type I phosphatidylinositol 4-phosphate 5-kinase. Preferentially phosphorylates PtdIns4P. Induced by water stress and abscisic acid in <i>Arabidopsis thaliana</i> . Expressed in procambial cells of leaves, flowers and roots. A N-terminal Membrane Occupation and Recognition Nexus (MORN) affects enzyme activity and distribution.
AT1G23080	PIN-FORMED 7 (PIN7)	Encodes a novel component of auxin efflux that is located apically in the basal cell and is involved during embryogenesis in setting up the apical-basal axis in the embryo. It is also involved in pattern specification during root development. In roots, it is expressed at lateral and basal membranes of provascular cells in the meristem and elongation zone, whereas in the columella cells it coincides with the PIN3 domain. Plasma membrane-localized PIN proteins mediate a saturable efflux of auxin. PINs mediate auxin efflux from mammalian and yeast cells without needing additional plant-specific factors. The action of PINs in auxin efflux is distinct from PGPs, rate-limiting, specific to auxins and sensitive to auxin transport inhibitors. PINs are directly involved of in catalyzing cellular auxin efflux.
AT1G28370	ERF DOMAIN PROTEIN 11 (ERF11)	encodes a member of the ERF (ethylene response factor) subfamily B-1 of ERF/AP2 transcription factor family. The protein contains one AP2 domain. There are 15 members in this subfamily including ATERF-3, ATERF-4, ATERF-7, and leafy petiole.
AT1G28680		HXXXD-type acyl-transferase family protein
AT1G29500		SAUR-like auxin-responsive protein family
AT1G29510	SMALL AUXIN UPREGULATED 68(SAUR68)	SMALL AUXIN UPREGULATED 68 (SAUR68);
AT1G33790		jacalin lectin family protein;
AT1G50660		unknown protein;
AT1G52830	INDOLE-3-ACETIC ACID 6 (IAA6)	An extragenic dominant suppressor of the <i>hy2</i> mutant phenotype. Also exhibits aspects of constitutive photomorphogenetic phenotype in the absence of <i>hy2</i> . Mutants have dominant leaf curling phenotype shortened hypocotyls and reduced apical hook. Induced by indole-3-acetic acid.
AT1G60010		unknown protein
AT1G62770		Plant invertase/pectin methyltransferase inhibitor superfamily protein
AT1G64405		unknown protein
AT1G69530	EXPANSIN A1 (EXPA1)	Member of Alpha-Expansin Gene Family. Naming convention from the Expansin Working Group (Kende et al, Plant Mol Bio). Involved in the formation of nematode-induced syncytia in roots of <i>Arabidopsis thaliana</i> .
AT1G70560	TRYPTOPHAN AMINOTRANSFERASE OF ARABIDOPSIS 1 (TAA1)	TAA1 is involved in the shade-induced production of indole-3-pyruvate (IPA), a precursor to IAA, a biologically active auxin. It is also involved in regulating many aspects of plant growth and development from embryogenesis to flower formation and plays a role in ethylene-mediated signaling. This enzyme can catalyze the formation of IPA from L-tryptophan. Though L-Trp is expected to be the preferred substrate in vivo, TAA1 also acts as an aminotransferase using L-Phe, L-Tyr, L-Leu, L-Ala, L-Met, and L-Gln.
AT1G70940	PIN-FORMED 3 (PIN3)	A regulator of auxin efflux and involved in differential growth. PIN3 is expressed in gravity-sensing tissues, with PIN3 protein accumulating predominantly at the lateral cell surface. PIN3 localizes to the plasma membrane and to vesicles. In roots, PIN3 is expressed without pronounced polarity in tiers two and three of the columella cells, at the basal side of vascular cells, and to the lateral side of pericycle cells of the elongation zone. PIN3 overexpression inhibits root cell growth. Protein phosphorylation plays a role in PIN3 trafficking to the plasma membrane.

Locus identifier	Primary Gene Symbol	Gene Model Description
AT1G73590	PIN-FORMED 1 (PIN1)	Encodes an auxin efflux carrier involved in shoot and root development. It is involved in the maintenance of embryonic auxin gradients. Loss of function severely affects organ initiation, pin1 mutants are characterised by an inflorescence meristem that does not initiate any flowers, resulting in the formation of a naked inflorescence stem. PIN1 is involved in the determination of leaf shape by actively promoting development of leaf margin serrations. In roots, the protein mainly resides at the basal end of the vascular cells, but weak signals can be detected in the epidermis and the cortex. Expression levels and polarity of this auxin efflux carrier change during primordium development suggesting that cycles of auxin build-up and depletion accompany, and may direct, different stages of primordium development. PIN1 action on plant development does not strictly require function of PGP1 and PGP19 proteins.
AT1G74660	MINI ZINC FINGER 1 (MIF1)	Encodes MINI ZINC FINGER 1 (MIF1) which has a zinc finger domain but lacks other protein motifs normally present in transcription factors. MIF1 physically interact with a group of zinc finger-homeodomain (ZHD) transcription factors, such as ZHD5 (AT1G75240), that regulate floral architecture and leaf development. Gel mobility shift assays revealed that MIF1 blocks the DNA binding activity of ZHD5 homodimers by competitively forming MIF1-ZHD5 heterodimers. Constitutive overexpression of MIF1 caused dramatic developmental defects, seedlings were non-responsive to gibberellin (GA) for cell elongation, hypersensitive to the GA synthesis inhibitor paclobutrazol (PAC) and abscisic acid (ABA), and hypersensitive to auxin, brassinosteroid and cytokinin, but normally responsive to ethylene.
AT1G77280		Protein kinase protein with adenine nucleotide alpha hydrolases-like domain
AT1G78100		F-box family protein;
AT2G03730	ACT DOMAIN REPEAT 5 (ACRS5)	Member of a small family of ACT domain containing proteins. ACT domains are thought to be involved in amino acid binding.
AT2G14960	(GH3.1)	encodes a protein similar to IAA-amido synthases. Lines carrying an insertion in this gene are hypersensitive to auxin.
AT2G18690		unknown protein;
AT2G18980	Peroxidase 16	Peroxidase superfamily protein
AT2G23170	(GH3.3)	encodes an IAA-amido synthase that conjugates Asp and other amino acids to auxin in vitro.
AT2G25790		Leucine-rich receptor-like protein kinase family protein;
AT2G30040	MITOGEN-ACTIVATEDPROTEIN KINASE KINASE 14 (MAPKKK14)	member of MEKK subfamily
AT2G33310	AUXIN-INDUCED PROTEIN13 (IAA13)	Auxin induced gene, IAA13 (IAA13).
AT2G34650	PINOID (PID)	Encodes a protein serine/threonine kinase that may act as a positive regulator of cellular auxin efflux, as a binary switch for PIN polarity, and as a negative regulator of auxin signaling. Recessive mutants exhibit similar phenotypes as pin-formed mutants in flowers and inflorescence but distinct phenotypes in cotyledons and leaves. Expressed in the vascular tissue proximal to root and shoot meristems, shoot apex, and embryos. Expression is induced by auxin. Overexpression of the gene results in phenotypes in the root and shoot similar to those found in auxin-insensitive mutants. The protein physically interacts with TCH3 (TOUCH3) and PID-BINDING PROTEIN 1 (PBP1), a previously uncharacterized protein containing putative EF-hand calcium-binding motifs. Acts together with ENP (ENHANCER OF PINOID) to instruct precursor cells to elaborate cotyledons in the transition stage embryo. Interacts with PDK1. PID autophosphorylation is required for the ability of PID to phosphorylate an exogenous substrate. PID activation loop is required for PDK1-dependent PID phosphorylation and requires the PIF domain. Negative regulator of root hair growth. PID kinase activity is critical for the inhibition of root hair growth and for maintaining the proper subcellular localization of PID.
AT2G35930	PLANT U-BOX 23 (PUB23)	Encodes a cytoplasmically localized U-box domain containing E3 ubiquitin ligase that is involved in the response to water stress and acts as a negative regulator of PAMP-triggered immunity.
AT2G35980	YELLOW-LEAF-SPECIFIC GENE 9 (YLS9)	Encodes a protein whose sequence is similar to tobacco hairpin-induced gene (HIN1) and Arabidopsis non-race specific disease resistance gene (NDR1). Expression of this gene is induced by cucumber mosaic virus, spermine and during senescence. The gene product is localized to the chloroplast.
AT2G36220		unknown protein
AT2G39370		unknown protein;
AT2G39700	EXPANSIN A4 (EXPA4)	putative expansin.
AT2G40540	POTASSIUMTRANSPORTER 2 (KT2)	putative potassium transporter AtKT2p (AtKT2) mRNA,
AT2G41100	TOUCH 3 (TCH3)	encodes a calmodulin-like protein, with six potential calcium binding domains. Calcium binding shown by Ca(2+)-specific shift in electrophoretic mobility. Expression induced by touch and darkness. Expression may also be developmentally controlled. Expression in growing regions of roots, vascular tissue, root/shoot junctions, trichomes, branch points of the shoot, and regions of siliques and flowers.
AT2G41380		S-adenosyl-L-methionine-dependent methyltransferases superfamily protein;
AT2G42430	LATERAL ORGANBOUNDARIES-DOMAIN 16 (LBD16)	LOB-domain protein gene LBD16. This gene contains one auxin-responsive element (AuxRE).
AT2G42440		Lateral organ boundaries (LOB) domain family protein; CONTAINS InterPro DOMAIN/s: Lateral organ boundaries, LOB (InterPro:PRO04883)
AT2G42870	PHY RAPIDLY REGULATED1 (PAR1)	Encodes PHYTOCHROME RAPIDLY REGULATED1 (PAR1), an atypical basic helix-loop-helix (bHLH) protein. Closely related to PAR2 (AT3g58850). Up regulated after simulated shade perception. Acts in the nucleus to control plant development and as a negative regulator of shade avoidance response. Functions as transcriptional repressor of auxin-responsive genes SAUR15 (AT4G38850) and SAUR68 (AT1G29510).
AT2G43590		Chitinase family protein
AT2G45400	(BEN1)	involved in the regulation of brassinosteroid metabolic pathway
AT2G45420	LOB DOMAIN-CONTAINING PROTEIN 18 (LBD18)	LOB domain-containing protein 18 (LBD18)
AT2G47130		NAD(P)-binding Rossmann-fold superfamily protein
AT2G47140		NAD(P)-binding Rossmann-fold superfamily protein
AT2G47260	WRKY DNA-BINDING PROTEIN 23 (WRKY23)	Encodes a member of WRKY Transcription Factor; Group I. Involved in nematode feeding site establishment.
AT3G02885	GAST1 PROTEINHOMOLOG 5 (GASAS)	GAST1 protein homolog 5 (GASAS); INVOLVED IN: response to gibberellin stimulus;
AT3G07010	Probable pectate lyase 8	Pectin lyase-like superfamily protein
AT3G07390	AUXIN-INDUCED IN ROOTCULTURES 12 (AIR12)	isolated from differential screening of a cDNA library from auxin-treated root culture. sequence does not show homology to any known proteins and is predicted to be extracellular.
AT3G09280		unknown protein
AT3G13380	Serine/threonine-protein kinase BRI1-like 3	Similar to BRI, brassinosteroid receptor protein.
AT3G15540	INDOLE-3-ACETIC ACIDINDUCIBLE 19 (IAA19)	Primary auxin-responsive gene. Involved in the regulation stamen filaments development.
AT3G16420	AT3G16420; AT5G54490 PINOID-BINDING PROTEIN 1 (PBP1)	Encodes a PINOID (PID)-binding protein containing putative EF-hand calcium-binding motifs. The interaction is dependent on the presence of calcium. mRNA expression is up-regulated by auxin. Not a phosphorylation target of PID, likely acts upstream of PID to regulate the activity of this protein in response to changes in calcium levels.
AT3G18560		unknown protein;
AT3G19200		unknown protein;
AT3G20830		AGC (cAMP-dependent, cGMP-dependent and protein kinase C) kinase family protein;
AT3G21700	(SGP2)	Monomeric G protein. Expressed in root epidermal cells that are destined to become atrichoblasts. Also expressed during pollen development and in the pollen tube tip.
AT3G23030	INDOLE-3-ACETIC ACID INDUCIBLE 2 (IAA2)	auxin inducible gene expressed in the nucleus
AT3G26760		NAD(P)-binding Rossmann-fold superfamily protein
AT3G28850		Glutaredoxin family protein

Locus identifier	Primary Gene Symbol	Gene Model Description
AT3G42800		unknown protein
AT3G49700	1-AMINOCYCLOPROPANE-1-CARBOXYLATE SYNTHASE 9 (ACS9)	encodes a member of the 1-aminocyclopropane-1-carboxylate (ACC) synthase (S-adenosyl-L-methionine methylthioadenosine-lyase, EC 4.4.1.14) gene family. Mutants produce elevated levels of ethylene as etiolated seedlings.
AT3G50660	DWARF 4 (DWF4)	Encodes a 22α hydroxylase whose reaction is a rate-limiting step in brassinosteroid biosynthetic pathway. The protein is a member of CYP90B gene family. CLM is an epi-allele with small, compressed rosette, reduced internode length, and reduced fertility, appears in selfed ddm mutant plants possibly due to loss of cytosine methylation. Transcripts accumulate in actively growing tissues, and GUS expression is negatively regulated by brassinosteroids. Localized in the endoplasmic reticulum. The in vitro expressed protein can perform the C-22 hydroxylation of a variety of C27-, C28- and C29-sterols. Cholesterol was the best substrate, followed by campesterol. Stolesterol was a poor substrate.
AT3G51410		Arabidopsis protein of unknown function (DUF241)
AT3G54000		Uncharacterised conserved protein UCPO22260
AT3G54950	PATATIN-RELATED PHOSPHOLIPASE IIIBETA (pPLAIIIBeta)	Encodes pPLAIIIBeta, a member of the Group 3 patatin-related phospholipases. pPLAIIIBeta hydrolyzes phospholipids and galactolipids and additionally has acyl-CoA thioesterase activity. Alterations of pPLAIIIBeta result in changes in lipid levels and composition.
AT3G55690		unknown protein;
AT3G55720		Protein of unknown function (DUF620)
AT3G58190	LATERAL ORGANBOUNDARIES-DOMAIN 29 (LBD29)	This gene contains two auxin-responsive element (AuxRE).
AT3G60550	CYCLIN P3;2 (CYCP3;2)	cyclin p3;2 (CYCP3;2);
AT3G60630	HAIRY MERISTEM 2 (HAM2)	Belongs to one of the LOM (LOST MERISTEMS) genes: AT2G45160 (LOM1), AT3G60630 (LOM2) and AT4G00150 (LOM3). LOM1 and LOM2 promote cell differentiation at the periphery of shoot meristems and help to maintain their polar organization.
AT3G60640	AUTOPHAGY 8G (ATG8G)	AUTOPHAGY 8G (ATG8G)
AT3G62100	INDOLE-3-ACETIC ACID INDUCIBLE 30 (IAA30)	Encodes a member of the Aux/IAA family of proteins implicated in auxin signaling. IAA30 lacks the conserved degen (domain II) found in many family members. IAA30 transcripts are induced by auxin treatment and accumulate preferentially in the quiescent center cells of the root meristem. Overexpression of IAA30 leads to defects in gravitropism, root development, root meristem maintenance, and cotyledon vascular development. Target of LEC2 and AGL15. Promotes somatic embryogenesis.
AT3G63440	CYTOKININOXIDASE/DEHYDROGENAS E 6 (CKX6)	This gene used to be called AtCKX7. It encodes a protein whose sequence is similar to cytokinin oxidase/dehydrogenase, which catalyzes the degradation of cytokinins.
AT4G00080	UNFERTILIZED EMBRYOSAC 11 (UNE11)	unfertilized embryo sac 11 (UNE11)
AT4G01870		tolB protein-related
AT4G11280	1-AMINOCYCLOPROPANE-1-CARBOXYLIC ACID (ACC) SYNTHASE 6 (ACS6)	encodes a member of the 1-aminocyclopropane-1-carboxylate (ACC) synthase (S-adenosyl-L-methionine methylthioadenosine-lyase, EC 4.4.1.14) gene family
AT4G12410		SAUR-like auxin-responsive protein family ; CONTAINS InterPro DOMAIN/s: Auxin responsive SAUR protein (InterPro:IPRO03676); BEST Arabidopsis thaliana protein match is: SAUR-like auxin-responsive protein family (TAIR:AT4G22620.1); Has 1137 Blast hits to 1128 proteins in 26 species: Archaea - 0; Bacteria - 0; Metazoa - 0; Fungi - 0; Plants - 1136; Viruses - 0; Other Eukaryotes - 1 (source: NCBI BLINK).
AT4G12720	Nudix hydrolase 7 (NUDT7)	Encodes a protein with ADP-ribose hydrolase activity. Negatively regulates EDS1-conditioned plant defense and programmed cell death.
AT4G13180		NAD(P)-binding Rossmann-fold superfamily protein).
AT4G13195	CLAVATA3/ESR-RELATED44 (CLE44)	Belongs to a large gene family, called CLE for CLAVATA3/ESR-related, encoding small peptides with conserved carboxyl termini. The C-terminal 12 amino acid sequence of CLE44 is identical to that of a dodeca peptide (TDIF, tracheary element differentiation inhibitory factor) isolated from Arabidopsis and functions as a suppressor of plant stem cell differentiation. TDIF sequence is also identical to the C-terminal 12 amino acids of CLE41 (At3g24770).
AT4G14130	XYLOGUCANENDOTRANSGLUCOSYLAS E/HYDROLASE 15 (XTH15)	xyloglucan endotransglycosylase-related protein (XTR7)
AT4G14560	INDOLE-3-ACETIC ACID INDUCIBLE (IAA1)	auxin (indole-3-acetic acid) induced gene (IAA1) encoding a short-lived nuclear-localized transcriptional regulator protein.
AT4G17350		DOMAIN/s: Pleckstrin-like, plant (InterPro:IPRO13666), Protein of unknown function DUF828 (InterPro:IPRO08546), Pleckstrin homology (InterPro:IPRO01849)
AT4G22530		S-adenosyl-L-methionine-dependent methyltransferases superfamily protein
AT4G22620		SAUR-like auxin-responsive protein family
AT4G22780	ACT DOMAIN REPEAT 7 (ACR7)	Member of a family of ACT domain containing proteins .ACT domains are involved in amino acid binding .
AT4G27260	(WES1)	encodes an IAA-amido synthase that conjugates Asp and other amino acids to auxin in vitro. Lines carrying insertions in this gene are hypersensitive to auxin.
AT4G27280		Calcium-binding EF-hand family protein;
AT4G28640	INDOLE-3-ACETIC ACID INDUCIBLE 11 (IAA11)	Auxin induced gene, IAA11 (IAA11).
AT4G30420		nodulin MtN21 /EamA-like transporter family protein
AT4G31910		HXXXD-type acyl-transferase family protein
AT4G32280	INDOLE-3-ACETIC ACID INDUCIBLE 29 (IAA29)	Auxin inducible protein.
AT4G37290		unknown protein
AT4G37295		unknown protein
AT4G37590	NAKED PINS IN YUCMUTANTS 5 (NPY5)	A member of the NPY gene family (NPY1/AT4G31820, NPY2/AT2G14820, NPY3/AT5G67440, NPY4/AT2G23050, NPY5/AT4G37590). Involved in auxin-mediated organogenesis.
AT5G01840	OVATE FAMILY PROTEIN 1 (OFP1)	Encodes a member of the plant specific ovate protein family. Members of this family have been shown to bind to KNOX and BELL-like TALE class homeodomain proteins. This interaction may mediate relocalization of the TALE homeodomain from the nucleus to the cytoplasm. Functions as a transcriptional repressor that suppresses cell elongation.
AT5G02760		Protein phosphatase 2C family protein
AT5G04980		DNase I-like superfamily protein
AT5G05160	REDUCED IN LATERAL GROWTH1 (RUL1)	Encodes a receptor-like kinase that activates secondary growth, the production of secondary vascular tissues.
AT5G06080	LOB DOMAIN-CONTAINING PROTEIN 33 (LBD33)	LOB domain-containing protein 33 (LBD33)
AT5G12050		unknown protein;
AT5G16110		unknown protein
AT5G17340		Putative membrane lipoprotein
AT5G18560	(PUCHI)	Encodes PUCHI, a member of the ERF (ethylene response factor) subfamily B-1 of ERF/AP2 transcription factor family. The protein contains one AP2 domain. There are 15 members in this subfamily including ATERF-3, ATERF-4, ATERF-7, and leafy petiole. PUCHI is required for morphogenesis in the early lateral root primordium of Arabidopsis. Expressed in early floral meristem (stage 1 to 2). Required for early floral meristem growth and for bract suppression. Triple mutant with bop1 and bop2 displays a strong defect in the determination of floral meristem identity with reduced LFY expression and the lack of AP1 expression.
AT5G26930	GATA TRANSCRIPTIONFACTOR 23 (GATA23)	Encodes a member of the GATA factor family of zinc finger transcription factors. Controls lateral root founder cell specification.
AT5G40540		Protein kinase superfamily protein

Locus identifier	Primary Gene Symbol	Gene Model Description
AT5G43700	AUXIN INDUCIBLE 2-11(ATAUX2-11)	Auxin inducible protein similar to transcription factors.
AT5G47370	(HAT2)	homeobox-leucine zipper genes induced by auxin, but not by other phytohormones. Plays opposite roles in the shoot and root tissues in regulating auxin-mediated morphogenesis.
AT5G48150	PHYTOCHROME A SIGNALTRANSDUCTION 1 (PAT1)	Member of GRAS gene family. Semi-dominant mutant has a reduced response to far-red light and appears to act early in the phytochrome A signaling pathway.
AT5G49448	AT5G49448	
AT5G51670		Protein of unknown function (DUF668)
AT5G52900		unknown protein
AT5G54490	PINOID-BINDING PROTEIN 1 (PBP1)	Encodes a PINOID (PID)-binding protein containing putative EF-hand calcium-binding motifs. The interaction is dependent on the presence of calcium. mRNA expression is up-regulated by auxin. Not a phosphorylation target of PID, likely acts upstream of PID to regulate the activity of this protein in response to changes in calcium levels.
AT5G54500	FLAVODOXIN-LIKEQUINONE REDUCTASE 1 (FQR1)	Encodes a flavin mononucleotide-binding flavodoxin-like quinone reductase that is a primary auxin-response gene.
AT5G54510	DWARF IN LIGHT 1 (DFL1)	Encodes an IAA-amido synthase that conjugates Ala, Asp, Phe, and Trp to auxin. Lines overexpressing this gene accumulate IAA-ASP and are hypersensitive to several auxins. Identified as a dominant mutation that displays shorter hypocotyls in light grown plants when compared to wild type siblings. Protein is similar to auxin inducible gene from pea (GH3).
AT5G57100		Nucleotide/sugar transporter family protein
AT5G57520	ZINC FINGER PROTEIN 2(ZFP2)	Encodes a zinc finger protein containing only a single zinc finger.
AT5G62280		Protein of unknown function (DUF1442)
AT5G64250		Aldolase-type TIM barrel family protein
AT5G65390	ARABINOGLACTANPROTEIN 7 (AGP7)	arabinogalactan protein 7 (AGP7)
AT5G67430		Acyl-CoA N-acyltransferases (NAT) superfamily protein

B. Appendix - LRRK1, a leucine rich repeat receptor-like kinase and its role in auxin-dependent PIN re-arrangement

Table S1

Table with results of statistical analysis from protein-protein interaction IP/MS experiment from Perseus software. List is sorted by fold change ratio between MS result from control Col-0 plants and *35S::LRRK1-GFP* with an arbitrary cut-off at 100. The p-value from two-sided t-test with a cut-off at 0.0001 represent statistical significance. Experiments and statistical analysis were performed by B.d.R..

Table S1.

RATIO	p-value	Protein IDs	Fasta headers
12877	1.38429E-08	AT1G30360.1	ERD4 Early-responsive to dehydration stress protein (ERD4) chr1:10715892-10718799 FORWARD LENGTH=724
12702	5.92279E-08	AT2G45960.2	PIP1B, TMP-A, ATHH2, PIP1;2 plasma membrane intrinsic protein 1B chr2:18910450-18911579 FORWARD LENGTH=274; PIP1B, TMP-A, ATHH2, PIP1;2 plasma membrane intrinsic protein 1B chr2:18910450-18911703 FORWARD LENGTH=286; PIP1
8933	6.51001E-08	AT3G11630.1	Thioredoxin superfamily protein chr3:3672189-3673937 FORWARD LENGTH=266
8163	2.69895E-09	AT3G61430.2	PIP1A, ATP1P1, PIP1, PIP1;1 plasma membrane intrinsic protein 1A chr3:22733657-22735113 FORWARD LENGTH=286; PIP1A, ATP1P1, PIP1, PIP1;1 plasma membrane intrinsic protein 1A chr3:22733657-22735113 FORWARD LENGTH=286
5783	2.64727E-06	AT1G31330.1	PSAF photosystem I subunit F chr1:11215011-11215939 REVERSE LENGTH=221
3921	2.14009E-08	AT4G30190.1	AHA2, PMA2, HA2 H(+)-ATPase 2 chr4:14770820-14775920 REVERSE LENGTH=948; HA2 H(+)-ATPase 2 chr4:14770820-14775920 REVERSE LENGTH=981
2827	1.39337E-10	AT4G00430.2	TMP-C, PIP1;4, PIP1E plasma membrane intrinsic protein 1;4 chr4:186569-187531 REVERSE LENGTH=219; TMP-C, PIP1;4, PIP1E plasma membrane intrinsic protein 1;4 chr4:186143-187531 REVERSE LENGTH=287
2745	6.61169E-07	AT5G62670.1	AHA11, HA11 H(+)-ATPase 11 chr5:25159495-25164957 FORWARD LENGTH=956; AHA4, HA4 H(+)-ATPase 4 chr3:17693015-17697801 FORWARD LENGTH=960
2593	2.93191E-06	AT2G39010.1	PIP2E, PIP2;6 plasma membrane intrinsic protein 2E chr2:16291564-16293746 FORWARD LENGTH=289
2125	1.69951E-11	AT5G23060.1	CaS calcium sensing receptor chr5:7736760-7738412 REVERSE LENGTH=387
2072	7.4686E-08	AT5G56030.1	HSP81-2, ERD8, HSP90.2, AtHsp90.2 heat shock protein 81-2 chr5:22686923-22689433 FORWARD LENGTH=699; HSP81-3, Hsp81.3, AtHsp90-3, AtHsp90.3 heat shock protein 81-3 chr5:22681410-22683911 FORWARD LENGTH=699; HSP81-2 hea
2047	1.05971E-08	AT3G28860.1	ATMDR1, ATMDR11, PGP19, MDR11, MDR1, ATPGP19, ABCB19, ATABCB19 ATP binding cassette subfamily B19 chr3:10870287-10877286 REVERSE LENGTH=1252
2015	2.3623E-08	AT5G14040.1	PHT3;1 phosphate transporter 3;1 chr5:4531059-4532965 REVERSE LENGTH=375
1929	7.1146E-09	AT1G23080.3	PIN7 Auxin efflux carrier family protein chr1:8180768-8183406 REVERSE LENGTH=615; PIN7, ATPIN7 Auxin efflux carrier family protein chr1:8180768-8183406 REVERSE LENGTH=619; PIN7 Auxin efflux carrier family protein chr
1884	9.6508E-08	AT1G79040.1	PSBR photosystem II subunit R chr1:29736085-29736781 FORWARD LENGTH=140
1424	1.57756E-08	AT4G35060.1	HIPP25 Heavy metal transport/detoxification superfamily protein chr4:16685874-16686419 REVERSE LENGTH=153
1388	1.2438E-06	AT3G09740.1	SYP71, ATSYF71 syntaxin of plants 71 chr3:2989615-2991354 FORWARD LENGTH=266
1319	3.26017E-05	AT5G01530.1	LHCB4.1 light harvesting complex photosystem II chr5:209084-210243 FORWARD LENGTH=290
1299	2.00804E-07	AT1G71500.1	Rieske (2Fe-2S) domain-containing protein chr1:26936084-26937331 FORWARD LENGTH=287
1297	1.48565E-06	AT1G48480.1	RKL1 receptor-like kinase 1 chr1:17918475-17920743 FORWARD LENGTH=655
1258	6.03511E-08	AT3G53420.2	PIP2A, PIP2, PIP2;1 plasma membrane intrinsic protein 2A chr3:19803906-19805454 REVERSE LENGTH=287; PIP2A, PIP2, PIP2;1 plasma membrane intrinsic protein 2A chr3:19803906-19805454 REVERSE LENGTH=287
1037	1.33522E-06	AT3G61470.1	LHCA2 photosystem I light harvesting complex gene 2 chr3:22745736-22747032 FORWARD LENGTH=257
1029	5.26239E-08	AT1G47128.1	RD21, RD21A Granulin repeat cysteine protease family protein chr1:17283139-17285609 REVERSE LENGTH=462
1006	2.98055E-07	AT1G45201.2	ATLL1, TLL1 triacylglycerol lipase-like 1 chr1:17123889-17127497 FORWARD LENGTH=387; ATLL1, TLL1 triacylglycerol lipase-like 1 chr1:17123889-17128462 FORWARD LENGTH=479
974	2.72972E-07	AT4G38920.1	AVA-P3, ATVHA-C3, VHA-C3 vacuolar-type H(+)-ATPase C3 chr4:18147330-18148853 FORWARD LENGTH=164; AVA-P1, VHA-C1, ATVHA-C1 ATPase, FO/VO complex, subunit C protein chr4:16568223-16569165 REVERSE LENGTH=164; ATPase, FO/
959	2.63231E-09	AT4G25960.1	PGP2 P-glycoprotein 2 chr4:13177438-13183425 FORWARD LENGTH=1273
900	1.22002E-08	AT5G60660.1	PIP2F, PIP2;4 plasma membrane intrinsic protein 2;4 chr5:24375673-24376939 REVERSE LENGTH=291
892	1.6685E-07	AT2G30950.1	VAR2, FTSH2 FtsH extracellular protease family chr2:13174692-13177064 FORWARD LENGTH=695; FTSH8 FTSH protease 8 chr1:1960214-1962525 REVERSE LENGTH=685
867	9.97073E-07	AT2G20990.1	SYTA, NTMC2TYPE1.1, ATSYTA, NTMC2T1.1, SYT1 synaptotagmin A chr2:9014827-9017829 FORWARD LENGTH=541; SYTA synaptotagmin A chr2:9014827-9017829 FORWARD LENGTH=565; SYTA synaptotagmin A chr2:9014827-9017829 FORWARD LEN
837	7.05455E-06	AT1G29930.1	CAB1, AB140, CAB140, LHCB1.3 chlorophyll A/B binding protein 1 chr1:10478071-10478874 FORWARD LENGTH=267; CAB2, AB165, LHCB1.1 chlorophyll A/B-binding protein 2 chr1:10475089-10475892 REVERSE LENGTH=267; CAB3, AB180, LHC
825	1.26696E-06	ATCG00770.1	RPS8 ribosomal protein S8 chrC:80068-80472 REVERSE LENGTH=134
819	1.88861E-09	AT4G35470.1	PIRL4 plant intracellular ras group-related LRR 4 chr4:16846531-16848448 FORWARD LENGTH=549
804	6.60294E-07	AT3G54140.1	ATPTR1, PTR1 peptide transporter 1 chr3:20045885-20048154 REVERSE LENGTH=570
731	1.01391E-09	AT1G12840.1	DET3, ATVHA-C vacuolar ATP synthase subunit C (VATC) / V-ATPase C subunit / vacuolar proton pump C subunit (DET3) chr1:4375584-4378220 FORWARD LENGTH=375
718	3.34151E-06	AT2G01420.1	PIN4, ATPIN4 Auxin efflux carrier family protein chr2:180478-183199 REVERSE LENGTH=612; PIN4 Auxin efflux carrier family protein chr2:180478-183199 REVERSE LENGTH=616
698	2.16065E-07	AT4G22890.4	PGR5-LIKE A PGR5-LIKE A chr4:12007157-12009175 FORWARD LENGTH=321; PGR5-LIKE A PGR5-LIKE A chr4:12007157-12009175 FORWARD LENGTH=322; PGR5-LIKE A PGR5-LIKE A chr4:12007157-12009175 FORWARD LENGTH=324; PGR5-L
688	5.11463E-07	AT3G61260.1	Remorin family protein chr3:22675403-22676701 REVERSE LENGTH=212
670	5.89795E-08	AT1G79920.2	Heat shock protein 70 (Hsp 70) family protein chr1:30058935-30062224 REVERSE LENGTH=831; Heat shock protein 70 (Hsp 70) family protein chr1:30058935-30062224 REVERSE LENGTH=831
665	1.96872E-09	AT3G51550.1	FER Malectin/receptor-like protein kinase family protein chr3:19117877-19120564 REVERSE LENGTH=895
658	5.36519E-06	AT2G38750.1	ANNAT4 annexin 4 chr2:16196582-16198431 REVERSE LENGTH=319
614	6.3431E-07	AT1G11260.1	STP1, ATSTP1 sugar transporter 1 chr1:3777460-3780133 FORWARD LENGTH=522
578	1.42624E-06	AT2G45820.1	Remorin family protein chr2:18863147-18864576 REVERSE LENGTH=190
573	1.2743E-07	AT2G37180.1	RD28, PIP2;3, PIP2C Aquaporin-like superfamily protein chr2:15617779-15618937 FORWARD LENGTH=285
555	5.01092E-11	AT4G35250.1	NAD(P)-binding Rossmann-fold superfamily protein chr4:16771401-16773269 REVERSE LENGTH=395

RATIO	p-value	Protein IDs	Fasta headers
554	4.37302E-08	AT4G30010.1	unknown protein;FUNCTIONS IN: molecular_function unknown;INVOLVED IN: biological_process unknown;LOCATED IN: mitochondrion, plastid;EXPRESSED IN: 26 plant structures;EXPRESSED DURING: 15 growth stages;Has 39 Blast hits to 39 proteins in
552	4.09484E-06	AT2G36880.2	MAT3 methionine adenosyltransferase 3 chr2:15479721-15480893 REVERSE LENGTH=390; MAT3 methionine adenosyltransferase 3 chr2:15479721-15480893 REVERSE LENGTH=390
547	3.43799E-07	AT3G16240.1	DELTA-TIP, TIP2;1, DELTA-TIP1, AQP1, ATTIP2;1 delta tonoplast integral protein chr3:5505534-5506788 FORWARD LENGTH=250
542	8.86788E-07	AT2G45140.1	PVA12 plant VAP homolog 12 chr2:18611029-18612971 FORWARD LENGTH=239
516	1.55059E-06	AT3G46780.1	PTAC16 plastid transcriptionally active 16 chr3:17228766-17231021 FORWARD LENGTH=510
515	2.04718E-06	AT4G02510.1	TOC159, TOC86, PPI2, TOC160, ATTOC159 translocan at the outer envelope membrane of chloroplasts 159 chr4:1104766-1109360 FORWARD LENGTH=1503
510	1.62474E-07	AT5G54500.1	FQR1 flavodoxin-like quinone reductase 1 chr5:22124674-22126256 FORWARD LENGTH=204; FQR1 flavodoxin-like quinone reductase 1 chr5:22124674-22126435 FORWARD LENGTH=244
499	8.57377E-09	AT5G51010.1	Rubredoxin-like superfamily protein chr5:20744615-20745344 FORWARD LENGTH=154
495	9.76711E-06	AT4G14960.2	TUA6 Tubulin/FtsZ family protein chr4:8548769-8550319 REVERSE LENGTH=450; TUA2 tubulin alpha-2 chain chr1:18517737-18519729 FORWARD LENGTH=450; TUA4, TOR2 tubulin alpha-4 chain chr1:1356421-1358266 REVERSE LENGTH=450
490	2.24985E-06	AT4G16370.1	ATOPT3, OPT3 oligopeptide transporter chr4:9247514-9250071 REVERSE LENGTH=737
480	1.33926E-05	AT5G10960.1	Polynucleotidyl transferase, ribonuclease H-like superfamily protein chr5:3464581-3465414 FORWARD LENGTH=277
479	2.66089E-08	AT5G52520.1	OVA6, PRORS1 Class II aarS and biotin synthetases superfamily protein chr5:21311112-21313875 FORWARD LENGTH=543
476	9.63624E-06	AT3G18830.1	ATPLT5, PMT5, ATPMT5 polyol/monosaccharide transporter 5 chr3:6489000-6491209 REVERSE LENGTH=539
474	1.0595E-06	AT1G04750.1	VAMP7B, VAMP721, ATVAMP721, AT VAMP7B vesicle-associated membrane protein 721 chr1:1331857-1333426 REVERSE LENGTH=219; SAR1, VAMP722, ATVAMP722 synaptobrevin-related protein 1 chr2:14043785-14045337 REVERSE LENGTH=221; S
464	1.47617E-06	AT5G57110.2	ACA8, AT-ACA8 autoinhibited Ca2+ -ATPase, isoform 8 chr5:23109729-23116857 REVERSE LENGTH=1074; ACA8, AT-ACA8 autoinhibited Ca2+ -ATPase, isoform 8 chr5:23109729-23116857 REVERSE LENGTH=1074
462	1.47793E-08	AT4G08850.2	Leucine-rich repeat receptor-like protein kinase family protein chr4:5637467-5640496 REVERSE LENGTH=1009; Leucine-rich repeat receptor-like protein kinase family protein chr4:5636693-5640496 REVERSE LENGTH=1045
455	1.24717E-05	AT1G51500.1	CERS5, D3, ABCG12, WBC12, ATWBC12 ABC-2 type transporter family protein chr1:19097967-19100972 REVERSE LENGTH=687
452	4.3859E-07	AT3G04120.1	GAPC, GAPC-1, GAPC1 glyceraldehyde-3-phosphate dehydrogenase C subunit 1 chr3:1081077-1083131 FORWARD LENGTH=338
426	1.85622E-07	AT4G01100.1	ADNT1 adenine nucleotide transporter 1 chr4:477411-479590 FORWARD LENGTH=352; ADNT1 adenine nucleotide transporter 1 chr4:477411-479590 FORWARD LENGTH=366; Mitochondrial substrate carrier family protein chr4:1326026
417	1.28116E-09	AT3G13920.1	EIF4A1, RH4, TIF4A1 eukaryotic translation initiation factor 4A1 chr3:4592635-4594128 REVERSE LENGTH=412; EIF4A1, RH4, TIF4A1 eukaryotic translation initiation factor 4A1 chr3:4592586-4594128 REVERSE LENGTH=415; EIF4A1
401	5.97254E-06	AT1G78570.1	RHM1, ROL1, ATRHM1 rhamnose biosynthesis 1 chr1:29550110-29552207 FORWARD LENGTH=669
399	6.7526E-07	AT3G23750.1	Leucine-rich repeat protein kinase family protein chr3:8558332-8561263 FORWARD LENGTH=928
396	3.07939E-07	AT3G28715.2	ATPase, V0/A0 complex, subunit C/D chr3:10778025-10780350 FORWARD LENGTH=343; ATPase, V0/A0 complex, subunit C/D chr3:10778025-10780350 FORWARD LENGTH=351; ATPase, V0/A0 complex, subunit C/D chr3:10773144-10775594
387	7.32483E-07	AT3G21810.1	Zinc finger C-x8-C-x5-C-x3-H type family protein chr3:7684852-7688360 FORWARD LENGTH=437
384	5.59388E-07	AT4G24190.2	SHD, AtHsp90.7, AtHsp90-7 Chaperone protein htpG family protein chr4:12551902-12555851 REVERSE LENGTH=823; SHD, HSP90.7, AtHsp90.7, AtHsp90-7 Chaperone protein htpG family protein chr4:12551902-12555851 REVERSE LENGTH=823
371	4.4446E-07	AT1G10200.1	WLIM1 GATA type zinc finger transcription factor family protein chr1:3346677-3347763 REVERSE LENGTH=190
364	3.45309E-06	AT5G59840.1	Ras-related small GTP-binding family protein chr5:24107450-24109049 REVERSE LENGTH=216; ARA3 RAB GTPase homolog 8A chr3:16917908-16919740 FORWARD LENGTH=216; ARA3 RAB GTPase homolog 8A chr3:16917908-16919740 FORWARD
359	4.43392E-06	AT2G44790.1	UCC2 uclacyanin 2 chr2:18462182-18463232 REVERSE LENGTH=202
354	3.89558E-06	AT2G26730.1	Leucine-rich repeat protein kinase family protein chr2:11388621-11391286 FORWARD LENGTH=658
353	1.91197E-06	AT5G19780.1	TUA5 tubulin alpha-5 chr5:6687212-6688926 FORWARD LENGTH=450; TUA3 tubulin alpha-3 chr5:6682761-6684474 REVERSE LENGTH=450
339	5.11807E-06	AT5G15350.1	ENODL17, AtENODL17 early nodulin-like protein 17 chr5:4985184-4986154 REVERSE LENGTH=172
335	1.29282E-06	AT3G56940.1	CRD1, CHL27, ACSF dicarboxylate diiron protein, putative (Crd1) chr3:21076594-21078269 FORWARD LENGTH=409; CRD1 dicarboxylate diiron protein, putative (Crd1) chr3:21076825-21078269 FORWARD LENGTH=332
333	3.53433E-08	AT4G09000.1	GRF1, GF14 CHI general regulatory factor 1 chr4:5775387-5777157 FORWARD LENGTH=267; GRF1, GF14 CHI general regulatory factor 1 chr4:5775387-5777157 FORWARD LENGTH=318; GRF2, 14-3-OMEGA, GF14 OMEGA general regulatory f
317	1.56569E-07	AT5G35360.1	CAC2 acetyl Co-enzyme a carboxylase biotin carboxylase subunit chr5:13584300-13588268 FORWARD LENGTH=537; CAC2 acetyl Co-enzyme a carboxylase biotin carboxylase subunit chr5:13584300-13587827 FORWARD LENGTH=499; CAC2 a
311	1.06802E-06	AT5G64740.1	CESA6, IXR2, E112, PRC1 cellulose synthase 6 chr5:25881555-25886333 FORWARD LENGTH=1084; CESA5 cellulose synthase 5 chr5:3073356-3077974 FORWARD LENGTH=1069; CESA2, ATH-A, ATCESA2 cellulose synthase A2 chr4:18297078-
308	4.05931E-06	AT3G17840.1	RLK902 receptor-like kinase 902 chr3:6106092-6108430 FORWARD LENGTH=647
305	7.30364E-07	AT5G67500.1	VDAC2, ATVDAC2 voltage dependent anion channel 2 chr5:26935223-26937123 FORWARD LENGTH=276; VDAC2 voltage dependent anion channel 2 chr5:26935223-26937123 FORWARD LENGTH=303
299	2.53305E-07	AT1G22710.1	SUC2, SUT1, ATSUC2 sucrose-proton symporter 2 chr1:8030911-8032970 REVERSE LENGTH=512
294	6.58566E-06	AT4G23650.1	CDPK6, CPK3 calcium-dependent protein kinase 6 chr4:12324967-12327415 REVERSE LENGTH=529
286	8.21849E-08	AT4G38630.1	RPN10, MCB1, ATMCB1, MBP1 regulatory particle non-ATPase 10 chr4:18057357-18059459 REVERSE LENGTH=386

RATIO	p-value	Protein IDs	Fasta headers
281	2.69652E-05	AT3G08930.1	LMBR1-like membrane protein chr3:2713562-2717058 FORWARD LENGTH=509
279	1.4983E-07	AT2G38940.1	ATPT2, PHT1;4 phosphate transporter 1;4 chr2:16258500-16260104 FORWARD LENGTH=534
278	2.66312E-05	AT3G58730.1	vacuolar ATP synthase subunit D (VATD) / V-ATPase D subunit / vacuolar proton pump D subunit (VATPD) chr3:21718495-21719280 REVERSE LENGTH=261
276	2.8762E-06	AT3G14840.2	Leucine-rich repeat transmembrane protein kinase chr3:4988271-4993891 FORWARD LENGTH=1020
274	3.16187E-07	AT5G38660.1	APE1 acclimation of photosynthesis to environment chr5:15473285-15475497 REVERSE LENGTH=286; APE1 acclimation of photosynthesis to environment chr5:15471208-15475497 REVERSE LENGTH=431
272	7.84044E-07	AT5G46110.2	APE2, TPT Glucose-6-phosphate/phosphate translocator-related chr5:18698019-18700212 FORWARD LENGTH=297; APE2, TPT Glucose-6-phosphate/phosphate translocator-related chr5:18697606-18700212 FORWARD LENGTH=399; APE2, TPT
270	3.10696E-08	ATCG00470.1	ATPE ATP synthase epsilon chain chrC:52265-52663 REVERSE LENGTH=132
268	8.39695E-07	AT5G53480.1	ARM repeat superfamily protein chr5:21714016-21716709 FORWARD LENGTH=870
256	4.67193E-08	AT5G39320.1	UDP-glucose 6-dehydrogenase family protein chr5:15743254-15744696 FORWARD LENGTH=480
254	7.5326E-07	AT5G38480.2	GRF3, RCI1 general regulatory factor 3 chr5:15410277-15411285 FORWARD LENGTH=254; GRF3, RCI1 general regulatory factor 3 chr5:15410277-15411285 FORWARD LENGTH=255
251	1.59556E-05	AT1G04410.1	Lactate/malate dehydrogenase family protein chr1:1189418-1191267 REVERSE LENGTH=332
244	1.96136E-07	AT1G79530.1	GAPCP-1 glyceraldehyde-3-phosphate dehydrogenase of plastid 1 chr1:29916232-29919088 REVERSE LENGTH=422
239	4.75485E-06	AT5G10450.2	GRF6, AFT1, 14-3-3lambda G-box regulating factor 6 chr5:3284452-3286261 REVERSE LENGTH=246; GRF6, AFT1, 14-3-3lambda G-box regulating factor 6 chr5:3284452-3286261 REVERSE LENGTH=248; GRF6 G-box regulating factor 6 c
238	1.69044E-07	AT1G79930.1	HSP91 heat shock protein 91 chr1:30063781-30067067 REVERSE LENGTH=831; HSP91 heat shock protein 91 chr1:30063924-30067067 REVERSE LENGTH=789
233	2.27603E-06	AT1G71880.1	SUC1, AT5UC1 sucrose-proton symporter 1 chr1:27054334-27056100 FORWARD LENGTH=513
230	5.9359E-09	AT3G08510.3	phospholipase C 2 chr3:2582626-2585556 REVERSE LENGTH=552; ATPLC2, PLC2 phospholipase C 2 chr3:2582626-2585556 REVERSE LENGTH=581; ATPLC2, PLC2 phospholipase C 2 chr3:2582626-2585556 REVERSE LENGTH=581
229	3.78227E-05	AT3G62530.1	ARM repeat superfamily protein chr3:23132219-23133121 FORWARD LENGTH=221
227	1.39013E-07	AT4G39090.1	RD19, RD19A Papain family cysteine protease chr4:18215826-18217326 REVERSE LENGTH=368
222	6.84084E-06	ATCG01060.1	PSAC iron-sulfur cluster binding;electron carriers;4 iron, 4 sulfur cluster binding chrC:117318-117563 REVERSE LENGTH=81
215	2.04062E-08	AT5G43060.1	Granulin repeat cysteine protease family protein chr5:17269784-17272117 REVERSE LENGTH=463
214	9.56515E-09	AT1G25450.1	KCS5, CER60 3-ketoacyl-CoA synthase 5 chr1:8938679-8940282 REVERSE LENGTH=492; CUT1, POP1, CER6, G2, KCS6 3-ketoacyl-CoA synthase 6 chr1:25712881-25714733 REVERSE LENGTH=497
211	1.23357E-07	AT3G48140.1	B12D protein chr3:17778471-17779299 FORWARD LENGTH=88
208	8.69143E-09	AT1G03860.2	ATPHB2, PHB2 prohibitin 2 chr1:979611-980870 REVERSE LENGTH=221; ATPHB6, PHB6 prohibitin 6 chr2:8842300-8843787 FORWARD LENGTH=286; ATPHB6, PHB6 prohibitin 6 chr2:8842300-8843787 FORWARD LENGTH=286; ATPHB2,
202	2.63526E-06	AT5G01460.1	LMBR1-like membrane protein chr5:186823-190008 FORWARD LENGTH=509
200	4.94303E-09	AT2G26250.1	FDH, KCS10 3-ketoacyl-CoA synthase 10 chr2:11170799-11173059 REVERSE LENGTH=550
199	1.51691E-06	AT1G73110.1	P-loop containing nucleoside triphosphate hydrolases superfamily protein chr1:27494344-27496844 REVERSE LENGTH=432
198	5.85619E-06	AT2G34430.1	LHB1B1, LHC1.4 light-harvesting chlorophyll-protein complex II subunit B1 chr2:14524818-14525618 FORWARD LENGTH=266
190	3.0048E-07	AT1G54780.1	TLP18.3 thylakoid lumen 18.3 kDa protein chr1:20439533-20440953 FORWARD LENGTH=285
188	1.02523E-06	AT3G44110.1	ATJ3, ATJ DNAJ homologue 3 chr3:15869115-15871059 REVERSE LENGTH=420; ATJ3, ATJ DNAJ homologue 3 chr3:15869179-15871059 REVERSE LENGTH=343
187	2.9347E-06	AT5G06320.1	NHL3 NDR1/HIN1-like 3 chr5:1931016-1931711 REVERSE LENGTH=231
185	6.94549E-05	AT4G03080.1	BSL1 BRI1 suppressor 1 (BSU1)-like 1 chr4:1359935-1365166 REVERSE LENGTH=881
184	4.00632E-06	AT3G08030.2	Protein of unknown function, DUF642 chr3:2564517-2565819 FORWARD LENGTH=323; Protein of unknown function, DUF642 chr3:2564191-2565819 FORWARD LENGTH=365
183	4.46132E-05	AT4G32150.1	VAMP711, ATVAMP711 vesicle-associated membrane protein 711 chr4:15526407-15527651 REVERSE LENGTH=219
179	3.36353E-07	AT5G38990.1	Malectin/receptor-like protein kinase family protein chr5:15608824-15611466 FORWARD LENGTH=880
174	1.25735E-07	AT1G54270.1	EIF4A-2 eif4a-2 chr1:20260495-20262018 FORWARD LENGTH=412; EIF4A-2 eif4a-2 chr1:20260495-20262018 FORWARD LENGTH=407; EIF4A1, RH4, TIF4A1 eukaryotic translation initiation factor 4A1 chr3:4592635-4594094 REVERSE LENG
171	6.41163E-08	AT3G07570.1	Cytochrome b561/ferric reductase transmembrane with DOMON related domain chr3:2418205-2420206 REVERSE LENGTH=369
167	8.29127E-06	AT5G59880.2	ADF3 actin depolymerizing factor 3 chr5:24120382-24121628 FORWARD LENGTH=124; ADF2 actin depolymerizing factor 2 chr3:16907743-16908822 REVERSE LENGTH=137; ADF4, ATADF4 actin depolymerizing factor 4 chr5:24122545-241
164	1.40883E-06	AT1G72150.1	PATL1 PATELLIN 1 chr1:27148558-27150652 FORWARD LENGTH=573
159	1.29152E-08	AT1G61250.1	SC3 secretory carrier 3 chr1:22586035-22588519 FORWARD LENGTH=274; SC3 secretory carrier 3 chr1:22586035-22588664 FORWARD LENGTH=289
158	8.09419E-05	AT5G23660.1	MTN3, SWEET12, AtSWEET12 homolog of Medicago truncatula MTN3 chr5:7971936-7973796 REVERSE LENGTH=285

RATIO	p-value	Protein IDs	Fasta headers
158	2.56291E-07	AT1G06700.2	Protein kinase superfamily protein chr1:2052750-2054552 REVERSE LENGTH=361; Protein kinase superfamily protein chr1:2052750-2054552 REVERSE LENGTH=361; Protein kinase superfamily protein chr2:13093145-13094677 FOR
156	6.58395E-06	AT5G25460.1	Protein of unknown function, DUF642 chr5:8863430-8865394 FORWARD LENGTH=369; Protein of unknown function, DUF642 chr5:3644655-3646991 FORWARD LENGTH=366
155	5.49579E-07	AT3G62830.1	UXS2, ATUXS2 NAD(P)-binding Rossmann-fold superfamily protein chr3:23232539-23235353 FORWARD LENGTH=445; UXS4
155	1.95335E-05	AT3G08530.1	Clathrin, heavy chain chr3:2587171-2595411 REVERSE LENGTH=1703
154	6.59875E-06	AT3G44320.1	NIT3, AtNIT3 nitrilase 3 chr3:15993419-15995493 FORWARD LENGTH=346
147	1.66704E-07	AT1G25490.1	RCN1, REGA, ATB BETA BETA, EER1 ARM repeat superfamily protein chr1:8951700-8954899 FORWARD LENGTH=588; PP2AA3 protein phosphatase 2A subunit A3 chr1:4563970-4567348 REVERSE LENGTH=537; PDF1, PR 65, PP2AA2 protein pho
144	1.49251E-05	AT1G68830.1	STN7 STT7 homolog STN7 chr1:25872654-25875473 REVERSE LENGTH=562
144	4.62424E-07	AT5G28540.1	BIP1 heat shock protein 70 (Hsp 70) family protein chr5:10540665-10543274 REVERSE LENGTH=669
143	2.18155E-05	AT1G12920.1	ERF1-2 eukaryotic release factor 1-2 chr1:4396555-4397859 REVERSE LENGTH=434; ERF1-3 eukaryotic release factor 1-3 chr3:9788854-9790161 FORWARD LENGTH=435; ERF1-1 eukaryotic release factor 1-1 chr5:19386555-19387865
142	7.66958E-07	AT3G17970.1	atToc64-III, TOC64-III translocon at the outer membrane of chloroplasts 64-III chr3:6148030-6151794 FORWARD LENGTH=589
141	9.77252E-07	AT3G58140.1	phenylalanyl-tRNA synthetase class IIc family protein chr3:21529988-21532386 REVERSE LENGTH=429
140	5.85708E-07	AT1G12000.1	Phosphofructokinase family protein chr1:4050159-4053727 REVERSE LENGTH=566; MEE51 Phosphofructokinase family protein chr4:1939250-1942765 FORWARD LENGTH=569
138	3.91752E-06	AT5G13430.1	Ubiquinol-cytochrome C reductase iron-sulfur subunit chr5:4305414-4307399 REVERSE LENGTH=272; Ubiquinol-cytochrome C reductase iron-sulfur subunit chr5:4308431-4310022 REVERSE LENGTH=274
132	1.14862E-05	AT3G21340.1	Leucine-rich repeat protein kinase family protein chr3:7511848-7515937 REVERSE LENGTH=899
130	2.25303E-08	AT5G47930.1	Zinc-binding ribosomal protein family protein chr5:19406423-19407329 REVERSE LENGTH=84
126	1.05517E-06	AT1G45688.1	unknown protein;FUNCTIONS IN: molecular_function unknown;INVOLVED IN: biological_process unknown;LOCATED IN: plasma membrane;EXPRESSED IN: 22 plant structures;EXPRESSED DURING: 13 growth stages;BEST Arabidopsis thaliana protein match is:
124	1.31377E-06	AT3G19760.1	EIF4A-III eukaryotic initiation factor 4A-III chr3:6863790-6866242 FORWARD LENGTH=408; DEA(D/H)-box RNA helicase family protein chr1:19047960-19049967 FORWARD LENGTH=392
123	1.1419E-07	AT5G17170.2	ENH1 rubredoxin family protein chr5:5649335-5650835 FORWARD LENGTH=224; ENH1 rubredoxin family protein chr5:5649335-5650975 FORWARD LENGTH=271
119	9.95157E-08	AT5G12370.3	SEC10 exocyst complex component sec10 chr5:4003002-4008445 REVERSE LENGTH=820; SEC10 exocyst complex component sec10 chr5:4003002-4008445 REVERSE LENGTH=825; SEC10 exocyst complex component sec10 chr5:4003002-4008445
118	5.59768E-07	AT3G54110.1	ATPUMP1, UCP, PUMP1, ATUCP1, UCP1 plant uncoupling mitochondrial protein 1 chr3:20038890-20040996 FORWARD LENGTH=306
117	1.07099E-05	AT3G18780.2	ACT2, DER1, LSR2, ENL2 actin 2 chr3:6475535-6476832 FORWARD LENGTH=377; ACT8 actin 8 chr1:18216539-18217947 FORWARD LENGTH=377; ACT2, DER1, LSR2, ENL2 actin 2 chr3:6475535-6476728 FORWARD LENGTH=371
116	1.7492E-06	AT5G33320.1	CUE1, PPT, ARAPPT Glucose-6-phosphate/phosphate translocator-related chr5:12588950-12591408 FORWARD LENGTH=408
115	1.31042E-08	AT5G55280.1	FTSZ1-1, ATFTSZ1-1, CPFTSZ homolog of bacterial cytokinesis Z-ring protein FTSZ 1-1 chr5:22420740-22422527 REVERSE LENGTH=433
114	1.76621E-06	AT4G33510.1	DHS2 3-deoxy-d-arabino-heptulosonate 7-phosphate synthase chr4:16116496-16118549 FORWARD LENGTH=507; Class-II DAHP synthetase family protein chr1:7912120-7914742 FORWARD LENGTH=527; DHS2 3-deoxy-d-arabino-heptulosonate
112	1.99533E-06	AT3G11800.1	unknown protein;FUNCTIONS IN: molecular_function unknown;INVOLVED IN: biological_process unknown;LOCATED IN: endomembrane system;EXPRESSED IN: 24 plant structures;EXPRESSED DURING: 15 growth stages;BEST Arabidopsis thaliana protein match
112	2.48766E-06	AT1G51805.2	Leucine-rich repeat protein kinase family protein chr1:19221187-19225590 REVERSE LENGTH=860; Leucine-rich repeat protein kinase family protein chr1:19221187-19225590 REVERSE LENGTH=884; Leucine-rich repeat protein k
111	1.06351E-05	AT5G59030.1	COPT1 copper transporter 1 chr5:23833945-23834457 REVERSE LENGTH=170
111	4.4564E-08	AT2G25110.1	SDF2, ATSDL, ATsDF2 stromal cell-derived factor 2-like protein precursor chr2:10684428-10685838 FORWARD LENGTH=218
110	2.64164E-07	AT4G25140.1	OLEO1, OLE1 oleosin 1 chr4:12900498-12901259 FORWARD LENGTH=173
106	1.60162E-07	AT3G01570.1	Oleosin family protein chr3:222152-222778 REVERSE LENGTH=183
104	2.98865E-07	AT5G48960.1	HAD-superfamily hydrolase, subfamily IG, 5-nucleotidase chr5:19849645-19853382 FORWARD LENGTH=642
102	3.6081E-06	AT5G49910.1	CPHSC70-2EAT SHOCK PROTEIN 70-2, HSC70-7, cpHsc70-2 chloroplast heat shock protein 70-2 chr5:20303470-20306295 FORWARD LENGTH=718
101	8.41888E-07	AT3G58500.1	PP2A-4 protein phosphatase 2A-4 chr3:21635503-21638911 REVERSE LENGTH=313; PP2A-3 protein phosphatase 2A-3 chr2:17698099-17701226 REVERSE LENGTH=313; PP2A-3 protein phosphatase 2A-3 chr2:17699029-17701226 REVERSE LEN
101	1.8258E-06	AT2G46820.2	PTAC8, TMP14, PSAP, PSI-P photosystem I P subunit chr2:19243729-19244870 FORWARD LENGTH=174; PTAC8, TMP14, PSAP, PSI-P photosystem I P subunit chr2:19243729-19244870 FORWARD LENGTH=174
101	2.84273E-05	AT4G35000.1	APX3 ascorbate peroxidase 3 chr4:16665007-16667541 REVERSE LENGTH=287
101	2.06227E-07	AT3G09820.1	ADK1, ATADK1 adenosine kinase 1 chr3:3012122-3014624 FORWARD LENGTH=344; ADK2 adenosine kinase 2 chr5:796573-798997 FORWARD LENGTH=345; ADK1 adenosine kinase 1 chr3:3012645-3014624 FORWARD LENGTH=302